Mechanical design of dynamic hand orthoses

Expanding technology with comprehensive overviews and alternative pathways

Bos, Ronald

DOI
10.4233/uuid:011f686f-5f5c-4fc5-9ba5-b613f95abfe2

Publication date
2019

Document Version
Final published version

Citation (APA)
Bos, R. (2019). *Mechanical design of dynamic hand orthoses: Expanding technology with comprehensive overviews and alternative pathways*. [Dissertation (TU Delft), Delft University of Technology]. https://doi.org/10.4233/uuid:011f686f-5f5c-4fc5-9ba5-b613f95abfe2

RONALD BOS

MECHANICAL DESIGN OF DYNAMIC HAND ORTHOSES

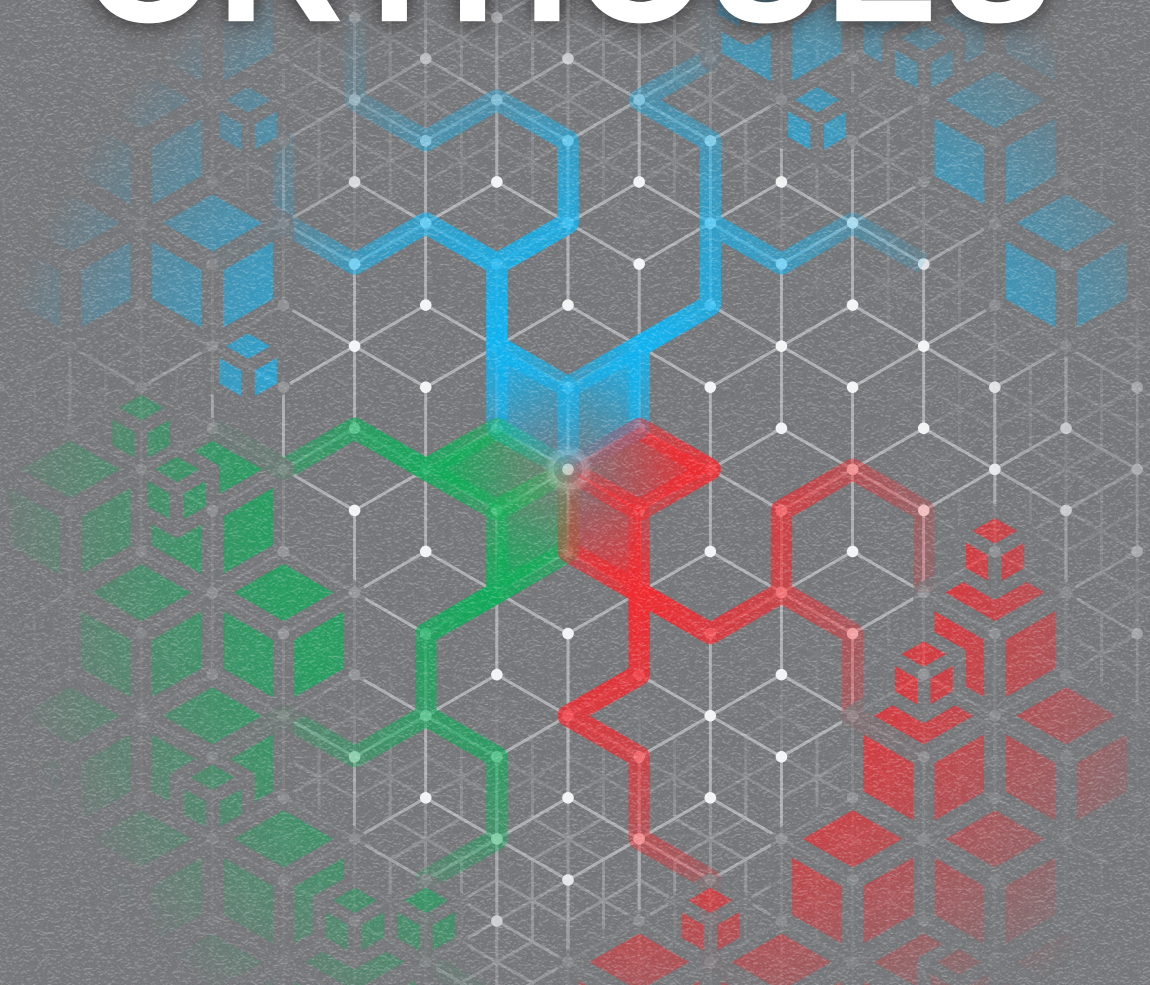

expanding technology with comprehensive overviews and alternative pathways

MECHANICAL DESIGN OF DYNAMIC HAND ORTHOSES

EXPANDING TECHNOLOGY WITH COMPREHENSIVE OVERVIEWS AND ALTERNATIVE PATHWAYS

MECHANICAL DESIGN OF DYNAMIC HAND ORTHOSES

EXPANDING TECHNOLOGY WITH COMPREHENSIVE OVERVIEWS AND ALTERNATIVE PATHWAYS

Proefschrift

ter verkrijging van de graad van doctor
aan de Technische Universiteit Delft,
op gezag van de Rector Magnificus prof. dr. ir. T.H.J.J. van der Hagen,
voorzitter van het College voor Promoties,
in het openbaar te verdedigen op donderdag 28 november 2019 om 15:00 uur

door

Ronald Alfons BOS

Master of Science in Biomedical Engineering,
Technische Universiteit Delft,
geboren te Houten, Nederland.

Dit proefschrift is goedgekeurd door de

promotor: prof. dr. ir. J.L. Herder
copromotor: dr. ir. D.H. Plettenburg

Samenstelling promotiecommissie:

Rector Magnificus	voorzitter
Prof. dr. ir. J.L. Herder	Technische Universiteit Delft
Dr. ir. D.H. Plettenburg	Technische Universiteit Delft
Onafhankelijke leden:	
Prof. dr.-ing. H. Vallery	Technische Universiteit Delft
Prof. dr.-ing. M. Hüsing	Rheinisch-Westfälische Technische Hochschule Aachen
Prof. dr. ir. R.H.M. Goossens	Technische Universiteit Delft
Dr. I.J.M. de Groot	Radboud universitair medisch centrum
Prof. dr. ir. D.M. Brouwer	Universiteit Twente

Keywords: Mechanical design, dynamic hand orthosis, grasp modeling, miniature hydraulics
Printed by: Gildeprint

"He turned left (...) in the hope of finding better fortune in that direction, but after a while lost his nerve and turned a speculative right, and then chanced another exploratory left, and after a few more such maneuvers was thoroughly lost."

— Douglas Adams, Dirk Gently's Holistic Detective Agency

CONTENTS

SUMMARY

Orthoses have evolved from simply maintaining bone fractures and correcting spinal deformities to full mechatronic systems that can read a person's intention and translate that into a desired motion or force path. A vast variety in pathologies (e.g., stroke, muscular dystrophies), applications (e.g., daily assistance, research) and environments (e.g., home, clinic) are possible. The term *dynamic hand orthosis* is able to cover this full range of applications and is therefore used as an umbrella term. In order to map the research field of dynamic hand orthosis and improve on the state-of-the-art, this thesis proposes a design methodology that categorizes mechatronic components and collects rationale to make specific design choices through scoping & optimization. Finally, a proof-of-principle dynamic hand orthosis was made and tested on a single participant in a case study experiment.

A total of 165 dynamic hand orthoses was collected, from recent history up to 2015, which included 9 research tools, 34 clinical tools, 56 home rehabilitation tools, 46 daily assistive tools, 16 haptic devices and 4 extra-vehicular activity (EVA) gloves for astronauts. Of these devices, 109 cases published changes between 2011–2015. These numbers support the claim that research in dynamic hand orthoses has been growing rapidly and that a clear majority focuses on their use in a home environment. The fact that only 18 were developed as a commercial product, however, indicates that the research field is still somewhat in its infancy and that it is not very straightforward to design a dynamic hand orthosis that meets all end user requirements.

The used mechatronic components were categorized in a tree-like structure and resulted in a hierarchical overview. This connected core functionalities with physical implementations, where each branching point symbolized a design choice. Corresponding trends showed that some mechatronic components were clearly more popular than others. These differences were mostly attributed to availability of components and common practice, rather than choosing the best component within the design constraints. Additionally, the overview revealed that not all pathologies were well-represented. Due to its high incidence rates, stroke is naturally dominating the research field. On the other hand, there are currently no dynamic hand orthoses available for people with Duchenne muscular dystrophy.

In an attempt to handle the multitude of trade-offs while designing a dynamic hand orthosis mechanism, different methods of modeling and optimization were explored. It turned out, however, that a model that requires accurate material properties (in this case for shape optimization of a compliant mechanism), cannot be combined with a less predictable manufacturing method like fused deposition modeling (FDM). Along with the fact that the early design phase is characterized by a lack of available details, a more simplified modeling approach was investigated to help make qualitative comparisons between concepts. This approach was based on a rigid multi-body model that estimated the grasping performance by evaluating the ability to hold a circular object. The equilibrium grasping position was determined using a static and dynamic approach. The

static model proved to be able to reach the same conclusions as the dynamic model, despite having no inertial effects, viscosity, friction and memory of previous states in time. On top of that, the static model was able to do this about 10 times faster with a greater variety of contact stiffnesses. This reduction in complexity due to less required details, makes the static model a feasible tool to help make complex trade-offs in an early design phase.

The majority of the categorized dynamic hand orthoses used cable systems as a method to transmit mechanical work, whereas hydraulic transmission systems were barely used. However, a hydrostatic transmission is able to be more efficient with a more predictable force transmission than cable systems, because the efficiency in a hydraulic system increases at higher pressures and is independent of hose routing. This makes the concept of using hydraulics particularly useful in situations that require a flexible coupling between the motor and end-effector, which include prosthetic and orthotic applications. Additionally, it became evident that piston-cylinder actuators become more efficient when miniaturized to a millimeter scale, which adds to the appropriateness of applying this technology in a dynamic hand orthosis.

As a proof-of-concept, a hydraulically operated dynamic hand orthosis was developed for people with Duchenne muscular dystrophy. This device, called SymbiHand, could move multiple fingers and joints with only a signal command signal that was taken from corresponding muscular activity (i.e., using electromyography). This was done by making use of a fluidic differential mechanism that distributed the pressure from a master hydraulic cylinder to multiple slave cylinders. Force was transferred via a compliant mechanism that was slid on each finger and was able to self-align itself according to the anatomical joint locations. This compact and simplistic design fitted within a 15 mm boundary on the dorsal side of the hand, left the fingertips available for tactile feedback and added only 241 g of mass to the hand. A single case study participant was able to increase his maximum grasping force on a cylindrical object from 2.6 to 8 N. Moreover, flexor and extensor muscular activation was reduced by 55 and 40% during a force tracking task without showing reductions in task performance.

The results from the case study experiment showed that the proposed design approach of a dynamic hand orthosis can result in the development of novel and suitable technologies, which are here characterized by the use of hydraulics and self-aligning compliant structures. This increase in technological diversity can increase the number of possibilities in terms of pathologies, applications and environments. Further development of these technologies can reach more fundamental research areas, connecting clinical issues with advanced and innovative technological solutions.

SAMENVATTING

Ortheses zijn geëvolueerd vanaf het simpelweg ondersteunen van botbreuken en corrigeren van vervormingen in de wervelkolom, tot aan volledig mechatronische systemen die de intentie van een persoon kunnen meten en vertalen naar een gewenste beweging of kracht. Een grote variatie in ziektebeelden (bijv. beroerte, spierdystrofie), applicaties (bijv. dagelijkse ondersteuning, onderzoek) en omgevingen (bijv. thuis, in een kliniek) zijn mogelijk. Deze variaties kunnen onder één overkoepelende term worden omvat: een *dynamische handorthese*. Om het onderzoeksveld van dynamische handortheses in kaart te brengen en de huidige stand van techniek verder te brengen, wordt er in deze dissertatie een ontwerpmethode voorgesteld wat bestaat uit een categorisatie van mechatronische componenten en een verzameling van redenaties achter specifieke ontwerpkeuzes, wat wordt verkregen door in te zoomen op technieken en door het gebruik van optimalisatie. Om de principiële bruikbaarheid aan te tonen, is er een concept dynamische handorthese ontwikkeld, gemaakt en getest op een enkel persoon in een casestudie experiment.

In totaal zijn er 165 dynamische handortheses verzameld uit de recente geschiedenis tot aan 2015. Uit deze collectie waren er 9 gebruikt voor onderzoeksdoeleinden, 34 voor gebruik in de kliniek, 56 voor thuisrevalidatie, 46 voor dagelijkse ondersteuning, 16 voor haptische applicaties en 4 voor tijdens ruimtewandelingen van astronauten. Van al deze handortheses zijn er van 109 nog veranderingen gepubliceerd tussen 2011–2015. Deze getallen ondersteunen de claim dat onderzoek in dynamische handortheses snel is gegroeid en dat er een duidelijke focus ligt op gebruik in een huiselijke omgeving. Het feit dat er slechts 18 van de 165 commercieel verkrijgbaar zijn toont tegelijkertijd aan dat het onderzoeksveld nog in de kinderschoenen zit, en dat het niet eenvoudig is om een dynamische handorthese te ontwerpen die voldoet aan de eisen van de eindgebruiker.

Uit deze 165 dynamische handortheses zijn alle gebruikte mechatronische componenten gecategoriseerd in een boomdiagram, waaruit een hiërarchisch overzicht is ontstaan. Dit overzicht is in staat om kernfuncties te verbinden met fysieke implementaties, waar elk splitstingspunt in de boomdiagram een ontwerpkeuze symboliseert. Corresponderende trends lieten zien dat sommige mechatronische componenten duidelijk populairder zijn dan anderen. Deze verschillen in gebruik zijn voornamelijk toebedeeld aan beschikbaarheid van de componenten en gewoontes, in tegenstelling tot het kiezen van de beste component binnen de ontwerpeisen. Verder liet het overzicht zien dat niet alle ziektebeelden evenredig zijn gerepresenteerd. Vanwege de hoge incidentie is beroerte het meest dominante ziektebeeld in het onderzoeksveld. Aan de andere kant zijn er geen dynamische handortheses beschikbaar gebleken voor mensen met Duchenne spierdystrofie.

In een poging om de hoeveelheid afwegingen te hanteren tijdens het ontwerpproces van een dynamische handorthese, zijn er verschillende modellerings- en optimalisatiemethoden verkend. Hier kwam naar voren dat minder precieze maar snelle vervaardigingsmethoden, zoals 3D-printen volgens de FDM-methode, niet is te

combineren met een model dat accurate materiaaleigenschappen nodig heeft (in dit geval ten behoeve van vormoptimalisatie van een flexibel mechanisme). Gecombineerd met het feit dat een vroege ontwerpfase wordt gekarakteriseerd door een gebrek aan detail, is er gekozen voor een versimpelde modelleringsaanpak waar voornamelijk kwalitatieve vergelijkingen tussen verschillende concepten kunnen worden gemaakt. Deze aanpak is uitgevoerd op basis van een stijve-massamodel, wat de grijpprestatie van een potentieel concept op een cirkel-vorming object kon evalueren. De evenwichtspositie tijdens het grijpen werd bepaald met zowel een statisch als een dynamisch model. Hier was het statisch model in staat om dezelfde kwalitatieve conclusies te maken als het dynamisch model, ondanks het gebrek aan traagheid, viscositeit, wrijving en een geheugen van voorgaande situaties in tijd. Daar bovenop kon het statisch model deze resultaten 10 keer zo snel bereiken met een groter werkgebied in mogelijke contactstijfheden. Deze afname in complexiteit, omdat er minder details benodigd zijn, maakt het statische model een beter hulpmiddel dan het dynamische model om in een vroege ontwerpfase complexe afwegingen te maken tussen verschillende concepten.

De meerderheid van dynamische handortheses gebruikt kabelsystemen om mechanische arbeid over te brengen, terwijl hydraulische overbrengingen slechts nauwelijks worden gebruikt. Een hydrostatische transmissie is echter in staat om efficiënter en meer voorspelbaar krachten over te brengen, omdat de efficiëntie toeneemt bij hogere drukken en onafhankelijk is van de buiging van de hydraulische slang. Dit maakt het concept van een hydraulisch systeem erg interessant in situaties die een flexibele koppeling nodig hebben tussen een stationaire motor en bewegende eindeffector. Vooral protheses en ortheses maken deel uit van deze situaties. Verder is het gebleken dat zuiger-cilinder actuatoren efficiënter kunnen worden als ze worden verkleind tot millimeterschaal, wat nog meer bijdraagt aan de toepasbaarheid van miniatuurhydrauliek in een dynamische handorthese.

Ten behoeve van bewijs van het concept is een hydraulisch aangedreven dynamische handorthese ontwikkeld voor mensen met Duchenne spierdystrofie. Dit hulpmiddel, genaamd SymbiHand, kan meerdere vingers en gewrichten ondersteunen met slechts een enkel aansturingssignaal, wat werd verworven door spieractiviteit te meten met elektromyografie bij de corresponderende spiergroepen. Dit is uitgevoerd door gebruik te maken van een fluïdisch differentiaalmechanisme wat druk kon verdelen van een enkele hoofdzuiger-cilinder (master) naar meerdere volgende zuiger-cilinders (slaves). Krachten op de vingers werden via flexibele structuren overgedragen. De vorm van deze structuren zorgde ervoor dat de buigpunten zichzelf konden uitlijnen om de anatomische gewrichten en konden daarnaast één voor één om de vinger geschoven worden. Dit compact en simplistisch ontwerp paste in een 15 mm grensgebied aan de dorsale zijde van de hand, liet de vingertoppen vrij van obstructie om zo nog gebruik te kunnen maken van tastsensoren in de huid en voegde slechts 241 g aan massa toe aan de hand. Een enkele casestudie deelnemer was in staat om zijn eigen grijpkracht om een cilindrisch object te verhogen van 2.6 N naar 8 N. Daarnaast was de spieractiviteit in de flexor en extensor spiergroepen verlaagd met 55 en 40% tijdens een taak waar een krachtprofiel gevolgd moest worden, zonder in te leveren in taakprestatie.

De resultaten van de casestudie hebben laten zien dat de voorgestelde ontwerpmethode kan leiden tot de ontwikkeling van vernieuwende en geschikte technologieën. Deze technologieën zijn in deze dissertatie gepresenteerd door

het gebruik van miniatuurhydrauliek en zelf-uitlijnende flexibele structuren. Deze toename in technologische diversiteit kan leiden tot een toename in mogelijkheden van dynamische handorthesen wat betreft de ondersteunde ziektebeelden, applicaties en omgevingen. Door deze technologieën nog verder door te ontwikkelen kunnen er raakvlakken gecreëerd worden met meer fundamentele onderzoeksgebieden, waardoor een verbinding kan ontstaan tussen klinisch gedreven vraagstukken en innovatieve technologische oplossingen.

1

INTRODUCTION

The quality of our health care is improving. Across the world, we have better access to health services and are able to live longer (World Health Organization, 2015). Unfortunately, not all years of our life are necessarily spent in perfect health. Some years, or perhaps all years, can be affected by disabilities caused by a disorder or disease. Between 2005 and 2015, the prevalence of health conditions that result in a severe disability has increased 23% (World Health Organization, 2017). Musculoskeletal disorders are one of the leading causes of disabilities, for which physical activity is one of the more vital recommendations for an improved health outcome (Vos et al., 2016). In many cases, a dynamic hand orthosis can be a viable tool to accommodate such physical activity.

This chapter aims to introduce the concept of dynamic hand orthoses by first asking the most elementary questions: what they are, why people use them, and what is the current state of the art. Answering these questions results in an explicit problem statement and how this thesis aims to approach that problem.

(a) (b) (c)

Figure 1.1: Characteristic Google image search results when looking for (a) hand exoskeleton (by Arata et al. (2013)), (b) hand rehabilitation device (HWARD by Takahashi et al. (2005)) and (c) robotic glove (RoboGlove by NASA Johnson Space Center ()).

1.1. WHAT IS A DYNAMIC HAND ORTHOSIS

The term *dynamic hand orthosis* covers a wide range of devices that are currently being called by many different names, e.g., hand exoskeletons, hand rehabilitation devices, robotic gloves and many others. A quick online image search using these exemplary names will result in probably the fastest way of getting an impression of the diversity of these devices, and how using different names can show implications on the shape of the device. See Figure 1.1 for some characteristic results.

Despite the implied differences, there is also a clear overlap. These devices can be grouped using a single description: they all aim to modify the structural or functional characteristics of the neuromuscular or skeletal system of the hand. This description was not chosen by coincidence, as it quotes the definition of an orthosis according to ISO/TC 168 (1989). This can involve stabilization of body segments or assistance, resistance, limiting or locking of anatomical joints (ISO/TC 168, 2007). Then, by adding the term 'dynamic', a scope is added towards those devices that allow some kind of movement in at least one joint of the limb in question—which, in this case, is the hand. Note how this meaning of 'dynamic' is slightly different from that used in mechanics which involves forces and motion of masses, which will also be used in this thesis. See Section 2.1 for a more extensive description on the history and evolution of used terminologies in dynamic hand orthoses.

1.2. WHY USE A DYNAMIC HAND ORTHOSIS

Many people suffer from impairments that affect their ability to carry out the functional movements of the hand, which can be due to the consequences of stroke, spinal cord injury, muscular dystrophy and many other pathologies. Hand impairments prevent them from performing activities of daily living (ADLs) and, depending on the pathology, require distinct approaches to reduce the impairment. For example, for traumatic events like stroke it becomes more important to recover hand functionality, whereas for progressive disorders it becomes more important to maintain hand functionality or perhaps even retard the progression of the disorder.

The ability to perform ADL and overall muscular fitness are strongly correlated with an individual's perceived quality of life (Haghgoo et al., 2013; Kell et al., 2001),

hence it is important to preserve these functionalities. By modifying the structural or functional characteristics of the hand with an external device, we can aid an individual's ability to perform ADL using modern technology. Characteristic advantages for this approach include the possibility for continuous assistance in daily environments, high repetitions of tasks for physical therapy, gathering of data and reduced workload on (professional) caregivers. Exemplary applications of dynamic hand orthoses are to provide assistance while executing ADL (In et al., 2015), to promote physical therapy using gaming environments (Amirabdollahian et al., 2014), to passively and continuously compensate for impairments like hypertonic finger flexor muscles (Brokaw et al., 2011) or to facilitate research to further improve treatment programs (Jones et al., 2014).

1.3. WHAT IS THE CURRENT STATUS

Over the past few decades, research into dynamic hand orthoses has been accelerating, their functionalities has been expanding and the design of these devices has become more complex. This has produced a large quantity of devices that can be found by bundling several review studies (Heo et al., 2012; Maciejasz et al., 2014; Basteris et al., 2014; Balasubramanian et al., 2010). It is quite clear that the majority of these devices focuses on post-stroke rehabilitation, which makes sense because stroke is one of the most prevalent causes of disability (Vos et al., 2016). Other pathologies are also represented, albeit in lower quantities, like tendon injuries (Ertas et al., 2014), spinal cord injuries (Moromugi et al., 2013) and overall muscular weakness due to aging (Hasegawa et al., 2010).

From the large quantity of dynamic hand orthoses, only very few devices have passed the research phase and have become available as a commercial product. Those that are available, mainly focus on a clinical environment and not at home. This does not coincide with the image one might get from reading scientific literature. It seems, therefore, that the current popularity of dynamic hand orthoses is out of balance with their availability. Moreover, many pathologies that are less prevalent than stroke are underrepresented in this field.

Studies on the effectiveness of dynamic hand orthoses with stroke survivors show that they are not necessarily improving traditional treatment, but not worsening it either (Kwakkel et al., 2008; Mehrholz et al., 2008; Timmermans et al., 2009). This does not necessarily make them useless, because there are other advantages not directly related to treatment effectiveness (e.g., reduced load on caregivers, continuous progress monitoring, new range of possible treatments). However, devices that do not meet the end user requirements are easily abandoned and not used at all (Radder et al., 2015), rendering any effect useless. Hence, before we can make use of these advantages and to further improve on the state-of-the-art, it means that we need to be more specific during the design of a dynamic hand orthosis and tailor it to the needs of the end user. Especially with the recent increase in global connectivity, as well as the development of rapid manufacturing methods like 3D-printing and laser cutting, state-of-the-art technology can be shared from/to almost any corner of the world. This overwhelming number of possibilities makes it more difficult to choose the right mechatronic components (e.g., control systems, actuators, mechanisms) for a dynamic hand orthosis.

1.4. PROBLEM STATEMENT

The expansion of functionalities in the recent history of orthoses, along with the vast diversity and complexity of current dynamic hand orthoses, indicates that this type of device can provide many opportunities. However, not much has been realized in practice. To ensure the orthosis delivers the desired outcome, it should still be carefully designed to accommodate the disability of the hand, while addressing the specific needs of the wearer of the orthosis. With the possibilities brought by today's state-of-the-art technology and easy access to high-tech components, it becomes easier to lose sight of this particular design problem. It can obscure the need for critical assessment of each design choice and optimization of the mechatronic components according to the pathology, application and environment. This impedes progress and development of novel technologies due to an abundance of choice and lack of overview.

1.5. THESIS GOAL

The goal of this thesis is to reveal and expand the current technological possibilities for dynamic hand orthoses in a broad range of pathologies, applications and environments. Focus will lie on a collection of the range of possible mechatronic components, identification of opportunities and gathering of rationale behind design choices. The most popular approaches and components will be questioned and compared to using alternative ways. To test this method, it will be applied to the design of a dynamic hand orthosis for people with Duchenne muscular dystrophy (DMD) in order to assist with daily activities. By using a general approach, however, the emerging method can be applied to a multitude of orthotic, prosthetic and other robotic applications.

Primarily, this thesis adheres to the following research objectives:

O1: Determine the spectrum of technological possibilities for dynamic hand orthoses.

O2: Investigate modeling approaches and justify model simplifications to help choose between concepts in the early design phase of a dynamic hand orthosis.

O3: Determine the value of using alternative technologies (i.e., fluidics, compliant mechanisms) as opposed to traditional technologies (i.e., Bowden cables, rigid links) in a dynamic hand orthosis.

O4: Assess the potential of these alternative technologies when applied to a dynamic hand orthosis to assist people with DMD during ADL.

1.6. APPROACH

The main approach to achieve this goal is to develop and follow a structured design approach that aims to reach towards an optimized mechatronic system based on well-considered design choices, while taking into account the surrounding factors that influence the design.

The structured approach helps with providing an overview of available solutions, identifying possibilities and gaps in technology, and developing a solution that fits the end user. This approach is characterized firstly by a *categorization* of mechatronic components that are used in current dynamic hand orthoses. By making sure the

categorization follows an all-inclusive structure, this allows for an expansive overview of mechatronic components that can be easily extended and possibly reveal new solutions as well.

Making well-considered design choices is essential in documenting rationale behind a specific design. Regardless of the success of its outcome, this will always provide a knowledge base for future iterations, fellow designers or interdisciplinary research fields. Learning from literature can help to make such choices, as well as using tools from optimization for more complex and multidimensional trade-offs. Wherever information is missing, conducting experiments can help to fill in these knowledge gaps. By aiming for an optimally designed mechatronic system, the designer can achieve greater insight in the constraints that are formed by the surrounding factors, which in the case of a dynamic hand orthosis are the pathology, application and environment. This process of collecting rationale to make specific design choices for an optimally designed system, is grouped under *scoping & optimization*.

As with any method, this approach requires verification. This approach will therefore be tested with a *proof-of-principle* development of a dynamic hand orthosis for people with DMD to help perform ADLs in their everyday environments.

1.7. THESIS OUTLINE

This thesis follows the structure of a 'sandwich thesis', meaning that a set of published papers are reproduced and make up the meat (or the avocado, for the vegetarians) of the sandwich. Additionally some appendices are added, which are studies that did not make it as a paper but can serve as, lets say, the lettuce and tomatoes of the sandwich. Everything is then bound together by the introduction, basic concepts and discussion & conclusions, which are the bread of the sandwich. All together, this hopefully leaves you with some food for thought, which can be enjoyed with a side of your own expertise.

The main body of this thesis (i.e., the sandwich filling) is divided into three parts and connect to the approach described in the previous section (see Figure 1.2). In the first part, *categorization*, Chapter 3 describes an overview of mechatronic components that were collected form a database of dynamic hand orthoses, shown in Appendix A, from which rationale behind design choices was gathered and possible gaps can be identified. In the second part, *scoping & optimization*, the outliers from this overview are analyzed at greater detail. In Chapter 4, the use of compliant mechanisms is explored together with using techniques from optimization. Chapter 5 presents a tool to make well-considered design choices, in particular aimed towards optimizing grasp performance for a dynamic hand orthosis mechanism. Additionally, Appendix B and C describe a more thorough look into the use of Bowden cable systems and miniaturized hydraulic systems. In the third part, *proof-of-principle*, the findings from the first and second part are combined into a prototype version of a dynamic hand orthosis for people with DMD. Chapter 6 presents the first version of this prototype using commercially available components, whereas Chapter 7 uses an optimized version in a case study on a single person with DMD. Finally, in Chapter 8, the results are discussed and conclusions are made with respect to the research objectives.

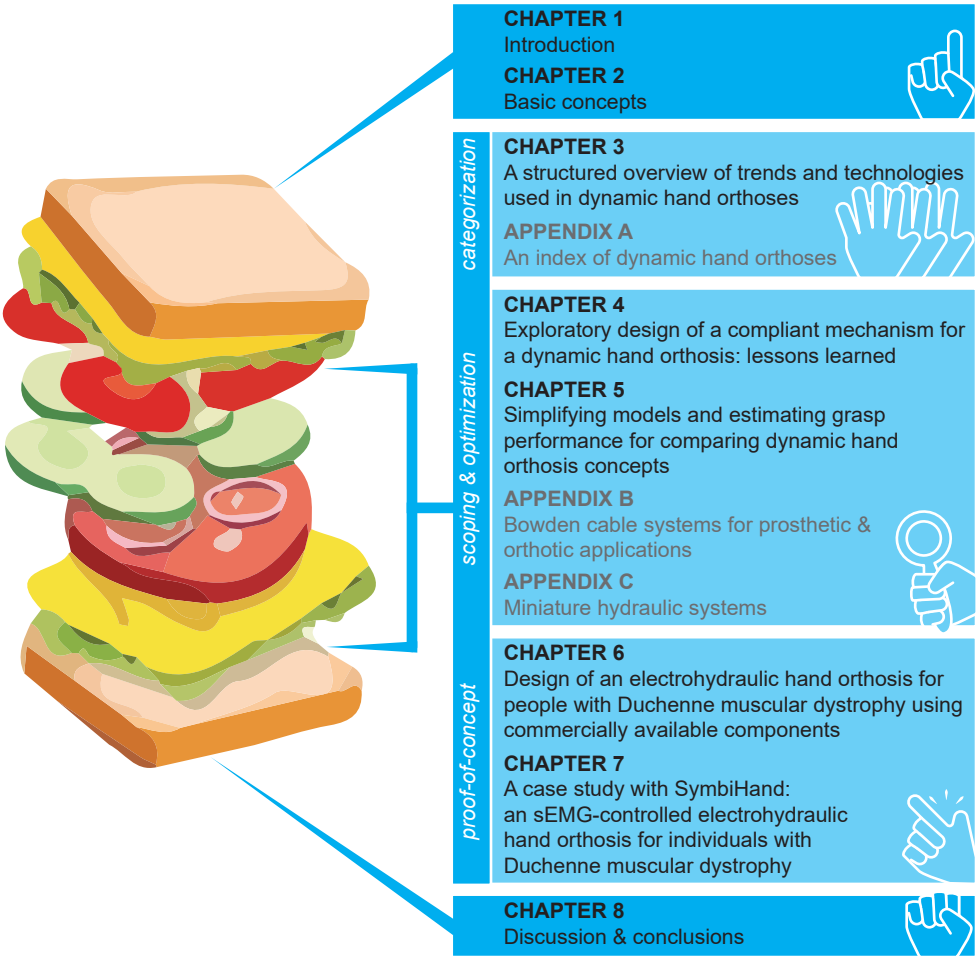

Figure 1.2: Schematic representation of the 'sandwich thesis' outline.

2

BASIC CONCEPTS

Hand function makes up a large portion of physical activity. It involves tasks like grasping and holding objects, operating equipment, feeling the environment and making gestures for non-verbal communication. Loss of hand function negatively affects the ability to do many of these tasks, which has consequences for an individual's independence and quality of life. A dynamic hand orthosis can help to regain hand function. However, the design of such a device is not very straightforward: it needs to take into account the source and symptoms of the disability, it needs to accommodate for the complex movement patterns of the hand, and it should be comfortable to the user. This chapter introduces the basic concepts behind a dynamic hand orthosis; how orthoses have evolved throughout history, how these concepts relate to the anatomy of the hand and how the design of a dynamic hand orthosis can be approached.

2.1. A BRIEF HISTORY OF ORTHOSES

Orthoses have been around for ages and make up a large part of the field of orthopedics. The earliest examples that were found date all the way back to the fifth Egyptian Dynasty (2730–2625 BC), where pieces of wood or bark were wrapped in cloth to maintain bone fractures (Smith, 1908). It was only until the 16th century when orthopedics was established as a science by the famous barber surgeon Ambroise Paré (1510-1590). He is not only considered a founding father in artificial limbs (Thurston, 2007; Plettenburg, 2006), he was also the first to design orthopedic boots for club foot and iron corsets to treat early stages of scoliosis (Williams and Williams, 2004). However, the first time that the term *orthosis* was actually used, is appointed to French physician Nicolas Andry (1658–1742). In his book *L'Orthopedie* (Andry, 1743, p.iv), along with the famous frontispiece (see Figure 2.1), he explains the title and the historical meaning becomes clear:

Original text	**Free translation**
Quant au titre en question, je l'ai formé de deux mots grecs, à savoir, d'Orthos qui veut dire droit, exempt de difformité, qui est selonla rectitude, & de Paidion, qui signifie Enfant. J'ai composé de ces deux mots, celui d'Orthopédie, pour exprimer en un feul terme, le dessein que je me propose, qui est d'enseigner divers moyens de prévenir & de corriger dans les enfans des difformités du corps.	As for the title in question, I have formed it with two Greek words: firstly Orthos, which means straight and free of deformity along the rectitude; and secondly Paidion, which means Child. I composed these two words into Orthopedics, to express in one term my intention which is to teach diverse means to prevent and correct deformities in the body of children.

In more recent history, particularly in the last 60 years, orthoses have undergone a new development where the addition of external sources of power play a large role. The start of these developments coincides with the invention of the McKibben muscle in the late '50s, an inflatable artificial muscle that was designed to approach the behavior of a human muscle. Joseph McKibben was a physicist (who supposedly pushed the button for the first atomic bomb) and collaborated with the orthopedists at the Ranchos Los Amigos Hospital (Landauer, 1958). He was asked to think of a mechanism that would help his own daughter, paralyzed by polio, to be able to move her fingers again (*LIFE*, March 14, 1960). He then invented the McKibben-type artificial muscle and fixed it to a simple flexor-hinge splint, which allowed for a very simplistic and light-weight method to power an orthotic device (see Figure 2.2). Other electric, hydraulic and pneumatic devices were reported to have been used before, but none provided the advantages that the McKibben muscle could provide (Landauer, 1958).

More devices like McKibben's powered hand orthosis emerged and are now more popularly described as *exoskeletons*, a term which is undoubtedly inspired by the shells from crustaceans that go by the same name. This, however, would imply the opposite of an endoskeleton, which would exclusively fulfill a structural purpose. The active movement, articulation and embedded control in many of these devices would actually imply an *exoneuromusculoskeleton*, which admittedly sounds a whole less catchy. Regardless of

Figure 2.1: Frontispiece of L'Orthopedie (Andry, 1743), illustrating the classical principle of orthotics.

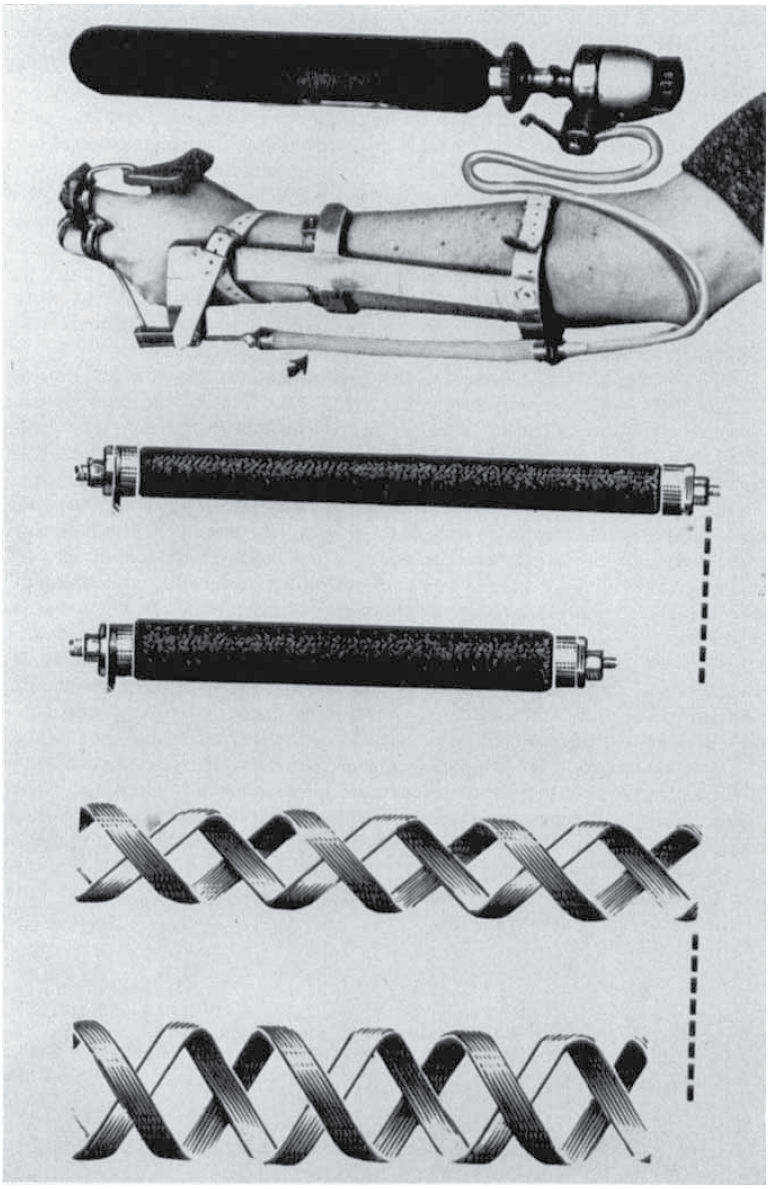

Figure 2.2: First use of the McKibben-type artificial muscle onto a flexor-hinge splint (top), the working principle upon inflation with pressurized gas (middle) and how the orientation of the cross-woven fibers contribute to this working principle (reproduced with permission from Landauer (1958)).

Figure 2.3: Arm module of the Hardiman powered exoskeleton (Croshaw, 1969), representing the role of an orthosis to augment human strength.

the origin of the name, however, exoskeletons are more often associated with power augmentation rather than rehabilitation (Dollar and Herr, 2008; Herr, 2009). This implied difference in terminology becomes apparent when looking for the first exoskeleton instead of the first orthosis. We can then find the earliest examples of exoskeletons in patent sketches from around the turn of the 20^{th} century, describing devices that aim to reduce fatigue during running with passive structures (Yagn, 1890) or even steam-powered mechanisms (Kelley, 1919).

One of the first cases where the term exoskeleton was used to describe a prototype that was actually built as well, can be found in the lab reports from the Hardiman project by General Electric (see Figure 2.3), which date back to the late 1960s (Mosher, 1967; Croshaw, 1969). The reports are interesting in the fact that they recognized the strengths and weaknesses of humans and robots, and tried to design a device that was able to combine the strengths of both. This resulted in the development of an electro-hydraulic exoskeleton, with the primary aim to increase humans' lifting capacity (e.g., to load bombs onto aircrafts during the Cold War). Sadly, the prototype was never used except as an inspiration for a barrel loader in the 1967 film 'The Ambushers'.

Around the same time, the Mihailo Pupin Institute in former Yugoslavia was also developing a device which they now refer to as an exoskeleton—who classified it as an active orthotic system at the time of development (Vukobratovic et al., 1974). With their pneumatically powered *kinematic walker* in 1969 they wanted to help paraplegics with an alternative to the wheelchair. Similar to the Hardiman project, they leveraged the strengths of a robotic system to take over a complex task that required additional strength, but their clinical application makes it one of the first externally powered orthoses after McKibben's hand orthosis. However, it were their advancements in controlling such a device that distinguished them from McKibben's efforts, leading to the origin of the Zero-Moment Point (ZMP) concept (Vukobratovic and Borovac, 2004), an important theory in maintaining balance during bipedal walking.

This increased focus on using control systems has seemingly caused a shift towards using electromagnetic actuators rather than pneumatics (Vukobratovic, 2007). An example is the electric arm orthosis for people with muscular dystrophies developed by the same institute (see figure 2.4), whose architecture is starting to resemble what is now commonly seen in current active orthoses: electromagnetic systems with elaborate control systems that can assist or take over several body functions and structures. In other words, active orthoses can now be seen as mechatronic systems. With this, the design of such a device seems to have shifted from the physician to the engineer.

It is clear that, throughout the historic examples that were described, the used terminology varies with almost every advancement and orthoses have evolved into extremely complex devices. Modern orthoses allow movement, add stiffness and support only where necessary, add external power sources and seem to be focused more on the (neuro-)muscular alterations rather than skeletal. The classical principle illustrated in Andry's frontispiece is therefore outdated, as they can now be used for more than just straightening deformities. Combined with the more recent growth from present literature in active orthoses, powered exoskeletons, rehabilitation robots and human extenders (Heo et al., 2012; Balasubramanian et al., 2010; Basteris et al., 2014; Maciejasz et al., 2014), it becomes harder to classify these devices under a single term. However, the present-day definition for *orthosis* from ISO 8549-1:1989 (ISO/TC 168, 1989a) is actually able accommodate to this development:

> **orthosis; orthotic device:** Externally applied device used to modify the structural and functional characteristics of the neuro-muscular and skeletal systems.

In this thesis, following the example from (Gopura et al., 2015) and in conformity with ISO 8549-1:1989 (ISO/TC 168, 1989a), the term *orthosis* is used to cover the full range of passive and externally powered devices, where a *dynamic orthosis* provides a scope towards devices that facilitate movement. Combined with a focus on assisting the hand, this thesis concentrates on *dynamic hand orthoses*.

2.2. THE EFFECT OF ORTHOSES ON DISABILITY

From the historic examples of orthoses, we can generalize that orthoses are designed to reduce a person's disability. For a more fundamental understanding, however, we need to

Figure 2.4: One of the first active arm orthoses powered by electromagnetic actuators, developed at the Mihailo Pupin Institute, being controlled with a joystick by an individual suffering from a muscular dystrophy (reproduced with permission from Stanic (2018)).

be aware of the different aspects of a disability and how exactly an orthosis can have an effect on this disability.

2.2.1. DEFINING DISABILITY

The International Classification of Functioning, Disability and Health (ICF) can be used as a basis to define disability (World Health Organization, 2011). In this framework, *functioning* describes an individual's body functions, activities and participation in society. In contrast, *disability* describes impairments, activity limitations and participation restrictions (World Health Organization, 2002). A disability negatively affects the interaction between an individual's health condition and the individual's contextual factors. These contextual factors include personal factors (e.g. age, life experiences) and environmental factors (e.g. social environment, policies) (World Health Organization, 2011). This framework nicely illustrates that a disability cannot be solely judged by its biological aspect, but involves complex and dynamic interactions with psychological and social aspects as well.

Imagine the example of Steve, who suffers from sarcopenia (a syndrome related to aging (Cruz-Jentoft et al., 2010)). Following the ICF model (see Figure 2.5), the impairment

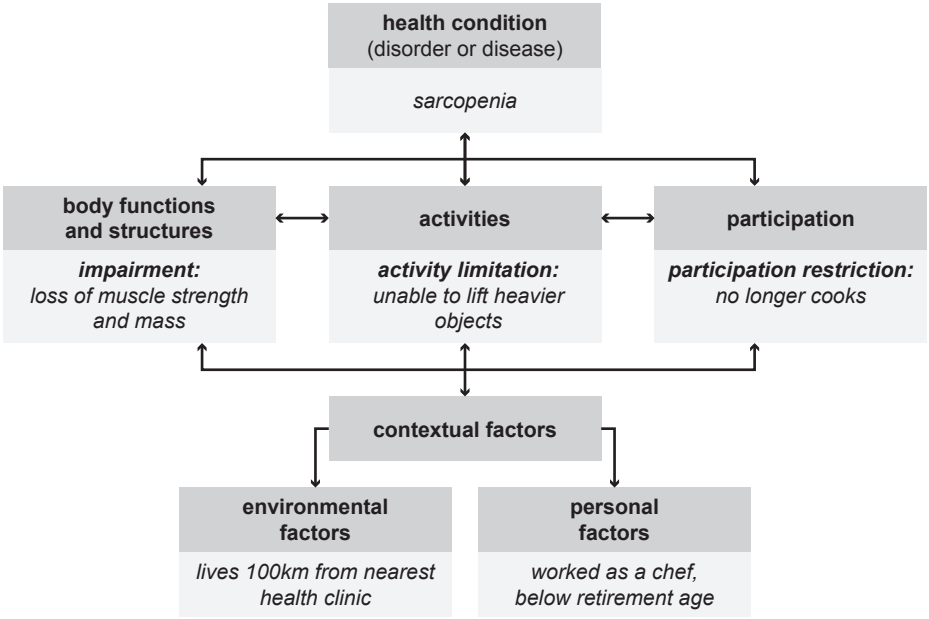

Figure 2.5: Graphical representation of the International Classification of Functioning, Disability and Health (ICF), including the example of Steve who suffers from sarcopenia.

(i.e., body function) is characterized by a loss of muscle strength and mass, the activity limitation is an inability to lift heavier objects and a possible participation restriction is that this individual no longer cooks. This can be seen as a loss of independence, because Steve now needs someone (or something) that prepares food for him. However, by including personal factors, the introduced disability can take another perspective. For example, Steve highly values cooking and used to work as a chef, but he was forced to quit just below the age for retirement. The participation restriction can be extended to the fact that Steve is now unemployed and no longer able to function in his main line of work. On top of that, it is hard for Steve to find help in the form of health care, because the nearest health clinic is about 100km away. Therefore, quality of life can already be improved if there is a solution that allows Steve to cook again. The implementation of an orthosis can be one of those solutions.

2.2.2. IMPLEMENTATION OF AN ORTHOSIS

An orthosis can help an individual in several ways. Following the ISO 13404:2007 standard (ISO/TC 168, 2007), the function of an orthosis may be:

- to manage (i.e., prevent, reduce or hold) a deformity;
- to change (i.e., increase or limit) the range of motion of a joint(s);
- to change the dimensions (i.e., add length or improve shape) of a limb segment(s);
- to manage abnormal neuromuscular function (i.e., compensate for weak muscle activity or control the effect of muscle hyperactivity); or,

- to reduce or redistribute the load on tissue.

This summation illustrates the diversity of functionalities for which an orthosis can be an appropriate intervention. For the example of Steve, an orthosis that compensates for weak muscle activity can help him to perform activities again that relate to cooking, which can help to reduce his restrictions on the participation level. Additionally, there is a chance that the orthosis manages a deformity, because increased muscle activity may reduce the progression of the loss of muscle strength and mass. This, however, does not reduce the impairment on the function level.

In conclusion, an orthosis can help to reduce disability of an individual. Depending on the health condition and contextual factors, an orthosis can have different effects on the function, activity and participation level.

2.3. THE HUMAN HAND

The human hand is an amazingly complex instrument. Merely imagining your daily morning routine already illustrates the diversity of tasks that can be performed: e.g., preparing your breakfast, brushing your teeth, tying your shoelaces, getting your keys, waving goodbye to your cats and opening the door. In order to be able to support these functions with an orthosis, for example by changing the range of motion of joints or managing neuromuscular function, one needs at least basic understanding of the underlying physiology. To make sense of the many bones, joints, muscles, tendons, ligaments and movements, this is divided into degrees of freedom and functional movements.

2.3.1. DEGREES OF FREEDOM

The motion of any mechanism can be described according to the number of degrees of freedom (DOFs), and can therefore also be done for the hand. Strictly speaking, however, every anatomical joint allows some movement in every direction due to the flexible nature of the tissues that hold everything together. In order to prevent the number of DOFs to get out of control, some small movements can be neglected. This lowers the total number of DOFs and simplifies the system, where the level of simplicity becomes the result of making modeling choices (i.e., which DOFs are considered small enough to neglect). In this thesis, for example, movements between the metacarpal joints to arch the palm of the hand are neglected and only the major active joint rotations in the fingers are considered. This results in a total of 23 DOFs due to flexion/extension (FE), abduction/adduction (AA) and radial/ulnar deviation (RUD) movements in the fingers and wrist (see Figure 2.6).

The thumb is considered to have 5 DOFs. From proximal to distal, it has 2 DOFs (FE and AA) in the carpometacarpal (CMC) joint, 2 DOFs (FE and AA) in the metacarpophalangeal (MCP) joint and 1 DOF (FE) in the interphalangeal (IP) joint. Opposition is sometimes considered as an additional DOF, but is mainly the result of combined FE and AA in the CMC joint which automatically inflicts an axial rotation (Li and Tang, 2007). The index, middle, ring and little fingers each have 4 DOFs. From proximal to distal, they each have 2 DOFs (FE and AA) in the MCP joint, 1 DOF (FE) in the proximal interphalangeal (PIP) joint and 1 DOF (FE) in the distal interphalangeal (DIP) joint.

It is almost impossible to define hand functionality without including the wrist. Firstly, the FE and RUD movements come from the carpal bones at the base of the hand and is

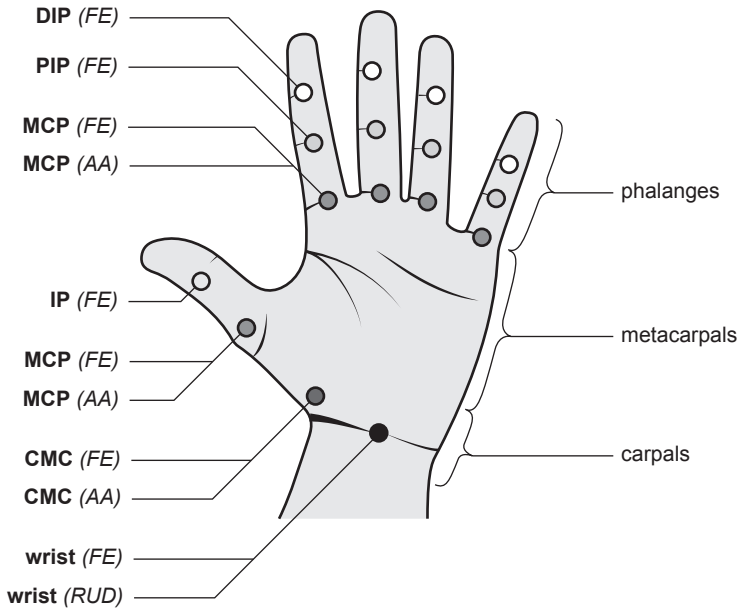

Figure 2.6: Simplified model of the movements of the human hand, indicating carpals, metacarpals and phalanges, along with the anatomical joints (CMC: carpometacarpal, MCP: metacarpalphalangeal, IP: interphalangeal, PIP: proximal interphalangeal, DIP: distal interphalangeal) and their possible movements (FE: flexion/extension, AA: abduction/adduction).

therefore part of the hand's anatomy (Taylor and Schwarz, 1955). Secondly, because the extrinsic finger muscles extend over the wrist, an extension of the wrist can pre-stretch the finger flexor muscles for increased grip strength and improved grasping stability in a dynamic environment (Carlson and Trombly, 1983). Lastly, and perhaps more obvious, the wrist positions the fingers to improve their function during particular tasks, most notably those associated with personal hygiene (Carlson and Trombly, 1983; Ryu et al., 1991). The pronation/supination can also be included as part of the hand function because it also positions the fingers. From an anatomical standpoint, however, this movement originates from the forearm and is therefore not considered to be part of the hand itself.

2.3.2. FUNCTIONAL MOVEMENTS

In between these DOFs, dependencies-—or synergies—exist due to couplings by control or by mechanical connection (Santello et al., 1998; Gustus et al., 2012), also called functional DOF (fDOF) (Li and Tang, 2007). For example, AA of the thumb's CMC and MCP joint are underactuated by the same tendon (Li and Tang, 2007), as well as the FE movement of the PIP and DIP joints in each of the other fingers (Rijpkema and Girard, 1991). Additionally, neural and muscular synergies have been detected as well, where multiple muscles work together as a unit to perform specific movements (Santello et al., 2016). Regardless of the origin of the synergy, it is clear that not every DOF can be (or has

to be) controlled independently and the possible functional movements of the hand can be further simplified. This reduction in dimensionality is not only useful in understanding the human hand, but also for designing (robotic) mechanisms that support or replace the hand (Santello et al., 2016).

By measuring the joint angles of the hand during a set of functional movements, these synergies can express themselves as correlations between these joint angles. This method, i.e. principle component analysis, can break down these functional movements of the hand into smaller building blocks, or principle components (Santello et al., 1998). As an example, this approach has been used in the design of the Pisa/IIT SoftHand. Although this is a robotic hand and not a dynamic hand orthosis, the use of biologically inspired synergies in a mechatronic device is relevant in both cases. The Pisa/IIT Softhand uses differential mechanisms to combine synergies according to the first few principle components, allowing to control 19 DOFs with only a single actuator (Catalano et al., 2014). If every principle component requires a separate differential module, however, these mechanisms can become quite complex. Moreover, if only a subset of functional movements is to be supported, the correlations may change and a new principle component analysis would be necessary for this subset of movements.

A more obvious ways of mapping the hand's functional movements is by looking at the grasping postures. A very simple but intuitive grasping taxonomy comes from Napier (1956), which defines a power grasp as a method to grasp large or heavy objects (e.g., a bottle, an apple), and a precision grasp for smaller or more light-weight objects (e.g., a pen, a cookie). In general, the power grasp is performed with an adducted thumb, providing the opposing force in plane with the palm of the hand. In the precision grasp, this opposing force is provided by the tip of the thumb in an opposed and slightly flexed position (Napier, 1956).

Napier was not the only one to classify grasping patterns and is surrounded by at least 20 more publications with different or supplementary views (Iberall, 1997). For example, Cutkosky (1989) expanded on Napier's taxonomy with more variations by further specifying the shape of the object and crudeness of the task. However, it is the reviewing effort by Iberall (1997) on all these studies that resulted in a clear and comprehensible overview of grasping postures. Similar to Napier (1956), the postures were classified by thumb opposition (combinations are also possible, see Figure 2.7):

- In pad opposition, object is clamped by force closure between the pads of flexed fingers and thumb.
- In palm opposition, object is clamped by both force and form closure between flexed fingers and palm of the hand.
- In side opposition, object is clamped by force closure between the lateral sides of the fingers and usually the pad of the thumb.
- In virtual finger, object is clamped by force closure between any finger of the hand and an external force (e.g., gravity).

Breaking down the functional grasping postures in these classes is useful because, compared to using synergies with a principle component analysis, they can be more easily coupled to particular tasks or activities. Therefore, by knowing which tasks or activities are necessary to support, the designer of a hand orthosis can decide which basic thumb and finger movements are most important. As a result, some DOFs can be locked, limited,

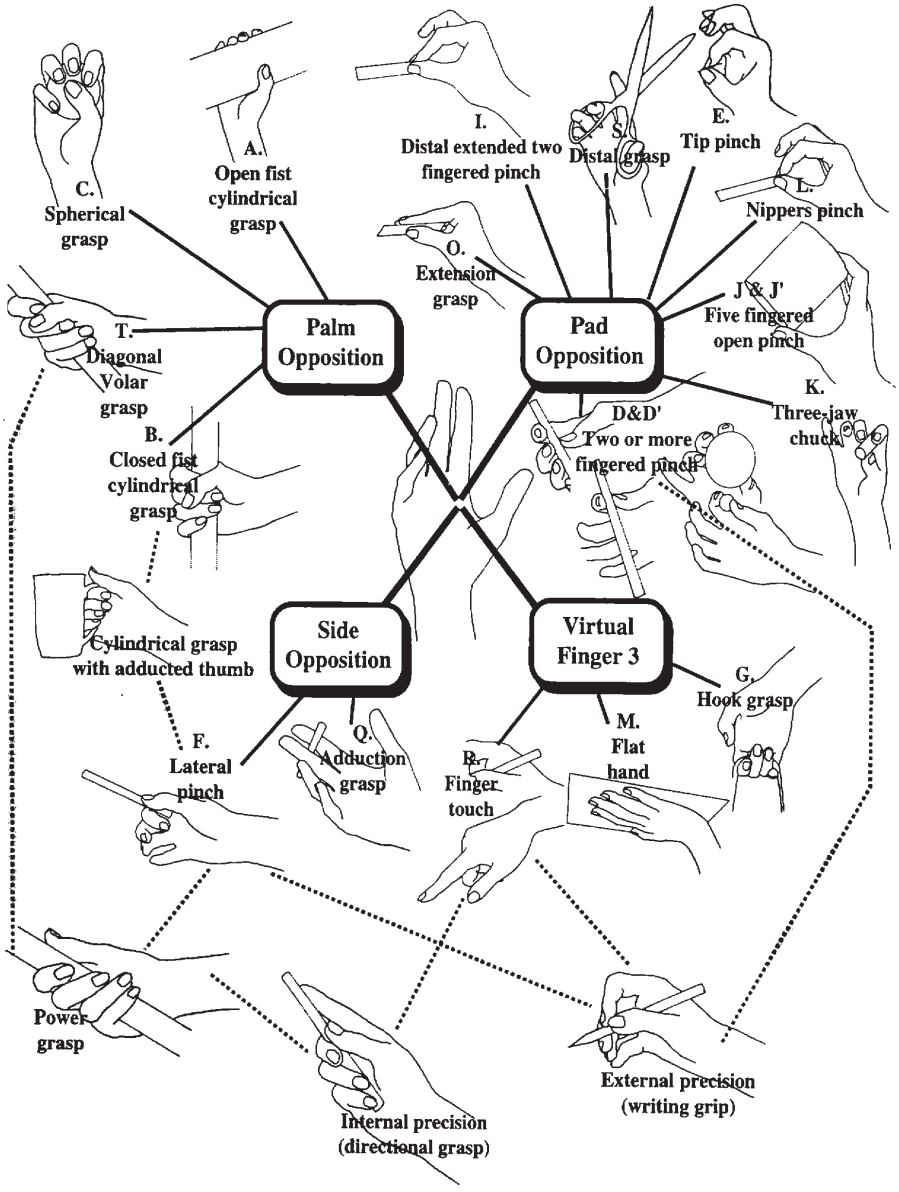

Figure 2.7: Grasping postures classified by thumb opposition (reproduced with permission from Iberall (1997)).

resisted or left unassisted (ISO/TC 168, 2007) to simplify the orthosis' design. It should be noted, however, that the movements described above do not include hand gestures for non-verbal communication (e.g., pointing with index finger, thumbs-up), which require more individual finger movements.

2.4. STROKE AND DUCHENNE MUSCULAR DYSTROPHY

As described in section 2.2, an orthosis can reduce an individual's impairment in many ways and it depends on the nature of the disorder or disease and the desired outcome. To illustrate these differences, two very distinct cases are described below, namely stroke and Duchenne muscular dystrophy (DMD).

2.4.1. STROKE

Stroke is a condition where brain cells are permanently damaged due to a rupture (hemorrhagic stroke) or obstruction (ischemic stroke) in the blood flow. This often results in hemiparesis in the upper limb and negatively affects the ability to perform functional movements (Hatem et al., 2016). In fact, motor deficits in the upper limb is the most common impairment following stroke (Lawrence et al., 2001). With a prevalence of more than 42 million worldwide in 2015 (Vos et al., 2016), which is expected to increase over the years (Truelsen et al., 2006), stroke is also one of the most prevalent health conditions.

Among the most common motor deficits following stroke are weakness or paralysis, which can trigger a train of problems that eventually lead to increased muscle stiffness and spasticity. Multiple forms of physiotherapy can help with rehabilitation from such impairments, like muscle strengthening exercises, passive stretching, assisted training and mirror therapy (Raghavan, 2016). Aside from countering muscle weakness, such methods can also stimulate motor learning through neuroplasticity (i.e., a reorganization of neural connections to re-learn specific movements), a leading theory in modern rehabilitation science (Reinkensmeyer and Boninger, 2012).

A dynamic hand orthosis can help with post-stroke rehabilitation by managing abnormal neuromuscular functions. These devices often include an external power source and control system, hence they are commonly classified under robot-assisted rehabilitation or robot-aided therapy. Multiple systematic reviews have shown mixed results on the effectiveness of these methods, as they are not necessarily better than traditional therapy (Kwakkel et al., 2008; Mehrholz et al., 2008; Timmermans et al., 2009). However, because the most effective treatments include high-intensity and highly repetitive training, a dynamic hand orthosis designed for such purposes can reduce the workload on responsible caregivers, improve monitoring of progress and consequently enhance effect of the treatment (Prange et al., 2006; Timmermans et al., 2009). Especially with the expected increase in stroke prevalence (Truelsen et al., 2006) and aging of society (Vos et al., 2016), this increases the potential for every stroke survivor to get sufficient treatment time. Dynamic hand orthoses can also be used as a diagnostic tool to better understand the underlying mechanisms and to help choose the right treatment (Kamper and Rymer, 2000). With improved understanding, the advantages of robot-assisted rehabilitation can be exploited even further to create treatments that were not possible before.

2.4.2. DUCHENNE MUSCULAR DYSTROPHY (DMD)

DMD is a congenital and progressive muscular disorder linked to the X-chromosome. It is found in approximately 1 of 5000–6000 live births, which makes it the most occurring type of muscular dystrophy in children (Ryder et al., 2017; Janssen et al., 2014). DMD is caused by a mutation in the gene responsible for the dystrophin protein, an important structural building block in the muscles. The absence of dystrophin inflicts a series of processes that eventually lead to death of muscle cells, reduced regenerative capacity of the muscles and replacement by connective tissue, which causes muscle tissue to waste away and eventually results in muscle weakness (Blake et al., 2002). There is currently no cure for DMD, but changes in health care (e.g., increased prescription of corticosteroids and better access to ventilation) has increased life expectancy from 25 to around 40 years old (Ryder et al., 2017). DMD progresses from the larger to the smaller muscle groups, where individuals with DMD quickly lose the ability to walk and become bound to a wheelchair at around 12 years old. This means that they are fully dependent on their upper extremity for the largest part of their life, which makes preservation of this functionality very important (Janssen et al., 2016).

The inability to move due to muscle weakness can result in non-use and static positioning of joints, which can develop into joint contractures. Regular physical therapy exercises can help to prevent the formation of such fixed deformities, along with static orthoses for improved joint positioning (Bushby et al., 2010b). Additionally, management of upper extremity function can be stimulated by maintaining an active life and participating in school- or work-related activities (Janssen et al., 2016).

A dynamic hand orthosis can help retard the progression of DMD by managing abnormal neuromuscular functions. By compensating for the muscle weakness through the addition of an external power supply or passive energy storage, movement of the joints can be encouraged. Similar to the physical therapy exercises and use of static splints, dynamic hand orthoses can possibly retard the formation of contractures and prolong the time period where an active life and participation in social activities can be maintained. The difference with doing exercises is that a dynamic hand orthosis can provide assistance during ADLs, instead of exercising before ADLs. Moreover, although this is currently still an unproven theory, continued use of the muscles can possibly retard the progression of muscle wasting as well.

2.4.3. CASE COMPARISON

Comparing the situations for stroke survivors and people with DMD reveals that similarities and dissimilarities both exist. For example, increased muscle stiffness and contractures are common in both pathologies and can result in an inability to open up the hand. For stroke survivors, however, this is often coupled with hyper-excitability of the stretch reflex (Raghavan, 2016) and can result in a much higher joint stiffness compared to people with DMD.

The function of a dynamic hand orthosis for either stroke or DMD would be fundamentally different, because stroke has a neurological origin and DMD a muscular origin. From the complications as described in the previous subsections, it appears that stroke survivors benefit from rehabilitation of motor function, with the final intention to regain hand function. The progressive nature of DMD, however, prevents rehabilitation to

be a feasible construct and a dynamic hand orthosis' primary function is to assist during ADLs, with the final intention to maintain hand function.

Clearly, different pathologies ask for different functionalities in a dynamic hand orthosis. On top of that, it also not unthinkable for a dynamic hand orthosis to assist stroke survivors with performing ADLs, or to provide regular exercises similar to rehabilitation for people with DMD to reduce joint stiffness. Then there is also the environment in which the orthosis is to be used. Whether it is at home, in the clinic or perhaps in a research setting, the environment has an important role in how a dynamic hand orthosis should look like. The design of a dynamic hand orthosis is therefore dependent on three factors: *pathology* (e.g., stroke, DMD), *application* (e.g., daily assistance, rehabilitation) and *environment* (e.g., home, clinic).

2.5. CONCLUSION

From pieces of bark to electromagnetic devices with control systems, the field of orthoses has seen many changes. Naturally, this is also coupled with a wide variety of terminology and corresponding implications. A typical example is the use of the term *exoskeletons*, which has become a sensational way of describing an ambiguous subset of orthosis applications and designs. In an attempt to cover all varieties of orthoses for the hand that facilitate movement, the term *dynamic hand orthosis* is introduced.

The increase in technical complexity of a dynamic hand orthosis has seemingly caused its design to shift from the physician to the engineer. From the historical developments, the introduction of electric motors and control systems around the '70s appeared to mark this key change. However, the design of a dynamic hand orthosis remains a multidisciplinary field of study. Important constructs include the effect of the device on a person's disability, modeling and classification of hand physiology, and the influences of pathology, application and environment on the design constraints. A structured overview of the available technological components (e.g., sensors, motors, mechanisms) can help a designer to make well-considered design choices according to these constructs.

3

A STRUCTURED OVERVIEW OF TRENDS AND TECHNOLOGIES USED IN DYNAMIC HAND ORTHOSES

Bos, R. A., C. J. W. Haarman, T. Stortelder, K. Nizamis, J. L. Herder, A. H. A. Stienen, and D. H. Plettenburg

published in: *Journal of NeuroEngineering and Rehabilitation*, 13: 62. 2016.
DOI: 10.1186/s12984-016-0168-z

A B S T R A C T

The development of dynamic hand orthoses is a fast-growing field of research and has resulted in many different devices. A large and diverse solution space is formed by the various mechatronic components which are used in these devices. They are the result of making complex design choices within the constraints imposed by the application, the environment and the patient's individual needs. Several review studies exist that cover the details of specific disciplines which play a part in the developmental cycle. However, a general collection of all endeavors around the world and a structured overview of the solution space which integrates these disciplines is missing. In this study, a total of 165 individual dynamic hand orthoses were collected and their mechatronic components were categorized into a framework with a signal, energy and mechanical domain. Its hierarchical structure allows it to reach out towards the different disciplines while connecting them with common properties. Additionally, available arguments behind design choices were collected and related to the trends in the solution space. As a result, a comprehensive overview of the used mechatronic components in dynamic hand orthoses is presented.

3.1. INTRODUCTION

Human hands are complex and versatile instruments. They play an essential role in the interaction between a person and the environment. Many people suffer from hand impairments like spasticity, lack of control or muscle weakness, which may be due to the consequences of stroke, paralysis, injuries or muscular diseases. Such impairments may limit an individual's independence in performing activities of daily living (ADL) and the ability to socially interact (e.g. non-verbal communication). Devices like hand exoskeletons, rehabilitation robots and assistive devices, here collectively termed as dynamic hand orthoses, aim to overcome these limitations. Their development is a fast-growing field of research and has already resulted in a large variety of devices (Heo et al., 2012; Balasubramanian et al., 2010; Basteris et al., 2014; Maciejasz et al., 2014).

Each individual has different demands for a dynamic hand orthoses. Some patients benefit from rehabilitation therapy (e.g. stroke patients (Kwakkel et al., 2008)) while others would more likely benefit from daily assistance (e.g. Duchenne Muscular Dystrophy (Janssen et al., 2014)). The resulting diversity between the different devices can be illustrated by the elaborate overviews on robotic devices (Maciejasz et al., 2014), training modalities (Basteris et al., 2014) and intention detection systems (Lobo-Prat et al., 2014b) they use. Clearly, there are many mechatronic components to choose from and are often the result of making particular design choices within the imposed design constraints. However, not everybody has the resources (i.e. time, accessibility) to investigate all possible design choices within these constraints. Moreover, not always are design choices reported in literature and are therefore hard to retrieve. The full potential of learning from each other's endeavors is therefore not yet fully exploited, leaving several questions in this field of research unanswered. For example, there is the discussion whether pneumatic or electric actuation is better for some applications.

The goal of this study is to collect a high quantity of dynamic hand orthoses and extract the mechatronic components which are used. Their collective properties are analyzed by using a framework which uses a generic categorization applicable for any mechatronic system: a signal domain (e.g. controllers, sensors), energy domain (e.g. energy sources, actuators) and mechanical domain (e.g. cables, linkages). Additionally, feasible technologies from other, but similar, disciplines are included (e.g. prosthetics, haptics). Trends are then visualized using bar charts and compared to available arguments behind design choices. This not only includes arguments from often-cited success-stories, but also from small-scale projects. Referring to the case of using pneumatic or electric actuation, this approach can answer how often each method is used and what arguments are reported, which may help in scoping further research and making a well-considered choice.

This paper is structured in different sections. The Scope section describes the boundaries and limitations of this study and Framework introduces the basis of the framework structure that is proposed. The Results section describes the quantitative results which illustrate the trends. How this relates to the functionality of the components, is discussed and summarized in the Discussions and Conclusions section, respectively.

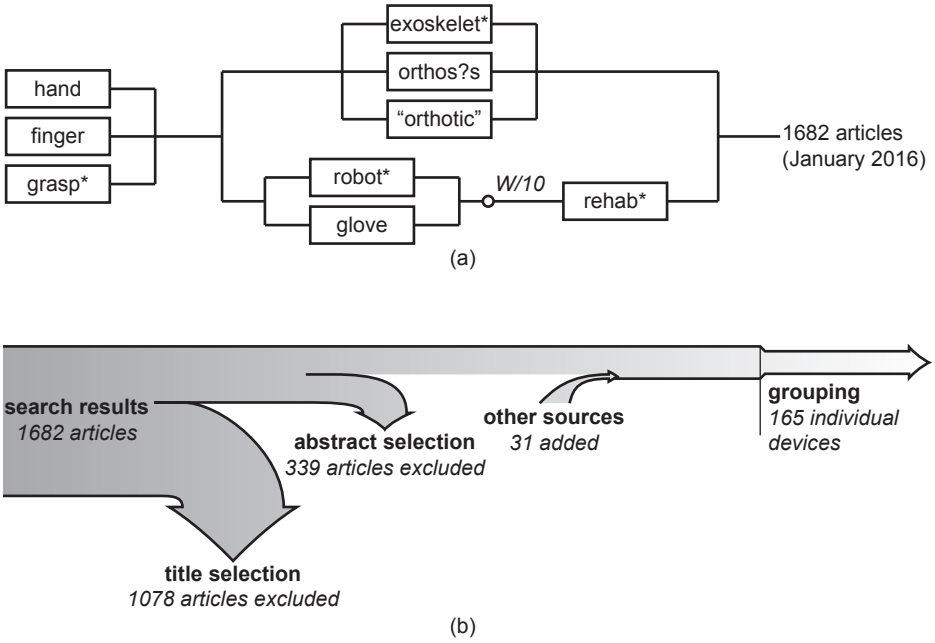

Figure 3.1: Search query and selection procedure. (a) A visualization of the search query is shown which resulted in 1682 articles. Here, connections in series represent 'AND' and proximity ('W/10') operators, those in parallel represent 'OR' operators. (b) The results underwent title/abstract selection based on inclusion criteria and more sources were added through references/citations. Finally, articles were grouped in order extract the individual devices.

3.2. SCOPE

3.2.1. SEARCH STRATEGY

The used terminology often varies between studies due to different backgrounds or field of application. For example, the term 'exoskeleton' has been presented as a type of rehabilitation robot (Maciejasz et al., 2014) or, conversely, as a device that is not used for limb pathologies but to augment the strength of able-bodied people (Herr, 2009). In this study, following the example from (Gopura et al., 2015) and in conformity with ISO 8549-1:1989 (ISO/TC 168, 1989a), the term 'orthosis' is used to cover the full range of applications. The added term 'dynamic' then provides a scope towards devices that facilitate movement.

In order to collect a large quantity of dynamic hand orthoses, sources of literature were searched in Scopus, where a set of keywords was used to search in titles and abstracts. A visual representation of the search query and selection procedure can be seen in Fig. 3.1.

Boolean operators and wildcard symbols were used to include alternative spellings and synonyms. The used search query was (hand OR finger OR grasp*) AND ((rehab* W/10 robot* OR glove) OR (exoskelet* OR orthos?s OR "orthotic")). The inclusion criteria were defined as regular articles in the English language which presented a dynamic orthosis,

supporting at least a finger joint. Using standardized terminology from ISO 8549-3:1989 (ISO/TC 168, 1989b), this includes the finger orthosis (FO), hand orthosis (HdO) and wrist-hand-finger orthosis (WHFO). The wrist-hand orthosis (WHO) was not included, as it stems from the deprecated term wrist orthosis (WO) (ISO/TC 168, 1989b) and therefore does not necessarily support a finger joint. Whenever a combined arm and hand support system was presented, e.g. a shoulder-elbow-wrist-hand orthosis (SEWHO), only the hand and wrist module was included. Based on the inclusion criteria, the search results underwent a title and abstract selection. Additional sources were added from relevant citations and references, as well as other possibly linked publications from the same author(s)/institution(s). Ultimately, this resulted in a total of 296 articles, describing 165 unique devices. Other supplementary sources of information used in this study include websites/brochures for commercial devices, key review studies, standards and articles describing fundamentals on specific topics.

Year of publication was considered to cover the temporal aspect of trends and technology. Devices were placed into groups of before 2006, 2006 to 2010 and 2011 to 2015, where a device's year was defined by the most recent publication in which change to the design is reported.

3.2.2. APPLICATIONS

As a preliminary classification, the dynamic hand orthoses were split up into different applications. These can be both medical and non-medical. Medical applications focus on enhancing or recovering hand function for a wide range of patients with disabilities in the hand. Non-medical applications, on the other hand, focus on haptic interfaces or providing additional strength for more demanding tasks. In many cases, a device's application was explicitly stated in available literature, whereas in other cases it needed to be derived from the imposed design constraints. In the latter case, the most restrictive constraints were used as distinguishing features (e.g. strict constraints on portability can indicate home use). The different applications which were used are described below.

A research tool is often used for making accurate measurements, investigating the fundamental working principle and properties of the hand (Fiorilla et al., 2011). Additionally, they can be used to simulate different treatments and analyze the ideal strategies for other applications (Jones et al., 2014). Emphasis is mostly put on accuracy and reliability, rather than size and ease of use.

A clinical tool can be used for diagnostic purposes, but are mostly used for robot-assisted rehabilitation at the clinic with reduced active workload for the professional caregiver (Prange et al., 2006; Kwakkel et al., 2008; Mehrholz et al., 2008; Timmermans et al., 2009).

A home rehabilitation tool can be similar to a clinical tool, but does not require personal supervision and poses more strict design constraints regarding to its size, portability and ease of use. Examples are systems that use continuous passive motion (CPM) and/or virtual reality (VR) environments, in which fun and gaming are critical aspects for increasing patient motivation (Timmermans et al., 2009; Reinkensmeyer and Boninger, 2012). In most cases, progress is remotely or occasionally monitored by a clinician, allowing for personalized rehabilitation programs and the ease of staying at home. This is an increasingly popular field in rehabilitation devices, as it ideally reduces time in the clinic and maximizes hours of physical therapy (Kwakkel et al., 2008).

A daily assistive tool is intended to assist during ADL. These types of devices are meant to be used for several hours a day without supervision from a caregiver. They are more invasive to a person's daily routine and, similar to prosthetics (Plettenburg, 2006), the comfort, cosmesis and control presumably become key factors. They differ from home rehabilitation tools as they aim to assist in task execution, rather than to perform physical therapy. Sometimes physical therapy can be offered through assistance (Polygerinos et al., 2015c), in which case the daily assistance imposes the most restrictive design constraints.

A haptic device is originally a non-medical device and is used as a master hand. They interact with a VR environment or perform teleoperation while providing the user with haptic feedback. Due to similar design constraints, haptic devices become comparable with medical applications and are sometimes reported to be able to perform both (e.g. (Mali and Munih, 2006; Festo AG & Co. KG, 2012)).

Lastly, Extra-Vehicular Activity (EVA) gloves for astronauts are included as a non-medical application. Their intended function is to compensate the high stiffness of an astronaut's gloves during activities that require a space-suit. Similar to haptic devices, these devices are included due to comparable design constraints (e.g. (Matheson and Brooker, 2011; Matheson and Brooker, 2012)).

3.3. FRAMEWORK

3.3.1. STRUCTURE

In order to collectively analyze a large quantity of dynamic hand orthoses, a framework was constructed which uses the concept of tree diagrams. Firstly, the basic components of a dynamic hand orthosis were identified. Their relations are illustrated in Fig. 3.2, along with the interactions with the human and environment. Also shown in this figure, is a division of these components into three different domains:

- **signal** domain (controller, command signal, user feedback): determines the training modalities, how the human can control the device and how the human is informed about the device's status;

- **energy** domain (energy storage, actuation): determines the source of energy and the conversion into mechanical work that is applied through the system;

- **mechanical** domain (transmission, mechanism): determines how mechanical work is transported and how the different joints are supported.

These domains were chosen such that they are all-inclusive and describe a generalized mechatronic system that interacts with a human. Starting from these general domains, tree diagrams were defined which describe the mechatronic components that make up the solution space. See Fig. 3.3 for a schematic. At each branching point, the level of detail increases. This method was chosen as it visualizes possible design choices at several levels of detail and categorizes them among three separable domains.

3.3.2. CHARACTERISTICS & LIMITATIONS

The proposed framework was used as a subjective tool from which objective observations could be made. This is because there are multiple ways of defining the branching points, as

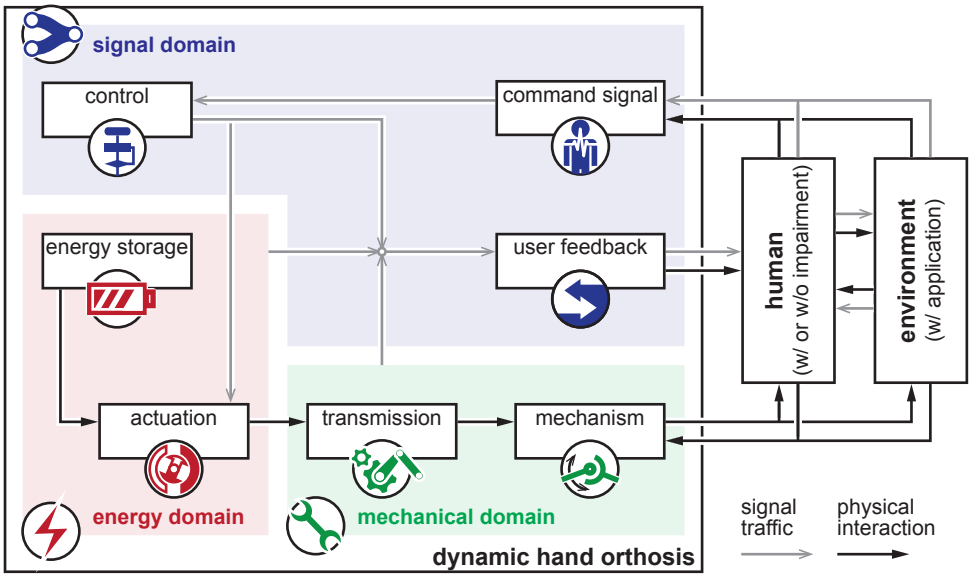

Figure 3.2: Basic interactions for a dynamic hand orthosis. The device consists of several components which can be categorized into the signal, energy and mechanical domain. Gray arrows represent signal traffic, which can be made of visual or auditory stimuli, as well as electrical currents used for artificial control or the nervous system. Black arrows indicate physical interactions in the form of forces and motions. The human interacts with the device through its mechanism, but additional interactions can be provided through the command signal or user feedback.

long as the divisions are as all-inclusive as possible to accommodate all possible solutions. Moreover, it was constructed in order to discuss components and trends as a whole, rather than scoping down into full detail which is already covered in other useful reviews and classifications (Basteris et al., 2014; Lobo-Prat et al., 2014b; Sigrist et al., 2013; Zupan et al., 2002; Poole and Booker, 2011). Existing relevant methods and terminology from these studies were used as much as possible, such that their definitions are covered in their respective sources.

The process of categorization involved investigating the available literature for each device and checking which ends of the tree branches were used. By counting all checked occurrences, the trends for each tree branch could be seen in terms of numbers grouped by year ranges. It is important to note that these numbers indicate a rate of popularity and does not always correlate to functionality, which is treated in the Discussion section. High numbers could arise because something is successful, easily accessible or common practice. Low numbers, on the other hand, could indicate that the respective solution is still experimental, not easily accessible, not well-known or it simply does not work for a given application.

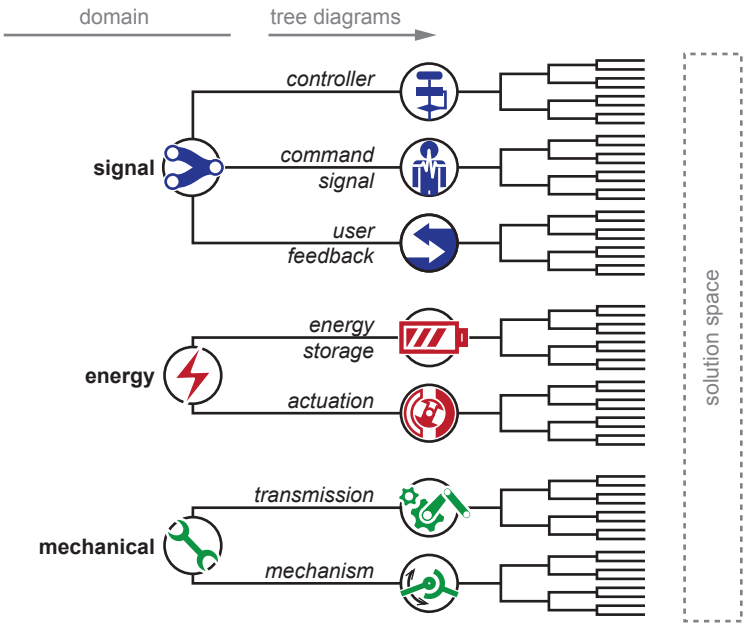

Figure 3.3: Conceptual framework. Several tree diagrams are categorized into the signal, energy and mechanical domain. Towards the right side, branches lead to the solution space in increasing level of detail.

A visualization of the completed framework can be seen in Figure 3.4–3.6 as part of the Results section. Embedded in this framework is a set of terms, which are discussed below per domain.

SIGNAL

The first tree diagram within this domain encompasses the training modalities from (Basteris et al., 2014) employed by the controller, subdivided according to who has authority over the device's movement (Abbink et al., 2012). The passive modality appears three times due to this additional subdivision. Automated passive training (machine authority) most resembles the traditional passive training modality. From a patient's perspective, self-triggered passive training (shared authority) can be considered to invoke different cognitive processes and—depending on the trigger—approaches the situation of an active-assistive modality. From the device's perspective, teleoperated passive training (human authority) implies different lower level control strategies. A second tree diagram covers the command signal required to activate the device, similar to (Lobo-Prat et al., 2014b). The third tree diagram describes the modes of feedback which are available to the user, using principles from motor learning (Sigrist et al., 2013). Here, standard physiological feedback is assumed and changes due the orthosis by augmentation or attenuation were considered.

ENERGY

Within the energy domain, the tree diagrams incorporate types of energy storage and actuation. The diagrams have a similar structure and are subdivided according to feasible types of energy and stimulus from (Zupan et al., 2002) and (Poole and Booker, 2011). Methods of energy storage were scoped towards portable solutions. Nuclear, wind and solar energy were considered infeasible, as well as using thermal energy for energy storage.

MECHANICAL

For an all-inclusive incorporation of components in the mechanical domain, one can refer to Reuleaux's classification of kinematic pairs from 1876, largely available as a digital library from the Cornell University (Cornell University, n.d.). Instead, to make the framework more compact, a more crude categorization is proposed in terms of principles encountered in dynamic hand orthoses. Hence, the first tree diagram includes transmission components which are used to transfer mechanical energy, whereas the second tree diagram describes the mechanism by its shape (i.e. structure), how the anatomical joints are supported (i.e. joint articulation) and which couplings are added to simplify the mechanism (i.e. underactuation and constraints). More specifically for joint articulation, the axis of rotation is monocentric or polycentric according to ISO 13404:2007 (ISO/TC 168, 2007). Jointless and external methods of articulation were added to also encompass glove and end-effector types of devices, respectively.

3.4. RESULTS

A total of 165 different dynamic hand orthoses were found, of which 109 cases presented changes most recently published between 2011 and 2015. A list of all devices is divided according to application and is shown in Table A.1–A.6. These tables contain relevant references and additional descriptive information per device.

The majority of devices were home rehabilitation tools (56), followed by daily assistive tools (46), clinical tools (34) and research tools (9). Additionally, 16 haptic devices and 4 EVA glove mechanisms were found.

The resulting framework is split up into three figures, which are shown in Figure 3.4–3.6. The number of occurrences are added at the ends of the branches and grouped by year ranges.

3.5. DISCUSSION

3.5.1. GENERAL

Results show that the development of dynamic hand orthoses has accelerated, as more than half of the found devices has undergone development in the last five years. Moreover, the amount of home rehabilitation and daily assistive tools indicate that the majority focuses on the development of devices that are used in a domestic setting, concentrating on being able to perform physical therapy at home or to help with ADL. Such observations can be linked to the trend where patient care is brought to their homes and workload on caregivers reduced (Takahashi et al., 2005; Lambercy et al., 2007a; Ates et al., 2014a).

The list of devices as presented in the tables, reveals several trends not covered in the framework. Only in rare cases, pathologies like tetraplegia, tendon injuries, arthritis or muscular weaknesses are specifically addressed in found literature. Consequently,

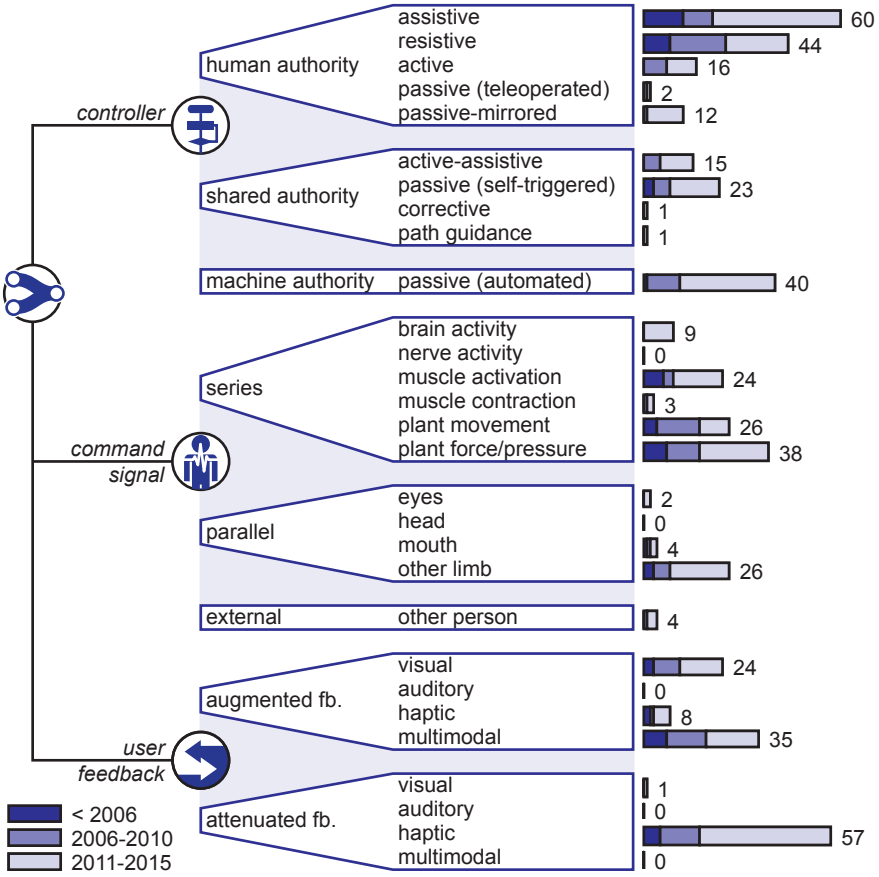

Figure 3.4: Signal domain. Tree diagrams within the signal domain and their number of occurrences in found devices, grouped by year ranges.

these less targeted patient groups may fall short in specialized devices compared to more prevalent groups like stroke survivors. The tables also show that the wrist is often supported, albeit locked or assisted. In some cases, it is because the size of the mechanism or actuator module simply extends over the wrist. In other cases, however, the wrist is considered to be a crucial element in supporting overall hand function. Especially in the case of synergies or muscular weakness, supporting the combination of wrist and grasping function can be essential.

The presented framework illustrates the large span and variety of the solution space. The emerged collection of solutions can help future developers to form morphological overviews, to contemplate on the many possible combinations and to make concept choices. The unbalanced distribution and presence of outliers (i.e. very high or low number of occasions) indicate that some solutions are clearly more popular than others. A few are also never used (i.e. zero occurrences), such solutions were found by means of the

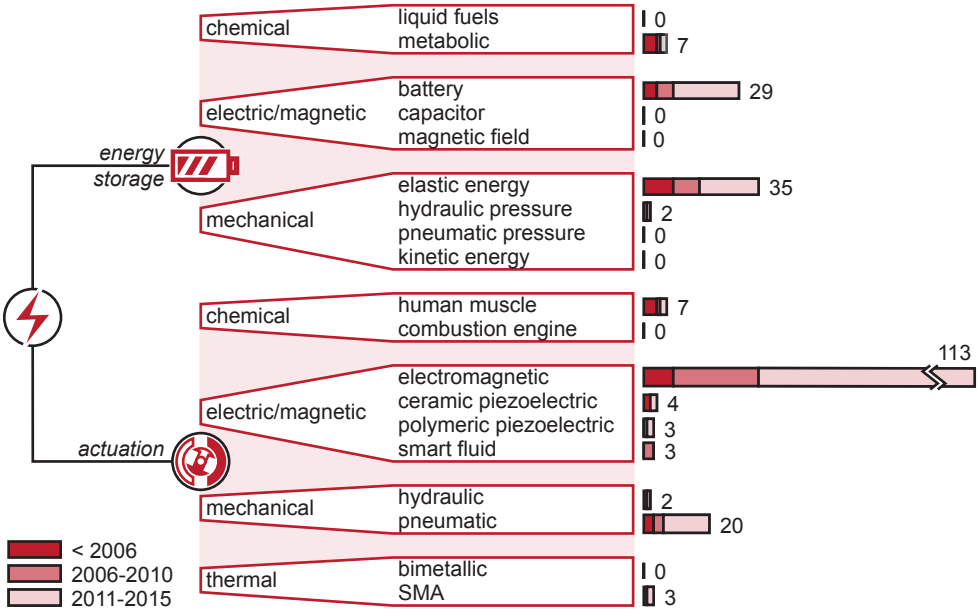

Figure 3.5: Energy domain. Tree diagrams within the energy domain and their number of occurrences in found devices, grouped by year ranges.

framework or by inspiration from other fields of research (e.g. cineplasty from prosthetics, (Sauerbruch, 1916; Weir et al., 2001)). It should be clear, however, that these numbers do not necessarily correlate to the functionality of the component. The reasons behind these differences remain speculations, but they can be due to performance, accessibility, popularity or because a solution is still experimental. Further detailed observations on the functionalities are described below per domain.

3.5.2. SIGNAL

CONTROLLER

Similar to the detailed review on training modalities (Basteris et al., 2014), the passive-mirrored, corrective and path guidance modalities are used the least. They are also the least similar to the type of therapy a physical therapist can provide, and their low use implies that these methods are still in experimental phase. Little can be said about their efficacy, as the exact working principles behind a successful rehabilitation program are not yet fully known (Reinkensmeyer and Boninger, 2012). Nonetheless, their development helps in understanding these principles and exploring the full potential of involving robotic technology.

In general, the training modalities which are mostly used in dynamic hand orthoses, have the human in full authority over the movement. Due to the large amount of daily assistive tools, home rehabilitation tools and the inclusion of haptic devices, the assistive, resistive and passive training modalities show the highest frequencies and skew

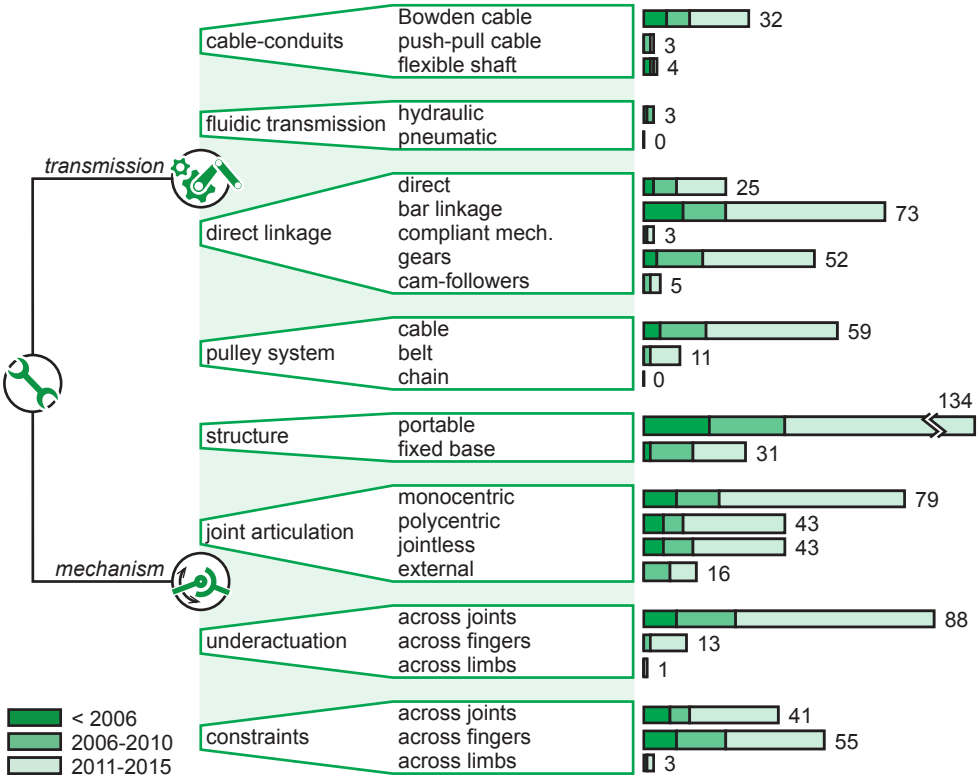

Figure 3.6: Mechanical domain. Tree diagrams within the mechanical domain and their number of occurrences in found devices, grouped by year ranges.

the distribution compared to a previous review on training modalities (Basteris et al., 2014). Especially for daily assistive tools, emphasis is more often put on regaining hand function rather than recovery of the physiological abilities. In these cases, assistive and self-triggered passive modalities are more popular.

COMMAND SIGNAL

Detecting the user's intention to serve as a command signal for the device is one of the larger challenges, because the control of the device is expected to be both intuitive and robust (Ison and Artemiadis, 2014). From the inspected dynamic hand orthoses, most state that measuring the command signal in series with the intended movement is most intuitive (Matheson and Brooker, 2012; Pedrocchi et al., 2013). This is also reflected in the results, as 100 cases use methods in series against 32 cases in parallel. The use of interaction forces and motions from the human plant is the most popular method of using a command signal in series. Here, issues due to sweat, sensor placement and signal quality are less interfering as compared to alternatives. Electromyography (EMG) as a measure of muscle activation is also often used and widely accepted in externally powered upper limb

prosthetics, but more challenges are encountered in electrode placement and separation of signals (Wege and Zimmermann, 2007; Takagi et al., 2009; Kadowaki et al., 2011; Ochoa et al., 2011; Sasaki et al., 2014). Nonetheless, recent studies have shown that both methods (plant forces/motions and EMG) are feasible as a control interface (Corbett et al., 2011; Lobo-Prat et al., 2014a).

Parallel methods are considered less complex, useful for self-controlled mirror therapy (Ueki et al., 2012; Bae et al., 2012), or sometimes inevitable due to the absence of physiological signals directly relating to the intended motion (Otsuka and Sankai, 2010; Pedrocchi et al., 2013). However, these methods can also take away useful functionalities (e.g. bimanual tasks, muscle use) and providing intuitive control is important to achieve user acceptance, stressing the advantages of using command signals in series whenever this fits within the design constraints.

Other methods that were encountered appear less feasible, less successful or experimental. For example, peripheral nerve interfaces (PNI) are not encountered as they can be considered as too invasive; measuring brain activity through electroencephalography (EEG) has an increased risk of false positives and negatives (even with a binary system (King et al., 2014)); force myography (FMG) remains in experimental phase (Lobo-Prat et al., 2014b); and, mechanomyography (MMG) is subject to environmental sounds and limb-movement artifacts (Lobo-Prat et al., 2014b).

USER FEEDBACK

A large portion of the investigated devices (67 out of 165) use augmented user feedback. Especially multimodal feedback is a popular method of providing the user with additional cues. Here, VR environments are often used as a platform to provide audiovisual cues (e.g. (Cruz and Kamper, 2010)), audiovisuohaptic cues (e.g. (Loureiro and Harwin, 2007)) or haptic rendering (e.g. (Sarakoglou et al., 2004)). Amongst others, this can enhance a sense of reality or provide information on performance. Augmenting unimodal feedback (i.e. visual, auditory or haptic) can also be used in various manners. For example, the force exerted by the device can be visualized (Benjuya and Kenney, 1990), music can facilitate motor output (Wolbrecht et al., 2011) and stimulation of the muscle spindles through vibrations can give an enhanced sensation of motion to further enhance rehabilitation success (Cordo et al., 2013; Backus et al., 2014).

From a different perspective, augmented feedback can be used to compensate for an attenuation of haptic feedback (Watanabe et al., 2007; Yamada et al., 2004). A spatial separation between the palmar surface and the environment can affect force perception (Jones and Piateski, 2006), hence facilitating tactile sensation is considered to be of great importance in dynamic hand orthoses (Heo and Kim, 2014b).

The design of augmented feedback signals, however, should be considered carefully. It does not always work effectively (Watanabe et al., 2007) and may even prove to be counterproductive (Rosati et al., 2013). Determining the ideal form of augmented feedback signals is challenging, hard to verify and in many cases related to task complexity (Sigrist et al., 2013). Nonetheless, proper designs have shown potential in robot-aided rehabilitation (Rosati et al., 2009).

3.5.3. ENERGY

ENERGY STORAGE

The usage of components for energy storage is rarely reported, which is reflected by the low number of cases where this could be determined (73 out of 165). Of these cases, the method of energy storage is usually a consequence of choices in actuation, which is why electric batteries are often used because of the high use of electric/magnetic actuators. It should be noted, however, that tapping energy from a centralized system (e.g. mains electricity or compressed air systems) was not considered. It's usage is in many cases hard to verify from available literature and its effects on portability are covered in the mechanical domain.

The most-often used form of energy storage is with elastic energy, of which a helical spring is the most straightforward example. They are often added to realize antagonistic movement when the primary actuation or transmission method is not able to do so (Tjahyono et al., 2013). Other usages include applications where unidirectional and passive forces are sufficient to overcome an impairment, which is the case when compensating hyperflexion (Brokaw et al., 2011). A special case of utilizing elastic energy lies in compliant structures. Aside from introducing mechanical potential energy, they can function like a mechanism and provide for an articulating and load-bearing structure. Compliant mechanisms are both efficient and inherently flexible (Arata et al., 2013), but also introduce complications in defining rotation centers and there is a careful balance between stiffness and elasticity (Matheson and Brooker, 2012).

ACTUATION

The most prominent result from the trends on actuation components is the large amount (113 out of 165) of devices that use a form of electromagnetic actuation. DC motors have the upper hand within this group, but reasonings behind this choice are hard to retrieve. Reported arguments include the increased possibilities for both position and torque control (Schabowsky et al., 2010), high mechanical bandwidth (Stergiopoulos et al., 2003) and general performance in the torque-velocity space (Jones et al., 2014). Such properties appear most useful in applications where variability in control strategies is sought-after or when high-frequent perturbations or interactions need to be applied. For applications that focus more on general assistance, the lower torque-to-speed ratios of DC motors need to be reduced to coincide with the higher ratio demands for human movement. As a result, gearheads are added to reduce the high speeds, adding backlash and reducing inherent backdrivability of the device (Stergiopoulos et al., 2003). An interesting development here lies in the twisted string actuation system, which reaches high reduction ratios by twisting strands on one end and creating linear motion on the other end (Würtz et al., 2010; Palli et al., 2013). Alternatively, ceramic piezoelectricity as used in ultrasonic motors can also provide for a more suitable torque-to-speed ratio. They are silent, have high power-to-weight ratio and are able to facilitate free motion (Choi and Choi, 2000). However, they also require high voltages (Ryu et al., 2008) and show hysteresis (Choi and Choi, 2000).

An often mentioned substitute for electromagnetic actuation, is the use of pneumatic actuation. They are intrinsically compliant, lightweight, act similar to natural muscles and high power-to-weight ratios are reported (Bouzit et al., 2002; Xing et al., 2008; Sun et al., 2009; Tadano et al., 2010; Matheson and Brooker, 2012; Surendra et al., 2012; Tjahyono

et al., 2013; Heo and Kim, 2014b). Still, no commercial pneumatically powered prosthesis or orthosis exists to date to our knowledge. The main reported drawbacks are difficulties in control, expensive components and low bandwidth (Ryu et al., 2008; Xing et al., 2008; Wu et al., 2010). The stated arguments, however, impress as ambiguous due to vague definitions and lack of comparison with design requirements. For example, definitions for power-to-weight ratios are often unclear (Plettenburg, 2005) and a distinction can be made between high- and low-force bandwidth (Stienen et al., 2010). Concerning the latter, human force control operates at around 7 Hz (Tan et al., 1994) and rehabilitation does not necessarily require high bandwidths (Maciejasz et al., 2014), displaying values that do appear within range of pneumatic actuators.

Other methods of actuation appear to be more experimental or impractical. The natural muscle can be used as an actuator and is the crux in body-powered prosthetics. Although applicable for local impairments at the hand, this becomes less practical in orthotics when the muscle itself requires support, as this would add the need for yet another force amplifier. Active polymers appear more promising, being thin, lightweight, compliant and able to perform both sensing and actuation. However, in (Biddiss and Chau, 2008), it was stated that fundamental enhancements would be required for feasible use in upper limb prosthetics. Similar to shape memory alloys (Makaran et al., 1993; Tang et al., 2013a; Zheng et al., 2013), forces are generally low and take time to build up (i.e. low bandwidths), which results in the need for large stacked configurations (Aw and McDaid, 2014; Lee et al., 2014a).

3.5.4. MECHANICAL

TRANSMISSION

No existing studies were found that presented a form of categorization on transmission components usable for dynamic hand orthoses. Consequently, the results and interpretation are based on (and limited by) a categorization from the authors' perspective. Some approaches can be considered as a direct consequence from design choices in the energy domain. For example, gears are most often used to alter DC motor speeds and compliant mechanisms integrate both energy storage and transmission. Other approaches are more a result of choice in mechanism, where n-bar linkages are well-known methods of facilitating path trajectories. Nonetheless, additional notable approaches can be reviewed and coupled with reported argumentations.

The most arguments are reported for pulley-cable and Bowden cable systems. Pulley-cable systems are spatially constrained and require a continuous control of cable tension to maintain traction on the pulleys (In and Cho, 2012; Iqbal et al., 2014; Jones et al., 2014). Bowden cable systems, on the other hand, are a type of cable-conduit and are essentially flexible, but introduce variable and high friction forces dependent on curvature (Wege and Hommel, 2005; Lelieveld et al., 2006; Masia et al., 2007; Fu et al., 2008; Li et al., 2011). Nonetheless, both cable systems most resemble the tendon mechanism in the natural hand (Baker et al., 2011; In et al., 2011; Nilsson et al., 2012; Tjahyono et al., 2013; Weiss et al., 2013; Cempini et al., 2014a; Lee et al., 2014b) and are often an effective method of proximally placing the actuators to reduce the inertia of moving parts (Chiri et al., 2012b; In and Cho, 2012; Delph II et al., 2013; Cempini et al., 2014a; Jones et al., 2014).

Fluidic transmissions are generally more efficient for larger channel diameters, which could explain the low use in dynamic hand orthoses (3 out of 165). Despite this, hydraulic transmissions remain promising at similar scales (Whitney et al., 2014) and are able to provide a more efficient alternative compared to a similar cable mechanism (Smit et al., 2013). In comparison with hydraulics, a pneumatic transmission can offer faster responses due to the use of low-viscosity fluids (Ryu et al., 2008; Whitney et al., 2014), but is not encountered in the included dynamic hand orthoses.

MECHANISM

The alignment of anatomical and mechanical joints is the essence of many mechanical design papers on hand orthoses, which is especially the case for exoskeleton-based devices (Maciejasz et al., 2014). Misalignments may cause numerous sources of discomfort to the user, resulting in possible frustration by the user, rejection of the device and eventual hindrance in the rehabilitation program (Meyer et al., 1979). Even tissue damage can occur, where pressure sores, joint dislocations or cartilage damage are among the possibilities depending on the user (Meyer et al., 1979; Schiele and van der Helm, 2006). The main design challenges lie in limited available space, differences in hand sizes and coping with the compliance of skin tissue. Additionally, the rotation axis of a finger joint is not constant (Gustus et al., 2012), i.e. polycentric. Despite the latter, however, almost half of the dynamic hand orthoses use monocentric rotation (79 out of 165). This includes the more straightforward hinge joints (Tjahyono et al., 2013), but also those that use a virtual center of rotation with fixed rotation axis (e.g. concentric rotation in (Ho et al., 2011)). In these cases, the rotation centers need to be manually aligned and results in a time-consuming process for different hand sizes (Fu et al., 2008). This is where self-aligning joint centers are often-used alternatives. They are able to adapt to various hand sizes (Ueki et al., 2012) and prevent strong discomfort for the user (Chiri et al., 2012b; Cempini et al., 2014a). Self-aligning mechanisms are essentially polycentric and conform to whatever rotation the anatomical joint imposes. Moreover, efficiency is increased as the device finds less resistance from the user.

End-effector-based devices omit the constriction of joint movement by only moving the most distal end of the fingers (Maciejasz et al., 2014), forming a kinematic chain with the ground. This makes it advantageous over exoskeleton-based devices (Yeong et al., 2009), but also less suitable for applications with more strict design constraints on portability (i.e. home rehabilitation and daily assistive tools).

A general trend towards simplification of the hand kinematics can be seen. This includes the introduction of couplings by force (i.e. underactuation) and by motion (i.e. constraints) in order to reduce the complexity of the device. These methods are similar to the mechanical couplings and control synergies that exist in the natural hand (Santello et al., 1998; Gustus et al., 2012). This concept can be generalized under the term functional degrees of freedom (fDOF) (Li and Tang, 2007), which means that complex movement patterns can be generalized and achieved by less complex actuation strategies. This is a viable approach for dynamic hand orthoses as complex multi-DOF movements are unnecessary for many rehabilitation purposes (Rosati et al., 2009; Ertas et al., 2014) and grasping patterns that are used during ADL can be generalized (Napier, 1956). Underactuation, in particular, is a popular method as it reduces weight and complexity (Shields et al., 1997; Stergiopoulos et al., 2003; In et al., 2011; Surendra et al., 2012; Ertas

et al., 2014; Iqbal et al., 2014; Lee et al., 2014b) and it facilitates passive adaptation for better object manipulation (Nilsson et al., 2012; Iqbal et al., 2014). From the results, it appears that intrafinger (i.e. across joints) underactuation is preferred, as opposed to interfinger (i.e. across fingers) underactuation which is an upcoming feature and allows passive adaptation to 3D objects (In et al., 2011; Smit et al., 2015).

3.6. CONCLUSION

A high quantity of dynamic hand orthoses was gathered and shows that their development is becoming increasingly prevalent. A framework was developed in an attempt to collectively analyze the diverse solution space, whose general methodology can be used for other mechatronic systems that interact with the human. The investigated solution space reveals several outliers, for example the preference for EMG or force/motion control and electromagnetic actuation. There are also less-used solutions that do seem feasible, like compliant mechanisms, fluidic transmission/actuation and interfinger underactuation. By no means is the framework complete, as more branches can be added to the tree diagrams that expand and extend further into the solution space at increased level of detail. Even so, a comprehensive analysis was performed that can be used as a general exploration on mechatronic design of dynamic hand orthotics—and possibly other related fields as well.

4

EXPLORATORY DESIGN OF A COMPLIANT MECHANISM FOR A DYNAMIC HAND ORTHOSIS: LESSONS LEARNED

Bos, R. A., D. H. Plettenburg, and J. L. Herder

published in: 2017 International Conference on Rehabilitation Robotics (ICORR), pp. 603–608. London, 2017.
DOI: 10.1109/ICORR.2017.8009314

A B S T R A C T

This study does not describe a success-story. Instead, it describes an exploratory process and the lessons learned while designing a compliant mechanism for a dynamic hand orthosis. Tools from engineering optimization and rapid prototyping techniques were used, with the goal to design a mechanism to compensate for hypertonic or contracted finger muscles. Results show that the mechanism did not reach its design constraints, mostly because it could not provide for the necessary stiffness and compliance at the same time. Hence, the presented approach is more suited for design problems with either lower forces or less displacement. It was concluded that physiological stiffness models are an important part when modeling hand orthoses. Moreover, further research on compliant mechanisms in dynamic hand orthoses should focus on the feasibility of implementing more complex three-dimensional shapes, i.e., compliant shell mechanisms.

4.1. INTRODUCTION

The human hand is an amazingly complex organ capable of doing many different tasks. Unfortunately, there are many individuals that are impeded even in the most basic functionality, e.g., to open the hand and grasp objects, which hampers their ability to perform activities of daily living (ADLs). There can be numerous causes, but common examples include muscle hypertonia or contractures due to the consequences of stroke (Kamper et al., 2003; Brokaw et al., 2011) or other neuromuscular disorders (Skalsky and McDonald, 2012), limiting the ability to fully extend the fingers. For these individuals dynamic hand orthoses can offer novel solutions, whose development is a fast-growing field of research (Balasubramanian et al., 2010; Heo et al., 2012; Maciejasz et al., 2014; Bos et al., 2016a). These solutions range from simple gloves that provide passive impairment compensation for daily assistance (Saebo, Inc., n.d.[b]) to more advanced devices that monitor and aid movement of the fingers for home rehabilitation (Ates et al., 2016).

The design of the mechanism for a dynamic hand orthosis, however, remains a challenge. Especially for devices used during ADLs, the mechanism should be compact, light-weight, comfortable (Radder et al., 2015), and prevent hindrance of tactile feedback as much as possible. Even more, the axes of rotation should align with those of the human hand, which becomes difficult within the limited available space. Meeting all these criteria while still providing sufficient force output, is something that seems to be missing from a large list of existing devices (Bos et al., 2016a). Moreover, it appeared that there remain some less-used solutions whose feasibility can still be further explored. One example is the use of compliant mechanisms.

Instead of having mechanical joints, compliant mechanisms make use of elastic deformation in materials to create a force or displacement. It opens possibilities for creating monolithic structures, allowing for the design of compact, light-weight mechanisms, and easy use of rapid manufacturing methods. Moreover, they can admit minor misalignments by offering flexibility. A few examples exist where a dynamic hand orthosis uses a compliant mechanism. These range from using simple piano wires for passive support (Watanabe et al., 1978) to a more complex active device using multiple parallel leaf springs (Arata et al., 2013; Nycz et al., 2016). Efficiencies for larger ranges of motion, however, are generally low and it is difficult to find the right combination of flexibility and stiffness (Matheson and Brooker, 2012).

The goal of this study is to explore the use of compliant mechanisms in a dynamic hand orthosis, using tools from engineering optimization. The main purpose of the mechanism is to facilitate active extension of the fingers in order to compensate for finger flexor hypertonia or muscle contractures, ultimately regaining hand function while performing ADLs. The exploratory nature serves as a method to examine the feasibility of the proposed mechanism, as well as to extract recommendations for future work.

4.2. DESIGN CRITERIA

This study uses tools from engineering optimization, which requires a well-defined set of design criteria as boundary conditions. A summary of the design criteria, along with their descriptions and implementations, is shown in Table 4.1. They are described below in more detail.

Table 4.1: List of design criteria for the mechanism.

Criterium	Metric/description	Implementation
Degrees offreedom	Functional degrees of freedom [#]	1
Design domain	Cross-section [mm×mm]	26×17 mm
Finger stiffness	Rotational stiffness [Nm/rad]	≈0.5 Nm/rad per joint
	Flexion/extension angle [°]	60/0° per joint
Comfort	Resultant interaction force [N]	<5 N
	Unpredictable environment	Compliant mechanism

4.2.1. DEGREES OF FREEDOM (DOFS)

Using a simplified model of the hand, each finger has three joints that facilitate flexion/extension (FE) and abduction/adduction (AA) movements. The thumb facilitates two DOFs (FE and AA) in the carpometacarpal (CMC) joint, two (FE and AA) in the metacarpophalangeal (MCP) joint, and one (FE) in the interphalangeal (IP) joint. All other fingers have two DOFs (FE and AA) in each MCP joint, one (FE) in each proximal interphalangeal (PIP) joint, and one (FE) in each distal interphalangeal (DIP) joint. In total, this gives 21 DOFs and illustrates the diversity of possible movements.

For functional use, the hand can be controlled by fewer DOFs. This occurs in the natural case through synergies and mechanical couplings between tendons and muscles, which often depend on the task to be executed and posture of the body. This phenomenon can be collectively termed as functional DOFs (fDOFs) (Santello et al., 1998), implying that not all DOFs need to be individually controlled for specific tasks (Santello et al., 2016).

For a dynamic hand orthosis, this means that not all DOFs of the impaired hand need to be individually assisted. In the presented case, merely being able to open the hand for grasping can be enough to regain hand function for ADLs, hence a single fDOF is considered sufficient. For further simplification, the mechanism is designed for a single finger, i.e., the index finger. The presented concept can be extended for multiple phalanges by using force-distributing mechanisms (e.g., whippletree).

4.2.2. DESIGN DOMAIN

The dynamic hand orthosis should affect the hand's natural movements as little as possible. Consequently, occupying space in between the fingers should be avoided. Moreover, the mechanism should reside on the dorsal side of the hand for conservation of tactile feedback on the palmar side. For a single finger module, the height and width should be no more than the hand's thickness and finger breadth. This results in an available cross-section of 26×17 mm (DINED anthropometric database, n.d.) above the finger, respectively. The longitudinal length is of lower impact, as long as the mechanism does not extend over the wrist or fingertip. Because linear actuators are commonly used in a hand orthosis (Bos et al., 2016a), a linear force input is assumed to actuate the mechanism.

4.2.3. FINGER STIFFNESS

The mechanism should be able to carry the forces necessary to extend the fingers for individuals that suffer from hypertonic or contracted muscles. In Brokaw et al. (2011), several subjects with a score of 1+ or 2 on the Modified Ashworth scale showed an order of magnitude of 0.2-0.8 Nm over roughly 60°, which translates into a rotational stiffness of around 0.5 Nm/rad per joint. An exact value, however, is almost impossible to determine because there exists a large variety in severity between individuals (Kamper and Rymer, 2000). As an initial exploration of the presented concept which is able to accommodate hypertonic muscles with similar scores on the Ashworth scale, a stiffness of 0.5 Nm/rad with equilibrium position at 60° flexion was used for each joint during optimization.

4.2.4. COMFORT

Comfort is an important aspect for a dynamic hand orthosis and may well determine its acceptance for daily use. Its interpretation in design criteria is difficult and can be considered subjective, but it is here defined in terms of interaction forces. Such forces occur during normal operation of the device, but also due to unpredictable forces or impacts which may occur while performing ADLs.

During normal operation, forces are applied on the hand on a regular basis and skin tissue damage may occur. A method of minimizing discomfort is to minimize the main contributor to skin tissue damage, which is internal strain in underlying tissue (Oomens et al., 2010), but can also be measured as reduction in blood flow (Zhang et al., 1994). In Johansson et al. (2002), an 85% reduction in blood flow was reported for pressures ranging between 30–52 kPa applied at the palmar side of the fingers and for a duration of several minutes. Additionally, shear forces equally contribute to internal stresses and the resultant force which is applied should be considered (Zhang et al., 1994). In the case of active extension of the fingers, forces are most likely applied at the palmar side of the fingers and for shorter durations. Resultantly, forces can be in the higher range before damage occurs due to a thicker layer of skin (Bennett, 1972) and short duration of loading (Oomens et al., 2010). When force is applied at a 1 cm^2 area on the finger, the maximum resultant force is defined as 5 N.

In practice, when considering a joint stiffness of 0.5 Nm/rad, a resultant force of 5 N would require a moment arm of >100 mm and is unrealistic. During the optimization process in this study, this constraint was therefore often altered to higher forces or even relaxed in order to find a more realistic design point.

Regardless of the operational forces, unpredictable forces or impacts can occur on the mechanism during ADLs. In this case, a compliant mechanism is beneficial and provides for a safe interaction between the user and device. Additionally, the lack of mechanical joints avoids frictional phenomena and the need for lubrication, but also allows for the design of monolithic, simplistic, and low-profile structures. More importantly, a compliant dynamic hand orthosis is robust against minor misalignments between the finger's joints and mechanism's joints. Such misalignments may cause numerous sources of discomfort to the user or even tissue damage, where pressure sores, joint dislocations or cartilage damage are among the possibilities depending on the user (Schiele and van der Helm, 2006).

4.3. MECHANISM SYNTHESIS

4.3.1. TOPOLOGY OPTIMIZATION

For initial inspiration on mass distribution of a compliant monolithic mechanism, a simplified topology optimization procedure was performed. The problem was reduced to a single-DOF mechanism actuated by a linear input force (F_{act}), where a desired output displacement at an angle (u_{out}) is maximized around a fixation point (see Fig. 4.1(a)). The basis of the algorithm was formed by the 99-line structural optimization code presented in Sigmund (2001), which contains a simple finite element model (FEM) using Q4 elements in a predefined design domain. The design was varied by scaling the stiffness of the individual elements by an artificial density factor, ρ.

As the ideal compliant mechanism is a trade-off between stiffness and flexibility, the objective function was defined as a ratio between these terms (Saxena and Ananthasuresh, 1998, Eq. P4):

$$\min_{\boldsymbol{\rho}} f(\boldsymbol{\rho}) = -\text{sign}(MSE)\frac{\left|MSE(\boldsymbol{\rho})\right|^m}{SE(\boldsymbol{\rho})^n} \tag{4.1}$$

Here, strain energy (SE) is the amount of elastic energy stored in the mechanism and serves as a measure of stiffness. Mutual strain energy (MSE) expresses a form of output deformation due to a virtual load and represents flexibility (Howell, 2001). The parameters m and n were taken at 2 and 1, respectively. Sequential linear programming with move limits (Sigmund, 1997) was then used to update the design variables.

4.3.2. SHAPE OPTIMIZATION

Results from the topology optimization procedure were interpreted and translated into a general shape of the mechanism, which was parameterized by defining member lengths, angles and in-plane material thicknesses. The shape optimization procedure was then performed by using `fmincon`'s SQP algorithm in Matlab (version 2013b, Mathworks, Natick, MA, USA). The mechanism's performance for each iteration was evaluated through a nested FEM using ANSYS Mechanical APDL (version 15.0, ANSYS Inc., Canonsburg, PA, USA).

In this FEM, the members were modeled as BEAM188 elements with rectangular cross-sections and connected with MPC184 joint elements. The finger was included to represent the load and was modeled as a double pendulum with fixed base, having joints with a linear rotational stiffness of 0.5 Nm/rad and equilibrium points at a 60° flexion angle. Distance between the mechanism and finger skeleton was ensured by adding stiff beam elements whose lengths were equal to half the finger's thickness. Compliancy of skin tissue was neglected.

All elements had an out-of-plane thickness of 15 mm. The mechanism's material properties originated from available data on 3D-printed Nylon (Taulman 645 Nylon, $E \approx 0.2$ GPa, $\sigma_Y \approx 35$ MPa), whereas the finger's material was taken as relatively stiff compared to the mechanism ($E = 200$ GPa). The FEM was evaluated by subjecting it to a 40 N linear force at the mechanism and recording the maximum extension angles of the finger joints, reaction loads at the fixation points and maximum equivalent stress in the mechanism.

The optimizer's constraints originate from the remaining design criteria as previously described. Additional constraints were added that limited the material stresses and

avoided infeasible configurations. All constraints were normalized to ensure equal contribution despite their differences in units.

The goal of the mechanism was to fully extend the fingers, hence the objective function was defined to minimize the difference between the obtained extension angle of the finger joints and full extension. This was formulated as:

$$\min_{\mathbf{x}} g(\mathbf{x}) = \left|\Delta\theta_{MCP}(\mathbf{x}) - \frac{\pi}{3}\right| + \left|\Delta\theta_{PIP}(\mathbf{x}) - \frac{\pi}{3}\right| \tag{4.2}$$

Here, $\mathbf{x}$ represents the collection of parameters to be optimized, $\Delta\theta_{MCP}$ the angular rotation of the MCP joint, and $\Delta\theta_{PIP}$ the angular rotation of the PIP joint. In order to account for the limited precision in rapid manufacturing methods, angles were rounded to the closest increment of 5 degrees and lengths were rounded to millimeters.

4.3.3. PROTOTYPING

The mechanism was evaluated by fitting it onto a mock-up finger, where a linear actuation force of 0–40 N was applied using a test bench. Position was determined with a camera that took pictures at increments of 5 N applied force. Using image processing software, the joint angles were then determined by the angle between the vectors imposed by the joint centers. This was considered to be accurate with a +/- 1° variation. Actuation force was measured and monitored using a load cell (Zemic Inc, Santa Fe Springs, California).

The effects of possible misalignments were evaluated by fixating the mechanism at three different points on the phalanges of the mock-up finger and detecting changes in the joint angles. The same alterations were applied in the FEM analysis for comparison. These locations were defined at 1/4, 1/2, and 3/4 of the proximal phalange's length and were labeled PP1, PP2, and PP3. The same was done for the intermediate phalange and the locations were labeled IP1, IP2, and IP3 (see top left illustration in Fig. 4.4).

The compliant mechanism was made out of 3D-printed Nylon plastic (Taulman 645 Nylon). The mock-up finger was made with 3D-printed ABS plastic and was a modified from the open source InMoov hand (Gael Langevin, n.d.). Main modifications included the addition of fixation points for the mechanism, a rectangular cross-section in the phalanges for simplicity, mechanical stops at 90° flexion and 20° extension, and free-rotating pulleys with bearings for reduced friction. The finger stiffness was simulated with a tendon-like system. Specifically, a linear spring was connected to a string that was routed through the pulleys at each joint.

4.4. RESULTS

4.4.1. TOPOLOGY OPTIMIZATION

The result from the topology optimization procedure is shown in Fig. 4.1(a), accompanied by an interpretation of this result over multiple joints in Fig. 4.1(b). The interpretation follows from the following observations:

- The bottom layer of elements (pixels) can be replaced by the finger's skeletal structure.

- The mechanism consists of a smooth arching element and connects with the finger through flexure elements.

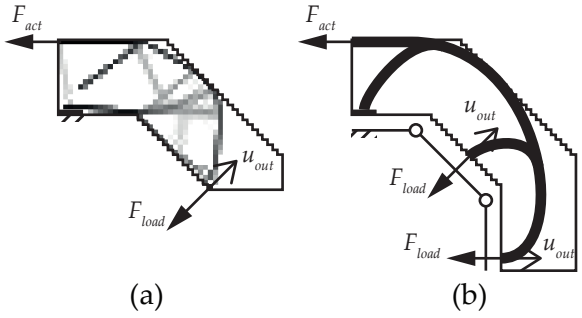

Figure 4.1: (a) Result of the topology optimization procedure, indicating the input force (F_{act}), load force (F_{load}) and desired output displacement (u_{out}). Each pixel represents an element in de FEM, where darker pixels represent a higher local material stiffness and indicate a form of mass distribution. In (b), an interpretation of the result is illustrated across multiple joints.

- To prevent interference with the finger's knuckles, the flexure elements can be connected at the center of the phalanges.

4.4.2. SHAPE OPTIMIZATION

The resulting mechanism showed significant similarities with the compliant finger prosthesis from Steutel (2010). In this study, signs of buckling were observed in the flexure elements and were reduced by creating S-shaped flexures. This was also used in the parameterization of the mechanism for shape optimization, where the S-shape was characterized by two angles. In Fig. 4.2, a full parameterization of the mechanism is shown. The position of points A–O determined the mechanism's overall dimensions with respect to the finger, which were defined by its joints MCP–PIP–DIP. To create smooth shapes, the main arch of the mechanism was defined by creating a spline through points K–C–O–E–F–G, whereas the flexures were defined as two fillets between points H–I–J–K (and equivalently for L–M–N–O) with maximum radius. The line between A–K was defined as a straight line to ensure it remained parallel to the dorsal surface of the hand.

The locations of the fixation points (defined by l_{mH}, l_{pL}, and l_{iG}) were kept constant (30, 26.5, and 14 mm, respectively) and the parameter vector to be optimized was set at $\mathbf{x} = [\alpha_1, \alpha_2, \beta_1, \beta_2, \gamma, h_a, h_b, h_c, h_1, h_2, h_3]$. The resulting values are shown in Table 4.2. In this shape and according to the FEM, the maximum equivalent stress was equal to 12.5 MPa and the final joint angles (negative indicating flexion) were predicted at -20° and -54° for the MCP and PIP joint, respectively. The resultant forces at the phalanges exceeded the constraints at approximately 7 N and 4 N at the proximal and intermediate phalange, respectively.

4.4.3. PROTOTYPING

The resulting prototype of the mechanism with mock-up finger is shown in Fig. 4.3. The mechanism protruded a maximum of 22 mm in equilibrium position (flexed finger). During initial tests, the mechanism appeared not able to extend the fingers when the intended stiffness of 0.5 Nm/rad was applied. For this reason, a lower finger stiffness of

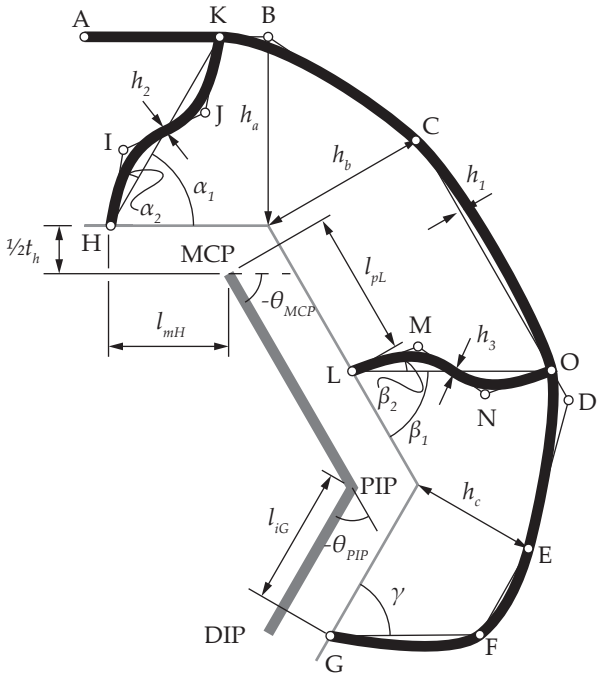

Figure 4.2: Full parameterization of the mechanism shape, showing the finger skeleton (thick gray), skin surface (thin gray) and mechanism (thick black) outlines.

approximately 0.2 Nm/rad was used and the model predictions were altered accordingly. The results from the FEM analysis and prototype measurements are shown in Fig. 4.4. In this graph, a range of curves due to imposed misalignments are also shown.

4.5. DISCUSSION

4.5.1. FINGER STIFFNESS

It is apparent from the results that the mechanism did not meet its design criteria and did not coincide with the model predictions. One of the major causes behind these differences was how the finger's joint stiffness was applied. In the FEM, each finger joint had an independent stiffness value, whereas the joints in the mock-up finger shared a stiffness through an underactuated tendon-like structure. This leads to a situation where an extension in the MCP joint would also increase the passive torque in the PIP joint. Because the mechanism had a more favorable moment arm around the MCP joint, it was more likely to extend and the PIP joint would remain flexed. A similar effect can be observed in the model results, which only occurred after reducing the joint stiffness down to 0.2 Nm/rad (see Fig. 4.4).

These effects mostly demonstrate the mechanism's sensitivity to the finger's stiffness. Specifically, it shows that the stiffness model used during mechanism synthesis can have a large influence on the mechanism's performance, especially when it relies on an optimization procedure. It is therefore recommended to use models that better approach

Table 4.2: Optimized shape for the parameterized mechanism.

Parameter	Angle	Parameter	Length
α_1	40°	h_a	15 mm
α_2	-5°	h_b	22 mm
β_1	45°	h_c	22 mm
β_2	-35°	h_1	4 mm
γ	75°	h_2	5 mm
		h_3	4 mm

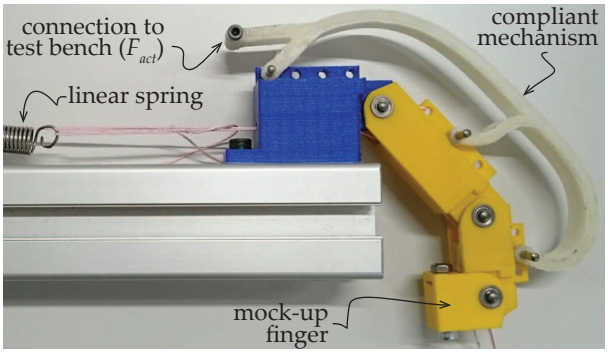

Figure 4.3: Photo of the compliant mechanism made out of 3D-printed Nylon plastic, fixed onto a mock-up finger for testing purposes.

physiological behavior. For example in Kamper et al. (2002); Deshpande et al. (2012), models are proposed with non-linear stiffness characteristics as well as dependencies on surrounding joint angles.

4.5.2. MECHANISM SHAPE

Due to a singularity around the PIP joint, the mechanism was not able to extend the PIP joint. This was caused by the direction of the forces on the phalanges and the mechanism's geometric shape. Depending on the PIP joint's angle, it would extend or flex as a result of the actuation force. Combined with the way how the joint stiffness was implemented in the mock-up finger (see previous subsection), this would cause the PIP joint to flex up to its mechanical stop (i.e., the 90° angle).

4.5.3. MATERIAL COMPLIANCE

Similar to the model's predictions, the joint angle decreased when the fixations were moved to more proximal locations and increased when moved to distal locations. The size of the effect, however, was much larger in the measured results, indicating that the mechanism did not provide sufficient flexibility to cope with these changes. These differences are mostly attributed to the unpredictable mechanical properties of the

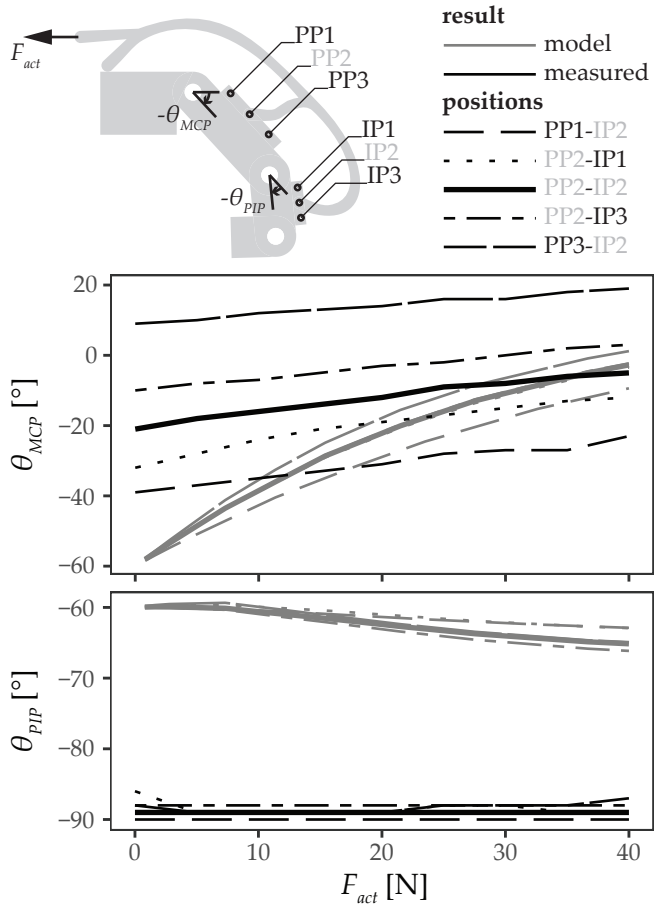

Figure 4.4: Joint angles as a result of the input force F_{act}, comparing the model (gray) and measured (black) results. Please note the difference in vertical axis scaling. The top left illustration shows the outline shape of the mechanism on the mock-up finger, as well as the labels used in the legend. Misalignments are implemented by varying the fixation positions from a reference position PP2-IP2 (solid lines). Moving the fixations proximally (PP1 or IP1) decreases the flexion angle, moving them distally (PP3 or IP3) increases it.

material, as they are highly dependent on the 3D-printing process. In general, the material appeared to be stiffer than anticipated, which largely reduced motion around the Y-junctions at points K and O (see Fig. 4.2). Additionally, warped shapes along the vertical printing direction (out-of-plane thickness) was a common effect when printing the Nylon material. This would distort the second moment of inertia of the mechanism's cross-section and thus the resistance to bending.

These observations show that, when relying on rapid manufacturing methods, the actual behavior of the mechanism can differ from the predictions. This implies that it would be more useful to investigate a range of design variations around an optimum, in order to investigate the prototype's sensitivities to these variations. Consequently, it can be

recommended to perform a sensitivity analysis that includes the manufacturing process, instead of focusing on a singular result from an optimization procedure that may not be that optimal in practice.

The presented concept needed to withstand relatively high forces and large displacements, evidently requiring stiffness and compliance at the same time. Even though the 3D-printed Nylon plastic appeared very strong and flexible, a compliant mechanism in the presented shape would not be very suited for its original goal, i.e., to actively compensate contracted or hypertonic finger muscles. It may, however, be appropriate for applications with lower forces. For example, a thinner version may aid in minor force assistance during ADLs for individuals that only lack in muscular strength. Alternatively, the design problem can be expanded to a three-dimensional case. Cross-sectional shapes can then be altered to better approach the desired stiffness profile and the abduction/adduction movement in the MCP joint can be included, resulting in a shell-like mechanism.

4.6. CONCLUSION

The mechanism did not reach its design criteria. It was not able to accommodate the intended joint stiffness of 0.5 Nm/rad and even at a lower stiffness of the finger, it would only extend for 20°. Nevertheless, several lessons were learned from the process and can be useful as recommendation for future work.

Including the prototype of a 3D-printed compliant mechanism in the sensitivity analysis, would give a better view on the mechanism's behavior in practice and includes the rapid manufacturing process. This can be a more powerful tool than relying on a single optimal result. Moreover, it is important to implement a physiological joint stiffness model when modeling a hand orthosis. Especially when relying on optimization tools, the design becomes highly dependent on how the finger behaves. A compliant mechanism will also change shape depending on the forces applied, hence it has a large influence on the mechanism's outcome.

The original goal of the mechanism, i.e., to compensate for contracted or hypertonic finger muscles, did not appear to be compatible with the presented concept. At this scale, the necessary forces to be transmitted required the mechanism to be relatively stiff, but the necessary range of motion also required it to be compliant in the same direction. This approach may be better suited for other hand impairments or purposes that require either lower forces or less displacement. For future work, it is recommended to investigate the feasibility of compliant mechanisms with more complex three-dimensional shapes (shell mechanisms).

ACKNOWLEDGMENT

The authors would like to thank Claudia J.W. Haarman for her support in making the 3D-printed components.

5

SIMPLIFYING MODELS AND ESTIMATING GRASP PERFORMANCE FOR COMPARING DYNAMIC HAND ORTHOSIS CONCEPTS

Bos, R. A., D. H. Plettenburg, and J. L. Herder

published in: PLOS ONE, vol. 14(7): pp. 1–16. 2019.
DOI: 10.1371/journal.pone.0220147

A B S T R A C T

While designing a dynamic hand orthosis to assist during activities of daily living, the designer has to know whether a concept will have sufficient grasp performance to support these activities. This is often estimated by measuring the interaction force at the contact interface. However, this requires a prototyping step and limits the practicality of comparing several concepts in an early design stage. Alternatively, this study presents and compares basic static and dynamic models to numerically estimate grasp performance. This was applied on an exemplary concept for a hydraulically operated hand orthosis grasping a circular object. The models were validated with an experimental set-up that does not require sensors at the contact interface. Static and dynamic model results were almost identical, where the static model could be around 10 times faster and is generally more robust to a high contact stiffness. Both models were unable to make accurate quantitative predictions, which is believed to be due to differences in used contact stiffness. However, the models were able to make correct qualitative comparisons, making it a valid method to compare and choose concepts in an early design stage.

5.1. INTRODUCTION

Sometimes, an impairment can affect the neuromuscular function of our hands. For example, the available strength in the hand muscles can be limited by the effects of aging or a muscular disorder. When an individual loses the ability to grasp objects, it becomes more difficult to perform daily activities, maintain independence and participate in social activities. In order to recover the ability to grasp, additional strength can be added to the hand by using a dynamic hand orthosis that provides assistance during activities of daily living.

There are numerous dynamic hand orthoses being developed, with over 160+ examples over the past 50 years Bos et al., 2016a. A certain diversity between these devices can be found in applications, system designs and testing procedures. Partly due to this diversity, there is also a wide range of methods to characterize the mechanical functioning of this type of device. For a daily assistive device, it is necessary to get an idea of the grasping performance. For example, a custom actuator can be evaluated by measuring actuator strength Polygerinos et al., 2015c, a particular mechanism can be evaluated by measuring tip force Gasser and Goldfarb, 2015, or the full orthosis design can be evaluated by having an individual wear the orthosis and measure grasping force with a sensorized object In et al., 2015. The advantage of these methods is that they provide a measure of actual performance and can be used to verify predictions. The disadvantage, however, is that they cannot be performed in an early design stage. Being able to estimate grasping performance during this stage can help with optimizing mechanism topologies and shapes. Because the early design stage is characterized by creating and weighing concepts, any step that requires manufacturing impedes the design process. To the author's knowledge, there is currently no generalized method presented that is able to estimate grasping performance of a dynamic hand orthosis in this conceptual design stage.

The purpose of this study is to present a method that is able to estimate the grasping force using a model that does not require much a priori knowledge, which can be used as a tool to aid in choosing between conceptual designs. The intention behind this method is not to be anatomically correct, but to minimize the amount of details while preserving the ability to make appropriate design choices. This way, one can get an idea of the grasping performance in an early design stage without fabricating and testing a prototype, or requiring accurate (subject-specific) anatomical properties. Moreover, beyond this study, the use of modeling techniques allows us to extract even more information like possible range of motion of the anatomical joints or interaction forces between the finger and orthosis, which can be used to maximize freedom of movement or to minimize shear forces.

In order to estimate the grasping force, one needs to find a stable grasping configuration and investigate the contact forces on the object. There are multiple ways to determine this configuration and can be narrowed down to finding a position where the system is in equilibrium. In this study, a dynamic model and a static model are compared and their applicability is discussed. Both models require several iterations to find the equilibrium position. A dynamic model performs an integration over time and a static model uses a minimization procedure for each individual position. To validate both models and assess the effect of the additional assumptions that come with a static model,

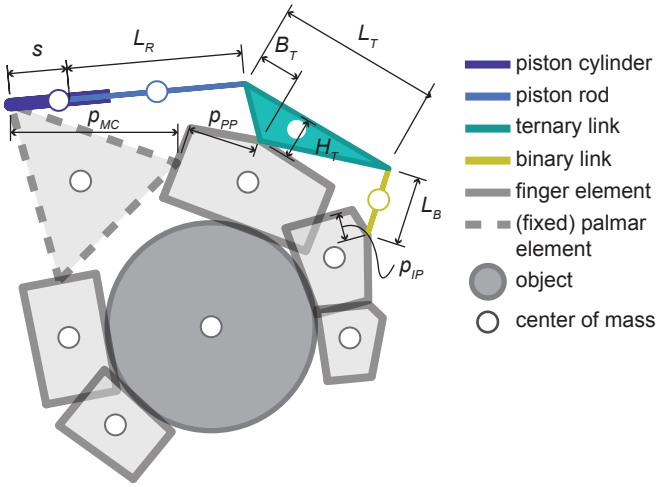

Figure 5.1: Basic illustration of the system as it appears in the model. Mechanism elements are indicated along with their lengths ($s, L_R, L_T, B_T, H_T, L_B$) and locations of the interfaces at the phalanges (p_{MC}, p_{PP}, p_{IP}). In this model, the length of the piston cylinder relates to the maximum stroke (s_{max}) and the length of the piston rod (L_R) equals the minimum distance between the hinge joints of the cylinder.

a prototype was made and tested. All methods were applied on an exemplary design of a hydraulically operated hand orthosis.

5.2. SYSTEM DESCRIPTION

For the purpose of this study, a hydraulically operated hand orthosis mechanism was used. An illustration of the system is shown in Fig 5.1. A single hydraulic cylinder pushes a linkage mechanism with two degrees of freedom (DOFs), which then applies force to the proximal and intermediate phalange of the finger. Because the number of actuators is less than the mechanical DOFs, this is an underactuated mechanism and allows it to passively adapt to an object's shape. The distal phalange is left free and does not actively contribute to grasping force during cylindrical grasps. Similar to the Delft Cylinder Hand Smit et al., 2015, multiple finger mechanisms can be connected by a single master cylinder. This study, however, is limited to a two-dimensional scenario supporting only a single finger.

The shape of the linkage mechanism is based on the first isomer of a seven-link mechanism with two DOFs from Suarez-Escobar et al. Suarez-Escobar et al., 2016. A mechanism with only two DOFs was chosen, because a two-phalange system is still able to perform stable underactuated grasping Kragten et al., 2011 and avoids any physical connection between the mechanism and the distal phalange, which minimizes the risk of attenuating tactile feedback at the fingertip. This particular isomer was chosen based on the ability to easily replace a revolute joint by a prismatic joint (i.e., piston cylinder), while maintaining the capability to create a low-profile mechanism.

5.3. METHODS

5.3.1. ABILITY TO HOLD AN OBJECT

As described in Kragten and Herder, 2010, a grasper can be assessed by calculating its ability to grasp and hold objects. In this context, the ability to grasp is defined by the geometry of the grasper, i.e., the number of phalanges and their lengths. A human hand is considered without limb-deficiencies in this study and so the ability to grasp is fixed. The ability to hold objects, on the other hand, remains variable. It is defined by the grasping force that the grasper is able to exert on an object. In Kragten and Herder, 2010, this was tested by determining the minimum force required to pull an object out of the grasper, in a direction that is perpendicular to the grasper's axes of rotation. Although a very effective method for robotic graspers, the joint stiffness of a human hand can greatly affect this metric. This is because the hand is opened while the object is being pulled out of the grasp, introducing the risk to measure joint stiffness rather than grasping force. Hence, in this study, the object was pulled in a direction that was parallel to the joint axes. The ability to hold an object can then be defined by the sum of normal forces of the finger's phalanges on an object at the instant when the grasp is stable. This way, the ability to hold an object is more dependent on the mechanism's ability to transfer and distribute forces, and less dependent on the grasper's inherent stiffness characteristics.

In order to assess the system's ability to hold an object, the interaction with a graspable object needs to be modeled. This is preferably done without requiring a priori knowledge on the contact configuration. For example, when modeling one finger with three phalanges and one opposing thumb with two phalanges, this gives a total of six possible contact points (i.e., five phalanges and one palm element). If all possible configurations with at least two contact points need to be investigated, this results in $(\sum_{k=2}^{6} \frac{6!}{k!(6-k)!} =)$ 57 different scenarios. Even though some of these configurations could be excluded, it would be much more efficient to let the model determine the stable grasp configuration.

In this study, the ability to hold an object is analyzed for an open fist cylindrical grasp Iberall, 1997. This particular grasp was chosen to be representable for picking up objects with a circular cross-section (e.g., bottles, cans). Because this grasp holds the objects by form-closure, friction will not have an effect on the grasping shape. Neglecting static friction will then result in a worst-case scenario, where the actual grasping force can only be higher. Additionally, the thumb was simplified with only two phalanges and acting in the same plane as the finger. Although this does not reflect the anatomy of the human hand, this was not deemed necessary because forces acting on or inside the thumb were not of interest in this exemplary study. The simplified thumb element fulfilled the purpose of providing an opposing force and allowing analysis of the finger elements that interface with the orthosis mechanism.

5.3.2. CONTACT MODEL

In order to determine whether a contact point is active, the model needs to detect the distance between the potential contact points. Using this distance, the appropriate contact force can be applied using a contact force model.

CONTACT DETECTION

The moment when the distance between two bodies becomes zero, they are in contact and the appropriate contact forces should be applied. Hence, contact is detected by

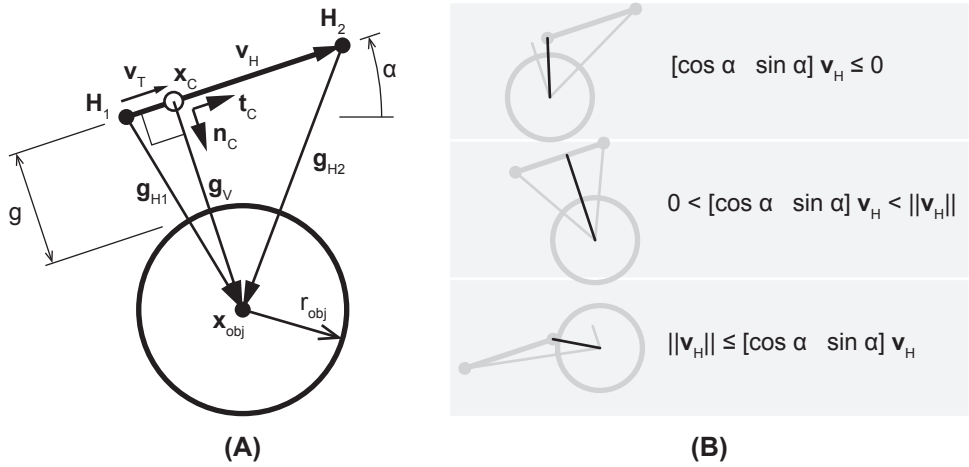

Figure 5.2: Determination of the shortest distance vector. (A) Potential distance vectors ($\mathbf{g}_{H1}$, $\mathbf{g}_V$, $\mathbf{g}_{H2}$) between a circular object (position $\mathbf{x}_{obj}$ and radius r_{obj}) and line segment (defined by vector $\mathbf{v}_H$ with endpoints $\mathbf{H}_1$ and $\mathbf{H}_2$). In the shown configuration, vector $\mathbf{g}_V$ is shortest and creates a contact point ($\mathbf{x}_C$) at the line segment, along with local tangential and normal unit vectors ($\mathbf{t}_C$, $\mathbf{n}_C$). (B) Three different configurations that illustrate when which distance vector should be used to determine the shortest distance.

monitoring the shortest distance between two potential contacting bodies. For the purpose of this study and similar to Kragten and Herder, 2010, only circular objects were considered and the contacting elements of the hand were represented by straight lines. This way, the shortest distance between the object and a hand element could be narrowed down to the shortest distance between a point and a line segment.

Fig 5.2A illustrates an arbitrary situation between two potential contacting bodies. It shows that, depending on the position of the circular object, three potential distance vectors can be defined. Using the symbols from Fig 5.2A, the distances between the object and the endpoints can be easily determined:

$$||\mathbf{g}_{H1}|| = ||\mathbf{H}_1 - \mathbf{x}_{obj}|| \tag{5.1}$$

$$||\mathbf{g}_{H2}|| = ||\mathbf{H}_2 - \mathbf{x}_{obj}|| \tag{5.2}$$

The distance vector $\mathbf{g}_V$, on the other hand, can be determined by using the projection of $\mathbf{g}_{H1}$ on $\mathbf{v}_H$, according to:

$$||\mathbf{g}_V|| = ||\mathbf{g}_{H1} - \mathbf{v}_T|| \tag{5.3}$$

where

$$\mathbf{v}_T = \left(\mathbf{g}_{H1} \bullet \hat{\mathbf{v}}_H\right)\hat{\mathbf{v}}_H \tag{5.4}$$

$$\hat{\mathbf{v}}_H = \frac{\mathbf{v}_H}{||\mathbf{v}_H||} \tag{5.5}$$

To determine which distance vector should be used for the shortest distance at a particular instant, the location of the potential contact point ($\mathbf{x}_C$) needs to be determined which is constrained to be on the line segment defined by $\mathbf{v}_H$. If $\mathbf{x}_C$ appears to lie on or beyond the boundaries defined by endpoints $\mathbf{H}_1$ and $\mathbf{H}_2$, it means that $\mathbf{x}_C$ needs a correction towards the nearest endpoint. This can all be done by using the projection vector $\mathbf{v}_T$ and determining its length and orientation with respect to $\mathbf{v}_H$ (see Fig 5.2B), resulting in the following conditional equations for the distance between the object and line segment:

$$g = \begin{cases} ||\mathbf{g}_{H1}|| - r_{obj} & \text{if } \begin{bmatrix}\cos\alpha & \sin\alpha\end{bmatrix}\mathbf{v}_T \leq 0 \\ ||\mathbf{g}_V|| - r_{obj} & \text{if } 0 < \begin{bmatrix}\cos\alpha & \sin\alpha\end{bmatrix}\mathbf{v}_T < ||\mathbf{v}_H|| \\ ||\mathbf{g}_{H2}|| - r_{obj} & \text{if } ||\mathbf{v}_H|| \leq \begin{bmatrix}\cos\alpha & \sin\alpha\end{bmatrix}\mathbf{v}_T \end{cases} \tag{5.6}$$

Additionally, by using Eqs 5.3–5.5, the coordinates of the contact point can be determined and a set of local unit vectors can be defined:

$$\mathbf{x}_C = \mathbf{H}_1 + \mathbf{v}_T \tag{5.7}$$

$$\mathbf{t}_C = \frac{\mathbf{v}_T}{||\mathbf{v}_T||} \tag{5.8}$$

$$\mathbf{n}_C = \frac{\mathbf{g}_V}{||\mathbf{g}_V||} \tag{5.9}$$

These expressions are particularly useful to apply the appropriate contact forces in the correct directions.

CONTACT FORCE

In both the dynamic and static model, contact with an object was added by using a continuous (or compliant) model. This approach was chosen to be favorable over using a discrete model, which limits itself to rigid contacts. Especially in a dynamic model, this causes instantaneous changes in the system and becomes inconvenient in numerical integration with multiple possible contact points Gilardi and Sharf, 2002. The continuous model, on the other hand, simulates a (visco-)elastic interface between the contacting bodies and allows to model flexible objects. Similar to Hertz's contact theory, the indentation between two objects can be related to a contact force. In Machado et. al Machado et al., 2012, several extensions to this model are discussed, including this dissipative contact force model:

$$F_N = K_c \delta^n \left(1 + \frac{3(1-c_r^2)e^{2(1-c_r)}}{4}\frac{\dot{\delta}}{\dot{\delta}^{(-)}}\right) \tag{5.10}$$

Here, F_N is the contact force perpendicular to the surface, δ the indentation, $\dot{\delta}$ the indentation velocity, $\dot{\delta}^{(-)}$ the initial velocity during contact, K_c the contact stiffness factor and c_r the coefficient of restitution. Assuming a parabolic pressure distribution, the power exponent (n) was taken as equal to $\frac{2}{3}$ Machado et al., 2012.

This contact force model is particularly suitable for situations with a low coefficient of restitution Machado et al., 2012, which is assumed to be the case in the presented situation

of a hand grasping an object. The model was coupled with Eqs 5.1–5.6, by defining the indentation as the overlap between the contacting bodies:

$$\delta = \min\left(g, 0\right) \tag{5.11}$$

It was assumed that the magnitude of indentation would not exceed the radius of the object. Because if $\delta > r_{obj}$, the direction of $\mathbf{n}_C$ would change and F_N will act in opposite direction. Even though this is unlikely to happen, it can produce invalid results when very small objects are chosen with a low contact stiffness.

5.3.3. DYNAMIC MODEL

When using a dynamic model, effects such as friction, viscosity and inertial forces can be implemented and the motion of the system can be investigated. The equilibrium position can be found by simulating a system over time until the accelerations approach zero. The basis of the dynamic model revolves around the equations of motion of a constrained system of rigid bodies. This combines Newton's second law of motion with constraint equations by using the technique of Lagrange multipliers:

$$\begin{bmatrix} \mathbf{M} & \mathbf{D}_{\mathbf{q}}^T(\mathbf{q}) \\ \mathbf{D}_{\mathbf{q}}(\mathbf{q}) & \mathbf{0} \end{bmatrix} \begin{bmatrix} \ddot{\mathbf{q}} \\ \lambda \end{bmatrix} = \begin{bmatrix} \mathbf{f}(\dot{\mathbf{q}}, \mathbf{q}, t) \\ -\mathbf{g}(\dot{\mathbf{q}}, \mathbf{q}, t) \end{bmatrix} \tag{5.12}$$

The bodies' states, velocities and accelerations are denoted by $\mathbf{q}$, $\dot{\mathbf{q}}$ and $\ddot{\mathbf{q}}$, respectively. Values for mass and inertia are stored in the mass matrix, $\mathbf{M}$. Contact forces, actuator forces and other viscoelastic elements were all applied as external forces that are stored in the force vector, $\mathbf{f}$. Constraint equations were implemented using their jacobian, $\mathbf{D}_{\mathbf{q}}$, and the convective terms that follow from the second order derivatives with respect to time, $\mathbf{g}$. Lastly, the Lagrange multipliers are denoted by λ and can be interpreted as the magnitude of constraint forces. These equations can be used to evaluate the system over time using numerical integration, where the values of the Lagrange multipliers can be used to inspect the internal forces of the system.

FRICTION FORCE

Friction is an extremely complex phenomenon and is strongly dependent on the types of materials that are interacting. Considering the high variability of graspable objects and dependency of the friction coefficient on numerous factors Derler and Gerhardt, 2012; Veijgen et al., 2013, the friction forces from this model were not considered to be representative for a real-life situation. Nonetheless, friction was implemented to provide for additional numerical stability. More specifically, it was added to avoid undamped sliding of the object along the finger elements.

In the classic Coulomb model, the friction force is equal to a friction coefficient times the normal force. This force is then applied in opposite direction of the relative movement between the contacting bodies. This results in a sudden change in forces on the system, which can severely slow down the numerical integration process around these events. Instead, the friction force was defined with a smooth transition around close-to-zero velocities:

$$F_T = \text{sgn}(\dot{\mathbf{t}}_C)\mu F_N \min\left(1, \frac{\dot{\mathbf{t}}_C}{v_T}\right) \tag{5.13}$$

Here, F_T represents the friction force which scales with the normal force according to the frictional coefficient, μ. Direction of the friction force is determined by the relative tangential velocity at the contact point between the two bodies, $\dot{\mathbf{t}}_C$. For relative velocities below a characteristic velocity, v_T, the friction force is scaled as a ramp function. The advantage of this method is that it stabilizes the numerical integration algorithm at low velocities compared to the classic Coulomb model Flores et al., 2006. However, it only models dynamic friction and neglects stick-slip effects caused by a higher static friction coefficient.

NUMERICAL INTEGRATION

The contact and friction force models conveniently provide a smooth transition from zero, thus giving a method suitable for numerical integration. Nonetheless, the sudden application of these forces still introduces an abrupt change in the system. For this reason, an event-detection scheme was used to detect the moment when a new contact force should be added (or an old one removed). This stops the integration process, adds the contact forces to the model, and continues the integration where it left off. This allows for larger time steps and overall faster computation. A standard solver (`ode15s` from Matlab) was used that is able to deal with stiff equations. To further speed up the numerical integration process, the functions that generate the matrices for Eq 5.12 were converted to faster MEX-files.

5.3.4. STATIC MODEL

As opposed to the dynamic model, a static model neglects inertial effects and makes accelerations of bodies obsolete. Instead of simulating the system over time, it already assumes that accelerations are zero and finds the appropriate system configuration. This configuration can be found by performing a constrained minimization procedure. In particular, it minimizes the total potential energy of the system according to:

$$\begin{aligned} \min_{\mathbf{x}} f(\mathbf{x}) &= \sum_{e=1}^{n_e} \int F_e(\mathbf{x}) ds_e(\mathbf{x}) - \sum_{a=1}^{n_a} \int F_a(\mathbf{x}) ds_a(\mathbf{x}) \\ \text{s.t.:} \quad & D_{eq}(\mathbf{x}) = 0 \\ & D_{ineq}(\mathbf{x}) \leq 0 \end{aligned} \tag{5.14}$$

In this expression, the elastic energy stored in all n_e elastic elements increase the potential energy, which also include the Hertzian contacts with the object. The work done by all n_a actuating elements decrease the total potential energy. The shape of the mechanism was represented by constraint equations. These can be equality constraints, D_{eq}, similar to what was used in the dynamic model, as well as inequality constraints, D_{ineq}. Lastly, the $\mathbf{x}$-vector contains the leftover degrees of freedom that are not connected by the constraint equations. In this study, these are the actuator strokes, finger joint angles and object position. By varying these variables and calculating their corresponding potential energies, a solution can be found within the constraints where the potential energy is minimal.

In contrary to the dynamic model, the minimization procedure allows for an easier implementation of inequality constraints. This provides for a convenient way to, for example, limit an actuator's stroke or prevent links from the mechanism to penetrate

finger elements. In a dynamic model, these need to be implied using contact models or non-smooth unilateral constraints.

Similar to the dynamic model, Lagrange multipliers can be used for all equality constraints to inspect the internal forces of the system. If the same constraint equations are used from the dynamic model, Eq 5.12 can be used with $\ddot{\mathbf{q}} = 0$:

$$\mathbf{D}_{\mathbf{q}}^T \lambda = \mathbf{f}(\dot{\mathbf{q}}, \mathbf{q}, t) \tag{5.15}$$

$$\mathbf{D}_{\mathbf{q}} \mathbf{D}_{\mathbf{q}}^T \lambda = \mathbf{D}_{\mathbf{q}} \mathbf{f}(\dot{\mathbf{q}}, \mathbf{q}, t) \tag{5.16}$$

$$\lambda = \left(\mathbf{D}_{\mathbf{q}} \mathbf{D}_{\mathbf{q}}^T \right)^{-1} \mathbf{D}_{\mathbf{q}} \mathbf{f}(\dot{\mathbf{q}}, \mathbf{q}, t) \tag{5.17}$$

FRICTION FORCE

Because friction is not a conservative force, it does not add to the total potential energy of the system and was therefore not included.

MINIMIZATION PROCEDURE

Because the minimization function and the constraint equations are highly non-linear, a robust minimization algorithm is needed. For this reason, the SQP-algorithm stored in Matlab's `fmincon` function was chosen. All constraint equations where added as non-linear equality and inequality constraint functions. To speed up the algorithm, variables and results from the objective function ($f(\mathbf{x})$) were shared with the constraint function expressions.

For different initial conditions, the SQP-algorithm can find different minima. Especially the initial guess for object position had a large influence on which local minimum was found by the algorithm, which could also be outside the grasp. To ensure that the algorithm finds the minimum that corresponds to a stable grasp, a range of initial object positions was used. This range was defined by a 15 mm square grid that fell within the possible range of motion of the hand. The solution with the lowest gradient around the found minimum was then selected, as this would represent the most stable solution.

5.3.5. EXPERIMENTAL SET-UP

In order to test the model outputs to a real-world situation, the ability to hold a circular object was measured using a prototype version of the hand orthosis system (see Fig 5.3). The prototype was fitted onto an anthropomorphically shaped mock-up hand, consisting of one finger and one opposing thumb. In this mock-up hand, the joints were fitted with torsional springs with a low stiffness (0.07 Nm/rad) in order to simulate a slightly flexed resting position of the phalanges. The thumb was fixed in opposition by strapping a 3D-printed splint onto the mock-up hand. The dimensions and material of this splint added a bending stiffness of approximately 8 Nm/rad parallel to each thumb joint. Fixation points were attached to the mock-up hand and facilitated a connection with the orthosis mechanism. These fixation points provided for a rigid connection between the mechanism and the finger, which is similar to the model representation.

In order to test the sensitivity of the mechanism to changes, the link length of the ternary link (L_T) and object diameter (D_{obj}) was varied. This simulated a crude sensitivity analysis and allowed to analyze how the outcome measure was affected by changing these

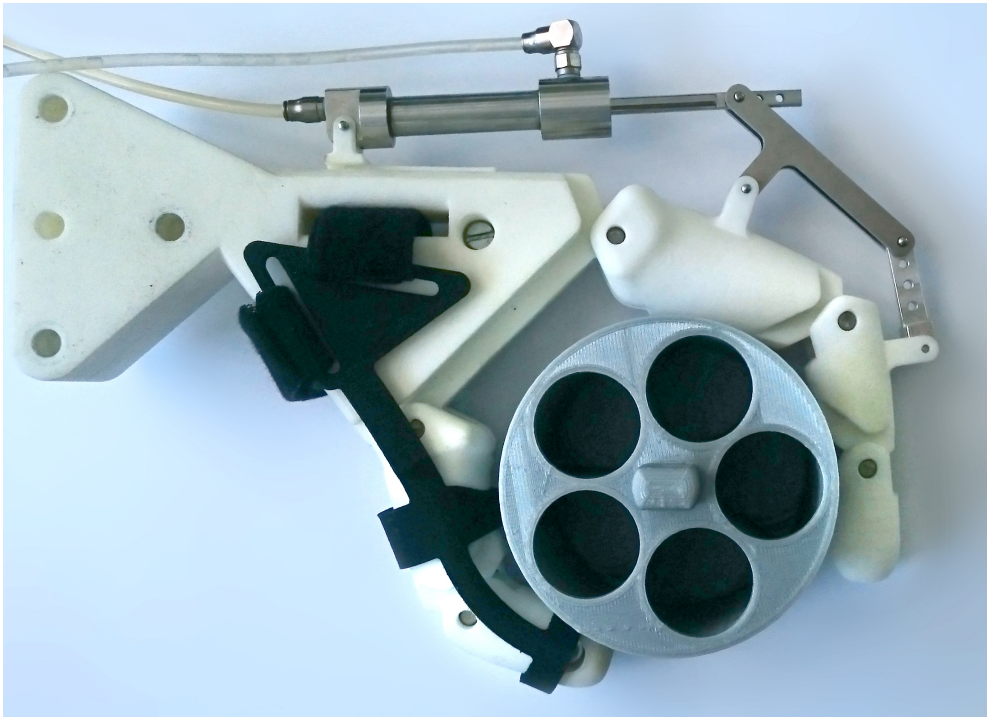

Figure 5.3: Picture of the manufactured prototype fixed on a mock-up hand, holding a circular object. The object was pulled out of the grasp with a cable connected to a force sensor. The hydraulic cylinder was connected to a master cylinder, onto which a weight was suspended for a constant system pressure.

parameters. The mechanism's shape was therefore varied with only one dimension, to prevent having to perform countless experiments and to maintain the ability to easily visualize the results. Naturally, a more realistic shape optimization scheme would include all key mechanism dimensions along with a sensitivity analysis around the optimum.

Changing L_T was expected to alter the range of motion and moment arm around the finger's proximal interphalangeal joint, affecting the attainable grasping force. Changing D_{obj} would test the mechanism's robustness to grasping different sizes of objects. The variations that were applied, along with the model and prototype dimensions, are shown in Table 5.1. In this table, hand interface locations describe the positions where the orthosis mechanism physically connects with a finger metacarpal or phalanx.

The objects were hollow cylinders and constructed using 3D-printed PLA. A diameter of 67.5 mm coincides with the average diameter of over 70 different 16 oz./500 mL bottles of popular brands Royal Vendors, Inc., n.d. and can be associated with an object mass of approximately 500 g. To accommodate this size and a range of 300-700 mL bottles as well, object diameters were varied between 60, 67.5 and 75 mm. All cylindrical objects had a height of 55 mm. Because the largest object had a mass of 80 g, gravitational effects were neglected.

Table 5.1: Dimensions used for modeling and construction of the mechanism.

VARIABLES		
Dimension	Symbol	Variations [mm]
Ternary link base length	L_T	40, 50, 60
Object diameter	D_{obj}	60, 67.5, 75
PARAMETERS		
Dimension	Symbol	Value [mm]
Mechanism dimensions		
Cylinder maximum stroke	s_{max}	36
Cylinder bore diameter	D_c	8
Piston rod length	L_R	63
Ternary link base position	B_T	15
Ternary link height	H_T	15
Binary link length	L_B	25
Hand dimensions		
Proximal phalange length	L_{PP}	55
Intermediate phalange length	L_{IP}	33
Distal phalange length	L_{DP}	26
Palm element length	L_P	60
Thumb proximal phalange length	L_{tPP}	43
Thumb distal phalange length	L_{tDP}	33
Proximal phalange thickness	t_{PP}	25
Intermediate phalange thickness	t_{IP}	19
Distal phalange thickness	t_{DP}	16
Thumb proximal phalange thickness	t_{tPP}	26
Thumb distal phalange thickness	t_{tDP}	22
Hand interface locations		
on metacarpals	p_{MC}	60
on proximal phalange	p_{PP}	25
on intermediate phalange	p_{IP}	10

The contact interaction between the 3D-printed mock-up hand and objects was considered as a stiff contact with a low coefficient of restitution ($c_r = 0.1$). The contact stiffness in the models was chosen as high as possible while maintaining a stable algorithm, which was mostly limited in the dynamic model. As a result, the dynamic model used a stiffness factor of $K_c = 1 \cdot 10^5$ Nm$^{\frac{2}{3}}$ (see Eq 5.10), whereas the static model was able to use a value of $K_c = 1 \cdot 10^9$ Nm$^{\frac{2}{3}}$. The fact that the models use different values for contact stiffness to simulate a rigid contact, is considered to be part of the models' traits and therefore part of the comparison between the modeling approaches.

Pressure on the cap-side of the hydraulic cylinder was applied by loading a master cylinder with a mass, until a pressure of 1.25 MPa was measured with a pressure sensor (SPAW-P50R-G12M-2PV-M12, Festo). A test bench was used to pull on the object in

a direction that was horizontal and parallel to the joint axes, where force (F_{pull}) was measured using a load cell (B3G-C3-50kg-6B, Zemic Inc). The object was pulled over a distance of at least 40 mm without losing contact with the object. In order to obtain the ability to hold the object (F_{hold}), this pulling force was divided by the friction coefficient between the object and mock-up hand. Vice versa, the inverse operation could be applied to estimate F_{pull} from the model outputs.

To avoid stick-slip effects that may influence the results, the object was pulled out at a constant velocity and the mean force was extracted. Furthermore, each configuration was measured five times. The dynamic friction coefficient was determined by measuring the average force necessary to move a 2, 4, 6 and 8 kg mass at the same velocity, resulting in a measured friction coefficient of 0.12.

In addition to the grasping force, the torque ratio between the proximal interphalangeal and metacarpophalangeal joint (M_{PIP}/M_{MCP}) was calculated from the contact forces to accompany the model results. This provided additional information on how the orthosis mechanism distributed force over these two phalanges. All contact forces should be similar for an equal force distribution Schuurmans et al., 2007 and so the ideal torque ratios can be scaled according to phalange lengths Kragten and Herder, 2010, which is approximately 0.52 for this situation.

5.4. RESULTS

The results for the force related to the ability hold objects are shown in Fig 5.4. Calculation times for the static model varied between 39–95 s, for the dynamic model this varied strongly between 118–1769 s. The results indicate, assuming a friction coefficient of 0.12, that F_{hold} for this mechanism ranged between 22–87 N according to the measured results, between 51–69 N according to the dynamic model predictions and between 44–68 N according to the static model predictions. The quantitative differences imply an agreement between the dynamic and static model, but a disagreement between these modeled outputs and the measured results.

Concerning relative differences, the outputs from the different methods (i.e., the measurements and models) agree within each object diameter. For instance, assuming D_{obj} = 67.5 mm, an optimization procedure would conclude with every method that L_T = 50 mm would give the highest possible grasping force. Compared to the measured results, however, the relative differences are very small between the model outputs.

In the static model, the torque ratios show more contrast than in the dynamic model. At L_T = 40 mm and D_{obj} = 60 mm, these torque ratios are (close to) zero for both models. This was also confirmed during the corresponding measurements, where it was observed that the intermediate phalange did not make contact with the object. Lastly, to illustrate the magnitude of the dynamic effects in the dynamic model, the individual masses of the finger elements were not larger than 6 grams and linear velocities of their centers of mass rarely exceeded 0.5 m/s.

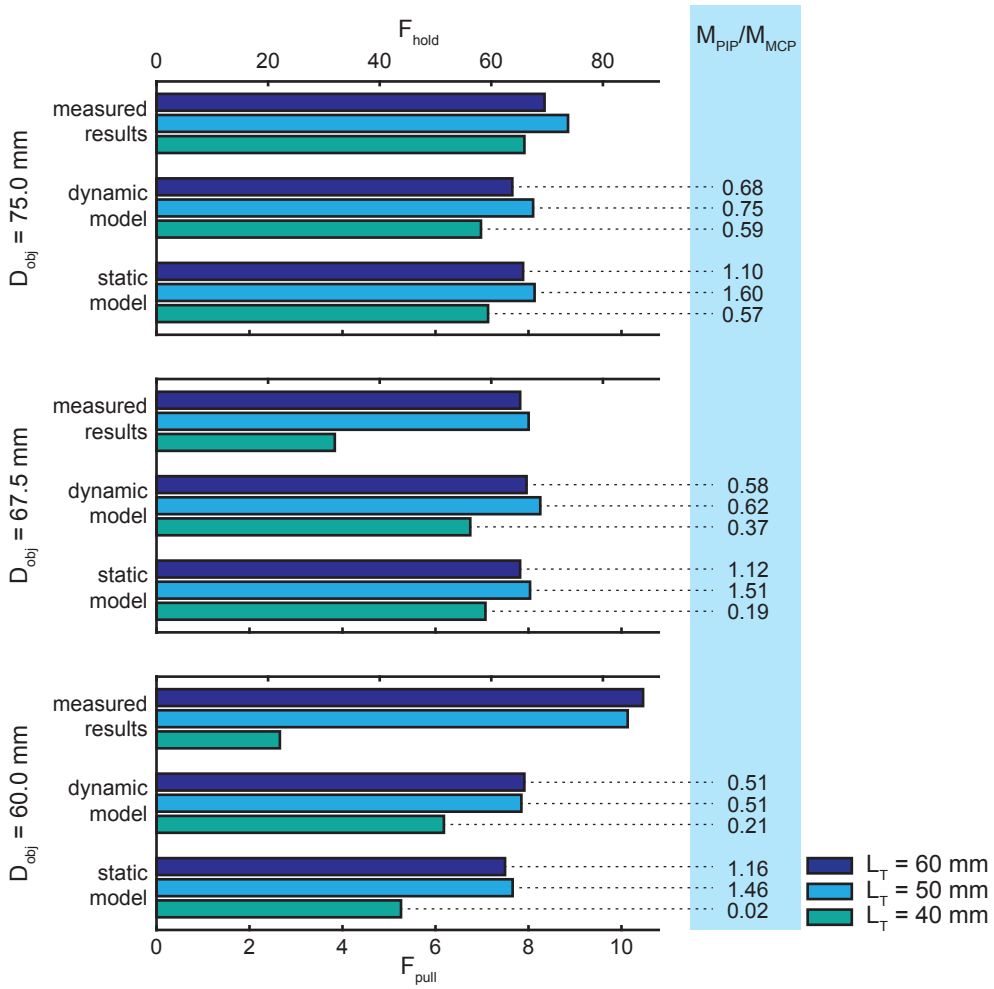

Figure 5.4: Measured and modeled results for forces related to the ability to hold objects. The sum all of normal forces (F_{hold}) is shown on the top horizontal axis. The force necessary to pull an object out of the grap (F_{pull}) is shown on the bottom axis. Additionally, the torque ratios (M_{PIP}/M_{MCP}) that accompany model outputs are displayed on the right.

5.5. Discussion

5.5.1. Dynamic versus static

In contrary to the dynamic model, the static model has no memory of previous states and can actually reach solutions that are not possible to reach or, in some cases, instable. A comparison of the outcomes of both models validates whether the static model is sufficiently constrained and able to reach the same conclusions as the dynamic model.

The results show that the grasping forces from the dynamic and static model are almost identical. This implies that the occurring velocities and inertial effects are indeed

small enough to be neglected. The torque ratios, however, show more variations. More specifically, the qualitative differences between these ratios are similar, but the contrast is increased in the static model. Because the static model used a higher value for contact stiffness, we argue that a compliant contact interface is more likely to equally distribute forces than a rigid contact interface.

In general, the torque ratios slightly increase towards a larger object size. This means that the emphasis shifts from the proximal phalange to the intermediate/distal phalange as the object diameter increases, which is more similar to human grasping Kargov et al., 2004; Rossi et al., 2012. However, comparison with existing literature is problematic because it usually describes grasping with a human hand Kargov et al., 2004 or a (symmetric) robotic grasper Dollar and Howe, 2011; Kragten et al., 2011. This study, on the other hand, uses only the first two phalanges of a human finger and a passive distal phalange. Moreover, the range of ratios that provide stable grasping strongly depends on the geometry of the grasper and several different grasping types are possible in each range Kragten et al., 2011. Therefore, in order to make more sense of these results, a grasping stability analysis is required for this particular situation.

5.5.2. MODEL AGREEMENT

Despite the agreement between the dynamic and static model, the measured results show larger quantitative differences and especially towards smaller object sizes. We attribute these differences to small dissimilarities in dimensions and contact stiffness.

While configuring the models, it was found that both approaches were sensitive to small changes in the hand dimensions. The experimental situation differed slightly from the model representation and may therefore account for a portion of the disagreement. The model used conical cylinders whereas the mock-up hand used more curved shapes to approximate an anthropomorphic shape.

The contact stiffness with the object was not adjusted to the experimental situation, which required a very high stiffness value in order to approach the stiff contact. Especially the dynamic model was not able to handle high values for contact stiffness ($k > 1 \cdot 10^5$), because this quickly resulted in the numerical integration algorithm to become instable (e.g., due to close to singular matrices). Similar to a previous argument, we believe that a rigid contact amplifies the contrast in the outcome measures, because it becomes less likely that multiple phalanges can contribute to the grasping force. This can most easily be visualized by referring to the results where D_{obj} = 60 mm and L_T = 40 mm. The results with the most rigid contact (i.e., measured results) showed no contact at all with the intermediate phalange and a low grasping force, whereas the most compliant contact (i.e., dynamic model) showed a more distributed pattern and higher grasping force. Alternatively, at D_{obj} = 75 mm, the hand is better able to envelop the object and make contact with all phalanges, reducing the dissimilarities between the different methods.

5.5.3. ORTHOSIS MECHANISM EVALUATION

It was found that the orthosis mechanism was able to achieve a stable cylindrical grasp for all configurations. From the results, it can be concluded that the mechanism configuration with L_T = 50 mm provided the highest overall grasping forces at a pressure of 1.25 MPa. The estimated grasping forces for this mechanism configuration are high, ranging between

22–87 N. Considering that a force of 25 N between the thumb and fingertips is sufficient to lift a 2.25 kg object of similar size Domalain et al., 2008, the presented orthosis mechanism is able to exceed the requirement to facilitate grasping of objects in daily living.

5.5.4. GENERALIZATION

Based on the presented system and experimental set-up, results cannot be generalized towards a situation that incorporates an anatomically correct human hand. However, conceptual designs can be compared in a qualitative way as they rely on the same simplifications. The connection with an anatomically correct hand is maintained by allowing the implementation of parametric stiffness characteristics in the anatomical joints and contact interfaces. Here, the static model allows for more freedom than the dynamic model, as it is not limited by stability issues that arise from the numerical integration process. By adding more details to the model, more similarities with the anatomical hand are introduced and quantitative outcomes are likely to further approach reality. For example, expanding to three-dimensional models can be helpful when other types of joints (e.g., spherical joints) are to be investigated, when a anatomically correct thumb is desired, or when multiple fingers are involved while grasping non-prismatic objects. Other pathological properties (e.g., stiff joints due to contractures) can be included in the model as well, for example by implementing joint stiffness profiles. However, further research is needed to investigate how such properties can affect the outcome of the model.

Beyond this particular example of a hydraulic hand orthosis with circular objects, the method presented in this study can be generalized towards a broader range of applications. The method is not limited by the use of hydraulic actuators, number of DOFs, object shape, two-dimensional scenarios or by hand orthoses. It allows any prescribed force, torque, translation or rotation to be used as an actuator, it allows any number of link elements to be connected by various joints and other convex-shaped objects can be used with the same contact detection scheme. When the mechanism becomes underactuated, however, it is important that enough stiffness elements (e.g., anatomical joint stiffness) are added to create a single valid equilibrium position.

The possibilities of the models can be further extended if the mechanism's bodies, constraints and their connectivity are represented by parameters that are irrespective of the topology. Potential applications are topology optimization or even automated mechanism design Kuppens and Wolfslag, 2018. Furthermore, flexible structures can be modeled using pseudo-rigid body modeling, but are more limited in accuracy. Addition of static friction can also include the analysis of grasps that are not bound by form closure.

The procedure to measure the grasping performance is simple and does not require an object to be equipped with pressure or force sensors. Therefore, any object can be pulled out of a hand that is fixed in position. This opens possibilities to validate the model predictions with human testing as well, which may also answer questions regarding compliancy of the contact interfaces.

5.6. CONCLUSION

The results from this study show that a static model provides for a fast and adequate alternative to a dynamic approach to investigate the ability to hold circular objects. Less

assumptions are required in order to estimate parameters related to dynamic effects (e.g., viscosity), rigid mechanical stops can be easily combined with compliant contact models and computation times can be around 10 times faster. However, there remain some discrepancies with experimental results that question the applicability of both models for real-world situations. These dissimilarities are mostly attributed to small differences in the used contact stiffness, where expansion to human testing can be the best method to determine model validity. Nonetheless, when relying on qualitative comparisons instead of quantitative predictions, the static model can be used to compare potential designs or even in optimization. Especially in an early design stage this is a useful tool for making well-supported design choices.

SUPPORTING INFORMATION

S1 File. Dataset. Matlab *.mat-file, which includes a structure that contains the simulation output data (e.g., grasping force, torque ratio, joint angles, simulation time) and measured values from the experimental set-up (average and minimum/maximum grasping force).
https://doi.org/10.1371/journal.pone.0220147.s001

S2 File. Figure generator. Matlab *.m-file, which uses the Dataset file and generates the results figure as displayed in this paper.
https://doi.org/10.1371/journal.pone.0220147.s002

6

DESIGN OF AN ELECTROHYDRAULIC HAND ORTHOSIS FOR PEOPLE WITH DUCHENNE MUSCULAR DYSTROPHY USING COMMERCIALLY AVAILABLE COMPONENTS

Bos, R. A., K. Nizamis, D. H. Plettenburg, and J. L. Herder

published in: 2018 International Conference on Biomedical Robotics and Biomechatronics (BioRob), pp. 305–311. Enschede, 2018.
DOI: 10.1109/BIOROB.2018.8487196

A B S T R A C T

People with Duchenne muscular dystrophy are currently in need of assistive robotics to improve their hand function and have a better quality of life. However, none of the available active hand orthoses is able to address to their specific needs. In this study, the use of hydraulic technology is proposed in the design of an active hand orthosis. Commercially available components were used to identify where customization is necessary for a new electrohydraulic hand orthosis. The presented prototype was able to move four finger modules with a single actuator. The finger modules were separable and had a total mass of only 150 g, whereas the valve manifold added another 250 g. Results revealed that the prototype was able to function well with full flexion/extension cycles up to 2 Hz, but with hysteretic losses between 37–81% of the total input energy. Specialized valves and slave cylinders are required to increase efficiency at higher speeds and to obtain more robust sealing performance.

6.1. INTRODUCTION

Duchenne muscular dystrophy (DMD) is an X chromosome-linked progressive neuromuscular disease, resulting in disability and shortened life expectancy (Bartels et al., 2011). It is the most common and severe form of muscular dystrophy (Darras et al., 2010). Recent advances in technology and medicine rapidly increased the life expectancy of people with DMD (Eagle et al., 2002). However, their hand function is rather limited (Mattar and Sobreira, 2008). Therefore, in order to have a better quality of life, they find themselves in need of assistive robotics (Janssen et al., 2014).

The importance of the hand function is highlighted by the great amount of orthotic devices developed in the last decades (Bos et al., 2016a). In contrast, at the moment, the only existing devices to support the hand function of people with DMD are static hand splints (Weichbrodt et al., 2018). Their aim is to postpone the development of contractures and maintain a satisfactory range of motion (Weichbrodt et al., 2018). Evidence suggests that people with DMD can greatly benefit from the use of orthotics (Bergsma et al., 2016), even passive (Weichbrodt et al., 2018). Nevertheless, those are not sufficient to assist in activities of daily living (ADLs).

As with any orthosis for daily assistance, it should be small, light-weight, comfortable (Radder et al., 2015) and provide enough force to support during ADLs. Creating a small and light-weight orthosis has proven to be challenging considering the small amount of design space that is available on the human hand. For people with DMD in particular, the interaction forces should not be too high due to an increased sensitive skin, and the hand orthosis needs to be donned onto the fingers one by one to more easily accommodate contracted fingers. Due to these factors, none of the existing devices meets the specific needs of people with DMD, hence a different approach is required in designing a dynamic hand orthosis.

The goal of this paper is to present the design of a hand orthosis that is actuated by an electric motor and uses miniature hydraulics as a method to transfer mechanical work. In particular, a prototype of the design is made as a platform to examine the use of commercially available components in terms of pressure and speed limitations. This helps to identify the bottlenecks of such a system and research focus for future iterations.

6.2. MINIATURE HYDRAULICS

In this study, the use of miniature hydraulics was explored for an active hand orthosis for people with DMD. The concept of using hydraulics to provide force and motion is certainly not new. Examples can be found at large scale in heavy machinery in construction (e.g., excavators, cranes). Also at micro-scale, hydraulics is being used in lab-on-a-chip systems. Between those scales, where hydraulic components are sized in the range of several millimeters, it becomes more feasible for orthotic applications. As long as this miniaturization is coupled with an increase in system pressure, hydraulic systems can be more compact and light-weight than an electromagnetic equivalent (Xia and Durfee, 2013). There are not many other applications that operate on this scale and therefore components are hard to find. Nonetheless, it is useful to find the limitations on what is currently commercially available and which components are hindering further miniaturization of hydraulics.

A hydraulic system can be largely characterized by the type of actuator that is used. Following the classification in de Volder and Reynaerts (2010), fluidic actuators can be either elastic or inelastic. Within the elastic class, McKibben-type actuators are easiest to obtain, whereas piston-cylinders with contact seals are the most widely available inelastic actuators. McKibben-type actuators can provide the highest forces relative to their cross-sectional area (i.e., actuator stress (Huber et al., 1997)). However, as is the case with all elastic actuators, available force from the actuator decreases as stroke is increased (Ryu et al., 2008) and system pressure is limited by the material (Polygerinos et al., 2015c). This is not the case with piston-cylinders, which can provide the maximum rated force over the full range of stroke (Plettenburg, 2005). Moreover, the available stroke relative to initial length (i.e., actuator strain (Huber et al., 1997)) is higher for piston-cylinders. Based on these observations, piston-cylinders were chosen as the most suitable type of actuator.

Hydraulic components can be connected with each other using flexible hoses, effectively providing a flexible transmission of mechanical energy. This makes it possible to place heavier equipment (e.g., pump, energy storage) away from the hand and, for example, fix it to the wheelchair. In contrary to a Bowden cable system, a hydraulic transmission can provide a more transparent force efficiency that is independent of any bends in the hose (LeBlanc, 1985). The only losses in efficiency are related to wall friction within the hoses and small added friction coefficients due to smooth bends (Janssen and Warmoeskerken, 2006). These were assumed negligible compared to O-ring friction in the actuators.

Only a few examples can be found where a hydraulic system was used in a hand orthosis (Ryu et al., 2008; Polygerinos et al., 2015c), but these systems use elastic actuators that limit the available force for larger joint angles and maximum system pressure. As a related application, more examples can also be found in hand prosthetics (Kargov et al., 2008; Love et al., 2009; Smit et al., 2015). Similar to orthotics, reported arguments are generally aimed towards minimization of added volume and mass—one of them resulting in the most light-weight hand prosthesis (Smit et al., 2015). All examples, however, rely on customized components and do not provide an insight on their accessibility compared to, for example, electromagnetic systems.

6.3. DESIGN CRITERIA

The design criteria for the presented hand orthosis were similar to a mechanism that was designed in a previous study by Bos et al. (2017). Specifically, the number of degrees of freedom, size of the design domain and maximum resultant force on the skin were kept the same. In this design, the thumb was not included but assumed to be fixed in opposition. Other criteria were adjusted and added in order to accommodate this particular target group. A summary of the criteria is given in Table 6.1. In this section they are elaborated in more detail.

The main objective of a hand orthosis that provides assistance during ADLs is to provide sufficient grasping force and range of motion. In Kargov et al. (2004), the highest joint moment in the human hand was measured at 0.1 Nm in order to grasp a bottle of approximately 0.5 kg. In order to be able to include a larger variety of graspable objects and levels of skin hydration (which affect attainable friction forces with the skin (Derler and Gerhardt, 2012)), a value of twice this magnitude was chosen, namely 0.2 Nm per

Table 6.1: List of design criteria for the hand orthosis.

Criterion	Description [metric]	Implementation
Grasping force	Joint moment [Nm]	0.2 Nm per joint
Range of motion	Flexion angle range [°]	20–80° per joint
Degrees offreedom	Functional degrees offreedom [#]	1
Design domain	Cross-section [mm×mm]	26×17 mm
Comfort	Resultant force on skin [N]	<5 N
	Shear force [N]	0 N
Mass	Mass on hand [kg]	<200 g
Speed	Cycle frequency [Hz]	2 Hz
Wearability	Easy donning/doffing	Separable finger modules

joint. To accommodate movement, an average range of finger flexion angles of 20–80° were chosen which relate to a functional range of motion (Bain et al., 2015).

Only forces normal to the fingers' skin surface contribute to an increase in grasping force. Shear forces, on the other hand, increase the resultant force and the related risk of skin tissue damage, while they do not contribute to grasping force. This means that shear forces should be avoided at all costs.

The orthosis should not interfere with the hand too much. This is reflected in the criteria for range of motion, but should also include a limit on the perceived mass. Similar systems mention a mass limit around 500 g (Aubin et al., 2014; Polygerinos et al., 2015c) that is placed on the hand, where heavier components can be placed on more proximal locations or even attached to the wheelchair. For people with DMD, however, it is believed that this value should be even lower because any additional weight will cause more strain on already weakened muscles or on the potential arm supports. Hence, a mass limit of 200 g was imposed on this design. Other factors that may increase the perceived mass are stiff elements that connect the hand module with the heavier components. We aimed to keep this added stiffness minimal.

The speed at which the hand orthosis is able to move, should not be a limiting factor to achieve natural human movement and to be able to respond to fast changes in intention. Based on speeds that occur in the hand while performing ADLs, cycle frequencies between 0.5-1.6 Hz have been reported in the design of hand orthoses and prosthesis (Wiste et al., 2011; Polygerinos et al., 2015c). Additionally, a recent study with one person with DMD, implies that people with DMD can process signals and respond successfully with finger movements no faster than 2 Hz (Nizamis et al., 2017). Hence, a full cycle frequency of 2 Hz was deemed sufficient and chosen as criterion.

One of the complications regarding people with DMD, is the occurrence of contractures (Wagner et al., 1989). This can make it difficult and even painful for these individuals to don glove-like systems, which requires all fingers to be stretched simultaneously. Therefore, in order to improve wearability of the hand orthosis, easy donning/doffing should be facilitated by incorporating separate finger modules, allowing each finger to be fitted one-by-one.

6.4. DESIGN DESCRIPTION

An illustration of a single finger module of the hand orthosis is shown in Fig. 6.1.

6.4.1. HYDRAULIC SYSTEM

SLAVE ACTUATORS

To the authors' knowledge, there is no commercially available hydraulic piston-cylinder that has a diameter of < Ø8 mm and states to be able to work with pressures of >2 MPa. Nonetheless, a line of small pneumatic cylinders from Festo were used. They are rated at 0.7 MPa for pneumatic use, but their ability to work with water and much higher pressures were tested. In particular, to maximize available actuator strain, Ø4 mm cylinders with 20 mm stroke were used (EG-4-20-PK-2, Festo).

MEDIUM

Because a hand orthosis requires a close interaction with a human operator, the medium should not cause damage to the skin or stains on fabric in case of any leakage. Therefore, water was chosen as medium. It is a neutral fluid and has been used in other miniature hydraulic systems as well (Ryu et al., 2008; Smit et al., 2015).

TRANSMISSION

The flexibility of the hydraulic transmission can have a large influence on the risk of leakages and perceived mass of the hand orthosis. Low-pressure hoses are generally more flexible than high-pressure hoses and available in the smallest diameters. Using them at higher pressures, however, can cause them to expand, which decreases the bulk stiffness and increases hysteresis of the hydraulic system. Maximizing flexibility was considered to be more important than overall system stiffness and hysteresis. For this reason, a standard polyurethane hose that was compatible with the fittings on the slave actuators was used (PUN-H-3x0.5, Festo).

CIRCUIT

To minimize the added stiffness from the hydraulic transmission between the heavier components and the hand orthosis, it was facilitated with only one hose. This way, only one master cylinder could be used and all supported degrees of freedom of the hand orthosis were underactuated. For each finger, this means that slave cylinders will curl around any object's shape. Across the fingers, the hand can adapt to three-dimensional shapes (e.g., spheres) as well (In et al., 2011; Smit et al., 2015). The overall schematic of the hydraulic system is shown in Fig. 6.2, which is very similar to the one shown in Smit et al. (2015). The only added feature is a set of electrically operated valves that allow to control which fingers to move and which to block—an approach which can also bee seen in Kargov et al. (2008).

VALVES

In order to support multiple fingers and be able to switch between different grasp types, a hydraulic hand orthosis should also contain valves that are able to facilitate this functionality. As displayed in Fig. 6.2, each valve can block or permit the flow of pressurized fluid so that specific groups of slave actuators can be selected to move. In the presented design, 2/2-way on/off normally-closed valves were chosen. The smallest

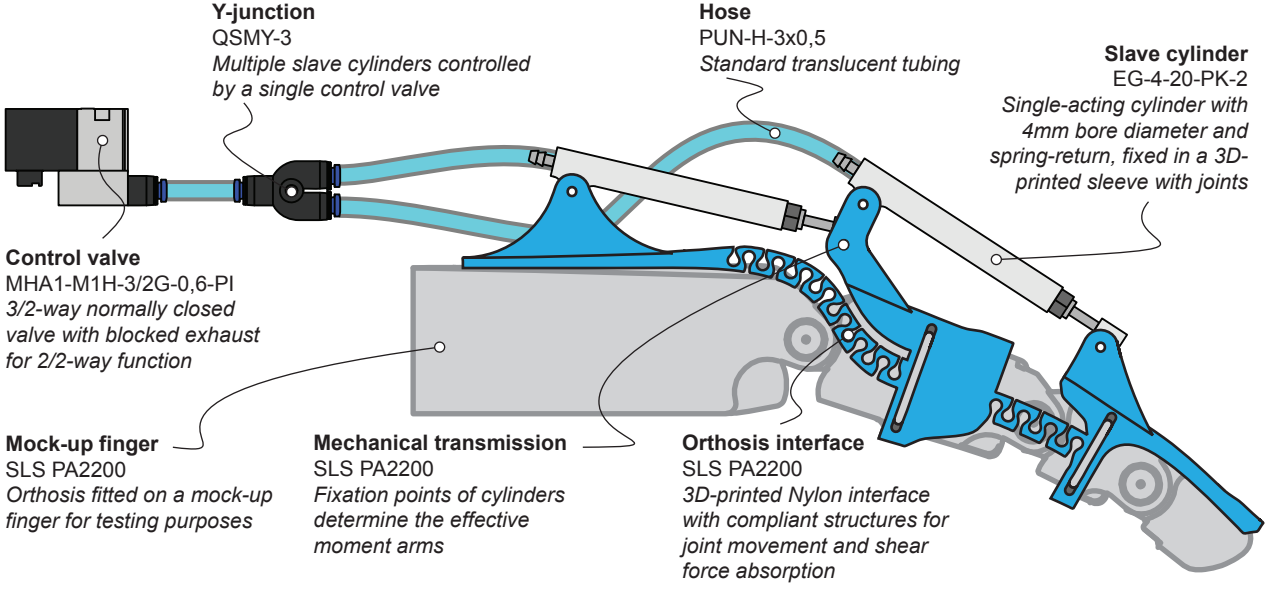

Figure 6.1: Illustration of a single finger module of the hand orthosis.

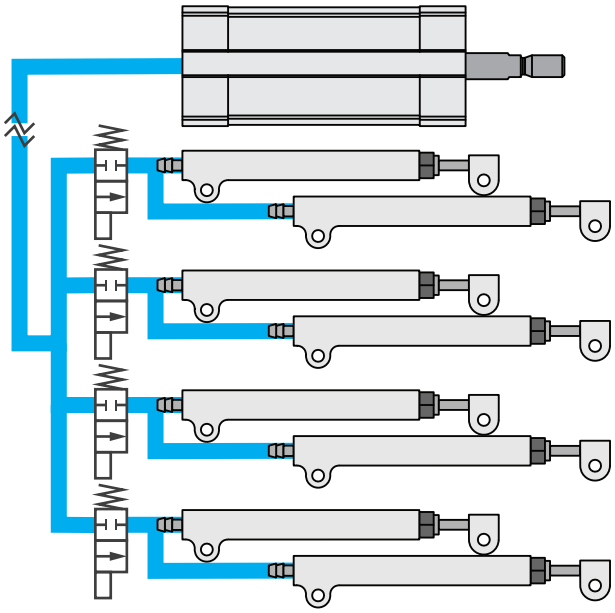

Figure 6.2: Schematic of the hydraulic system, where one master cylinder underactuates several slave cylinders. Each finger is equipped with two slave cylinders, whose movement can be blocked or allowed by the 2/2-way valves.

available valves with highest rated pressure from Festo were explored. Because it used a smaller nozzle diameter of 0.65 mm, a 3/2-way miniature valve with blocked exhaust provided the 2/2-way function at a rated pressure of 0.8 MPa (MHA1-M1H-3/2G, Festo).

6.4.2. HAND ORTHOSIS MECHANISM

MODULAR APPROACH

In order to accommodate the specific needs of people with DMD, the hand orthosis should allow each finger to be fitted individually. The weaker hand muscles combined with possible contractures make it very difficult to align all fingers properly at the same time. This restricts the use of any glove-like orthosis. As an alternative, we chose to design separate finger modules that can be donned one-by-one.

COMPLIANT MECHANISM

To minimize the shear forces, a compliant mechanism was developed with the purpose of absorbing shear forces. More specifically, the parts that interface with the metacarpals and phalanges of each finger were connected by flexure elements. These flexures should be strong enough in tensile direction to absorb the shear forces, but should also accommodate the joint motion with minimal added stiffness and allow small joint misalignments. This part was made by 3D-printing polyamide (PA 2200) using selective laser sintering (SLS). Due to the strength of the material, the flexures were implemented with a zig-zag-like shape in order to reduce overall bending stiffness. Additionally, this

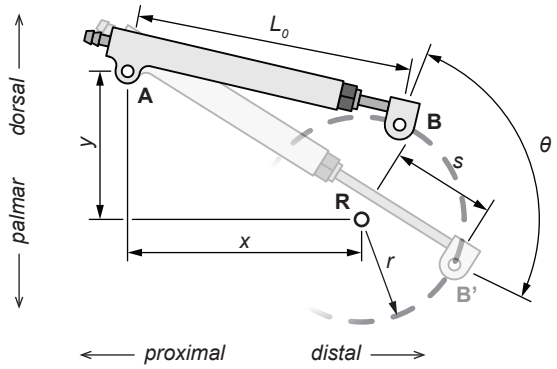

Figure 6.3: Illustration showing the relation between the slave actuator's stroke (s), initial length (L_0) and placement of the proximal connection (x, y) with the moment arm (r) and resulting joint range of motion (θ) around the finger joint ($\boldsymbol{R}$).

also allowed for slight elongations of the flexures, making the interface compliant to disturbances.

MECHANICAL TRANSMISSION

The total range of motion for each finger joint that can be achieved by direct actuation with a linear actuator is limited to a certain amount. In Fig. 6.3, it can be seen that the desired moment arm (r) and range of motion (θ) affect the (x, y)–placement of the proximal connection ($\boldsymbol{A}$) of the actuator. Moving the distal connection ($\boldsymbol{B}$) as proximal as possible is desirable, because this maximizes the attainable range of motion and avoids the actuator rod to hit the skin. However, this placement is limited by the slave cylinder's initial length (L_0) and possible interference with the second cylinder. Especially due to these factors, placement was also a practical consideration, where a moment arm of $r = 20$ mm was used for each slave cylinder and the dorsal distance from the joint center was limited to $y = 30$ mm. In combination with the chosen slave cylinders, this allowed for a theoretical flexion angle range of 10–80°.

Only the two proximal joints of the finger (i.e., metacarpophalangeal and proximal interphalangeal joint) were supported in flexion/extension. Using results from robotic grasping, two phalanges are sufficient to reach a stable grasping position (Kragten and Herder, 2010). The most distal joint (distal interphalangeal joint) was only protected against overextension by extending the orthosis interface (see Fig. 6.1).

6.5. DESIGN CHARACTERIZATION

6.5.1. PROTOTYPE

A photo of the resulting prototype in several poses is shown in Fig. 6.4. For purposes of characterizing the hand orthosis, it was fitted onto mock-up fingers. They were manufactured by 3D-printing polyamide (PA 2200) and showed an anthropomorphic shape. Each joint contained an integrated leaf spring of the same material which added a small but non-linear dummy stiffness, whose resting position was in a slightly

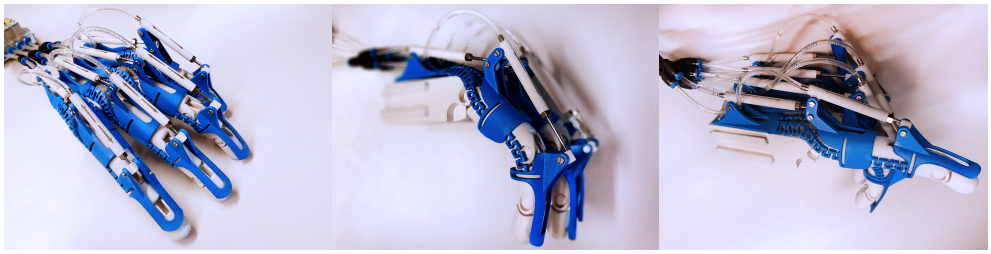

Figure 6.4: Photos of the prototype fitted on a mock-up left hand with, from left to right, fully extended position, fully flexed position and pointing with index finger.

flexed position of 20°. The added stiffness was characterized with a linear stiffness of approximately 0.01 Nm/rad around its resting position.

Each metacarpophalangeal joint expressed an active range of motion of 30–65° flexion, for each proximal interphalangeal joint this was 10–45°. The amount of finger elements involved in the (grasping) motion could be selected with on/off valves and, for example, allowed it to switch from a power grasp to pointing with the index finger (see Fig. 6.4). The maximum occupied cross-section on top of each finger was 33×19 mm (height×width). Each finger module could be donned/doffed separately, where the mass on the hand for all four modules was measured at 150 g. The valve manifold added a mass of 250 g. The grasping force and interaction forces were not measured in this study.

6.5.2. DYNAMIC BEHAVIOR

To evaluate the dynamic behavior of the system, a large electric motor (AKM22C-BNCNC-00, Kollmorgen) with spindle drive was used to move the master cylinder. The master cylinder was subjected to full stroke cycles at different frequencies and the resulting system pressure was recorded with a pressure sensor (3500-B-0040-A-01-B-0-00RS, Gems Sensors & Controls). The range of frequencies were chosen to be between 0.5–5 Hz with steps of 0.5 Hz, well below and above the required full cycle frequency of 2 Hz. All valves were opened such that all slave cylinders and mock-up fingers moved along, imposing the maximum load for free movement (i.e., no grasping).

Fig. 6.5 shows the measured system pressures as a function of the master cylinder stroke. Each curve represents the average of 10 cycles during steady-state operation. Due to the return springs in the single-acting cylinders and stiffness in the joints of the mock-up fingers, the curves show a distinguished loading (i.e., fingers flexing) and unloading (i.e., fingers moving back to resting position) curve. The peak value of the loading curve clearly increases with increasing frequency, whereas the unloading curve shows a lower limit due to the passive elements. After approximately 2.5 Hz the shape of the load curves slightly changes, where pressures below atmospheric pressure were measured and an overall delayed increase towards the peak pressure can be observed.

Fig. 6.6 shows energy values that correspond to the tested frequencies. The energy expenditure of the system was estimated by integrating the measured pressure over displaced volume ($E = \int pdV$), where the loading curves determined the input energy and the unloading curves the output energy. The difference between these values was determined as the hysteresis for one full cycle. In these results it can be seen that an

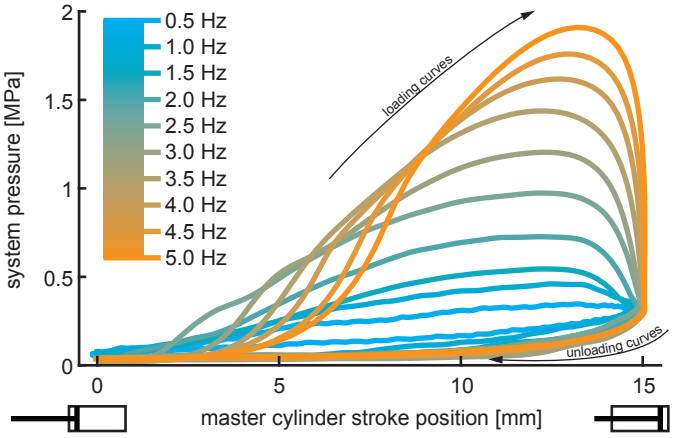

Figure 6.5: Loading and unloading curves of the system pressure versus master cylinder stroke. Different full cycle frequencies were imposed at the master cylinder and affect the measured system pressure.

increase in speed comes at the cost of increased hysteresis and total input energy. The system is most sensitive to changes in speed around 2 Hz, which is also be reflected by the altered shapes of the pressure curves in Fig. 6.5 and implies a change in dynamic behavior. At 2 Hz, both relative hysteresis and total input energy have doubled in magnitude compared to the results at 0.5 Hz.

6.5.3. COMPONENTS

The components of the hydraulic system that were used in the design showed high resilience to increased system pressures. A static measurement revealed that the valves were no longer able to block fluid flow at pressures above 1.5 MPa. The slave cylinders showed no signs of leakage at pressures up to 2 MPa. With closed valves, a decrease in bulk stiffness was observed for increased system pressure, which imply radial expansion of the hose material. At full cycle frequencies higher than 2.5 Hz, a substantial increase in air bubble formation was observed in the hydraulic hoses and coincide with the observed changes in dynamic behavior. Additionally, after one month, one of the valves showed signs of corrosion inside and needed to be cleaned in order to function properly.

6.6. DISCUSSION

The valves were the main limiting factor in terms of speed, pressure and mass. They contained the smallest orifices in the system with 0.65 mm in which fluid speeds can rapidly increase, making turbulent flow possible after 1 Hz in this design. This caused fluid friction to increase in magnitude and can be seen by the fast increase in hysteresis for increasing cycle frequencies. The Venturi effect caused local pressures to drop below the medium's vapor pressure and cavitation bubbles were clearly visible. Additionally, the valves had the lowest maximum pressure and the valve manifold added a mass which was

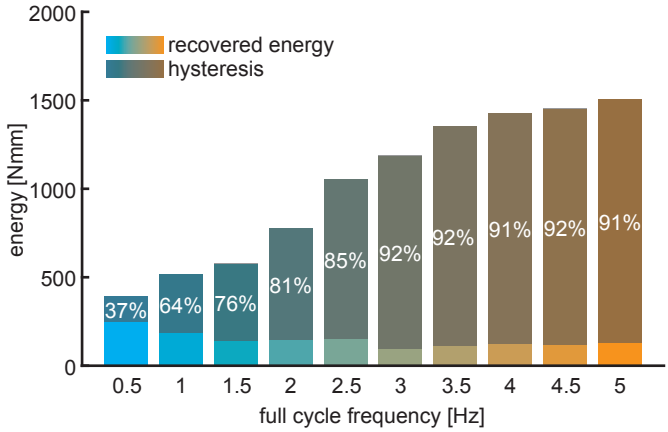

Figure 6.6: Calculated energy values for each tested full cycle frequency. The total height indicates the required input energy to fully load the system (reaching maximum finger flexion). After unloading, a percentage (indicated in white) is lost due to hysteresis and the rest is recovered from the passive elements.

almost twice as much as all the finger modules. Combined with the observed corrosion, different valves are required with increased water compatibility, larger nozzle diameter, higher pressure limit and lower mass.

The slave cylinders were able to accommodate water at higher pressures and did not add much volume and weight to the orthosis. Their initial length, however, required the fixation points to be stacked on top of each other. This caused the mechanism to have larger protrusions and have a lower margin on the range of motion to make up for relative movement of the compliant interface. Moreover, it did not allow for much variations in moment arms, which can provide more human-like force distributions (Kargov et al., 2004) and increased grasping stability (Kragten and Herder, 2010). The U-cup sealing elements in the slave cylinders were not able to seal against vacuum pressures, which occurred when the master cylinder was retracting faster than the return springs could follow. Custom slave cylinders can improve the design when they have a higher actuator strain, stronger return springs and more robust sealing elements.

A substantial number of air bubbles were visible in the system at higher cycle frequencies and affected the dynamic behavior of the hand orthosis. This is due to the combination of pressure drops below vapor pressure inside the valves and air being sucked in at the slave cylinders' sealing elements. The compression and expansion of the air bubbles slightly increased the amount of recovered energy and the added volume caused the pressure at rest to increase. More importantly, the added compliancy delayed the system pressure's response to the master cylinder's position input. At the highest frequencies, it attenuated the motion of the slave cylinders—explaining the lower increase rate in required input energy. Vacuum treatment of the water or using a different medium with lower vapor pressure can decrease these effects. Alternatively, the speed of the master cylinder needs to be limited according to the system's capabilities.

Even at the lowest frequency, the total efficiency is quite low compared to a previous hydraulic master-slave system (LeBlanc, 1985). Naturally, the mechanism and mock-up hand add more losses to the system, but expansion in the hoses' material also add hysteresis to the system. Hoses with higher radial stiffness can alleviate this effect. In its intended application, this will become more important as system pressures will be higher when objects need to be grasped and more realistic joint stiffnesses are present—including the possibility of increased stiffness due to muscle contractions. Human testing is required to validate this increase in pressure, but was considered out of scope of this study.

The presented design lacks an integrated energy storage and pump that controls the master cylinder. For a fully functional and controllable electrohydraulic hand orthosis, these components are indispensable as well and need to be optimized for minimal volume occupation. It is also possible to replace the master cylinder with a different fixed displacement pump (e.g., gear pump), but this would also require the addition of a reservoir with return line or additional valve.

To further decrease weight and increase portability, less finger modules can be used. For example, depending on the wearer's situation, supporting only the index and middle finger can already suffice in improving the ability to grasp some daily objects (In et al., 2015). However, supporting as many fingers as possible also encourages more finger movement and can possibly retard the development of contractures. It is unclear whether such an increased portability can outweigh this potential rehabilitative effect and requires further research. Either way, with the modular approach of the presented design it is relatively easy to attach or detach finger modules.

6.7. CONCLUSION

This study has shown that it is possible to create an electrohydraulic hand orthosis using commercially available hardware components, with the only exception being the 3D-printed structure which was custom-printed by a 3D-printing company. The prototype underactuated all flexion/extension movements with a single functional degree of freedom and consisted of separable finger modules. It was able to operate within the 2 Hz limit, but came at the cost of a large increase in energy losses. The mass was exceeded due to a heavy valve manifold and the desired range of motion and design domain were not reached due to low actuator strains in the slave cylinders. Evaluating the feasibility of the design and the individual components revealed possible bottlenecks and further improvements, indicating that the used methodology may still be a feasible solution for people with DMD. Specifically, specialized valves can decrease hysteresis, increase attainable system pressures and decrease mass; custom slave cylinders can reduce actuator strain, reduce occupied volume and improve sealing performance; and, stiffer hoses can reduce bulk stiffness and hysteresis, which can increase the system's overall efficiency.

ACKNOWLEDGEMENTS

The authors would like to thank Dr. Metin Giousouf from Festo for his help with realizing the prototype and Kyrian Staman for his support with the measurement set-up.

7

A CASE STUDY WITH SYMBIHAND: AN SEMG-CONTROLLED ELECTROHYDRAULIC HAND ORTHOSIS FOR INDIVIDUALS WITH DUCHENNE MUSCULAR DYSTROPHY

Bos, R. A., K. Nizamis, M. Sartori, H. F. J. M. Koopman, J. L. Herder, and D. H. Plettenburg

Accepted for publication in Transactions on Neural Systems & Rehabilitation Engineering

A B S T R A C T

With recent improvements in healthcare, individuals with Duchenne muscular dystrophy (DMD) have prolonged life expectancy, and it is therefore vital to preserve their independence. Hand function plays a central role in maintaining independence in daily living. This requires sufficient grip force and the ability to modulate it with no substantially added effort. Individuals with DMD have low residual grip force and its modulation is challenging and fatiguing. To assist their hand function, we developed a novel dynamic hand orthosis called SymbiHand, where the user's hand motor intention is decoded by means of surface electromyography, enabling the control of an electrohydraulic pump for actuation. Mechanical work is transported using hydraulic transmission and flexible structures to redirect interaction forces, enhancing comfort by minimizing shear forces. This paper outlines SymbiHand's design and control, and a case study with an individual with DMD. Results show that SymbiHand increased the participant's maximum grasping force from 2.4 to 8 N. During a grasping force-tracking task, muscular activation was decreased by more than 40% without compromising task performance. These results suggest that SymbiHand has the potential to decrease muscular activation and increase grasping force for individuals with DMD, adding to the hand a total mass of no more than 241 g. Changes in mass distributions and an active thumb support are necessary for improved usability, in addition to larger-scale studies for generalizing its assistive potential.

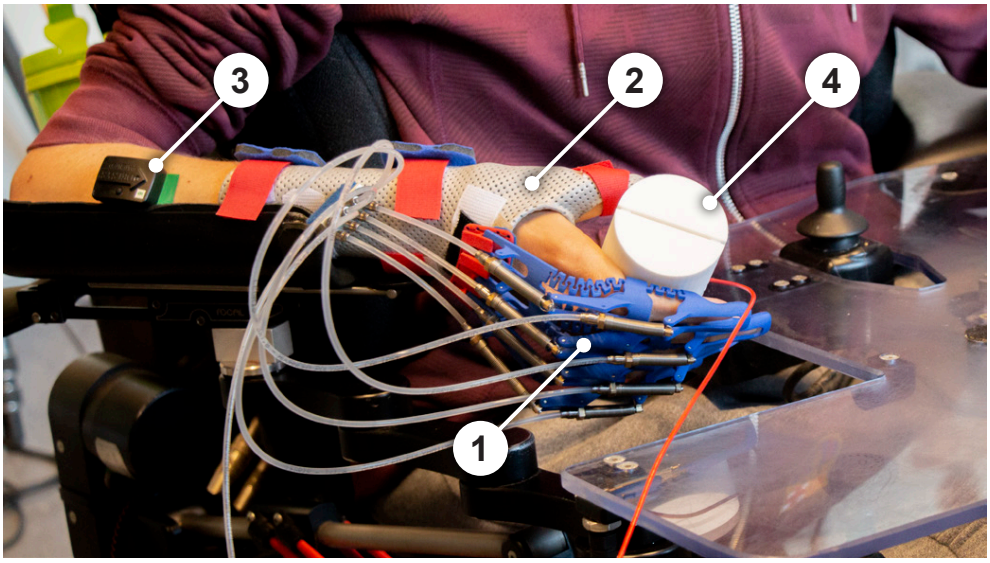

Figure 7.1: The participant with DMD grasping the sensorized object while wearing SymbiHand orthosis. 1) SymbiHand, consisting of four finger modules. 2) The thermoplastic hand splint, used to stabilize the wrist and thumb while providing an anchoring surface for the four finger modules. 3) Wireless sEMG sensor, placed on the extensor digitorum communis muscle. 4) The cylindrical sensorized object, used for measuring grasping force.

7.1. INTRODUCTION

Duchenne muscular dystrophy (DMD) is a progressive neuromuscular disease and is the most common form of muscular dystrophy, affecting approximately 1 in 5000–6000 live births (Janssen et al., 2014; Ryder et al., 2017). It results in severe disability, a strong dependence on care (Pangalila et al., 2015), and a subsequent decline in functional abilities (Haley et al., 2010). Recent scientific advances have increased the life expectancy of individuals with DMD up to 40 years (Bushby et al., 2010a), leading to an increase in the number of adults with DMD living with severe physical impairments and decreased functionality (Rahbek et al., 2005).

The hand plays a central role in performing activities of daily living (ADL), and its use is related to an increased quality of life in individuals with DMD (Lue et al., 2017). ADL require sufficient grip forces and additionally the ability to modulate those, without additional effort or fatigue. In DMD, the hand grip force significantly declines after the age of 12, accompanied by early fatigue onset (El-Aloul et al., 2019), leading in increasing inability of performing ADL (Mattar and Sobreira, 2008). However, hand treatment for such individuals is not receiving a lot of attention (Wagner et al., 2007), and there is no evidence of training grip force modulation or hand fatigue reduction in individuals with DMD. Existing studies highlight the importance of hand function in DMD and the need for more studies regarding grasping force that showcase that early interventions might slow the deterioration process (Wagner et al., 1993).

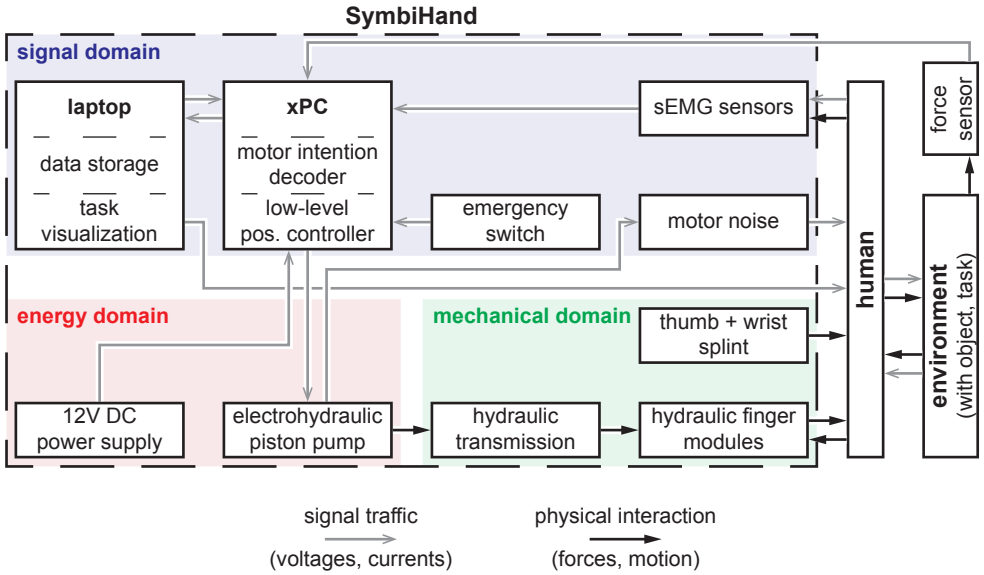

Figure 7.2: System overview of the different components of SymbiHand, subdivided into a signal, energy, and mechanical domain.

Current hand treatment for individuals with DMD, includes physical therapy (Wagner et al., 2007) or the use of hand splints during the night, which preserve the passive range of motion of the wrist and thumb (Weichbrodt et al., 2018), yet do not train grip force modulation or attenuate fatigue. Active assistive devices, however, can improve the quality of life of individuals with DMD and enhance their social participation (Bergsma et al., 2016), by addressing those issues. Evidence is increasingly highlighting the need for a comprehensive and multidisciplinary rehabilitation of individuals with DMD (Bushby et al., 2010a; Bushby et al., 2010b) that favors the use of dynamic hand orthoses.

Dynamic hand orthoses require a robust and intuitive way of decoding the user's intention and controlling the resulting mechanical output (Lenzi et al., 2012). Surface electromyography (sEMG) is a well-established method of decoding the motor intention of a user (Farina and Sartori, 2016) and is broadly used to enable the control of active hand orthoses (Bos et al., 2016a). Direct sEMG control was successfully tested in the past with individuals with DMD, combined with a first-order admittance model to control active elbow/shoulder orthoses (Lobo-Prat et al., 2016; Lobo-Prat et al., 2017). Two conference proceedings from Polygerinos et al. (Polygerinos et al., 2015a; Polygerinos et al., 2015b) with participants suffering from muscular dystrophy show promising results for the motor intention decoding of the hand motion. Additionally, there is work measuring weak sEMG signals in other patient populations such as stroke (Lee et al., 2011), and designing active orthoses for people with stroke or spinal cord injury (SCI) (Cappello et al., 2018; Yap et al., 2017). However, these conditions are not directly comparable to DMD due to differences in muscle activation, muscle strength and the presence of spasticity (Nizamis et al., 2019). To the authors' best knowledge, there is no evidence of the use of this sEMG for the

real-time decoding of hand motor intention with individuals with DMD, in combination with a first-order admittance model and hydraulic transmission. This is applied for the first time in the current study combined with a new dynamic hand orthosis.

A large number of existing hand orthoses can be found (Bos et al., 2016a), but none of them were deemed suitable for individuals with DMD. Important requirements are the ability to don individual finger elements, minimum shear forces on the skin and minimum perceived mass on the hand (Bos et al., 2018b). This resulted in choosing for a hydraulic transmission for its high energy density and transparent force transmission, and flexible structures to minimize the shear force components on the skin. Additionally, a hydraulic circuit is able to couple each finger element by force with flexible tubing, allowing for each finger element to be donned one-by-one while also providing a self-adaptive grasp. However, small-scale hydraulic components are not easily available as commercial products (Bos et al., 2016a). In this study, hydraulic components were customized to fit into a low-profile mechanism while still providing sufficient pressure resilience. Additionally, a first order admittance model was employed, in order to manipulate the virtual dynamics of the hand orthosis and add an extra level of control customization for the participant as proposed in (Nizamis et al., 2019). In combination with sEMG control, the combined system is called SymbiHand.

The objective of this study was to assess SymbiHands' potential to actively assist the grasping function of an individual with DMD in a case study. The primary purpose of SymbiHand is to augment the user's grasping force and additionally reduce the muscular activation needed to open/close the hand. This can help to extend the hand functionality of individuals with DMD and delay the onset of fatigue related to grasping.

7.2. METHODS

7.2.1. PARTICIPANTS

One 23-year-old male participant, diagnosed with DMD, took part in this study. He had not used hand splints in the past, and his dominant right arm was actively assisted by an arm support (TOP/HELP, Focal Meditech, Tilburg, Netherlands). He had a Brooke score (Jung et al., 2012) of 5 (range 0 - 6), meaning that he cannot raise hands to the mouth, but could use his hands to hold a pen or pick up pennies from the table. The Performance of Upper Limb (PUL) score (Mayhew et al., 2013) was 8 out of a maxmimum of 74 (summation of: 0 on the shoulder dimension, 1 on the elbow dimension, and 7 on the wrist/hand dimension). Minimal contractures relevant to finger movement were observed, and the range of motion (ROM) of the fingers was quite well preserved, yet slightly limited. However, he was experiencing early fatigue onset and a substantial decrease in grasping force. The severe hand/wrist weakness of the participant could highlight the effect of SymbiHand, combined with the absence of extensive finger contractures (that would made donning/doffing challenging and would not allow a large ROM support) and his availability for participation in the needed time-frame, made him an ideal participant for this case study.

The study design, experimental protocol, and procedures were approved by the Delft Human Research Ethical Committee (HREC) under ID 482. The study was conducted according to the ethical standards given in the Declaration of Helsinki of 1975, as revised

in 2008. The participant was informed via a letter and signed a consent form prior to the experiment.

7.2.2. SYMBIHAND

A picture of the manufactured prototype of SymbiHand worn by the participant is shown in Fig. 7.1 and a video of the participant controlling SymbiHand in real-time in Bos et al. (2018). The total mass on the hand was 241g. Table 7.1 shows a more detailed mass distribution. The piston pump assembly, which includes the master cylinder, had a mass of 526g.

SymbiHand consists of components in the signal, energy, and mechanical domain (Fig. 7.2) (Bos et al., 2016a). It aids the user in performing tasks by exchanging signals and physical interactions with the user, who, in turn, interacts with the environment. The intention of the participant was decoded in real time with the use of direct sEMG control, combined with a first-order admittance model and enabled voluntary opening/closing of the hand orthosis. A sensorized cylindrical object (Fig. 7.1) was used to measure the grasping force, as input for a real-time force-tracking task. The following paragraphs describe the key components in detail and are supported by a visual representation of the working principle of the device's actuators, sensors and control methods in Fig. 3.

SIGNAL DOMAIN

In this study, direct sEMG control (Lenzi et al., 2012) was used to decode a one degree-of-freedom (DOF) hand motion (open/close). After cleaning the participant's skin with alcohol to enhance signal quality, two dry wireless electrodes (Trigno, Delsys Inc., Natick, MA, USA) were put in place. One above the muscle belly of the extensor digitorum communis (EDC) and one above the muscle belly of the flexor digitorum superficialis (FDS). The exact placement was performed by palpation until a clear signal was found in relation with the requested motion (i.e hand closing for FDS and hand opening for EDC). The two sEMG signals were used to decode the hand opening-closing motor intention of the participant and enable the direct sEMG control of the orthosis. The EDS signal (Fig. 7.1) corresponded to hand opening and the FDS to hand closing. The same sEMG signals were used to measure muscular activation during the task.

Table 7.1: Mass distribution of the parts on the hand

Part	Mass (g)
Finger interfaces (4x)	29
Slave cylinders (8x)	65
Manifold	25
Hoses with fluid	24
Wrist and thumb splint	70
Trigno Avanti Sensor (x2)	28
Total mass on hand	*241*

The lower part of Fig. 7.3 presents a detailed diagram of the signal processing. Raw sEMG signals were initially digitally filtered with a high-pass filter (2^{nd} order Butterworth filter, $f_{c,hp} = 20Hz$) to reduce any movement artefacts. The envelopes of the sEMG signals ($\mathbf{E}_{env}$) were obtained by applying full-wave rectification and a low-pass filter (4^{th} order Butterworth filter, $f_{c,lp} = 2Hz$). The offsets of both the EDS and FDS envelopes were corrected by subtracting the resting sEMG envelope ($\mathbf{E}_{res}$), which was measured while the participant was completely relaxed. The resulting signals ($\mathbf{E}_{vol}$) were subsequently normalized to their own maximum voluntary contraction (MVC) value. Lastly, the normalized extensor envelope (U_{EDS}) was subtracted from the normalized flexor envelope (U_{FDS}) in order to create the normalized sEMG control signal (U_{vol}). This was multiplied by a conversion gain of 1N in order to acquire the estimated force (F_{est}), which served as input to a first-order admittance model similar to that carried out by Lobo-Prat et al. (2017):

$$H_{adm}(s) = \frac{1}{As+B} \tag{7.1}$$

Here, A represents the parameter related to virtual inertia (10^{-1}) and B the parameter related to virtual damping (10). The values were chosen in accordance with the participant's preferences and determined during a pre-trial. The manipulation of the virtual dynamics with the help of the admittance model aimed to create a responsive (dictated by inertia) yet stable (dictated by damping) interaction between the user and the device. The admittance model expected a force (estimated from the sEMG signals) as an input, i.e., a normalized signal that is negative for hand opening and positive for hand closing. The output of the admittance model was the reference velocity for the linear spindle (V_{ref}) based on the participant's intention. The reference position was obtained through integration (P_{ref}) and was sent to the low-level position controller (Fig. 7.2 in the signal domain and Fig. 7.3), in order to control the position of the linear spindle. The PID controller sent the calculated voltage to the motor driver (ESCON 24/2, Maxon Motor AG, Sachseln, Switzerland which in turn controlled the current of the motor (118743, RE25 10W, Maxon Motor AG, Sachseln, Switzerland).

The grasping force was measured in real time with the use of a sensorized cylindrical object (Fig. 7.1). For this purpose, a miniature S-beam load cell (FH04086, FUTEK Advanced Sensor Technology, Irvine, CA, USA) was incorporated in a 3D-printed cylindrical object with a diameter of 60 mm. The measured grasping force was normalized to the maximum voluntary force (MVF) produced by the participant without the orthosis and used for the visualization of the force-tracking task. The object included an indentation where the thumb could be placed in order to ensure that the grasping force direction was aligned with the axis of the load cell.

The analog signals of the sEMG electrodes and the force sensors were measured with the use of a real-time computer (xPC Target, MathWorks Inc., Natick, MA, USA) and by means of a data acquisition card (PCI-6229, National Instruments Corp., Austin, TX, USA). The analog data was converted to a digital signal with a 16 bit resolution and at a sampling frequency of 1 kHz.

ENERGY DOMAIN

In order to minimize the perceived mass on the hand, the actuation module was separated from the finger modules that were donned on the hand. This required a flexible force transmission to accommodate free movement of the hand in space. Due to the constant friction value and its independence on hose routing (LeBlanc, 1985), a hydraulic transmission was chosen over a Bowden cable transmission. This makes the force transmission more transparent for the user, which ideally leads to a more predictable link between the generated sEMG signal and desired assistive force.

To support this transmission, a hydraulic piston pump was used to convert electrical energy from the power supply into mechanical work in the form of hydraulic pressure. Differently than our previous design (Bos et al., 2018b), a custom-made pump was used, because an off-the-shelf version could not be found that was able to provide the desired pressures and flow rates. The pump was able to create pressures well up to 5.0 MPa. However, because of the frailness of the fingers among individuals with DMD, and thus to reduce the risk of harming the participant, the current to the piston pump was limited to approximately 35% of the motor's maximum continuous current. This way, pressures could not exceed 1.5 MPa during the study.

Fig. 7.3 shows the working principle of the electrohydraulic pump. It used a 12V DC motor (118743, RE25 10W, Maxon Motor AG, Sachseln, Switzerland) to move a spindle drive via a belt transmission. The spindle was directly connected to the piston of the master cylinder with a < Ø8 mm bore diameter and was able to generate pressure in a closed hydraulic circuit. The spindle drive's travel distance was limited with mechanical stops at 60 mm, which resulted in a maximum fluid displacement of 3 mL. The linear velocity of the spindle was limited to 10 mm/s (i.e., flowrate of 0.5 mL/s, 6 s for full flexion/extension). This value was, after a few trials, chosen by the participant as the maximum velocity that gave him a feeling of stable and safe control.

MECHANICAL DOMAIN

Mechanical work was transmitted using a hydraulic master-slave system (Bos et al., 2018b). The master cylinder was integrated in the electrohydraulic piston pump, dividing its pressure among all slave cylinders that were fixed on the finger modules, creating an underactuated system with an adaptive grasp. Fig. 7.3 shows how the slave cylinders were connected. Each finger module was equipped with two slave cylinders that acted on the metacarpophalangeal (MCP) and proximal interphalangeal (PIP) joint. The distal interphalangeal (DIP) joint was not actuated but was protected from overextension using passive structures. Valves can be used to selectively move one or multiple finger modules, allowing for individual finger movements or movement patterns (Bos et al., 2018b). In this study, in the interest of a simple control method, only a single DOF was controlled, and the use of valves was therefore omitted. The mechanical structure of SymbiHand was previously described in more detail in Bos et al. (2018).

The slave cylinders were custom-made single-acting hydraulic cylinders, with an active protraction and passive retraction using return springs. The return springs were fixed on the outside of the cylinder and could easily be interchanged with springs with a higher or lower stiffness, allowing for adjustments towards the preferences and conditions of an individual. In this study, all cylinders were equipped with stainless steel springs with a stiffness of 0.01 N/mm (T40740E, Tevema Technical Supply BV, Almere, Netherlands).

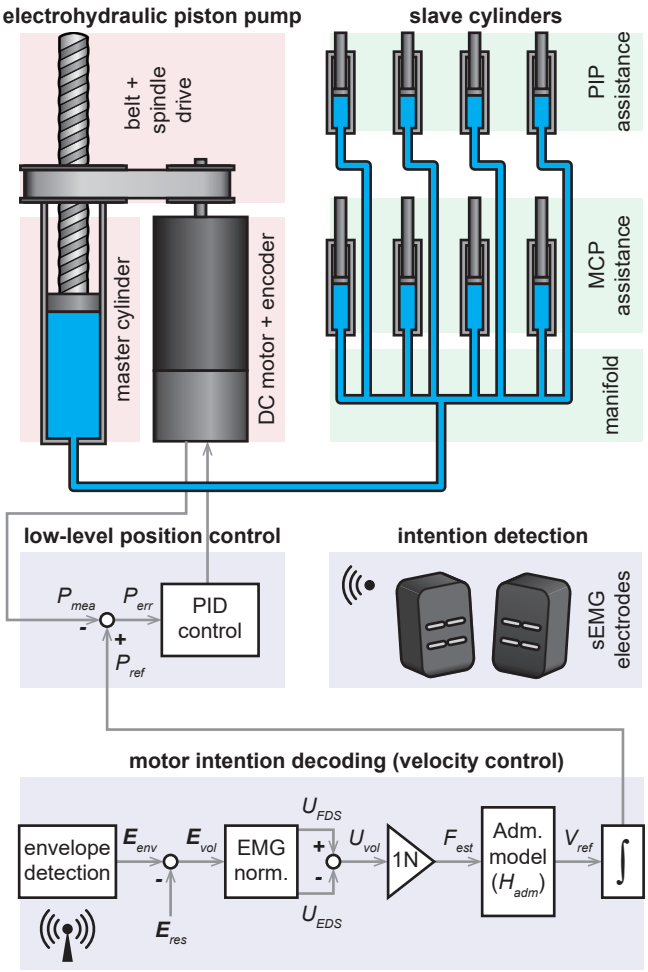

Figure 7.3: Detailed overview of the system, illustrating overall working principle and key components.

Water was used as the hydraulic fluid, which was degassed before filling the hydraulic circuit. A < Ø3 mm tubing material (Legris 1025P03 00 18, Parker Hannifin Corporation, Cleveland, OH, USA) was used to connect all slave cylinders to a manifold, which was connected to the piston pump using a single tube.

The finger modules served as the interface between the slave actuators and each finger, where the size was adjusted to the measurements of the participant's fingers (Bos et al., 2018b). In addition, the wrist and thumb were fixed in a functional position using a thermoplastic splint (Rolyan PAT-081572429, Performance Health, Warrenville, IL, USA). The wrist was slightly extended with the thumb in opposition, such that the tip of the thumb could oppose the tip of the index and middle fingers to allow for a three-jaw chuck

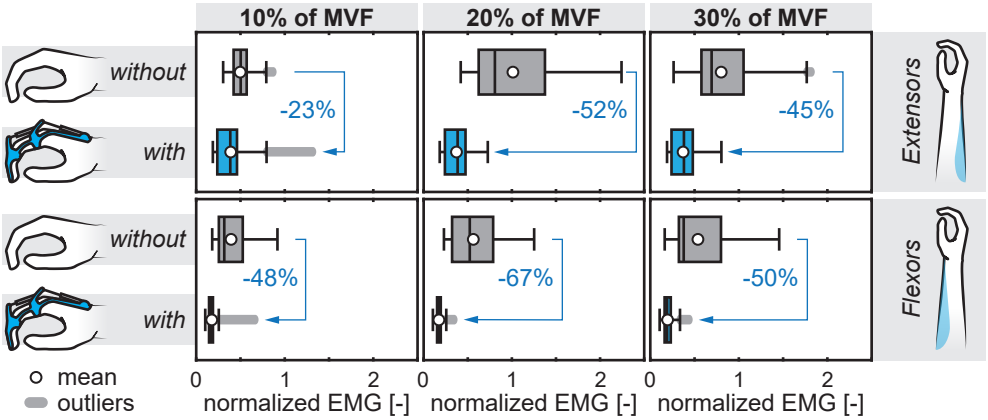

Figure 7.4: Normalized muscular activation of the extensor and flexor muscles while performing the task at 10%, 20%, and 30% of the participant's MVF, without and with SymbiHand. For each level of MVF, the muscular activation was averaged over the duration of the 6 trials, corresponding to that level. Percentages inside the figure windows indicate drops according to the median value. sEMG was normalized according to the MVC without SymbiHand (Flexor: 8.3 mV, Extensor: 12.3 mV). Horizontal lines represent the median while circles represent the mean values. The outliers were used for the calculation of the median and were visualized as those observations falling below Q1 – 1.5·IQR or above Q3 + 1.5·IQR.

grasp. Similar to all other fingers, the thumb's most distal joint (interphalangeal (IP) joint) was only protected against overextension, leaving the palmar area and as much as possible of the lateral side available for tactile feedback.

The orthosis could be donned by first securing the wrist and thumb splint using Velcro straps. Each finger module could then be slid on the fingers one by one, and attached to a snap-fit mechanism on the dorsal side of the splint. These snap-fit mechanisms were attached to the splint using Velcro, allowing for corrections in the distal or proximal direction.

7.2.3. EXPERIMENTAL PROTOCOL

The participant took part in two sessions, the first of which included the construction of the thermoplastic hand splint with the help of an occupational therapist and the measurement of the fingers for customizing SymbiHand. During the second session, and in order to assess whether SymbiHand could potentially provide assistance during activities of daily living, the participant was asked to perform a force-tracking task using the grasping force as input. For this purpose, an open-fist cylindrical grasp (Iberall, 1997) was carried out on a sensorized cylindrical object, without and with the hand orthosis.

At the start of the second session, and prior to the force-tracking task, the participant was asked to grasp the object as hard as possible for two seconds, simultaneously giving an MVF measured with the sensorized object and an MVC measured with both sEMG signals. Both MVF and flexor MVC were acquired as the mean signal over the period of two seconds of active grasping. The extensor MVC was recorded separately by asking the subject to extend his fingers against resistance. The envelopes were used for the calculation of the

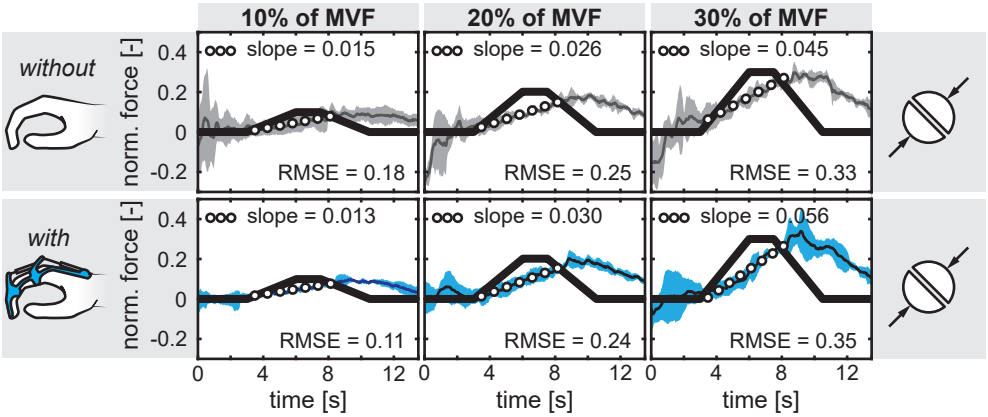

Figure 7.5: Normalized force-tracking performance while performing the task at 10%, 20%, and 30% of the participant's MVF, without and with SymbiHand. Generated force with and without SymbiHand was normalized according to the MVF (2.4 N) and averaged across the 6 trials per MVF level. The root mean square error (RMSE), between the imposed force trajectory and the average grasping force exerted by the participant is showed as well as the slope of the participant's average grasping force (equidistant circles) with and without SymbiHand.

MVC. During the force-tracking task, the participant was asked to grasp the same object, while also tracking a reference force trajectory that ramped up (hand close) to a specific percentage of the MVF for 3 s, remained there (hold) for 1.5 s, and then ramped down (hand open) to zero again for 3 s. These percentages were varied between 10, 20, and 30% of the MVF, in order to keep the participant effort low and avoid fatigue onset. The chosen reference trajectory (similar to the one applied by Kurillo and Bajd (2005)) provided a complete task with a proportional component that required force tuning (necessary for various ADL tasks) and a force steadiness component (necessary for holding objects). Each force level was repeated three times in a group of nine trials, and each group was repeated twice, resulting in a total of 18 trials without and 18 trials with the orthosis, and 6 trials per MVF level. After every nine trials, a resting period of at least two minutes was given to the participant to avoid the effects of fatigue in our data. All trials were executed in a randomized order to avoid order effects on our data.

Afterwards, the participant was fitted with SymbiHand, while the sEMG sensors remained donned. At first, the participant was allowed to familiarize himself with the device and its control for 10 minutes. This was followed by the same task as described previously, including a new measurement of the maximum attainable grasping force, only now with SymbiHand. To conclude the experiment, any additional informal feedback was registered. The datasets generated for this study can be found online in the IEEEDataPort repository (DOI: 10.21227/gerz-8s29).

7.2.4. DATA ANALYSIS

MUSCULAR ACTIVATION & GRASPING FORCE

Muscular activation and grasping force were taken as the main outcome measures in this study. The raw force signal was low-pass filtered (2^{nd} order Butterworth filter, $f_{c,lp}$ =

$20Hz$), before the analysis. The grasping force was used to determine force-tracking performance, defined as the root mean squared error (RMSE) between the imposed force trajectory and the average grasping force exerted by the participant, per MVF level. Additionally, force generation rate was calculated as the slope of the average normalized force exerted by the participant during the grasping phase. MVC and MVF measurements were taken as a measure of the participant's maximum capacities and used to normalize force and sEMG. All data were recorded both without and with SymbiHand.

MAXIMUM FLEXION ANGLE

Maximum flexion angle of the index finger was assessed by photogrammetry (de Carvalho et al., 2012). Photographic images (EOS 70D, EF-S 18–135mm, Canon Inc, Tokyo, Japan) were taken from the radial side of the participant's hand and analyzed in image processing software to quantify the angle between the phalanges. This was done both without and with the hand orthosis to evaluate any differences that the orthosis may impose. We chose to perform this analysis only for the index finger in order to create a representative example without encumbering the participant further by taking photos of each finger separately.

7.3. RESULTS

7.3.1. MUSCULAR ACTIVATION & GRASPING FORCE

Muscular activation from the extensors and flexors for all repetitions at every force level are shown in boxplots in Fig. 7.4 (The relevant raw and filtered sEMG data can be found online: DOI: 10.21227/gerz-8s29). The average and minimum/maximum values of the force-tracking tasks for every force level are shown in Fig. 7.5. SymbiHand was able to increase the participant's maximum grasping force of the cylindrical object from 2.4 to 8 N, with a slight increase in flexor muscular activation (+12%). This slight increase in flexor muscular activation may be the results of donning the orthosis (external finger load, changes in muscle length and stabilization of the wrist). Moreover, without compromising force-tracking performance, extensor muscular activation was reduced by an average of 40% and flexor by an average of 55%. The participant exhibited a similar reaction delay in the onset of tracking both with and without the orthosis during the force-tracking task, but exhibited higher force generation rate in all conditions except the 10% MVF, while wearing SymbiHand (Fig. 7.5).

7.3.2. MAXIMUM FLEXION ANGLE

Since the participant was experiencing minimal contractures,(which was reflected by a slightly reduced active maximum flexion angle), we limited the range of motion of the SymbiHand to accommodate the participant's comfortable limits. Taking the index finger as an illustrative example, maximum flexion angles without/with the hand orthosis were approximately 46°/51°, 91°/84° and 39°/22° for the MCP, PIP, and DIP joint, respectively. The hand orthosis therefore barely limited the active maximum flexion angle.

7.3.3. PARTICIPANT FEEDBACK

The participant indicated that the finger modules did not feel comfortable. Despite a polished finish, the 3D-printed material felt rough and had a few ragged edges. Because

the participant's fingers and skin were much more sensitive than that of a healthy individual, a cutting feeling was experienced at the skin creases on the palmar side of the finger joints. The wrist and thumb splint was quite comfortable for the participant while he was wearing it, and it provided sufficient support. However, donning the splint was quite cumbersome; in particular, when the MCP knuckles had to be slid through an opening that was a little bit too small, it was unpleasant to the participant.

7.4. DISCUSSION

7.4.1. MOTOR INTENTION DECODING

The combination of direct sEMG control with a first-order admittance model enabled the participant to control SymbiHand, by providing an additional level of control customization. Results showed a decrease in muscular activation while wearing the orthosis, without the loss of tracking performance. This is supporting evidence for the intuitiveness of the proposed motor intention decoding method. The participant adapted within 10 minutes of training, showing a strong training effect, as already suggested in previous studies with individuals with DMD (Lobo-Prat et al., 2017).

Being able to open and close the hand allows for a large variety of power grasps frequently used during household activities (Bullock et al., 2013), such as medium wrap and power sphere. Our choice for direct sEMG was largely motivated by the fact that only a single DOF needed to be controlled. For more DOF, however, direct sEMG control requires the generation of independent sEMG signals and the identification of independent sites for their acquisition, which can be cumbersome for the user and may result in a limited number of simultaneously controlled DOF (Wurth and Hargrove, 2014). In order to increase the range of assistance provided by SymbiHand (e.g., with an active thumb), in addition to enabling the control of more grasps used during dynamic ADL (Saudabayev et al., 2018) (e.g., by adding valves), different sEMG-based motor decoding approaches should be explored. Future work will investigate the possibility of employing regression (Hahne et al., 2017), pattern recognition (Wurth and Hargrove, 2014), or EMG-driven model-based techniques (Sartori et al., 2018; Sartori et al., 2019). Nevertheless, such approaches are still not broadly applied in clinical practice for hand orthoses, mainly due to the challenges they present for daily use in a home environment compared to direct sEMG control. Such challenges include the larger number of electrodes, longer and more frequent training and calibration, and a lack of robustness to electrode shift due to arm movements (e.g., pronation/supination as opposed to the fixed resting arm position used in this study).

In addition to an intuitive intention detection, it was essential that the participant could use his own intrinsic physiological feedback mechanisms (e.g., tactile and auditory feedback, proprioception, and vision) during the experiment. Hence, no explicit forms of augmented feedback were applied, resulting in a simple and easy-to-use approach. Implicitly, aside from the interaction force between the orthosis and the participant, motor noise could also be used as additional auditory information on the orthosis' operating conditions.

The reaction delay in tracking onset that the participant exhibited during the force-tracking task was similar both with and without the orthosis and cannot be attributed to the motor intention decoding. This delay in reaction time may be the result

of the limited training time and the specific condition of the participant. Despite this, the participant was able to modulate forces of the same magnitude, albeit with lower muscular activation, and additionally, in two out of three conditions (20% and 30% conditions) his force generation rate was higher while wearing SymbiHand.

7.4.2. MECHANICAL DESIGN

The hardware components of SymbiHand were well able to provide the necessary assistance to improve the participant's grasping performance. The mass on hand is slightly less than the comparable soft hydraulic hand orthosis from Polygerinos et al. (Polygerinos et al., 2015a; Polygerinos et al., 2015b), with the added advantage that the rigid pistons are capable of providing maximum assistance across the ROM. Yap et al. (2017) and Cappello et al. (2018) achieved masses of 180g and 77g respectively for their orthoses. However, these studies used a compressible gas as medium as opposed to a hydraulic fluid. Using a gas can indeed result in a lower mass, but it decreases energy density and reduces transparency of force transmission due to its compressible nature. Nonetheless, even though these hand orthoses were subject to different design choices due to differences in target groups (i.e., spasticity and different level of assistance in stroke and SCI survivors compared to individuals with DMD), it implies that further mass reductions are required to compare with the state-of-the-art.

The output force of SymbiHand is comparable with and in many cases exceeds that of the devices listed in Bos et al. (2016). However, it is emphasized that these capabilities exceed the assistance needs of this participant, which provides an opportunity for further device optimization by miniaturization of components and improvement of comfort, if this is generalizable across individuals with DMD. The flexure elements proved to be effective in aligning the orthosis' rotational centers with those of the anatomical joints. The bending shape of the flexure elements was able to self-align to the location of the anatomical joints. The use of standard hand sizes (e.g., small, medium, and large) are therefore possible, avoiding the need to manufacture bespoke parts. The retraction springs on the slave cylinders were strong enough to extend the fingers back to a slightly flexed resting position. These factors indicate that the overall design of the hand orthosis works as intended and has the potential to help increase the hand functionality of an individual with a muscular weakness.

Donning the different parts of the hand orthosis was difficult and uncomfortable for the participant. First, the tight fit of the wrist and thumb splint made it unpleasant to don. Second, because the fingers were so sensitive, sliding the finger modules on the fingers was not quite comfortable. As a result, the finger modules could not be donned easily one by one because the stiffness of the hydraulic hoses would add additional forces to the fingers. We believe that a modular or hinged splint with additional straps could help to reduce these problems, as well as finger modules that allow for quick and easy donning from the dorsal side of the hand. Changes in material may also contribute to a more comfortable interaction, as long as the load-bearing portions provide sufficient rigidity to transfer the loads without deformations. Third, positioning the thumb in opposition to the volar pads of the index and middle finger put it in an awkward resting position. This means that an additional thumb mechanism that is able to switch between a resting and functional position is necessary.

Despite the low mass of SymbiHand, the added mass was still an issue for the participant. The arm support could help with lifting the arm, but the high concentration of mass on the dorsal side of the hand made it impossible to pronate/supinate. A more strategic distribution of mass could be used to reduce the moment of inertia around the center of rotation of this particular movement. Additionally, overall mass reductions are possible, e.g., by making the hydraulic parts more lightweight. We also believe that the little finger does not need active support because the corresponding finger module only seemed to get in the way while grasping an object or while orienting the hand along the wheelchair tray. The ring finger can possibly be omitted as well, but further research is required with regard to how this reduction in mass and complexity affects the attainable grasping performance.

7.4.3. RELEVANCE

As this paper presents a case study, we cannot generalize the results over all individuals with DMD that might benefit from SymbiHand. For our participant, the assisted grasping force was still low (8 N), yet fitting to the individual's comfortable limits and still sufficient for a subset of ADL that require a maximum of 7.4 N (such as drinking, using a fork/pen or lifting a can/book (Memberg and Crago, 1997; Hart et al., 1998; Inmann and Haugland, 2001)). Especially compared to the original 2.4 N the participant could exert without SymbiHand, that is barely sufficient for any ADL. Due to various levels of contractures, preferred assistance or time for familiarization with the device that may help the user build confidence in its control, the magnitude of (assisted) grasping force and muscular activation may vary. This can lead to larger grasping forces and broaden the range of ADL that the user can perform. The applied current limit to the motor, however, implies that the device was over-dimensioned for this particular participant. The main reason for this added limit was to prevent exerting excessively high forces and flexion velocities on the sensitive fingers and skin of an individual that is not familiar in being assisted by a dynamic hand orthosis.

The increased muscular activation observed during the tracking task without the orthosis - especially in the extensor muscles, which were not expected to be that active during a grasping task - may be attributed to the effort of the participant to stabilize his wrist without the orthosis. While wearing SymbiHand, the wrist was supported by a thermoplastic splint, which may have contributed to the large reduction in baseline muscular activation. This may be a strong indication of the importance of supporting the wrist. However, further research is needed to investigate the effect of passively supporting the wrist on the reduction of muscular activation during functional hand use. Additionally, since many individuals with DMD suffer from strong contractures of their finger flexor muscles (Weichbrodt et al., 2018), it is interesting, in the future, to test the capacity of SymbiHand to assist an extension focused task.

The fact that the participant was able to control the hand orthosis without any artificial sensors at the end-effector (i.e., strain gauges and potentiometers placed on the hand) shows that the hydraulic transmission provided a predictable link between muscular activation and the speed of the orthosis. This makes the use of miniature hydraulic technology very interesting in the field of assistive devices controlled by the means of human intention detection schemes. In the presented hand orthosis, however, pressures are still quite low for a hydraulic system (<1.5 MPa). Even smaller hydraulic cylinders can

be used to further improve efficiency, and a smarter way of integrating the hydraulic circuit within the mechanism can result in a more inconspicuous design. The hydraulic hoses in the presented prototype, for example, decrease overall cosmesis and may get in the way in a daily environment.

The combination of SymbiHand with elbow/shoulder (Lobo-Prat et al., 2017) and trunk (Verros et al., 2018) orthoses for individuals with DMD can increase the reachable workspace, by allowing individuals with DMD to functionally interact with their environment. Furthermore, we believe that the use of SymbiHand can be extended to more pathologies, e.g., the daily assistance of elderly individuals with weakened muscles due to sarcopenia or individuals with stroke and SCI that have reduced hand strength. However orthoses for such conditions would require different control in order to decouple voluntary from involuntary sEMG due to spasticity and additionally offer assistance as needed. They may also require different mechanical and hardware design choices, tailored to the specificity of each condition (i.e. different power output or donning/doffing). Another interesting application is a combination with augmented reality for a broad range of physical therapy exercises, as proposed by Bushby et al. (2010); Bushby et al. (2010).

Future work will include more participants with similar condition as the participant of this study (low grip strength and preserved ROM). A more extensive protocol including ADL relevant tasks and measurements both in clinical and home settings would offer further insight in the long-term changes of the control over time and the feasibility of our approach for daily support. Nonetheless, the presented quantitative differences without and with Symbihand show that this participant was able to preserve force-tracking task performance, reduce muscular activation while wearing the hand orthosis, and his maximum grip force was tripled. As we mainly focused on force reference tracking, we did not provide any analysis on force steadiness or smoothness. Acknowledging the need for an intervention to address the hand function of individuals with DMD (Wagner et al., 1993; Wagner et al., 2007; Weichbrodt et al., 2018) we believe that after the recommended design improvements, SymbiHand can reduce the burden on the muscles, delay the onset of fatigue, and lengthen the time span in which the user can use his own hand.

7.5. CONCLUSION

This case study has shown that an individual with DMD underwent an amplification of grip strength, with no loss of tracking performance, while wearing SymbiHand. The results have shown that, along with grip strength amplification, SymbiHand enabled reduction in muscular activation during a force-tracking task. This was realized using a direct sEMG control approach with a tuned admittance model, in combination with a hydraulic transmission and differential mechanism. This has never been demonstrated before for individuals with DMD, highlighting the potential of this approach to enhance hand function and reduce fatigue while grasping. For use in a daily setting, however, adjustments need to be made to facilitate more comfortable donning of the device and reduce unfavorable effects due to its total mass and mass distribution. These adjustments can assist the development of SymbiHand towards a larger-scale study and broaden its use for a larger group of potential users and applications.

ACKNOWLEDGEMENTS

The authors would like to thank the participant for his time and dedication, Andrea Derks for her help fitting the splint and advice on functional complications and benefits, and Jeroen Gijzenmijter for his work on the design of the electrohydraulic piston pump and hydraulic slave actuators.

8

Discussion & conclusions

The main goal of this thesis was to reveal and expand the current technological possibilities for dynamic hand orthoses. Emphasis was put on comparing alternative technologies with those of highest popularity. This process was undertaken with a variety of steps, ranging from a large-scale exploration of current state-of-the-art, comparison of modeling methods and transmission technologies, and the fabrication and testing of a proof-of-concept dynamic hand orthosis for people with DMD. This chapter glues all these results together and indicates where the main opportunities lie. Finally, we will look back at the research objectives that emerged from the thesis goal and summarize the conclusions with respect to these objectives.

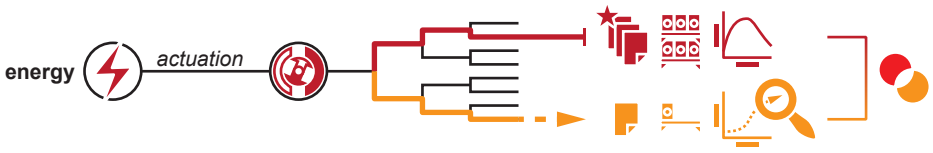

Figure 8.1: By way of categorization in a design process, one can choose for a traditional (red) or alternative pathway (orange). Traditional pathways are often accompanied by plentiful literature, available components and a well-known performance. Alternative pathways are characterized by the opposite, which means that research is required to map their potential and make a well-considered design choice.

8.1. OVERVIEW OF TECHNOLOGY

8.1.1. CATEGORIZATION OF COMPONENTS

Through the collection of a large quantity of dynamic hand orthoses, a database of mechatronic components was established. By categorizing this database into separate domains (i.e., signal, energy and mechanical domain) and tree diagrams, an overview of technology was created that can be viewed at multiple levels of detail. This method proved to be very useful in mapping the current technological possibilities in dynamic hand orthoses. Moreover, by aiming to make each branching point all-inclusive, new ideas could arise as well. This is most definitely not limited by its use in dynamic hand orthoses. In fact, almost any mechatronic device can make use of the same categorization structure and tree diagrams that were developed in this thesis. Going through this process of categorization, however, is cumbersome because only a small percentage of the (new-)found technologies may be feasible or truly innovative.

Regardless, the formation process of the tree diagrams creates a larger scale understanding of each subcomponent in the full mechatronic system. Each branching point signifies a design choice that requires rationale to support it. This includes rationale for going towards this particular path, but also for *not* going towards a different direction. Therefore, by going through this process, a designer is confronted with supporting choices which may otherwise have been implicit. For example, choosing a lithium-ion battery as energy storage includes choosing for: an electric energy output as opposed to other forms of energy (e.g., thermal, mechanical, nuclear); energy storage in a electrochemical unit rather than an electromagnetic field; a dry cell as opposed to a wet cell battery; a rechargeable as opposed to disposable battery; and, a battery with lithium electrodes as opposed to, for example, nickel-cadmium electrodes. This sequence of design choices can be seen as a pathway through the tree diagram that ends up at the component level, i.e., the lithium-ion battery.

8.1.2. RESEARCHING ALTERNATIVE PATHWAYS

In addition to this structured approach, a component's popularity was pitted against its feasibility. Just because DC motors are used in almost every assistive device, should not mean that they are also always the best choice. Regardless of performance, a component can also be popular because of high (off-the-shelf) availability, ease of use and previous experience. Researching alternative pathways, on the other hand, increases

technological diversity. This can potentially expand the possibilities and functionalities of the mechatronic device, making these alternative pathways worthwhile to investigate (see Figure 8.1). To support this statement, this thesis has demonstrated the potential of using miniature hydraulic technology as opposed to using more popular Bowden cable and pulley-cable mechanisms.

8.2. MECHANICAL DESIGN METHODS

8.2.1. USING OPTIMIZATION

Already in the early phase of the design process, a designer is exposed to a multitude of trade-offs that need to be evaluated. Sometimes, meeting one design criterion means violating another. The design of a dynamic hand orthosis is, in that sense, not an exception. One of the key trade-offs is size versus assistive force, because high assistive forces often require larger structures to increase moment arms and to prevent prominent shear force components. Wearable devices that are intended to be used in a home setting, however, should not be too large in size. A perfectly functioning dynamic hand orthosis can be immediately rejected if you cannot pick up your cookie without knocking over your cup of tea. Tools from engineering optimization can help with dealing with these trade-offs, but their success strongly relies on the underlying models.

In Chapter 4, the use of optimization algorithms in combination with a compliant mechanism was explored as an attempt to tackle this size-versus-force trade-off. The concept of a distributed compliant structure was interesting because it could bend anywhere you want by varying both shape and material thickness. Moreover, a single part design would allow it to be manufactured in one go with a 3D printer. A rigid linkage mechanism would require a multitude of joints and corresponding bearings, severely limiting miniaturization and the number of parts. It turned out, however, that accurate modeling of the compliant mechanism's behavior required a great amount of detail on the material, manufacturing process and finger joint stiffness. Because not all of this information was available at the time, the optimization algorithm came up with a design that did not behave as predicted. Aside from the fact that it is impractical for a flexible structure to follow a finger's full range of motion while also transmitting high loads in the same direction, this study also showed that it is important to align a model's complexity to the stage of the design process. For the early design phase, it meant that a minimalistic modeling approach was required.

8.2.2. MINIMALISTIC MODELING

Consequently, a less detailed model of a hand orthosis was developed and its simplifications were more carefully assessed. Within this model, a static approach proved to be able to reach the same conclusions as a dynamic approach—and much faster as well—despite having no inertial effects, viscosity, friction and memory of previous states in time. These results indicate that very comprehensive and accurate models are not always the best choice and that a more simplistic approach is more effective in reaching fast conclusions and dealing with complex trade-offs in an early design stage.

This, however, also poses the question as to how far these simplifications can be generalized. Grasping of non-circular objects, for example, is dependent on the initial orientation of the object (imagine picking up a cube by its sides or by its corners). A

dynamic model will come with a solution that has a causal relation with this initial condition, whereas a static model does not possess this aspect of causality. Namely, the static solution will depend on the minimization procedure's ability to find a minimum based on the initial search point. A smarter way is therefore necessary to deal with these limitations, which ideally finds all local minima (and thus all stable grasping configurations) in one go in order to maintain its advantage over time-expensive dynamic modeling. Examples include a brute force mapping of the potential energy field as a function of a subset of variables (e.g., object position and orientation), an increase in the number of initial search points, or biologically inspired search methods (e.g., evolutionary algorithms).

8.2.3. REDIRECTING INTERACTION FORCES

In a system where forces need to be transmitted in very small volumes, it becomes more important to minimize energy dissipation. In the case of a dynamic hand orthosis, this means that a pure moment needs to be applied around the anatomical joints. The underactuated mechanisms presented in Chapters 4 and 5 do not provide this pure moment. In fact, when using the modeling approach, we find out that the interaction force at the proximal phalange is pulling rather than pushing on the finger during flexion (see also concept A in Figure 8.2). Additionally, at the interaction with the metacarpal region, a very high shear force component can be identified. This means that a large portion of the assistive forces will be dissipated by the passive elements in the anatomical joints and by movement of the skin.

A solution that is suggested in this thesis resembles the opposite of a biological joint, where pulling actuators (i.e., muscles) are used and the shear components are absorbed by a rigid joint loaded in compression. Instead, pushing actuators are coupled with a flexural element alongside the anatomical joint that is loaded in tension. This way, shear forces no longer act on biological tissue but on the material of the flexural elements. This particular working principle was not confirmed in this thesis, but the observations that were made indicate its potential for any type of force transfer around an articulating component where shearing should be avoided (e.g., assistive devices for other limbs, reclining seats).

During pilot measurements, demonstrations and the case study experiment, all wearers of the hand orthosis design from Chapters 6 and 7 indicated a comfortable fit and did not feel any pronounced shearing on the skin. Additionally, because the flexure elements will bend according to the least amount of resistance, they can easily self-align themselves to the anatomical joints within a large margin. This was implied by the fact that the placement of the flexible structures in proximal-distal direction did not affect the force transfer for the case study participant. Therefore, a future study that scopes on the exact effect of these flexure elements on the (direction of the) interaction forces is warranted. For example, it is unknown how properties like overall (visco-)elasticity and flexure shape can affect this concept.

8.2.4. TRANSMITTING FORCES

In this thesis, the use of fluidic actuators and transmission systems was considered as a feasible method to generate and transmit relatively high forces. Because the force from a fluidic actuator largely depends on the pressure of the working fluid, force can be easily increased by increasing pressure without enlarging the actuator (for as long as the actuator

Table 8.1: Comparison of force efficiency and design implications between a Bowden cable and hydraulic transmission system.

	Bowden cable transmission	**Miniature hydraulic transmission**
Force efficiency	Friction force increases with transmission force. Static force efficiency highly depends on cable routing and material. Dynamic force efficiency slightly depends on cable speed.	Friction force decreases with hydraulic pressure. Static force efficiency independent of hose routing. Dynamic force efficiency depends on flow resistance.
Design implications	Requires very little space. Dyneema cables are least sensitive to changes in cable speed and highly repetitive bending.	Allows integration with fluidic differential mechanisms. Fluid should be protected from vacuum pressures and very small orifices (<0.6mm) should be avoided.

can handle the pressures). This can be particularly exploited in a hydraulic system, where it is much easier to reach these high pressures when compared to a pneumatic system. Choosing a hydraulic system, however, also results in many implications that affect the rest of the design. These design implications, along with force efficiencies, of a hydraulic transmission as opposed to a Bowden cable transmission were measured and discussed in Appendices B and C. Their core differences are summarized in Table 8.1.

Based on these differences, it became apparent that one solution is not always better than the other. However, as transmission force increases, pressure will increase in a miniature hydraulic transmission system and consequently shows a higher force efficiency. Additionally, because hose routing does not affect force efficiency, a hydraulic transmission facilitates a more predictable force transfer and can therefore be seen as a more transparent method. This is especially advantageous for human-in-the-loop control methods, as the human operator would be better able to estimate the forces at the end-effector from the operating signal. Combined with the fact that fluidic differential mechanisms can be more easily integrated to distribute forces, a hydraulic transmission proved to be the best option, even though a Bowden cable transmission would require less space to operate a mechanism.

8.3. LEVERAGING MINIATURE HYDRAULICS

8.3.1. DISTRIBUTING FORCES

The components inside an orthosis mechanism need to be able to transmit relatively high forces and distribute them over the phalanges. Ideally, force is distributed equally across all phalanges of each finger, as well as across all fingers, to allow for a fully adaptive grasp. In Chapter 4, however, the compliant mechanism was not able to accommodate full range of motion and transfer assistive forces in the same direction. In Chapter 5, the force distribution over the phalanges was affected by the size of the object (i.e., the joint angles). Therefore, a different approach was required, and this was found in using fluidic technology in a smaller scale. Instead of underactuating the finger by a linkage design,

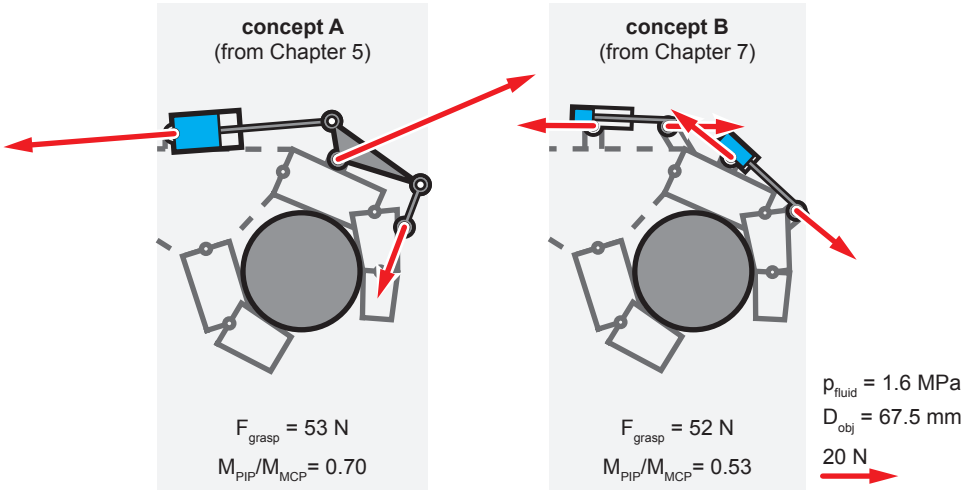

Figure 8.2: Using the static model developed in Chapter 5, two different concepts can be compared. Concept A underactuates the finger by a linkage design, whereas concept B does this by multiple fluidic actuators which are connected by pressure. Red arrows indicate the direction and magnitude of the interaction forces from the mechanism on the hand.

a fluidic differential mechanism with multiple smaller fluidic actuators can achieve the same function. Combined with the findings from Section 8.2.4, this could easily be combined with a hydraulic transmission.

Using the static model developed in Chapter 5, this design with a fluidic differential mechanism (concept B) was compared against the linkage-based design (concept A). Here, concept A used a single cylinder with a diameter of 6 mm and concept B used two connected cylinders with a diameter 4 mm each, giving both concepts a similar total surface area of the pistons. As shown in Figure 8.2, the interaction forces in concept B are more distributed along the finger and of lower magnitude, while the grasping force (F_{grasp}) on the object is very similar. Additionally, the torque ratio (M_{PIP}/M_{MCP}) in concept B is closest to the ideal ratio of 0.52 for this finger size (this ratio was determined according to phalange lengths (Kragten and Herder, 2010)). Other torque ratios can be easily obtained by changing the moment arm of the cylinders with the anatomical joints. A disadvantage of concept B, however, is that the shear force components are larger than in concept A. In combination with the flexible structures (see Section 8.2.3), this became less of a problem.

8.3.2. INTEGRATION OF MINIATURE HYDRAULIC COMPONENTS

A disadvantage of miniature hydraulics is that there is little room available for fluid transport. Fluid channels that are too small give rise to large pressure drops and energetic losses due to flow resistance. Bigger channels, on the other hand, quickly increase the bulk size of the system and can possibly cancel out the advantages of miniaturizing the fluidic actuators. Therefore, it becomes more important to integrate functions like fluid transport in the structural and articulating components of a miniature hydraulic system. With the

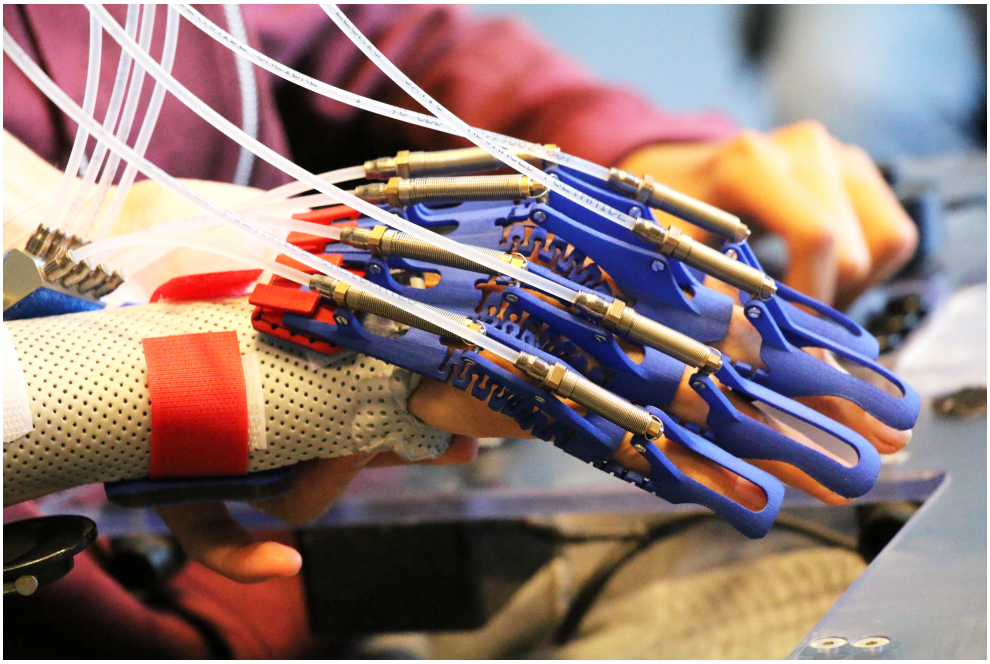

Figure 8.3: Case study participant wearing SymbiHand.

recent advancements in 3D-printing technology, integration of fluidic channels is starting to become feasible for channel diameters between 1–2 mm. However, even with a 1 mm channel, this is still a large relative increase in size when trying to integrate this in a hinge joint that already requires a 2 mm steel axis to transfer the loads.

One area that has not been encountered yet, is the integration of fluid transport in compliant mechanisms. As a straightforward example, one can treat a hydraulic hose as a compliant mechanism and use this to transmit mechanical work as an articulating component in a very volume-efficient manner. Concepts from fiber-reinforced tubing are particularly interesting in this case, which are able to achieve high pressure resilience while preserving bending flexibility (e.g., high-pressure tubing from RAUMEDIC AG (2018)).

8.4. A DYNAMIC HAND ORTHOSIS FOR ADL ASSISTANCE

The overview of technology, mechanical design methods and use of miniature hydraulics were all combined into the design of a new dynamic hand orthosis. This device, called SymbiHand (see Figure 8.3), serves as a proof-of-principle of the design approach that is advocated in this thesis.

The fact that the case study participant was able to maintain force tracking performance with SymbiHand, which does not include any sensors at the end-effector, indicates that the hydraulic system provided for a transparent link between the command signal (i.e., EMG activity) and the assisted grasping force. Moreover, with a mechanism

that resides within a 15 mm boundary around the hand, grasping force was increased from 2.5 to 8 N at only 35% of the pump's maximum capacity. Hence, at full capacity, this design can potentially provide 23 N of grasping force for this individual. From the researched state-of-the-art in Chapter 3, there is no other dynamic hand orthosis that can provide this magnitude of assistance within this volume, which also self-aligns to the anatomical joints, leaves the majority of the palmar area available for tactile feedback and provides intrinsic underactuation across all fingers. In addition to this, the case study experiment with SymbiHand has shown that muscular effort can be decreased for an individual with DMD by more than 40%. This implies that a dynamic hand orthosis for ADL assistance can delay the onset of muscle fatigue, which potentially increases the amount of daily tasks that can be performed and maintain hand function for a longer period of time.

However, there remain points of improvement that do not necessarily relate to further development at the component or technology level, which are elaborately discussed in the previous sections. Additionally, at the application level, the contact interface between the compliant finger modules and the fingers, and the process of donning/doffing the orthosis proved to be a more challenging issue than expected. The modular approach (i.e., donning the finger modules one-by-one) did not work well due to the stiffness of the hoses and experienced discomfort while sliding the finger modules along the fingers. Preferably, the user should be able to don the orthosis without external help and the tightness of the fit should be adjustable or self-adjusting. In combination with the self-aligning flexure elements, this allows for using standard sizes rather than bespoke parts. These functionalities, while maintaining the palmar area free as much as possible, results in a complex design problem that has yet to be solved.

The fact that SymbiHand only required 35% of the pump's capacity for an increase in grasping force by more than a factor 3, suggests that the device was overdimensioned for this participant. However, the preferred amount of assistance is difficult to predict as the participant gets used to the device and it is unknown by how much this preference can vary between different users. Therefore, we cannot make any recommendations regarding the required amount of assistance for people with DMD. Nonetheless, we feel that SymbiHand's design is capable of a very wide range of assistance. Especially with improvements in the miniature hydraulic system, pressure can be increased for even higher levels of assistance and valves can be added for more complex movement patterns. This makes SymbiHand an interesting device for a wider range of pathologies and applications, which may include the high-force requirements that come with hypertonic muscles among stroke survivors. We believe, however, that the added advantage of the flexible hydraulic transmission is only maintained if the device should be portable and light-weight on the hand. For research (and possibly clinical) applications and environments, volume and mass become less of an issue and actuators can be placed closer to the hand, which make rigid transmissions (e.g., linkages, rolling links, gears) more suitable.

8.5. CONCLUSIONS

Taking the preceding discussion in mind, and following from the work that is included in the chapters and appendices in this thesis, the following conclusions are made with respect to the posed research objectives:

O1: Determine the spectrum of technological possibilities for dynamic hand orthoses.

- With an extensive collection of existing dynamic hand orthosis, their mechatronic components can be extracted and subdivided into a signal, energy and mechanical domain.
- Within each domain, a tree-like categorization structure that uses mutually exclusive subdivisions is able to visualize the full spectrum of technological possibilities in terms of mechatronic components, and can reveal those that have barely (or not) been used but are still feasible.
- When choosing to expand a single branch in the tree-like categorization structure, a level of detail can be reached that coincides with more fundamental research areas. In the case of assistive devices like dynamic hand orthoses, this can create a clinically driven demand for advanced and innovative technologies.

O2: Investigate modeling approaches and justify model simplifications to help choose between concepts in the early design phase of a dynamic hand orthosis.

- Current methods of Fused Deposition Modeling (FDM) were not found to be predictable enough to make accurate predictions of the behavior of compliant mechanisms in a dynamic hand orthosis. This prevents the use of shape optimization procedures for the design of a compliant mechanism that is manufactured in this way.
- In an early design stage, modeling approaches that minimize the required amount of details are recommended. This avoids large time investments and erroneous predictions due to the uncertainties and lack of details that characterize the early design phase.
- A static model provides a faster and easier modeling method compared to a dynamic model when comparing concepts for a dynamic hand orthosis that are tested by their ability to hold objects. The outcome of qualitative comparisons was preserved while dimensioning a conceptual hydraulically operated dynamic hand orthosis with the static model, but quantitative results were in this case not consistent with the dynamic model. This makes the static model particularly useful in the early design phase, but loses its advantage in later phases as more details are required.

O3: Determine the value of using alternative technologies (i.e., fluidics, compliant mechanisms) as opposed to traditional technologies (i.e., Bowden cables, rigid links) in a dynamic hand orthosis.

- Compliant mechanisms are very well suited to self-align an orthosis mechanism with the anatomical joint centers and to facilitate a comfortable force interaction. However, they were not found suited to cover the full range of motion of a finger with a low-profile (<17 mm protrusions) mechanism while also providing assistive/resistive forces in the same direction.
- Hydraulic systems provide a higher force efficiency and more predictable force transmission (i.e., hose routing-independent) than Bowden cable systems in prosthetic and orthotic applications that require a variable hose/cable routing.
- Hydraulic systems are especially suitable for dynamic hand orthoses intended to assist during activities of daily living when miniaturized to millimeter-scale.
- Optimal implementation of a miniature hydraulic system in assistive devices requires customized components (e.g., piston-type actuators, high-pressure tubing, miniature valves), improved dynamic sealing methods on sub-millimeter scale, research on ideal fluids and integration of fluid transport with structural and articulating components.

O4: Assess the potential of these alternative technologies when applied to a dynamic hand orthosis to assist people with DMD during ADL.

- A hydraulically operated dynamic hand orthosis that is operated with direct EMG control (i.e., SymbiHand) can be operated by a person with DMD, without compromising in force tracking performance that uses grasping force as input.
- Maximum grasping force of an individual with DMD can be increased from 2.5 N to 8 N (potentially up to 23 N) with SymbiHand, which fits inside a 15 mm boundary around the hand.
- While wearing SymbiHand, muscular effort during a grasping task can be reduced by more than 40% for an individual with DMD.

A

AN INDEX OF DYNAMIC HAND ORTHOSES

This appendix features work from the following publication:

R. A. Bos, C. J. W. Haarman, T. Stortelder, K. Nizamis, J. L. Herder, A. H. A. Stienen, and D. H. Plettenburg (2016a). "A structured overview of trends and technologies used in dynamic hand orthoses". In: *Journal of NeuroEngineering and Rehabilitation*, 13: 62. DOI: 10.1186/s12984-016-0168-z

A.1. RESEARCH TOOLS

Table A.1: Overview of included dynamic hand orthoses classified as research tool.

Name/source	Country	Year range[1]	ISO abbr.	Reported function	Actuator DOF[2]	Wrist support[2]
MR_CHIROD v.2 (Khanicheh et al., 2005; Khanicheh et al., 2006; Khanicheh et al., 2008)	USA	2005–2008	HdO	post-stroke measurement	1	N/A
FingerBot (Cruz and Kamper, 2010)	USA	2010	FO	post-stroke measurement	3	N/A
ATX (Wang et al., 2011a)	USA	2011	FO	post-stroke measurement	5	N/A
Fiorilla et al. (2009); Fiorilla et al. (2011)	Italy	2009–2011	FO	normal measurement	2	Limited (PS) Locked (FE, RUD)
Ramos et al. (2009); Ramos-Murguialday et al. (2012)	Germany	2009–2012	WHFO	post-stroke therapy	4	Locked (PS, FE, RUD)
Tang et al. (2011); Tang et al. (2012); Tang et al. (2013); Tang et al. (2013)	Japan	2011–2013	FO	post-stroke measurement/therapy	1	Limited (FE)
CAFE (Worsnopp et al., 2007; Jones et al., 2010; Jones et al., 2014)	USA	2007–2014	FO	post-stroke measurement	6	Locked (FE, RUD)
Kim and Kim (2015)	South Korea	2015	WHFO	general measurement/therapy	1	Limited (PS, FE, RUD)
Lee and Bae (2015)	South Korea	2015	HdO	post-stroke measurement	5	N/A

[1]Year ranges are determined by the year span between found literature sources and my differ from the actual time of development.
[2]Actuator DOF = number of individually controlled actuators (zero means fully passive).
[3]Wrist can be assisted, resisted, limited or locked (ISO/TC 168, 2007) in pronation/supination (PS), flexion/extension (FE) and radial/ulnar deviation (RUD).

A.2. CLINICAL TOOLS

Table A.2: Overview of included dynamic hand orthoses classified as clinical tool.

Name/source	Country	Year range[1]	ISO abbr.	Reported function	Actuator DOF[2]	Wrist support[2]
HWARD (Takahashi et al., 2005)	USA	2005	WHFO	post-stroke therapy	2 (+1 wrist)	Locked (PS, RUD) Assisted (FE)
HIFE (Mali and Munih, 2006)	Slovenia	2006	FO	general physical therapy	2	Locked (PS, FE, RUD)
Gentle/G hand device (Loureiro and Harwin, 2007)	UK	2007	WHFO	post-stroke therapy	3	Locked (FE, RUD)
InMotion Hand Robot (Masia et al., 2007; Interactive Motion Technologies, 2013; Interactive Motion Technologies, n.d.)	USA	1991–2007	HdO	post-stroke therapy	1	N/A
CPM/CAM (Birch et al., 2008)	Canada	2008	HdO	general CPM/CAM	2	N/A
Fu et al. (2007); Fu et al. (2008)	China	2008	FO	general CPM	2	N/A
ADLER FES grasp glove (Nathan and Johnson, 2007; Nathan et al., 2009)	USA	2007–2009	HdO	post-stroke therapy	Not clear	Not clear
IntelliArm hand module (Park et al., 2008; Ren et al., 2009)	USA	2008–2009	WHFO	post-stroke measurement/therapy	1 (+2 wrist)	Assisted (PS, FE) Locked (RUD)
Sun et al. (2006); Sun et al. (2009)	China	2006–2009	WHFO	post-stroke therapy	2	Limited (PS, FE, RUD)
Wang et al. (2009); Wang et al. (2009); Wang et al. (2010); Wang et al. (2010); Wang et al. (2011)	China	2009–2011	FO	general physical therapy	4	Limited (FE, RUD)
Yamaura et al. (2009)	Japan	2009	FO	general physical therapy	2	N/A
HenRiE grasp module (Mihelj et al., 2008; Podobnik et al., 2009; Podobnik and Munih, 2010)	Slovenia	2008–2010	WHFO	post-stroke therapy	0	Locked (FE, RUD)

Table A.2: (continued)

Name/source	Country	Year range[1]	ISO abbr.	Reported function	Actuator DOF[2]	Wrist support[2]
HEXORR (Schabowsky et al., 2010)	USA	2010	WHFO	post-stroke therapy	2	Locked (PS, FE, RUD)
PneuGlove (Kline et al., 2005; Connelly et al., 2009; Connelly et al., 2010)	USA	2006–2010	HdO	post-stroke therapy	5	N/A
Unluhisarcikli et al. (2010)	USA	2008–2010	WHFO	post-stroke therapy	2 (+1 wrist)	Assisted (PS)
ExoHand (Festo AG & Co. KG, 2012)	Germany	2012	WHFO	tele-operation, post-stroke therapy	8	Limited (FE, RUD)
iHandRehab (Wang et al., 2009a; Li et al., 2011; Li et al., 2012)	China	2009–2012	HdO	general physical therapy	8	N/A
Kim and Kim (2013)	South Korea	2013	WHFO	post-stroke therapy	10	Locked (PS) Limited (FE, RUD)
Sooraj et al. (2013)	India	2013	WHFO	general physical therapy	5	Locked (PS, FE, RUD)
Amadeo (Tyromotion GmbH, n.d.; Mayr et al., 2010; Hartwig, 2014)	Austria	2010–2014	WHFO	general measurement/therapy	5	Locked (PS, FE, RUD)
AMES hand module (Cordo et al., 2009; Cordo et al., 2013; Backus et al., 2014; AMES Technology, Inc., n.d.)	USA	2009–2014	WHFO	post-stroke therapy	1 (+1 wrist)	Locked (PS, RUD) Assisted (FE)
AssistOn-Finger (Ertas et al., 2009; Ertas et al., 2014)	Turkey	2009–2014	FO	tendon injury treatment	1	Locked (FE, RUD)
Bi and Yang (2011); Bi et al. (2013); Bi and Yang (2014)	China	2011–2014	WHFO	post-stroke therapy	5	Locked (FE, RUD)
Chan et al. (2014)	Malaysia	2014	HdO	post-stroke therapy, general assistance	3	N/A
FINGER (Wolbrecht et al., 2011; Taheri et al., 2012; Taheri et al., 2014)	USA	2011–2014	FO	post-stroke therapy	1	Locked (PS, FE, RUD)

Table A.2: (continued)

Name/source	Country	Year range[1]	ISO abbr.	Reported function	Actuator DOF[2]	Wrist support[2]
HIT-Glove (Zheng and Li, 2010; Fu et al., 2011; Zhang et al., 2013; Zhang et al., 2014)	China	2010–2014	FO	post-stroke therapy	6	N/A
Kawasaki et al. (2004); Kawasaki et al. (2007); Ito et al. (2011); Ueki et al. (2012); Kawasaki et al. (2014)	Japan	2004–2014	WHFO	post-stroke therapy	16 (+2 wrist)	Assisted (PS, FE) Locked (RUD)
Moromugi et al. (2009); King et al. (2011); King et al. (2014)	USA	2009–2014	HdO	post-stroke therapy	7	N/A
PMHand (McConnell et al., 2014)	UK	2014	HdO	post-stroke therapy	1	N/A
ReachMAN2 (Yeong et al., 2009; Yeong et al., 2010; Zhu et al., 2014)	UK	2009–2014	WHFO	post-stroke therapy	1 (+1 wrist)	Assisted (PS) Locked (FE, RUD)
Reha-Digit (Hesse et al., 2008; Reha-Stim Medtec GmbH & Co. KG, 2012; Reha-Stim Medtec GmbH & Co. KG, n.d.)	Germany	2008–2014	HdO	general CPM	1	Limited (PS, FE, RUD)
Ushiba et al. (2014)	Japan	2014	WHFO	post-stroke therapy	1	Locked (FE, RUD)
IHRG (Popescu et al., 2013a; Popescu et al., 2013b; Hartopanu et al., 2013; Popescu et al., 2014; Hartopanu et al., 2014; Popescu et al., 2015)	Romania	2013–2015	HdO	post-stroke therapy	4	N/A
READAPT (Gupta et al., 2008; Agarwal and Deshpande, 2015; Agarwal et al., 2015; Pehlivan et al., 2015; Rose et al., 2015)	USA	2008–2015	WHFO	post-stroke measurement/therapy	8 (+3 wrist)	Assisted (PS, FE, RUD)

[1]Year ranges are determined by the year span between found literature sources and my differ from the actual time of development.
[2]Actuator DOF = number of individually controlled actuators (zero means fully passive).
[3]Wrist can be assisted, resisted, limited or locked (ISO/TC 168, 2007) in pronation/supination (PS), flexion/extension (FE) and radial/ulnar deviation (RUD).

A.3. HOME REHABILITATION TOOLS

Table A.3: Overview of included dynamic hand orthoses classified as home rehabilitation tool.

Name/source	Country	Year range[1]	ISO abbr.	Reported function	Actuator DOF[2]	Wrist support[2]
Sarakoglou et al. (2004)	UK	2004	HdO	general physical therapy	7	N/A
Luo et al. (2005); Luo et al. (2005)	USA	2005	HdO	post-stroke therapy	1	N/A
Mulas et al. (2005)	Italy	2005	WHFO	general physical therapy	2	Limited (PS, FE, RUD)
Haptic Knob (Lambercy et al., 2007a; Lambercy et al., 2007b)	Singapore	2007	WHFO	post-stroke therapy	1 (+1 wrist)	Assisted (PS) Limited (FE, RUD)
MRAGES (Winter and Bouzit, 2007)	USA	2007	HdO	general physical therapy	5	N/A
Wege and Hommel (2005); Wege et al. (2005); Wege and Hommel (2006); Wege et al. (2006); Wege and Zimmermann (2007)	Germany	2005–2007	HdO	general physical therapy	20	N/A
Carpi et al. (2008)	Italy	2008	WHFO	general impairment compensation	1	Locked (FE, RUD)
HandCARE (Dovat et al., 2008)	Singapore	2008	HdO	post-stroke therapy	1	Limited (PS, FE, RUD)
Chen et al. (2009)	China	2009	WHFO	post-stroke therapy	5	Locked (FE, FE, RUD)
HIRO III (Hioki et al., 2010)	Japan	2010	HdO	general physical therapy	15	N/A
Mohamaddan and Komeda (2010)	Malaysia	2010	HdO	post-stroke therapy	2	N/A
NeReBot hand add-on (Rosati et al., 2009; Oboe et al., 2010)	Italy	2009–2010	WHFO	post-stroke therapy	1	Locked (PS, FE, RUD)
Burton et al. (2011); Burton et al. (2012)	UK	2011–2012	WHFO	post-stroke therapy	6	Limited (FE, RUD)

Table A.3: (continued)

Name/source	Country	Year range[1]	ISO abbr.	Reported function	Actuator DOF[2]	Wrist support[2]
J-Glove (Ochoa et al., 2009; Ochoa et al., 2011)	USA	2009–2011	WHFO	post-stroke therapy	1	Locked (FE, RUD)
PRoGS (Wee and Ling, 2011)	Singapore	2010–2011	WHFO	post-stroke therapy	5	N/A
SaeboFlex (Hoffman and Blakey, 2011; Saebo, Inc., n.d.[a])	USA	2011	WHFO	post-stroke therapy, hypertonia compensation	0	Locked (FE, RUD)
Tzemanaki (Tzemanaki et al., 2011)	UK	2011	HdO	general therapy	5	N/A
DULEX-II (Kim et al., 2009; Bae et al., 2012)	South Korea	2009–2012	WHFO	post-stroke therapy	2 (+1 wrist)	Assisted (FE) Locked (RUD)
ExoFlex (Holmes et al., 2012)	USA	2012	HdO	general therapy	4	N/A
HANDEXOS (Chiri et al., 2009; Chiri et al., 2012b; Chiri et al., 2012a)	Italy	2009–2012	FO	post-stroke therapy	1	N/A
JACE H440 Hand CPM (JACE Systems, n.d.)	USA	2012	WHFO	general physical therapy	1	Locked (PS, FE, RUD)
Kazemi et al. (2012)	Canada	2012	WHFO	post-stroke measurement/therapy	1 (+1 wrist)	Assisted (PS)
Naidu et al. (2011); Naidu et al. (2012)	South Africa	2011–2012	WHFO	post-stroke therapy	2 (+1 wrist)	Assisted (PS) Locked (FE, RUD)
Polotto et al. (2012)	Canada	2012	FO	post-stroke therapy/assistance	4	N/A
WaveFlex Hand CPM (QAL Medical, LLC, n.d.; QAL Medical, LLC, 2012; Torgerson, 1997)	USA	1997–2012	WHFO	general physical therapy	1	Locked (FE, RUD)
Xing et al. (2008); Wu et al. (2009); Xing et al. (2009); Wu et al. (2010); Tu et al. (2012); Wu et al. (2012)	China	2008–2012	WHFO	post-stroke therapy	2	Limited (PS) Locked (FE, RUD)
CAFEx (Ab Rahim et al., 2013)	Malaysia	2013	HdO	post-stroke therapy	1	N/A

Table A.3: (continued)

Name/source	Country	Year range[1]	ISO abbr.	Reported function	Actuator DOF[2]	Wrist support[2]
Gloreha Lite (Idrogenet, srl, n.d.; Idrogenet, srl, 2013)	Italy	2013	HdO	general physical therapy	5	N/A
Hand of Hope (Tong et al., 2010; Ho et al., 2011; Tong et al., 2013; Ockenfeld et al., 2013; Rehab-Robotics Company Ltd., n.d.)	China	2010–2013	HdO	post-stroke therapy	5	N/A
mRes (Weiss et al., 2013)	Germany	2013	HdO	post-stroke therapy	4	N/A
Orlando et al. (2010); Ngeo et al. (2013)	India	2010–2013	FO	post-stroke therpapy	3	N/A
Rahman and Al-Jumaily (2012); Rahman and Al-Jumaily (2013)	Australia	2012–2013	WHFO	post-stroke therapy	5	N/A
Shafi et al. (2013)	Pakistan	2013	HdO	general physical therapy	4	N/A
Song and Chai (2013)	Taiwan	2013	HdO	post-stroke therapy/assistance	3	Limited (FE)
UoA hand exoskeleton (Surendra et al., 2012; Tjahyono et al., 2013)	Australia	2012–2013	WHFO	post-stroke therapy	11	Limited (PS, FE, RUD)
BiomHED (Lee et al., 2014b; Park et al., 2014; Kim et al., 2014)	USA	2014	WHFO	post-stroke therapy	7	Limited (PS) Locked (FE, RUD)
Coffey et al. (2014)	Ireland	2014	WHFO	post-stroke therapy	1	Limited (PS, RUD) Assisted (FE)
Guo et al. (2014)	China	2014	FO	post-stroke therapy	1	N/A
HEXOSYS-I (Iqbal et al., 2010b; Iqbal et al., 2011c; Iqbal et al., 2014)	Italy	2010–2014	HdO	general physical therapy	2	N/A
IOTA (Aubin et al., 2014)	USA	2014	WHFO	pediatric rehabilitation	2	N/A
Maestra (Kinetec SAS, n.d.; Kinetec SAS, 2014)	France	2014	WHFO	general physical therapy	1	Assisted (PS, FE, RUD)

Table A.3: (continued)

Name/source	Country	Year range[1]	ISO abbr.	Reported function	Actuator DOF[2]	Wrist support[2]
Maestra Portable (Kinetec SAS, n.d.; Kinetec SAS, 2014)	France	2014	WHFO	general physical therapy	1	Locked (FE, RUD)
PAFEx (Takagi et al., 2009; Ab Patar et al., 2014)	Japan	2009–2014	HdO	post-stroke therapy	3	N/A
Pu et al. (2014); Pu et al. (2015)	Taiwan	2014–2015	WHFO	general physical therapy	4	Locked (FE, RUD)
ReHand-II (Meng et al., 2014b; Meng et al., 2014a)	China	2014	HdO	post-stroke therapy	2	N/A
ReHapticKnob (Metzger et al., 2011; Metzger et al., 2012; Metzger et al., 2014)	Switzerland	2011–2014	WHFO	post-stroke measurement/therapy	1 (+1 wrist)	Assisted (PS)
SPO (Ates et al., 2013; Ates et al., 2014a; Amirabdollahian et al., 2014)	Netherlands	2013–2014	WHFO	post-stroke therapy	0	Resisted (F) Assisted (E) Locked (RUD)
Tang et al. (2013); Chen et al. (2014)	China	2013–2014	HdO	general physical therapy	10	N/A
ULERD hand module (Wei et al., 2013; Wei et al., 2014)	China	2013–2014	WHFO	post-stroke therapy	1 (+2 wrist)	Assisted (PS, FE) Locked (RUD)
Ab Patar et al. (2015); Ab Patar et al. (2015)	Japan	2015	HdO	post-stroke therapy	3	N/A
HEXOSYS-II (Iqbal et al., 2010a; Iqbal et al., 2011b; Iqbal et al., 2011a; Iqbal et al., 2015)	Italy	2010–2015	WHFO	general physical therapy	5	Limited (FE, RUD)
HX (Cempini et al., 2013; Cempini et al., 2014a; Cempini et al., 2014b; Cempini et al., 2015; Cortese et al., 2015)	Italy	2013–2015	WHFO	general physical therapy	2	Locked (RUD)

Table A.3: (continued)

Name/source	Country	Year range[1]	ISO abbr.	Reported function	Actuator DOF[2]	Wrist support[2]
NESS H200 (IJzerman et al., 1996; Bioness, Inc., 2013)	USA	1996–2015	WHFO	general physical therapy	Not clear	Not clear
Ramirez et al. (2015)	Mexico	2015	WHFO	general physical therapy	6	Limited (PS) Locked (FE, RUD)
Richards et al. (2015)	UK	2015	HdO	post-stroke rehabilitation	2 (+1 palm)	N/A
SAO-i3 (Ates et al., 2014b; Ates et al., 2015)	Netherlands	2014–2015	WHFO	post-stroke therapy	1	Assisted (FE, RUD)

[1]Year ranges are determined by the year span between found literature sources and my differ from the actual time of development.
[2]Actuator DOF = number of individually controlled actuators (zero means fully passive).
[3]Wrist can be assisted, resisted, limited or locked (ISO/TC 168, 2007) in pronation/supination (PS), flexion/extension (FE) and radial/ulnar deviation (RUD).

A.4. DAILY ASSISTIVE TOOLS

Table A.4: Overview of included dynamic hand orthoses classified as daily assistive tool.

Name/source	Country	Year range[1]	ISO abbr.	Reported function	Actuator DOF[2]	Wrist support[2]
Hardiman project (Mosher, 1967; Croshaw, 1969; Makinson, 1971)	USA	1967-1971	WHFO	power assistance	2 (+2 wrist)	Assisted (PS, FE) Locked (RUD)
Hamonet and DeMontgolfier (1974)	France	1974	HdO	tetraplegic assistance	1	N/A
K U finger splint S-type (Watanabe et al., 1978)	Japan	1978	WHFO	general impairment compensation	0	Limited (FE, RUD)
K U finger splint W-type (Watanabe et al., 1978)	Japan	1978	WHFO	general impairment compensation	0	Limited (FE, RUD)
WDFHO (Meyer et al., 1979; Kang et al., 2013; North Coast Medical, Inc., n.d.)	USA	1978–2013	WHFO	tetraplegic assistance	1	Assisted (FE) Locked (RUD)
Dollfus and Oberlé (1984)	France	1984	HdO	tetraplegic assistance	1	N/A
Benjuya and Kenney (1990)	USA	1990	HdO	tetraplegic assistance	1	N/A
Slack and Berbrayer (1992)	Canada	1992	WHFO	tetraplegic assistance	1	Limited (PS, FE, RUD)
Brown et al. (1993)	USA	1993	HdO	tetraplegic assistance	5	N/A
SMART WHO (Makaran et al., 1993)	Canada	1993	WHFO	tetraplegic assistance	1	Limited (FE) Locked (RUD)
DiCicco et al. (2004)	USA	2004	WHFO	tetraplegic assistance	2	Limited (FE, RUD)
Watanabe et al. (2005); Watanabe et al. (2007)	Japan	2005–2007	WHFO	arthritis assistance	1	Locked (FE, RUD)
Alutei et al. (2009)	Romania	2009	WHFO	general assistance	1 (+1 wrist)	Assisted (PS) Locked (FE, RUD)
Moromugi et al. (2009)	Japan	2009	HdO	general assistance	7	N/A
Exo-Finger (Otsuka and Sankai, 2010)	Japan	2010	HdO	post-stroke assistance	1	N/A

Table A.4: (continued)

Name/source	Country	Year range[1]	ISO abbr.	Reported function	Actuator DOF[2]	Wrist support[2]
Moromugi et al. (2010)	Japan	2010	HdO	tetraplegic assistance	1	Locked (RUD)
Tadano et al. (2010)	Japan	2010	HdO	power assistance	10	N/A
HandSOME (Brokaw et al., 2011)	USA	2011	WHFO	post-stroke impairment compensation	0	Locked (FE, RUD)
PowerGrip (Broadened Horizons, Inc., n.d.)	USA	2011	WHFO	general assistance	1	Locked (FE, RUD)
Toya et al. (2011)	Japan	2011	HdO	general assistance	4	N/A
Baqapuri et al. (2012)	Pakistan	2012	WHFO	tetraplegic assistance	4	Limited (PS, FE, RUD)
SEM Glove (Nilsson et al., 2012)	Sweden	2012	HdO	general assistance	3	N/A
Arata et al. (2013)	Japan	2013	HdO	general therapy/assistance	1	Limited (FE, RUD)
KULEX grasping module (Hong et al., 2012; Hong et al., 2013a; Hong et al., 2013b)	South Korea	2012–2013	WHFO	general assistance	1 (+3 wrist)	Assisted (PS, FE, RUD)
Lambercy et al. (2013)	Switzerland	2013	FO	post-stroke therapy/assistance	1	N/A
Moromugi et al. (2013)	Japan	2013	HdO	tetraplegic assistance	3	N/A
MUNDUS hand orthosis (Pedrocchi et al., 2013)	Italy	2013	HdO	tetraplegic assistance	1	N/A
Zheng et al. (2013)	China	2013	HdO	general assistance	Not clear	Not clear
Aw and McDaid (2014)	Australia	2014	HdO	general assistance	14	N/A
Kudo et al. (2014)	Japan	2014	HdO	tetraplegic assistance	1	N/A
Lee et al. (2012); Lee et al. (2014)	South Korea	2012–2014	HdO	general assistance	5	N/A

Table A.4: (continued)

Name/source	Country	Year range[1]	ISO abbr.	Reported function	Actuator DOF[2]	Wrist support[2]
Nishad et al. (2014)	India	2014	HdO	general therapy/assistance	8	Limited (FE, RUD)
OFX (Heo et al., 2013; Heo and Kim, 2014b; Heo and Kim, 2014a)	South Korea	2013–2014	WHFO	general assistance	1	Locked (FE, RUD)
Puzo et al. (2014)	USA	2014	HdO	general therapy/assistance	5	N/A
SaeboGlove (Saebo, Inc., n.d.[a])	USA	2014	WHFO	general impairment compensation	0	Locked (FE, RUD)
Sasaki et al. (2004); Kadowaki et al. (2011); Sasaki et al. (2014)	Japan	2004–2014	HdO	general assistance	5	N/A
BRAVO Hand Exoskeleton (Bergamasco et al., 2011; Loconsole et al., 2013; Leonardis et al., 2015)	Italy	2011–2015	HdO	post-stroke therapy/assistance	2	N/A
Conti et al. (2015)	Italy	2015	HdO	general assistance	4	N/A
Cui et al. (2015)	Australia	2015	HdO	general assistance	5	N/A
Delph II et al. (2013); Nycz et al. (2015)	USA	2013–2015	HdO	post-stroke therapy/assistance	5	N/A
ExoGlove (Low et al., 2015; Yap et al., 2015b; Yap et al., 2015a; Yap et al., 2015c)	Singapore	2015	HdO	general therapy/assistance	1	N/A
Gasser and Goldfarb (2015)	USA	2015	HdO	post-stroke assistance	2	N/A
Hasegawa (Hasegawa et al., 2008; Hasegawa et al., 2010; Hasegawa et al., 2011; Hasegawa et al., 2012; Hasegawa and Muto, 2013; Hasegawa and Suzuki, 2015)	Japan	2008–2015	WHFO	power assistance	8 (+4 wrist)	Assisted (PS, FE)

Table A.4: (continued)

Name/source	Country	Year range[1]	ISO abbr.	Reported function	Actuator DOF[2]	Wrist support[2]
OHAE (Rotella et al., 2009; Martinez et al., 2010; Baker et al., 2011; Colon et al., 2014; Cincotti et al., 2015)	USA	2009–2015	WHFO	general assistance	3	Limited (FE, RUD)
Polygerinos et al. (2013); Polygerinos et al. (2015); Polygerinos et al. (2015)	USA	2013–2015	HdO	general therapy/assistance	4	N/A
SNU Exo-Glove (In et al., 2011; In and Cho, 2012; Jeong et al., 2013; Jeong et al., 2015; In et al., 2015)	South Korea	2011–2015	WHFO	general therapy/assistance	3	N/A

[1]Year ranges are determined by the year span between found literature sources and my differ from the actual time of development.
[2]Actuator DOF = number of individually controlled actuators (zero means fully passive).
[3]Wrist can be assisted, resisted, limited or locked (ISO/TC 168, 2007) in pronation/supination (PS), flexion/extension (FE) and radial/ulnar deviation (RUD).

A.5. EXTRA-VEHICULAR ACTIVITY (EVA) GLOVES

Table A.5: Overview of included dynamic hand orthoses classified as EVA glove.

Name/source	Country	Year range[1]	ISO abbr.	Reported function	Actuator DOF[2]	Wrist support[2]
Shields et al. (1997)	USA	1997	HdO	power assistance	3	Limited (FE, RUD)
SkilMate (Yamada et al., 2001; Yamada et al., 2004)	Japan	2001–2004	HdO	power assistance	3	N/A
Matheson and Brooker (2011); Matheson and Brooker (2012)	Australia	2011–2012	WHFO	general assistance	1	Limited (PS, FE, RUD)
Matheson and Brooker (2011); Matheson and Brooker (2012)	Australia	2011–2012	FO	general assistance	2	Limited (PS, FE, RUD)

[1]Year ranges are determined by the year span between found literature sources and my differ from the actual time of development.
[2]Actuator DOF = number of individually controlled actuators (zero means fully passive).
[3]Wrist can be assisted, resisted, limited or locked (ISO/TC 168, 2007) in pronation/supination (PS), flexion/extension (FE) and radial/ulnar deviation (RUD).

A.6. HAPTIC DEVICES

Table A.6: Overview of included dynamic hand orthoses classified as haptic device.

Name/source	Country	Year range[1]	ISO abbr.	Reported function	Actuator DOF[2]	Wrist support[2]
SKK Hand Master (Choi and Choi, 1999; Choi and Choi, 2000)	South Korea	1999–2000	HdO	VR feedback	7	N/A
Koyama et al. (2002)	Japan	2002	HdO	VR feedback, teleoperation	0	N/A
Rutgers Master-II-ND (Bouzit et al., 2002)	USA	2002	HdO	VR feedback	4	N/A
LRP hand master (Tzafestas, 2003)	France	2003	HdO	VR feedback	14	N/A
Stergiopoulos et al. (2003)	France	2003	HdO	VR feedback	2	N/A
Lelieveld et al. (2006); Lelieveld and Maeno (2006)	Japan	2006	FO	VR feedback	4	N/A
Nakagawara et al. (2005); Sato et al. (2007)	Japan	2005–2007	HdO	tele-operation	6	N/A
Ryu et al. (2008)	South Korea	2008	WHFO	VR feedback	3	Not clear
CyperGrasp (CyberGrasp Systems LLC, 2009)	USA	2009	HdO	VR feedback	5	N/A
Fang et al. (2009); Fang et al. (2009)	China	2009	HdO	teleoperation	5	N/A
Charoenseang and Panjan (2011)	Thailand	2011	HdO	VR feedback	9	N/A
Fontana et al. (2009); Fontana et al. (2013)	Italy	2009–2013	HdO	VR feedback, tele-operation	6	N/A
Dexmo F2 (Dexta Robotics, n.d.[b]; Dexta Robotics, n.d.[a])	China	2014	HdO	VR feedback	5	N/A

Table A.6: (continued)

Name/source	Country	Year range[1]	ISO abbr.	Reported function	Actuator DOF[2]	Wrist support[2]
SPIDAR-10 (Liu et al., 2014)	Japan	2014	WHFO	VR feedback	20 (+1 wrist)	Assisted (PS) Limited (FE, RUD)
Jo and Bae (2013); Jo and Bae (2015)	South Korea	2013–2015	HdO	VR feedback	5	N/A
SAFE Glove (Ben-Tzvi and Ma, 2015; Ma and Ben-Tzvi, 2015)	USA	2015	HdO	VR feedback	6	N/A

[1]Year ranges are determined by the year span between found literature sources and my differ from the actual time of development.
[2]Actuator DOF = number of individually controlled actuators (zero means fully passive).
[3]Wrist can be assisted, resisted, limited or locked (ISO/TC 168, 2007) in pronation/supination (PS), flexion/extension (FE) and radial/ulnar deviation (RUD).

B

BOWDEN CABLE SYSTEMS FOR PROSTHETIC & ORTHOTIC APPLICATIONS

This appendix features work from the following publication:

R. A. Bos, M. N. Mahmood, P. N. Kooren, S. Verros, M. I. Paalman, H. F. J. M. Koopman, and D. H. Plettenburg (2016b). "Measuring dynamic friction properties of Bowden cable systems". In: *The Anthology of the ISPO European Congress on Prosthetics and Orthotics*. Rotterdam, p. 45

The transmission of mechanical work from an actuator to an output location is an imperative element in mechanical systems. For many applications, this transmission requires a flexible coupling. This allows the output location, e.g. end-effector, to move freely in space with respect to the actuator. The Bowden cable system is widely used in this aspect and finds many applications. In body-powered prosthetics, the human muscle serves as an actuator and the Bowden cable then facilitates the harnessing of muscle strength to operate a prosthesis (Pursley, 1955), while minimally impeding free movements of the body. In the case of externally powered prosthetics, orthotics and other robotic applications, Bowden cables are used to move the actuators away from the end-effector, effectively reducing its size and mass (Kaneko et al., 1991; Schiele, 2008; Goiriena et al., 2009; Palli et al., 2009).

B.1. BOWDEN CABLE WORKING PRINCIPLE

The working principle of the Bowden cable is more than a century old and little has been changed in its design compared to the original patents from Ernest Bowden (Bowden, 1896; Bowden, 1897). In fact, the original patent drawing still provides a good description of how Bowden cables are being used today (see Figure B.1). This requires the use of an incompressible outer cable and an inextensible inner cable. By fixing the ends of the outer cable, the inner cable is able to transfer a tensile force and displacement from one side to the other. The simplicity of the working principle of the Bowden cable allows it to be used in very narrow spaces and finds well-known applications as a throttle or brake cable in bicycles, cars and planes. Other variations of this working principle are also possible, for example in a push-pull cable or flexible shaft which are able to transfer compressive forces or torques, respectively. These types of cables—along with the Bowden cable—can be grouped as cable-conduit systems.

B.2. SLIDING FRICTION

One of the intrinsic disadvantages of the Bowden cable lies in the energy dissipation due to sliding friction between the inner and outer cable, which decreases force efficiency. For body-powered prosthetics, this increases the necessary input forces and, as a result, decreases overall comfort (LeBlanc, 1985; LeBlanc, 1990; Smit et al., 2013). Additionally, the frictional behavior is non-linear, depends on the cable routing, material properties and construction in the mechanical system (Carlson et al., 1995; Schiele et al., 2006; Agrawal et al., 2010; Palli et al., 2012; Agrawal et al., 2013). This makes it difficult to model the system's transmission characteristics and poses challenges for control (Schiele et al., 2006; Agrawal et al., 2010; Palli et al., 2012). Over time, different variations in windings of the cable's strands, cable materials, coatings and liners were introduced to decrease the frictional forces. For example, newly developed materials such as braided Spectra/Dyneema cables (Carlson et al., 1991) and Nylon/Teflon liners (LeBlanc, 1985; Gwynne, 1956; Chen et al., 2014a) have shown to be effective in increasing efficiency.

Several studies have successfully characterized Bowden cable friction for several variations (LeBlanc, 1985; Carlson et al., 1995; Goiriena et al., 2009; Chen et al., 2014a). Knowing the effect of these variations on the efficiency is important for a correct actuator and cable selection (Goiriena et al., 2009). Several phenomena influence the frictional properties of a Bowden cable system, which are here subdivided in the capstan effect, the effect of curvature radius and dynamic friction.

B.2.1. CAPSTAN EFFECT

Usually, the Bowden cable experiences some curvatures between the in- and output location and can be characterized as a cable running over a circular surface. This causes friction and is translated into a loss of tension in the cable. This variation in tension before and after the contact surface can be described by the capstan equation, or also called the Euler-Eytelwein equations (Schiele et al., 2006; Agrawal et al., 2010; Palli et al., 2012):

$$\frac{F_2}{F_1} = e^{\text{sign}(v)\mu\theta} \tag{B.1}$$

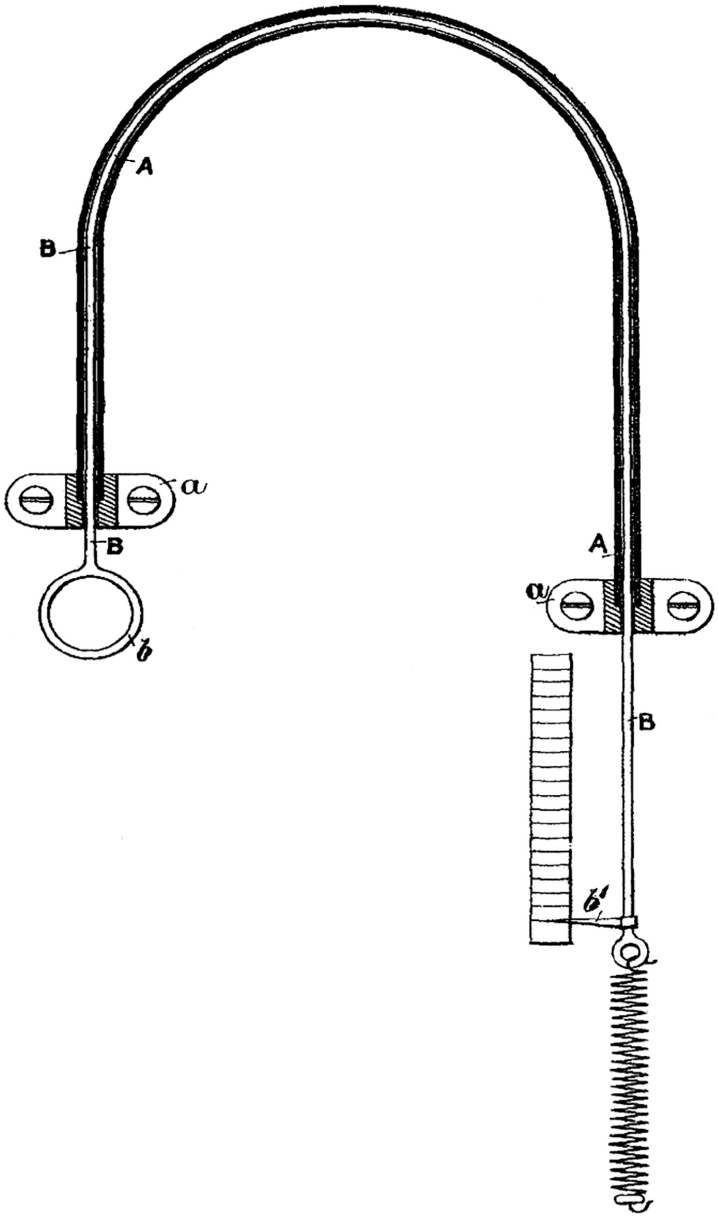

Figure B.1: Working principle of the Bowden as it appears in the original patent (Bowden, 1896). The illustration indicates the outer cable (**A**), inner cable (**B**), outer cable fixations (**a**) and the input and output side of the inner cable (**b** and **b'**, respectively).

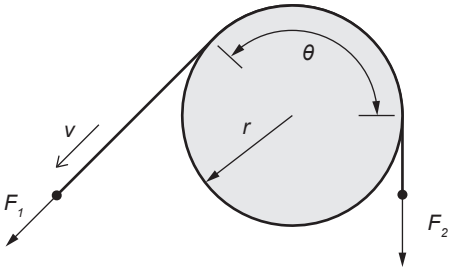

Figure B.2: Variables used in the capstan equation.

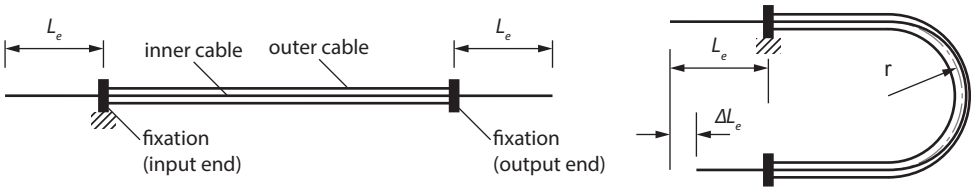

Figure B.3: Illustration of how bending the Bowden cable with a small curvature radius can cause the inner cable to lose conformity, and have a larger arc length than the outer cable. This shortens the free end length L_e at the output side by ΔL_e.

The capstan equation shows that the relative loss of tension ($\frac{F_2}{F_1}$) grows exponentially with the total angle of the curvature (θ) and the friction coefficient (μ). See Figure B.2 for an illustration of these variables. This capstan effect can be exploited by wrapping cables several times over pulleys or sheaves in order to carry and hold higher loads at the output with a lower input force. When transmission of mechanical work is the main purpose of the system, however, it becomes an undesirable effect and needs to be minimized (Gwynne, 1956). Hence, in order to minimize frictional losses, one needs to minimize the total angle of the cable's curvature and friction coefficient. Both effects were tested and verified for upper limb prosthetic and orthotic applications by Carlson et al. (1995); LeBlanc (1985); Goiriena et al. (2009); Chen et al. (2014).

B.2.2. CURVATURE RADIUS

The capstan equation does not include the effect of radius of curvature (r), hence the frictional losses should not be affected by this (Palli et al., 2009; Schiele et al., 2006). For very small radii, however, other phenomena come into play which may affect overall efficiency and force transmission transparency. For example, the inner cable's bending stiffness may cause a decreased conformity to the outer cable's curvature, decreasing the capstan effect (Shashaty, 1981). This, in turn, shortens the length of the free ends (L_e) of the inner cable. This can alter the output position of the Bowden cable (ΔL_e), or this can be compensated by increasing the cable tension to increase conformity. See Figure B.3 for an illustration of this effect.

In practice, manufacturers recommend a minimum curvature radius of about 20 times the inner cable's diameter, such that the effects of very small radii are avoided (Schiele

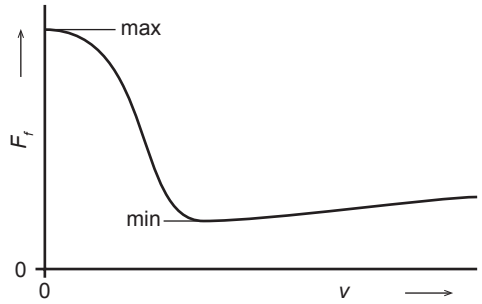

Figure B.4: Expected curve of velocity-dependent friction in Bowden cables, following the shape of a Stribeck curve.

et al., 2006). Although one study confirms this and shows a negligible influence of radius on overall Bowden cable efficiency (Carlson et al., 1995), a significant effect is reported by (Goiriena et al., 2009) at a radius of 38 times the inner cable's diameter.

B.2.3. DYNAMIC FRICTION

Dynamic friction is slightly different from static friction. The Coulomb friction model is a simple model that is able to describe stick-slip behavior, and does this with a larger static friction coefficient ($\mu = \mu_s$) and lower dynamic friction coefficient ($\mu = \mu_d$). In other words, to move the inner cable at a certain velocity, a higher initial force needs to be overcome to start the movement. Once there is movement, there is a constant dynamic friction. In reality, however, the amount of friction can vary for different velocities. The Stribeck curve describes a more realistic behavior.

The Stribeck curve is a general friction model for lubricated sliding contacts, with which dry contacts show similar behavior (Andersson et al., 2007). It describes maximum friction in static condition, a drop in magnitude for lower (non-zero) velocities, and an increase, decrease or constant magnitude for higher velocities. Within the limits of the considered applications in this study, however, it is uncertain whether the high-velocity region would be reached. Moreover, this region is largely characterized by hydrodynamic effects, which may only be apparent when a lubricant is added. Nonetheless, an expected curve is shown in Figure B.4.

Only one study was found that measured the effect of cable velocity on force efficiency (Chen et al., 2014a) and indicates that friction slightly increases for higher velocities. An extensive friction-velocity characteristic, however, remains missing. Characterization of the dynamic friction properties therefore seems underrepresented in current literature, whereas Bowden cables are mostly used in a dynamic setting. A reasonable justification is that most applications that employ a Bowden cable system, accept the unpredictable transmission characteristics and implement sensors at the output (e.g., end-effector). By fully relying on the sensor readings at the output, a suitable controller can compensate for the majority of non-linearities. In applications that do not make use of such technology (e.g., in body-powered prostheses or unsensorized end-effectors), mapping dynamic friction properties is of higher importance.

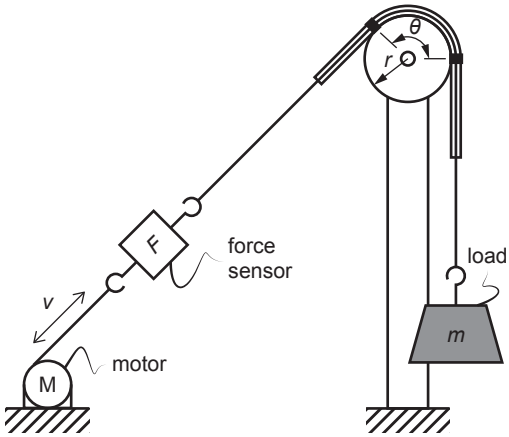

Figure B.5: Experimental set-up for measuring Bowden cable dynamic friction characteristics.

B.3. FRICTION MEASUREMENTS

Due to shortage of evidence in current literature, the effect of curvature radius and dynamic friction was tested, up to violation of the manufacturer's recommendations. Additionally, a comparison of currently available materials was deemed valuable as well.

B.3.1. EXPERIMENTAL DESIGN

The overall experimental set-up, similar to the set-up in (Carlson et al., 1995), is shown in Figure B.5 and is formed by a Bowden cable running over a stationary sheave. By fixating the outer cable to the sheave at the marked locations, a curvature was imposed with angle θ and radius r. The inner cable then ran freely through the outer cable and was fixated to a force sensor on one end, and a load with known mass (m) on the other end. A motor pulled on the other side of the force sensor and provided the force necessary to lift the load up- and downwards at a constant velocity v.

Acceleration to reach the desired velocity was adjusted such that no inertial effects were observed in the force measurements. A constant curvature angle of $\theta = 135°$ was ensured across all measurements (as shown in Figure B.5). A mass of $m = 17.5$ kg was chosen as load.

B.3.2. VARIABLES

The sheave radius (r), inner cable linear velocity (v) and cable material were the variables in this set-up. Their variations are summarized in Table B.1. The cable materials, in particular, were based on current standards and state-of-the-art. The two steel cables from Fillauer are standard light-duty cables used in body-powered prostheses. The Igus Dyneema cable is a type of non-metallic cable used in robotic applications. The Jagwire cable originates from a high-end bicycle derailleur cable, representing the state-of-the-art of metallic Bowden cable systems and uses a Teflon-coated cable with slick-lube liner (i.e. silicon grease). Every combination of radius, velocity and cable material was repeated three times. All trials were performed in a randomized order.

Table B.1: Overview of the variables and their variations as used in the experimental set-up.

Variable	Metric	Variations
Sheave radius (r)	mm	12.5, 20, 27.5, 35, 42.5, 50
Cable velocity (v)	mm/s	5, 15, 25, 35
Cable material	-	Fillauer 1.19 mm cross-lay 7x7 stainless steel cable with Teflon liner
		Fillauer 1.19 mm cross-lay 7x7 stainless steel cable with 0.2 mm Nylon coating and Teflon liner
		Igus Robolink 2 mm 12x braided Dyneema cable with jointed iglidur® RN54 outer cable & liner
		Jagwire Road Pro 1.1 mm Teflon-coated derailleur cable with slick-lube liner

B.3.3. RESULTS & DISCUSSION

The measured frictional losses as a function of linear velocity are shown in Figure B.6 for the different cable materials and bending radii. In general, it can be seen that only the Fillauer prosthetic cables show a slight increase in friction towards higher velocities, whereas the Teflon-coated cable from Jagwire and Dyneema cable from Igus seem to be more or less constant over the measured range of velocities. The steel cable, without any coatings, performed worst of all tested materials in terms of predictability across the range of velocities and overall efficiency. The most efficient cable material with barely any dependency on cable velocity was the bicycle cable from Jagwire, which included a Teflon coating and a silicon grease (slick-lube) as additional lubricant.

It stands out that there is barely any difference in relative losses due to changes in bending radii. It is only the steel cable from Fillauer that shows higher quantitative differences. However, the qualitative differences seem to be at random, and may be a result of badly controlled experimental conditions. For example, the bending radius of the outer cable was enforced by wrapping it around a drum using tie-wraps. These tie-wraps could have introduced additional compressive forces on the outer cable when too tight, or the outer cable could slide through these connections when too loose. Combined with the fact that the bare steel cable showed to have the highest coefficient of friction, these imperfections might have been amplified under these conditions.

B.4. DESIGN IMPLICATIONS

In this study, we are particularly interested in applications where space is a limiting factor and all components need to be fit into a small volume. For this purpose, Bowden cables are especially simple in design and can fit in the smallest of spaces. As can be seen in the original patent drawing (Figure B.1), it only needs an outer cable fixation at each end and the cable can be connected to a mechanism with any kind of cable terminator (e.g., thimble, socket) or pulley mechanism.

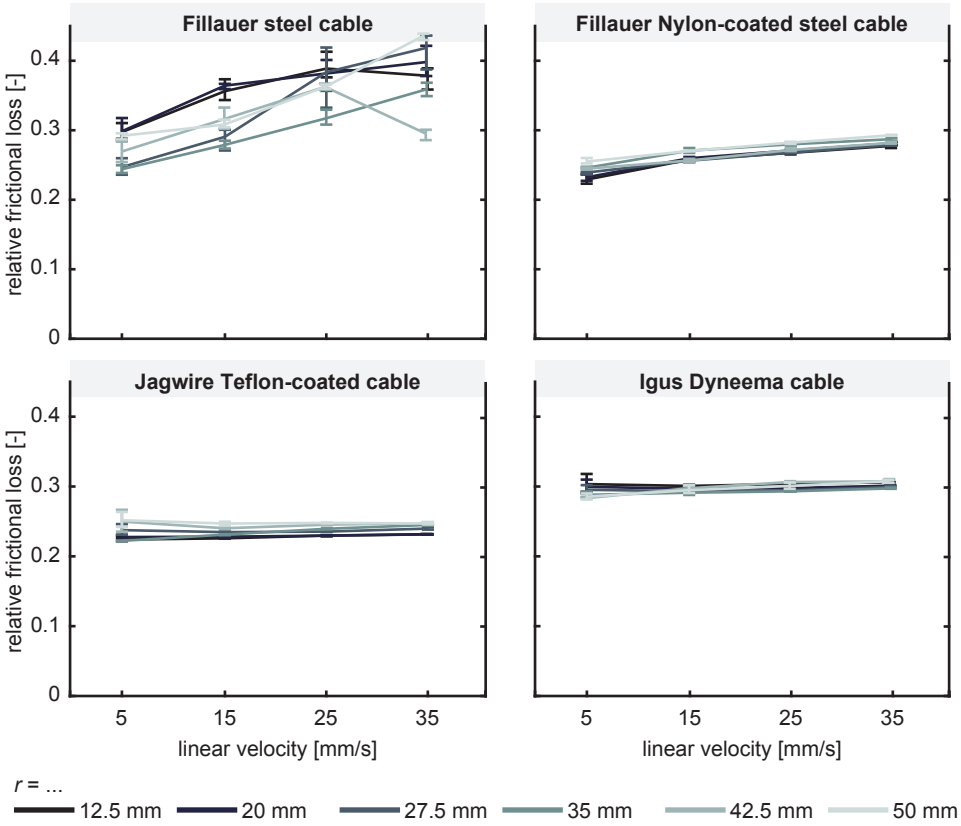

Figure B.6: Mean relative frictional losses of Bowden cable systems, comparing friction-velocity characteristics for different cable materials that are bent at different radii. Error bars indicate minimum and maximum values.

B.4.1. MAINTAINING TENSION

The inner cable inside a Bowden cable mechanism always requires some amount of tension. A slack cable can derail from a pulley or introduce a dead zone, where the initial onset of input force will not result in any force transmission towards the output. Controlling for cable slackness is therefore important for a more predictable force transmission. Pretension can be added to minimize cable slackness, for example with passive elastic elements (Schiele et al., 2006), but this also increases overall friction (Agrawal et al., 2010). Other examples of dealing with cable slackness are with agonist-antagonist setups (Jones et al., 2014) to prevent slackness as a whole, or with the addition of cable guides to prevent derailment of the cable from a pulley (Jeong et al., 2015).

B.4.2. ADDING CABLE-PULLEY MECHANISMS

In some cases, the mechanism is required to do more than just transferring mechanical work from one place to the other. Underactuation is an often-used example in this case (see Figure 3.6). With underactuation, there are more mechanical degrees of freedom than independently controlled actuators, which results in the need of a differential mechanism to distribute the force of an actuator over multiple mechanical degrees of freedom. When this is desired in combination with a Bowden cable mechanism, either pulley or link mechanisms are used. Such mechanisms can become increasingly complex when more degrees of freedom need to be underactuated.

Not only for underactuation, combining a Bowden cable-like mechanism with a pulley mechanism is a viable and popular implementation. Of the 32 hand orthotic devices that were found in the structured overview in Chapter 3 that make use of a Bowden cable, 19 were used in combination with a cable-pulley mechanism. However, adding pulley mechanisms inflicts repetitive bending of the cable over a small pulley and will eventually result in failure due to bending fatigue. How this affects the endurance of the system, strongly depends on the cable material. This is a well-known problem in larger scale cable systems (e.g., elevators, bridges), but very little information is available on the bending endurance of small-diameter cables (<2.5 mm).

How exactly the material can influence a cable's bending endurance, was briefly tested in an experimental setup. In Figure B.7a this setup is illustrated, which was designed to measure the fatigue life of small-diameter cables, subject to cyclical bending around a certain radius. The setup is very similar to the standard machines described in Feyrer (2015). The cable is wound around a traction sheave and a follower sheave. A back-and-forth motion is imposed by the traction sheave, causing a certain portion of the cable to be bent and stretched around the follower sheave. By making sure that the traction sheave diameter is always larger than that of the follower sheave, the cable should fail at the follower sheave. Additionally, the follower sheave is constrained in horizontal direction and suspended by the cable in vertical direction. This way, a constant preload can be imposed on the cable—independent on the cable's elongation—by loading the follower sheave with weights.

Five different cable materials were tested: stainless steel and nylon-coated steel (same as in the Bowden cable measurements); and, three types of Dyneema, namely SK99, SK78 and SK78 with a polyester jacket. The cables were tested at a constant tension in the cable of 150 N. This, however, makes comparison difficult as the diameters of the cables differed between 1.2–2.5 mm due to a limited choice in available cable diameters. Hence, for normalized results, additional measurements were done with a constant tensile stress of 20 N/mm^2. Between these two loading conditions, a straight line can be drawn on a log-log graph for visual interpolation. There is also a turning point where the slope suddenly changes to a steeper drop (Feyrer, 2015). Therefore, from only these two loading conditions, we cannot say for sure if the results are before, during or after this drop. Considering that the applied stresses are far below the materials' yield strength (<15% of cable strength), we assume that the results are before this turning point.

In Figure B.7b the results are shown, showing the mean cycles until failure over three repetitions. It can be seen that in both loading conditions, Dyneema cables are far better then steel cables in terms of bending fatigue, even though the relative bending radius (D_f/d_c) was much smaller. However, both cables with Dyneema SK78 show a steeper

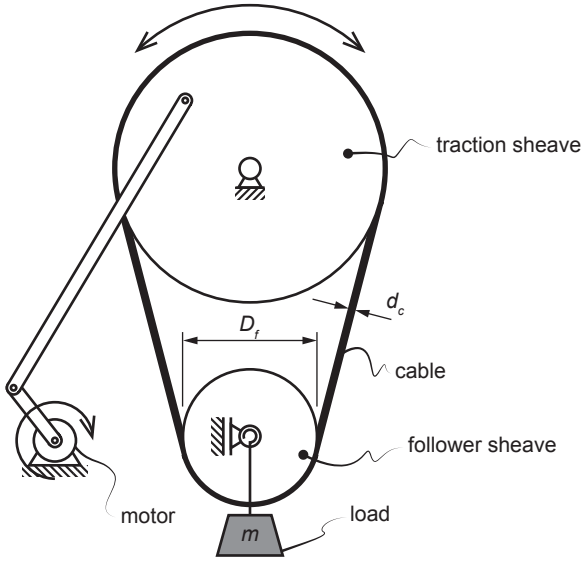

(a)

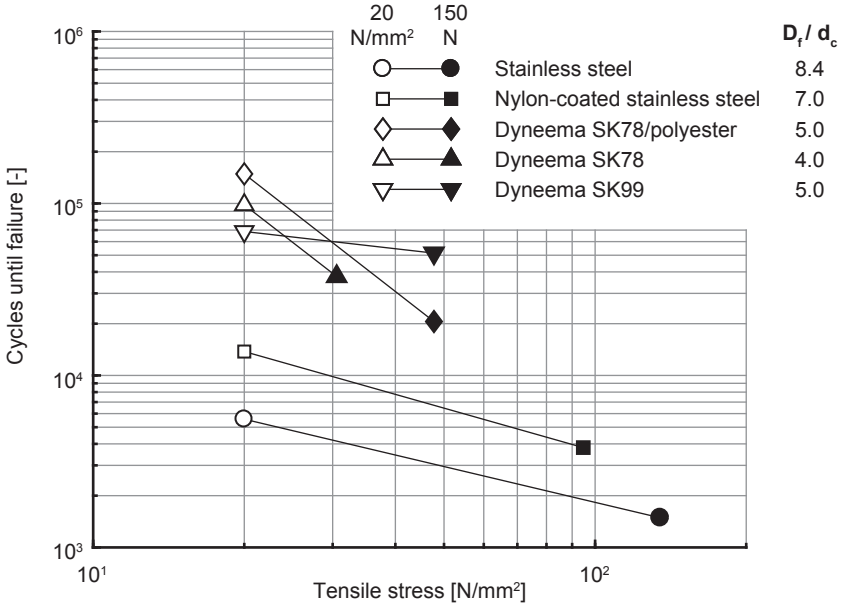

(b)

Figure B.7: (a) Experimental setup for measuring cable bending endurance. (b) Mean bending endurance of five different cable materials, each tested at a constant tensile stress of 20 N/mm^2 and a constant load of 150 N. The types of cables differed slightly in outer diameter, resulting in different ratios of sheave over cable diameter (D_f/d_c).

drop in bending endurance than the steel cables, hence it might be possible for these lines to cross at higher stresses. With that in mind, it seems that the Dyneema SK99 cable is the best option when optimizing for the longest fatigue life in a cable being bent over a pulley.

These cable bending enduring measurements were tested at only two different loading conditions and only one bending radius. It would be interesting to see how each material responds to different bending radii, as well as a multitude of loading conditions. Moreover, within small volumes, it makes more sense to use cables that are smaller in diameter than 1.2 mm. There were no suppliers found that could deliver off-the-shelf Dyneema cables in this order of magnitude. Smaller cables of the same material are expected to have a longer bending endurance at the cost of a decrease in tensile strength. The Dyneema cables that were tested, however, could handle tensile forces up to 6 kN, which indicates that a decrease in tensile strength is still acceptable for prosthetic and orthotic applications.

B.5. CONCLUSIONS & RECOMMENDATIONS

Overall, it can be concluded that Bowden cable transmission systems can be very simplistic in design and can fit in very small spaces. If materials are chosen correctly, force efficiencies of more than 70% can be obtained with very little dependence on operating velocity. However, force efficiency also depends on factors that can change during operation, mostly curvature angle, which makes it very hard to obtain a transparent force transmission. Moreover, tension needs to be maintained and combinations with pulley mechanisms introduce reductions in lifetime due to bending fatigue.

The results from the Bowden cable friction measurements have shown that bending radius has very little effect on dynamic friction and, in the case of the cables from Jagwire and Igus, friction remains approximately constant at velocities between 5–35 mm/s. It can be recommended to utilize the technology from bicycle cables and use Teflon-coated cables with a silicon grease for optimal efficiency and predictability. However, bending radius does have an effect on the cable's bending endurance. In this case, Dyneema was tested as the most suitable cable material with cycles to failure that far exceed those of steel cables. However, there are variations of Dyneema material that behave differently over a range of loading conditions. More testing is required to properly map these trends of bending endurance.

In addition to bending endurance, currently available literature also leaves room for a more complete mapping of dynamic friction, where especially close-to-zero (<5 mm/s) and high (>35 mm/s) velocities are missing. Additionally, for better reproducible results than presented in this study, the fixations of the outer cable need to be adjusted to a scenario that more resembles a practical implementation. Because, in reality, the Bowden cable is allowed to bend freely and no curvature radii are enforced. Considering that bending radius has negligible effect, this is also no longer necessary.

C

MINIATURE HYDRAULIC SYSTEMS

This appendix features work from the following publication:

R. A. Bos and D. H. Plettenburg (2019). "Miniaturization of hydraulic components". In: *7th Dutch Bio-Medical Engineering Conference*. Egmond aan Zee

Hydraulic systems are a type of a fluidic system and can be used in many ways. It can be a transmission system by transporting mechanical work from one location to another by using a working fluid. Or, it can be an actuation system by transforming potential energy (i.e., a pressurized fluid) or kinetic energy (i.e., a fluid with momentum) into mechanical work. In hydraulics the working fluid is a liquid and is generally incompressible, in contrary to pneumatics where compressible gases are used. This can be very advantageous, because of lot of pressure can be generated without losing heat during compression. Moreover, the incompressible nature allows for a very transparent force transmission. A lot of knowledge is available on hydraulics, where applications can range from micro-scale lab-on-chips to large-scale construction equipment. In between these two scales lies the millimeter-range of applications. This range is not explored as much, whereas it can be a very interesting alternative to electromagnetic actuation in orthotics, prosthetics and other robotic applications. Many terms are used to describe this scale of fluidic actuation, among them are miniature fluidics (Solano and Rotinat-Libersa, 2011; Pillsbury et al., 2015; Chakravarthy et al., 2014; Pourghodrat and Nelson, 2014), small-scale fluidics (Hocking and Wereley, 2013) and mesofluidics (Love et al., 2009). In this chapter, the term miniature fluidics is used and will be discussed with a focus on using hydraulics.

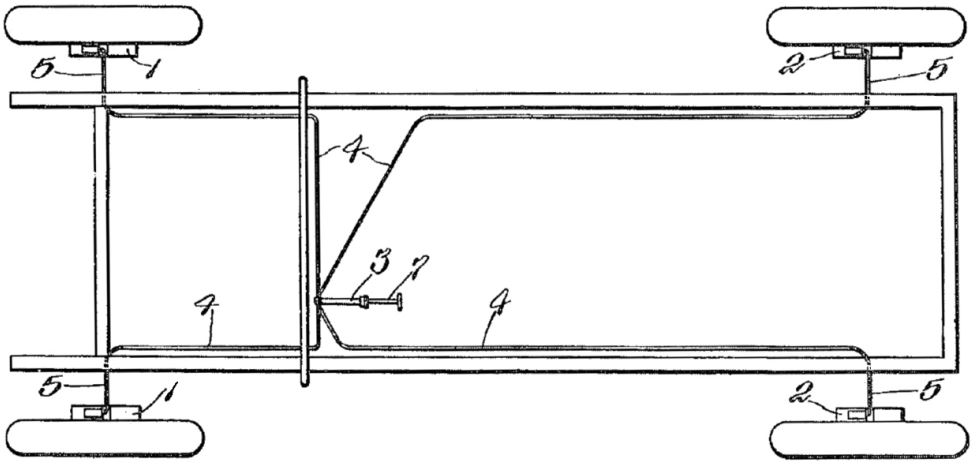

Figure C.1: Working principle of the hydraulic brake system from Loughead (1917). The illustration indicates a master cylinder (no. **3**) that, upon pressing on the brake pedal (no. **7**), distributes pressure among all slave cylinders at the front (no. **1**) and rear wheels (no. **2**) by connecting them with hydraulic lines (no. **4**).

C.1. HYDRAULIC TRANSMISSION WORKING PRINCIPLE

As an alternative to Bowden cables, hydraulic systems can also provide a means of transporting mechanical work through the use of flexible hoses and an incompressible fluid. Similar to the Bowden cable, hydraulic transmissions have been around for quite a while. Of course, hydraulic technology itself is as old as time (Ewbank, 1847), but it was only at the end of the 18th century that Joseph Bramah made use of the benefits of closed hydraulic circuits in the first hydraulic press (Bramah, 1897). A more relevant example is the first hydraulic brake system by Loughead (1917) (see Figure C.1), which later would become one of the founders of the Lockheed Corporation.

Both inventions rely on Pascal's principle, which states that pressure is uniform and acts in all directions in a fluid at rest. Hence, by coupling the chambers of two fluidic cylinders, force can be transmitted in the form of fluidic pressure. In the case of hydraulics, an incompressible fluid is used and so the motion of these cylinders will be coupled as well with little delay. In addition, the presence of a hydraulic circuit creates the opportunity to utilize some phenomena of fluidic systems. For example, by varying the surface area between the hydraulic cylinders, which is exploited in the hydraulic press (Bramah, 1897), a leverage system emerges and force can be amplified. Pressure can also be distributed among multiple output cylinders, creating a differential mechanism much like the hydraulic brake system (Loughead, 1917). These aspects make hydraulic transmission systems particularly useful as they can potentially transfer, amplify and distribute forces and movements inside one system.

Additional advantages that can be leveraged in a hydraulic transmission that uses a closed hydraulic circuit are high transmission stiffness, backdrivability and a routing-independent high efficiency (LeBlanc, 1985; Smit et al., 2013; Whitney et al., 2014).

Because there is no continuous flow of hydraulic fluid, the use of return lines, a reservoir, valves and flow sensors are not essential and can be omitted.

However, as is the case with all fluidic systems, the necessity to seal the working fluid to prevent leakages remains the biggest issue. A leakage can be defined as an undesired mass transport of the working fluid outside of the fluidic circuit. The most obvious form of leakage is due to a clearance somewhere along the fluidic circuit, allowing the fluid to escape. A rupture in a hose or a bad connector are examples of such leaks. Additionally, some sealing methods (like O-ring seals) will always have a small film of fluid between the sealing element and sealed component (see Section C.3). In this scenario, no matter how small, there will always be some leakage present and minimizing this is usually coupled with an increase in energy losses due to friction. Aside from that, after prolonged operation of a hydraulic system—even without mechanical failures—all these small leakages add up and the circuit will still need to be refilled (and possibly de-aired). Next to failures due to fatigue, this is an important aspect when long-term use is considered.

C.2. FLUIDIC ACTUATORS

C.2.1. OVERVIEW

From a more general perspective, a hydraulic transmission is a type of fluidic system. This system contains a working fluid with a certain momentum, which can be inflicted by pressure forces, gravity forces and viscous forces (White, 2011). For example, a pressure differential can cause a flow or net force on moving components, i.e. actuators, which are then used to actuate certain parts of a mechanism. From this perspective, the working fluid can be considered as a source of potential energy and the fluidic actuator transforms this into usable mechanical work, rather than using the fluid as a method of transporting and distributing mechanical work in a hydraulic transmission. To avoid confusion, the actuation, transmission, leverage and distribution properties are here grouped under the umbrella terms *hydraulics* and *hydraulic system*.

For the purpose of miniaturizing hydraulics for wearable systems, systems that use gravity forces (e.g., hydropower) are omitted in this study. The actuators can rely on a static or dynamic fluid and, similar to the classification in de Volder and Reynaerts (2010), fluidic actuators can be either elastic or inelastic. Figure C.2 shows how the different types of fluidic actuators relate to these properties, which can also be seen as an expansion to the overview in Chapter 3. Among these types, the balloon-, bellow-, artificial muscle- and piston-type actuators are considered to be the most feasible for miniaturization. The very small strokes of membrane actuators make them more suited for micro-scale applications, and the other actuators are generally more complex and require more (moving) parts.

In order to assess the state-of-the-art of these selected types of fluidic actuators on a miniature scale, a collection of actuators was searched in scientific literature. Scopus was used as search engine with the following search query in March 2016: `(miniature OR small-scale) AND (pneumatic OR hydraulic OR fluidic) AND (actuator) AND NOT (pump OR valve)`. Studies that used miniature fluidic actuators which were already found in Bos et al. (2016) were included as well. Additionally, products from Festo, SMC, Parker and Airpot were also scanned for actuators that fall within the miniature scale (< 20 mm). In some cases, a single article or product line contained multiple actuators

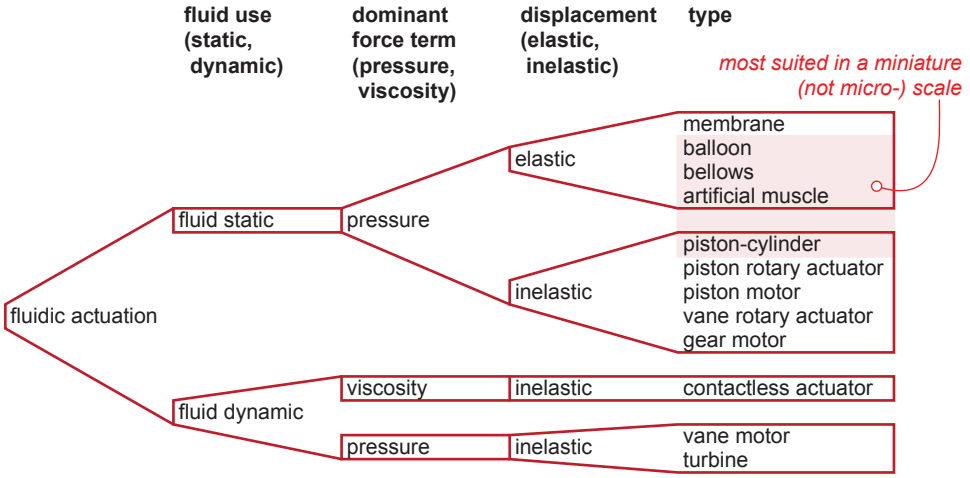

Figure C.2: Classification of fluidic actuators for wearable applications according to fluid use, dominant force term and elasticity of the displacement mechanism. Actuators that are considered most feasible for miniaturization are marked in red.

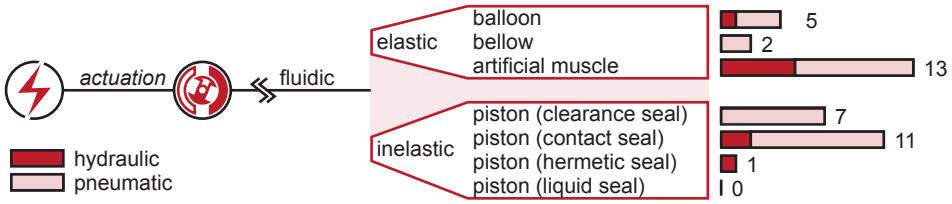

Figure C.3: Classification of fluidic actuators according to de Volder and Reynaerts (2010), along with the quantities of actuators that were found in scientific literature and industrial products.

at different scale ranges (e.g., multiple piston diameters). This ultimately resulted in 39 different actuators originating from 18 scientific articles and 7 product lines from industry. See Figure C.3 for a visualization of the results in a classification scheme.

In Tables C.1 and C.2, these fluidic actuators are listed along with properties that are independent on scale. Here, maximum actuation stress (Huber et al., 1997) is determined by dividing the highest reported actuator force by the cross-sectional area. Maximum actuation strain is determined by dividing the reported stroke by the initial length of the actuator (Huber et al., 1997). Some actuators operate in a radial direction, like bending balloon- or bellow-type actuators. For these cases the initial length and stroke were approximated from the arc length of the actuator. Lastly, the maximum supply pressure was collected for each entry, which illustrates the actuator's capacity to withstand higher pressures. A comparison with the maximum actuation stress gives an indication on how efficiently an actuator is able to utilize the system pressure of the working fluid.

Table C.1: Tabular overview of found elastic miniature fluidic actuators, along with their maximum actuation stress, actuation strain en supply pressure. Entries are sorted according to scale, after being subdivided according to the type of actuator and whether they were used as a pneumatic or hydraulic component.

P/H[1]	scale[2]	source	maximum actuation stress [Pa]	maximum actuation strain [-]	maximum supply pressure [Pa]
Balloon (linear):					
P	$4{\cdot}10^{-4}$	Chishiro et al. (2013)	$47.92{\cdot}10^{3}$	$208.33{\cdot}10^{-3}$	$150.00{\cdot}10^{3}$
P	$1{\cdot}10^{-2}$	Ionescu et al. (2012)	$378.61{\cdot}10^{3}$	$920.00{\cdot}10^{-3}$	$500.00{\cdot}10^{3}$
Balloon (radial):					
P	$8{\cdot}10^{-3}$	Kadowaki et al. (2011)	$162.40{\cdot}10^{3}$	$104.72{\cdot}10^{-3}$	$200.00{\cdot}10^{3}$
P	$2{\cdot}10^{-2}$	Toya et al. (2011)	$19.81{\cdot}10^{3}$	$224.40{\cdot}10^{-3}$	$350.00{\cdot}10^{3}$
H	$1{\cdot}10^{-2}$	Polygerinos et al. (2015)	$40.00{\cdot}10^{3}$	$545.42{\cdot}10^{-3}$	$345.00{\cdot}10^{3}$
Bellow (radial):					
P	$2{\cdot}10^{-3}$	Wakimoto et al. (2011)	700.28	$837.76{\cdot}10^{-3}$	$40.00{\cdot}10^{3}$
P	$6{\cdot}10^{-3}$	Udupa et al. (2014)	$6.01{\cdot}10^{3}$	$195.48{\cdot}10^{-3}$	$180.00{\cdot}10^{3}$
Artificial muscle:					
P	$1{\cdot}10^{-3}$	Chakravarthy et al. (2014)	$3.71{\cdot}10^{6}$	$180.00{\cdot}10^{-3}$	$827.00{\cdot}10^{3}$
P	$1{\cdot}10^{-3}$	Chakravarthy et al. (2014)	$3.09{\cdot}10^{6}$	$170.00{\cdot}10^{-3}$	$827.00{\cdot}10^{3}$
P	$1{\cdot}10^{-3}$	Chakravarthy et al. (2014)	$2.65{\cdot}10^{6}$	$160.00{\cdot}10^{-3}$	$827.00{\cdot}10^{3}$
P	$4{\cdot}10^{-3}$	Hocking and Wereley (2013)	$10.13{\cdot}10^{6}$	$77.20{\cdot}10^{-3}$	$552.00{\cdot}10^{3}$
P	$6{\cdot}10^{-3}$	Pillsbury et al. (2015)	$5.37{\cdot}10^{6}$	$310.00{\cdot}10^{-3}$	$621.00{\cdot}10^{3}$
P	$6{\cdot}10^{-3}$	Pillsbury et al. (2015)	$3.95{\cdot}10^{6}$	$75.00{\cdot}10^{-3}$	$552.00{\cdot}10^{3}$
P	$6{\cdot}10^{-3}$	Pillsbury et al. (2015)	$3.63{\cdot}10^{6}$	$240.00{\cdot}10^{-3}$	$621.00{\cdot}10^{3}$
P	$1{\cdot}10^{-2}$	Festo fluidic muscle DMSP	$1.47{\cdot}10^{6}$	$194.36{\cdot}10^{-3}$	$600.00{\cdot}10^{3}$
H	$2{\cdot}10^{-3}$	Solano and Rotinat-Libersa (2011)	$3.40{\cdot}10^{6}$	$29.70{\cdot}10^{-3}$	$1.46{\cdot}10^{6}$
H	$2{\cdot}10^{-3}$	Solano and Rotinat-Libersa (2011)	$3.40{\cdot}10^{6}$	$204.92{\cdot}10^{-3}$	$1.00{\cdot}10^{6}$
H	$2{\cdot}10^{-3}$	Solano and Rotinat-Libersa (2011)	$3.82{\cdot}10^{6}$	$116.09{\cdot}10^{-3}$	$1.77{\cdot}10^{6}$
H	$2{\cdot}10^{-3}$	Ryu et al. (2008)	$1.27{\cdot}10^{6}$	$108.70{\cdot}10^{-3}$	$550.00{\cdot}10^{3}$
H	$3{\cdot}10^{-3}$	Solano and Rotinat-Libersa (2011)	$2.44{\cdot}10^{6}$	$144.79{\cdot}10^{-3}$	$1.53{\cdot}10^{6}$

[1] P = pneumatic; H = hydraulic.
[2] Determined by the length of the smallest dimension in meters (e.g., outer diameter).

C.2.2. ACTUATOR COMPARISON

From Figure C.3, it can be seen that artificial muscle-type actuators and pistons with contact seals are the most popular. This is because artificial muscle-type actuators are easiest to obtain as an off-the-shelf product, whereas piston-cylinders with contact seals (e.g., O-rings) are the most widely available inelastic actuators. Some types of actuators are also missing from the overview or barely represented, like bellow-type actuators and pistons with a hermetic or liquid seal. The two classes of actuators (elastic versus inelastic) and their sub-types are described in more detail below.

Table C.2: Tabular overview of found inelastic miniature fluidic actuators, along with their maximum actuation stress, actuation strain en supply pressure. Entries are sorted according to scale, after being subdivided according to the type of actuator and whether they were used as a pneumatic or hydraulic component.

P/H[1]	scale[2]	source	maximum actuation stress [Pa]	maximum actuation strain [-]	maximum supply pressure [Pa]
Piston (clearance seal):					
P	$9{\cdot}10^{-4}$	Obara and Konishi (2012)	$5.00{\cdot}10^{3}$	$454.55{\cdot}10^{-3}$	$400.00{\cdot}10^{3}$
P	$1{\cdot}10^{-3}$	Obara and Konishi (2012)	$1.56{\cdot}10^{3}$	$454.55{\cdot}10^{-3}$	$500.00{\cdot}10^{3}$
P	$6{\cdot}10^{-3}$	Airpot self-aligning	$260.26{\cdot}10^{3}$	$701.66{\cdot}10^{-3}$	$860.00{\cdot}10^{3}$
P	$6{\cdot}10^{-3}$	Airpot Plus Air	$226.70{\cdot}10^{3}$	$592.59{\cdot}10^{-3}$	$700.00{\cdot}10^{3}$
P	$6{\cdot}10^{-3}$	Bouzit et al. (2002)	$567.65{\cdot}10^{3}$	$450.00{\cdot}10^{-3}$	$650.00{\cdot}10^{3}$
P	$9{\cdot}10^{-3}$	Airpot Plus Air	$295.13{\cdot}10^{3}$	$801.28{\cdot}10^{-3}$	$700.00{\cdot}10^{3}$
P	$9{\cdot}10^{-3}$	Airpot self-aligning	$206.36{\cdot}10^{3}$	$780.34{\cdot}10^{-3}$	$690.00{\cdot}10^{3}$
Piston (contact seal):					
P	$3{\cdot}10^{-3}$	Festo Round cylinders EG	$249.45{\cdot}10^{3}$	$263.16{\cdot}10^{-3}$	$700.00{\cdot}10^{3}$
P	$3{\cdot}10^{-3}$	SMC CJ1 series	$183.03{\cdot}10^{3}$	$263.16{\cdot}10^{-3}$	$700.00{\cdot}10^{3}$
P	$4{\cdot}10^{-3}$	Festo Round cylinders EG	$315.76{\cdot}10^{3}$	$312.50{\cdot}10^{-3}$	$700.00{\cdot}10^{3}$
P	$4{\cdot}10^{-3}$	SMC CJ1 series	$294.37{\cdot}10^{3}$	$298.51{\cdot}10^{-3}$	$700.00{\cdot}10^{3}$
P	$6{\cdot}10^{-3}$	Festo Round cylinders EG	$185.89{\cdot}10^{3}$	$233.64{\cdot}10^{-3}$	$700.00{\cdot}10^{3}$
P	$9{\cdot}10^{-3}$	Parker SR series	$1.26{\cdot}10^{6}$	$533.33{\cdot}10^{-6}$	$1.70{\cdot}10^{6}$
P	$1{\cdot}10^{-2}$	Peerdeman et al. (2012)	$920.65{\cdot}10^{3}$	$495.05{\cdot}10^{-3}$	$1.20{\cdot}10^{6}$
P	$1{\cdot}10^{-2}$	Parker P1A series	$504.78{\cdot}10^{3}$	$412.37{\cdot}10^{-3}$	$1.00{\cdot}10^{6}$
P	$2{\cdot}10^{-2}$	Plettenburg (2005)	$1.05{\cdot}10^{6}$	$896.06{\cdot}10^{-3}$	$1.20{\cdot}10^{6}$
H	$3{\cdot}10^{-3}$	Peirs et al. (2001)	$990.30{\cdot}10^{3}$	$333.33{\cdot}10^{-3}$	$1.00{\cdot}10^{6}$
H	$4{\cdot}10^{-3}$	Sindrey and Bone (2009)	$740.07{\cdot}10^{3}$	$312.50{\cdot}10^{-3}$	$738.00{\cdot}10^{3}$
Piston (hermetic seal):					
H	$1{\cdot}10^{-2}$	Pourghodrat and Nelson (2014)	$73.66{\cdot}10^{3}$	$263.16{\cdot}10^{-3}$	$380.00{\cdot}10^{3}$

[1] P = pneumatic; H = hydraulic.
[2] Determined by the length of the smallest dimension in meters (e.g., outer diameter).

ELASTIC ACTUATORS

Elastic actuators all depend on the expansion of a material to provide enough stroke, whereas the material should also be strong enough to withstand a high enough pressure for output force. Increased actuator forces are therefore accompanied by a decrease in stroke and vice versa. To illustrate this, both the balloon- and bellow-type actuators clearly show very high attainable actuation strains but with pretty low actuation stresses and supply pressures. The artificial muscle-type actuator is a little different, as it converts a radial expansion of elastic material in a linear shortening of the actuator. The most occurring type, i.e. the McKibben muscle, does this by covering the material with braided strands. This allows the actuation stress to exceed the supply pressure, allowing for a very volume-efficient actuator in the transverse direction. On the other side, however, these types of actuators have low available strain, which is clearly visible in Table C.1, and are therefore not that volume-efficient in the longitudinal direction.

One of the largest disadvantages of elastic actuators is that output force decreases as stroke increases. This is because at maximum stroke, all the potential energy is stored in the elastic material in the form of elastic energy and nothing is left to be converted into mechanical work. As a result, the maximum actuation stresses and strains never occur at the same time. In fact, maximum actuation stress is always at zero stroke and maximum actuation strain is at zero force.

INELASTIC ACTUATORS

As can be seen in Table C.2, inelastic actuators generally show more moderate stresses, strains and pressures. However, the list is also mostly made up of industrial products and, because they are designed for a much longer lifetime, mainly show lower achievable strains and pressures. The actuators from Parker are an exception, but are unfortunately limited in miniaturization with a minimum diameter of 9 mm. Custom piston-type actuators, on the other hand, are able to work with higher pressures and achieve higher actuation stesses and strains. Depending on the design of the actuator, strains can be comparable to some of the elastic actuators. Actuation stresses, however, will always be lower than those of artificial muscles, as it is physically impossible for a piston-type actuator to have an actuation stress that is higher than its supply pressure.

As opposed to elastic actuators, inelastic piston-type actuators do not have the disadvantage of limited pressures due to bursting of elastic material or decreasing output force with increasing stroke. Instead, the sealing element becomes a determining factor. A stronger seal introduces more friction and a weaker seal introduces more leakage.

Nonetheless, the disadvantage of sealing friction is considered less of problem compared to a limit in actuation force and stroke. Especially with the application of an orthosis, large strokes are required in very small volumes. Therefore, inelastic piston-type actuators are considered to be most feasible. How sealing exactly affects the performance in this type of actuator, is described below.

C.3. SEALING

Leaks in a fluidic system result in a loss of pressure and fluid volume, thus a loss in potential energy and decrease in overall efficiency. Moreover, when working with toxic and/or non-biodegradable fluids like oils, leakages can even become hazardous to the environment. Hence the necessity to seal fluidic components and maintain the fluid within the system is apparent.

Sealing the components comes with a cost, as it requires tight barriers between the fluid and the environment. These barriers decrease force efficiency (e.g., friction between parts, (visco-)elastic material expansion) and immediately forms an important trade-off: tighter seals decrease force efficiency, whereas weaker seals would increase the risk and amount of leakage. It strongly depends on the application and the desired fluid pressures as to which factor is more important.

There are different types of seals for a piston-type actuator that can contain the working fluid. According to de Volder and Reynaerts (2010) these are the clearance seal, contact seal, hermetic seal and liquid seal. Table C.3 displays a summary of their properties regarding friction, leakage and pressure limitations in a basic piston-cylinder configuration. Because of the combination of high attainable fluid pressures, low leakage rates and ease of miniaturization, contact seals were chosen as the most suited method

Table C.3: Tabular overview of sealing methods, along with their estimated friction, leakage, pressure limitations and other notes. Data is based on a basic piston-cylinder configuration with a 4 mm diameter piston moving at 30 mm/s while using water at a gauge pressure of 1.6 MPa, which should be able to achieve 20 N of force in a frictionless situation.

Seal	Friction	Leakage	Pressure limitations	Notes
Clearance seal	-0.2 N	1.3 mL/s	None	Continuously leaking fluid aids with increasing output force.
Contact seal	2.3 N	0.4 μL/s	10–70 MPa	Break-out friction can be 3 times the running friction.
Hermetic seal	-	None	0.62–6.9 MPa	More stiff seal materials increase pressure limits, but decrease available stroke. Energy losses not characterized by friction, but hysteretic losses from material expansion.
Liquid seal	0.001 N	None	10–100 kPa	1.6 MPa possible when combined with a clearance seal, but also introduces leakage.

of sealing despite their high friction. The following sections describe these seals in more detail and how this table was filled.

C.3.1. CLEARANCE SEAL

The clearance seal is the most basic seal. The leakage is limited by keeping the clearance gap between the cylinder bore and piston very small. The main advantage is that there is no direct contact between the piston and cylinder, which decreases the friction when compared to other types of seals. Moreover, there are no real pressure limitations to this seal, because the sealing method cannot fail under increased pressures. A disadvantage is that there will always be a considerable amount of leakage. This is also why only pneumatic actuators were found with a clearance seal in Table C.2, because leakage is then less of a problem compared to a hydraulic system.

USING NAVIER-STOKES EQUATIONS

Determining friction and leakage for a clearance seal can be done through the basic scenario of a piston moving concentrically in a hollow tube (i.e., cylinder). Under normal operating conditions, there is no direct contact between the piston and the cylinder. The total friction force is then dominated by the viscous friction caused by the working fluid in the clearance gap, which can be determined by using the Navier-Stokes equations. These equations essentially describe the fluid's momentum in all axial directions. Solving these equations is very cumbersome and requires a lot of computational power, hence it is common to make several convenient assumptions. In this case, the following set of assumptions can be used:

- fluid is at constant temperature;

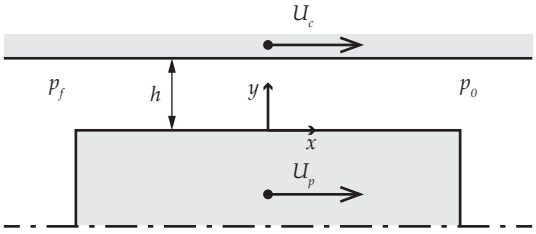

Figure C.4: A piston and cylinder separated by a clearance gap (h) and moving with a linear velocity (U_p and U_c, respectively). The piston is subject to the fluid's working pressure (p_f) on side, and the surrounding pressure (p_0) on the other side.

- viscosity does not change with pressure;
- fluid is incompressible (Mach number (Ma) ≤ 0.3);
- fluid flow is steady;
- pressure gradient is linear and only in longitudinal direction; and,
- clearance gap size between piston and cylinder wall is much smaller compared to piston diameter (flat plate approximation).

Combined with the conservation of mass in a control volume, this then leads to the following expressions for viscous friction (F_v) and leakage (q_l) in a clearance seal:

$$F_v = \pi D_p \left(-\frac{1}{2} h p_g + \frac{1}{h} \eta L_p U_p \right) \tag{C.1}$$

$$q_l = \pi D_p \left(\frac{h^3 p_g}{12 \eta L_p} + \frac{1}{2} h U_p \right) \tag{C.2}$$

In these equations, D_p is the piston diameter, h the gap between the piston and cylinder wall, p_g the pressure differential across the piston, η the fluid's dynamic viscosity, L_p the length of the piston and U_p the linear velocity of the piston (see Figure C.4.

In Xia and Durfee (2011), they indicate the equation for viscous friction to be a superposition of pressure-induced (Poiseuille) and velocity-induced (Couette) flow, which are specific solutions to the Navier-Stokes equations and give the same result when combined. This also reveals that when the gauge pressure is zero, the friction is solely dependent on the piston velocity and in opposite direction. If pressure is added, an additional force acts in the opposite direction of the pressure gradient and can reduce the overall viscous friction experienced by the moving piston. Figure C.5 visualizes the flow profile and shows that the added pressure gradient adds a parabolic shape to the velocity profile, which can reverse the direction of the velocity gradient close to the piston wall and thus the direction of viscous friction force. Leakage, on the other hand, is always positive as both types of flow contribute to fluid exiting the control volume through the gap.

APPLICATION

When scaling the dimensions of a fluidic piston-cylinder, equation (C.1) shows that the gap size (h) becomes an essential parameter to consider. For decreasing values of h,

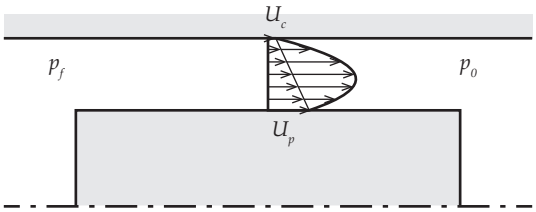

Figure C.5: Flow velocity profile for a clearance seal between a piston and cylinder. The overall profile can be considered as a superposition of velocity-induced flow (linear Couette flow) and pressure-induced flow (parabolic Poiseuille flow).

the pressure-induced friction will decrease and velocity-induced friction will increase, resulting in a less advantageous viscous friction force. Consequently, a minimum gap size will not always be beneficial, as larger gaps can aid in reducing the overall viscous friction. On the other hand, larger gaps will also give rise to increased fluid leakage.

This can be illustrated by choosing, for example, $D_p = 4$ mm, $h = 20$ μm, $p_g = 1.6$ MPa, $\eta = 1.002$ mPa·s (water), $L_p = 10$ mm and $U_p = 30$ mm/s. In this scenario, the piston speed is in some way constrained to move at 30 mm/s, which can be due to loading conditions (in an unloaded situation, this speed can be much higher). In this situation, we find a viscous friction of -0.2 N, which actually helps with increasing the output force. This is because the pressure-induced flow has a very high effect on the viscous forces, causing the velocity-induced flow to be almost negligible. On the downside, of course, there is a continuous leak (also at zero velocity) of substantial proportions.

Equation (C.2) reveals that a fair amount of leakage can exist through the clearance gap. Using the same values of before, already 1.3 mL/s of leakage occurs. Considering that a 4 mm cylinder is not likely to contain more than 1 mL of fluid, its own volume will be leaked within a second. For this reason, the leaking fluid will need to be recovered and recycled in the hydraulic circuit (e.g., in the reservoir), or tighter seals are necessary which can better contain the working fluid within the system. There are piston-cylinders with clearance seals commercially available (Airpot Corporation, Norwalk, CT, USA), but their engineering guides indicate that radially squeezing the cylinder by hand can already cause it to deform and affect the clearance gap size. Moreover, because these piston-cylinders are used in pneumatics, leakage becomes less of a problem. To avoid the necessity of such high-precision equipment and allowing a more robust solution suitable for hydraulics, contact seals are an often-used alternative in this case and are discussed in the next section.

C.3.2. CONTACT SEALS

Contact seals are characterized as elastic rings pressed between the piston and cylinder. Figure C.6 shows a few examples of seal shapes, where the O-ring is the most accessible at very small sizes. Essentially, the working principle is similar to that of a clearance seal. There remains a small fluid film of thickness h between the seal and sealed element, which

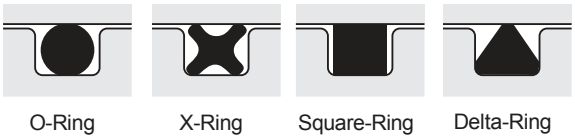

Figure C.6: Examples of different types of contact seals. Reproduced from Parker Hannifin Corporation O-ring Division (2007) (Figure 5-17) with permission.

influences the viscous friction and leakage rate. However, the elasticity of a contact seal allows it to conform to the shape of the rigid parts under pressure, evidently resulting in very small values of h. Moreover, a lubricant can occupy this small fluid film to further reduce friction and leakage.

EMPIRICAL FORMULAS

When predicting the friction and leakage of a contact seal, the complexity lies in determining the value for h and the influence of the lubricant. The Reynolds equation is often used as a starting point for many problems that involve hydrodynamic lubrication with very small fluid film thicknesses (Karaszkiewicz, 1987; White, 1991; Nikas and Sayles, 2006; Nikas, 2010; van Beek, 2009). Similar to the approach with a clearance seal, the equation finds it origin from the Navier-Stokes equations and the continuity equation. Unfortunately, the Reynolds equation does not have a closed form solution and requires a numerical procedure (Nikas and Sayles, 2006). However, there also exist empirical formulas that are more practical to use in their range of validity.

An empirical formula is inherently based on measurements that are subject to specific surrounding conditions, it is therefore important to know about these conditions to judge the applicability. Moreover, an empirical formula is usually based on a starting point that represents the most influential phenomena. In Plettenburg (2002), a method from the Parker Seal Company is described and was noted as the most practical method at the time. It breaks the friction of an O-ring down into two components: friction resulting from applied fluid pressure and friction resulting from the initial compression of the O-ring:

$$F_O = f_c(\alpha, H_S)L_w + f_h(p_g)A_{proj} \tag{C.3}$$

In this formula, f_c is a factor depending on the relative squeeze of the O-ring's cross-section (α) and material Shore hardness (H_S), which is multiplied by the length of the seal's wetted (rubbing) surface (L_w). In case of a piston seal, L_w equals the outside circumference of the seal (πD_c), for a rod seal this is the inside circumference (πD_r). Representing friction caused by the fluid's pressure, f_h is a factor depending on gauge pressure (p_g) and is multiplied by the seal's projected area ($A_{proj} = \frac{\pi}{4}\left(D_c^2 - D_g^2\right)$, where D_g is the piston groove diameter). Both f_c and f_h need to be looked up in graphs, which contain measured data based on the following conditions (Parker Hannifin Corporation O-ring Division, 2007):

- AN6227 rings (O-rings with standardized sizes for general use);
- room temperature;
- using MIL-H-5606 hydraulic oil;

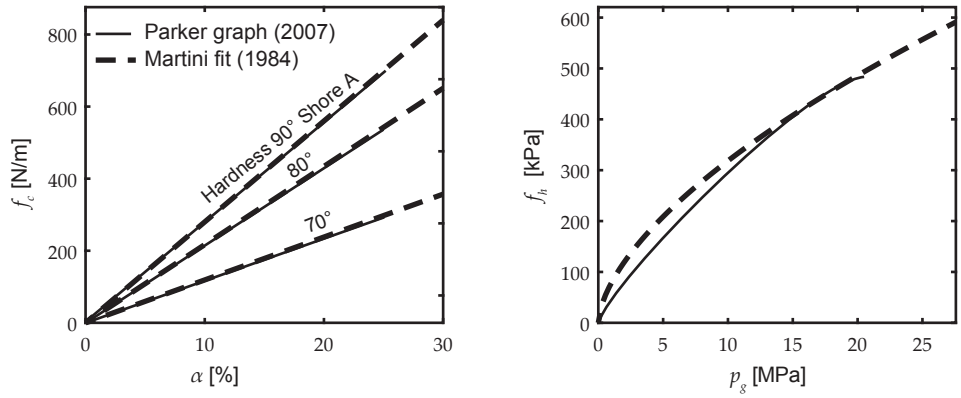

Figure C.7: Comparison between the graphical method from Parker and fit from Martini (1984) on the same data. Adapted from Parker Hannifin Corporation O-ring Division (2007) (Figures 5-9 and 5-10) with permission.

- seals rubbed against chrome plated surface with 35 μm surface finish; and,
- speeds in excess of 0.005 m/s.

Although using look-up graphs can be more convenient than numerical procedures in some cases, it is still cumbersome when trying to visualize overall behavior or sensitivity to changes. On this same dataset, a formula has been fitted by Martini (1984) that can approximate these factors with:

$$\begin{aligned} f_c = &\quad 1.75 \cdot 10^4 \left(-0.884 + 0.0206 H_S - 0.0001 H_S^2\right) \alpha \\ f_h = &\quad 17.1 p_g^{0.61} \end{aligned} \tag{C.4}$$

Although the year of publication differs by more than 20 years with the most recent Parker O-Ring Handbook, an overlap of both methods reveals that the fit by Martini (1984) still holds (see Figure C.7). Especially the approximation of f_c is very accurate, considering it is a linear fit. However, at pressures between 0-10 MPa, equation (C.4) will slightly overestimate f_h. Moreover, at pressures higher than 20 MPa, the dataset for determining f_h from Parker ends and so does the validity of using equation (C.4).

A different approach for estimating O-ring efficiency comes from Xia and Durfee (2011), who based their approximation on an analytical solution from Al-Ghathian and Tarawneh (2005):

$$F_O = \pi D_p d_O \mu_f E \alpha \sqrt{2\alpha - \alpha^2} \tag{C.5}$$

In this expression, d_O represents the O-ring's cross-sectional diameter, E the elastic modulus and μ_f the friction coefficient between the sealing element and cylinder wall. In contrary to the Parker/Martini approach, equation (C.5) does not distinguish explicitly between a pressure-induced and O-ring compression-induced friction, but are incorporated in a different way. O-ring compression is represented by the elastic modulus and squeeze ratio of the sealing element, whereas the pressure is hidden in the used definition for wall friction:

$$\mu_f = \begin{cases} C_1\sqrt{\frac{\eta U_p}{p_g}} & \text{if } p_g \neq 0 \\ C_2\sqrt{\eta U_p} & \text{if } p_g = 0 \end{cases} \tag{C.6}$$

Here, the constants equal to $C_1 = 12650$ and $C_2 = 4$ and are based on nominal operating conditions where $\eta = 0.1$ Pa·s, $U_p = 0.1$ m/s, $p_g = 10$ MPa and the assumption that μ_f should be in the range of 0.4 (Xia and Durfee, 2011). These are reasonable conditions for lubricated O-ring sealing in miniature applications.

COMPARISON

Using equations (C.5) and (C.6) seems less convenient compared to using equations (C.3) and (C.4). Firstly because material hardness is more easily reported for sealing materials than the elastic modulus. Although there exist empirical relations between hardness and elastic modulus for rubbers (ERIKS bv, n.d., p.26), the extra step and accompanying uncertainty adds inconvenience.

Secondly, equation C.6 requires quite some knowledge on the frictional properties between the O-ring and the cylinder wall, which now assumes a square root dependence on piston velocity and frictional values based on common practices in order to obtain the constants C_1 and C_2. Moreover, a follow-up paper from the same authors found that friction was actually decreasing with velocity (Xia and Durfee, 2014). A more accurate approximation for friction in lubricated contacts would be that of a Stribeck curve (Xia and Durfee, 2014; Andersson et al., 2007), which includes high break-out friction, a drop at low-to-moderate speeds and either an increase or decrease in friction at higher speeds. Going into such depth, however, would defeat the purpose of an empirical model, which is to obtain a fast and easy approximation.

A comparison of both estimations of O-ring friction reveals that they do not give similar results. At the previously mentioned nominal operating conditions, along with $D_p = 4$ mm, $d_O = 1$ mm, $\alpha = 0.1$, $H_S = 70$ Shore A and $E = 5.5$ MPa (ERIKS bv, n.d., p.26), the formula from Xia & Durfee predicts approximately 1.1 N of friction, whereas the output from Martini gives 3.8 N. These are large differences and imply that either one of the methods is wrong (or both). However, combined with the earlier mentioned disadvantages of using equations (C.5) and (C.6) and the proven industrial applicability of Parker's dataset, the use of equations (C.3) and (C.4) was chosen to be the best available empirical approach for O-ring friction.

APPLICATION

O-ring seals provide for a very robust sealing method and is probably the most-used solution as well. In contrary to the clearance seal, the elastic nature of an O-ring allows for a more forgiving fabrication accuracy. At $D_p = 4$ mm, $p_g = 1.6$ MPa, $H_S = 70$ and $\alpha = 0.1$, there is a constant friction of approximately 2.3 N. It should be noted that this describes the running friction of the seal. At the initiation of movement, a much higher friction force needs to be overcome. This break-out friction increases when the piston-cylinder assembly has been stationary for a longer time, as it allows the rubber of the O-ring to further conform to the irregularities on the cylinder wall. According to Parker Hannifin Corporation O-ring Division (2007), the break-out friction can reach a maximum of 3 times

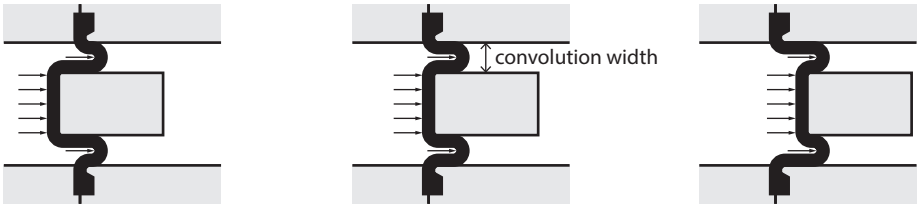

Figure C.8: Working principle of a rolling diaphragm seal, which consists of an elastic membrane (in black) that folds itself inside-out.

the running friction in the case of a seal with 70 Shore A hardness on a cylinder wall with 0.2 μm surface finish.

The amount of leakage is more difficult to determine. Although Xia and Durfee (2011) also presented a method to estimate this, their validity is questionable because it is based on similar empirical relations as their models for O-ring friction. However, in (Nikas and Sayles, 2006), maximum film thicknesses of approximately 0.1–1 μm are reported. Using equation (C.2) from the clearance seal, a worst-case-scenario would then result in a leakage of approximately 0.4 μL/s. If a piston needs 1 s to cover the full stroke, 625 full cycles of pro- and retraction result in a 50 μL droplet of leakage.

O-ring seals do have a pressure limit, but can be quite high if proper sealing materials are used. If there is a clearance of 0.1 mm between the piston and cylinder wall, pressures of more than 10 MPa can be easily achieved with 70 Shore A hardness and up to 70 MPa with 90 Shore A hardness seals (Parker Hannifin Corporation O-ring Division, 2007, p.3-3).

C.3.3. HERMETIC SEALS

A hermetic seal means that there is an elastic material inside the cylinder that either fully encompasses the fluid or completely seals the piston. This ensures the cylinder to be leak-free (except for possible permeation through the material) and to have no strict requirements on fabrication accuracy. The most common example is a rolling diaphragm seal, which uses an elastic material to seal a moving piston by folding itself inside-out (see Figure C.8). Because this seal does not involve sliding contact, there is no stick-slip behavior like in a contact seal. The main source of energy loss comes from the hysteresis due to rolling and unrolling of the convolution (Whitney et al., 2014).

However, as can be inferred from the working principle in Figure C.8, a rolling diaphragm has a maximum stroke and requires radial clearance to amount for the convolution width and attachment of the diaphragm. Towards the stroke limits, the hysteretic losses at the convolution increase (Burkhard et al., 2017). Additionally, pressure is limited by the bursting strength of the diaphragm material, which generally ranges between 1.0–1.7 MPa (Whitney et al., 2014) but can also reach values of 6.9 MPa (Bellofram Corporation, 1998). Naturally, higher working pressures result in higher hysteretic losses and ask for more stiff materials that require more space in an assembly. Such factors hinder miniaturization of a piston-type actuator and limits the applicability in miniature fluidics.

It is also possible to use a bladder-like structure inside the cylinder chamber to function as a hermetic seal. This more or less resembles the situation of an elastic

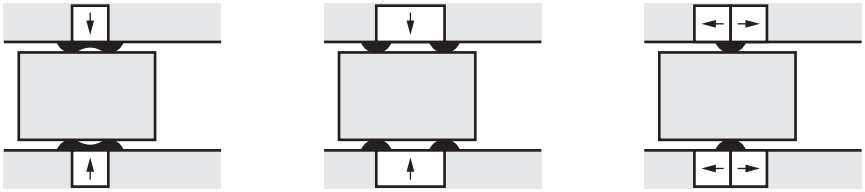

Figure C.9: Working principle of a liquid seal, where variations in magnetic fields can result in different shapes and dimensions of the seal. Adding additional magnetic rings can reduce leakage of the magnetic field and increase seal pressure (Ravaud et al., 2009).

balloon-type actuator, where the cylinder chamber and a moving piston act as guides to direct the expansion of the balloon. The advantage of this method is to ensure a leak-free actuator in a small scale while maintaining relatively large strokes, which can be particularly interesting in invasive medical devices (Pourghodrat and Nelson, 2014). However, because this method is also limited by the burst pressure of the balloon, pressures are very limited down to 0.62 MPa (Pourghodrat and Nelson, 2014).

C.3.4. LIQUID SEALS

A piston-type actuator can be equipped with a liquid seal by using magnetic rings and a ferrofluid. With a sufficiently strong magnetic field and small gap, the ferrofluid is able to seal a pressurized fluid and simultaneously function as a bearing. By varying magnetic orientation or even multiple magnets, different shapes of the seal can be obtained with different attainable seal pressures (see Figure C.9). Because the fluid will always conform to the surface of the piston and cylinder wall, a very efficient seal can be obtained with relatively rough surface qualities (de Volder and Reynaerts, 2009). Ferrofluid bearings have already gained interest as an alternative to ball and air film bearings and in precision positioning systems due to their low friction, inherent stability and no stick-slip effects (Ochonski, 2005; Lampaert et al., 2018), and are now also making their way towards cylindrical sealing elements (Ravaud et al., 2009; de Volder and Reynaerts, 2009).

Friction of a ferrofluid seal can be determined similar to that of a clearance seal, with the added condition that there is no leakage because the ferrofluid is being pushed back by the magnetic field (Lampaert et al., 2018). Using the same flat-plate approximation, this results in the following expression for experienced viscous friction:

$$F_L = 4\pi D_p \frac{1}{h} \eta_{ff} L_L U_p \tag{C.7}$$

In this equation, η_{ff} represents the viscosity of the ferrofluid and L_L the total length of the ferrofluid layer along the piston. Using $\eta_{ff} = 150$ mPa·s, $h = 180$ μm (Lampaert et al., 2018) and $L_L = 1$ mm (de Volder and Reynaerts, 2009), along with $D_p = 4$ mm and $U_p = 30$ mm/s, a very low friction of 0.001 N emerges.

Equation (C.7) is very similar to equation (C.1), with the difference that it does not include pressure-induced friction and multiplies the velocity-induced friction by 4. This is because it assumes that the magnetic force pulls the ferrofluid back in place such that there is no net fluid transport (Lampaert et al., 2018), which compensates for the

pressure-induced flow and its associated friction component. This property ensures that the friction of a liquid seal is no longer dependent on pressure.

However, maximum attainable pressures are quite limited and currently range between 10–100 kPa in centimeter-scale (Ravaud et al., 2009) and micro-scale applications (de Volder and Reynaerts, 2009). Smarter solutions are required to increase the attainable pressures. For example, a combination of a liquid seal with a clearance seal is reported to reach up to 1.6 MPa in a micro-scale application, albeit with additional complexity and introduction of leakage (de Volder and Reynaerts, 2009).

Although liquid seals show promise with very low attainable friction and zero leakage of working fluid, the pressure limitations prevent it to be a better alternative compared to contact seals. For a 4 mm cylinder to reach an output force of 20 N, a minimum pressure of 1.6 MPa is already required, which is just on the edge of the current capabilities of liquid seals. Nonetheless, continued research efforts on this sealing method can hopefully increase the attainable pressures and find its way to be applied in miniature hydraulics.

C.4. DESIGN IMPLICATIONS

Making a miniature hydraulic system work for a particular design means that, aside from optimizing the fluidic actuators and sealing methods, it should also be compatible within the practical limits. Several design implications therefore need to be considered, which include how size affects force efficiency, whether valves can provide a feasible method in this scale to expand functionalities, and how other fluidic components (e.g., hoses, bleeding valves) can present limitations to a design.

C.4.1. SCALING LAWS

With the sealing method chosen in favor of O-ring seals, we can use the corresponding formula and inspect how the performance changes when scaled to a millimeter scale. Given that a hydraulic cylinder can be designed to have almost any stroke length, the output force becomes the most determining factor. Specifically, from the perspective of a designer, we are interested in the efficiency of the hydraulic cylinder given a certain output force. By using equations (C.3)–(C.4) and assuming a single-acting hydraulic cylinder with only a piston seal, the following expression can be obtained for the actuator's output force, F_A:

$$F_A = \frac{\pi}{4} D_p^2 p_g - \frac{17.1\pi}{4} \left(D_c^2 - D_g^2 \right) p_g^{0.61} - 1.75 \cdot 10^4 \pi \left(-0.884 + 0.0206 H_S - 0.0001 H_S^2 \right) \alpha D_c \tag{C.8}$$

For a given value of F_A, it would be interesting to know how the efficiency responds when changing piston/cylinder dimensions. To do this, we first need to know how the pressure needs to be adjusted in order to accommodate the desired output force. However, because of the strange power exponent (0.61) on the differential pressure term, it becomes very difficult to analytically isolate this term. Therefore, a minimization procedure was performed on each combination of dimensions and desired output force, in order to find the required differential pressure:

$$\min_{p_g} f(p_g) = |F_A - F_{desired}| \quad \text{s.t.:} \quad p_g \geq 0 \tag{C.9}$$

Using the resulting value for the differential pressure, the relative losses of the actuator due to O-ring running friction can then be estimated according to:

$$f_{loss} = \frac{F_O}{\frac{\pi}{4} D_p^2 p_g} \tag{C.10}$$

Figure C.10 shows the relative losses as a function of the diameter scale for several desired output forces when using an O-ring with 70 Shore A hardness, squeeze ratio of 10% (Plettenburg, 2002) and cross-sectional thickness of 1 mm. Because of the O-ring's cross-sectional thickness, the minimum diameter is physically limited to approximately 3 mm in order to maintain a groove diameter of more than 1 mm. Moreover, the frictional losses should not exceed 0.33, because then the differential pressure is no longer able to overcome the maximum break-out force of 3 times the running friction.

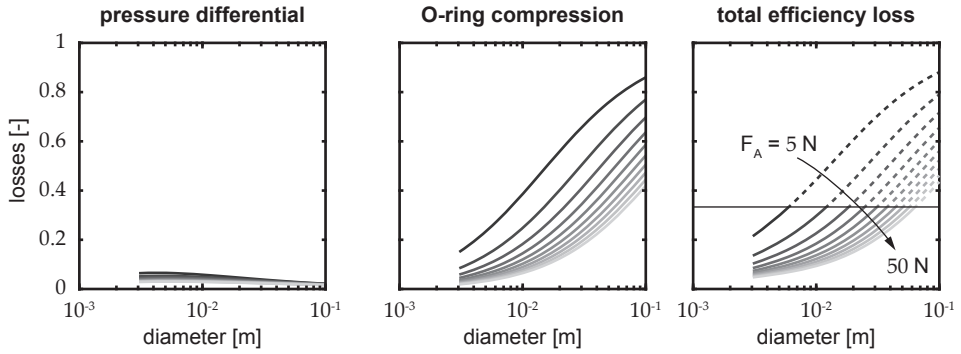

Figure C.10: Effect of scaling of a fluidic piston-type actuator on the relative frictional losses, using an O-ring with 70 Shore A hardness, squeeze of ratio of 10% and cross-sectional thickness of 1 mm. Frictional losses are broken up into losses due to the pressure differential and compression of the O-ring (see equations (C.3)–(C.4)). The total frictional losses should remain below 0.33, in order to be able to overcome maximum break-out force.

The total frictional losses can be broken up into losses due to the pressure differential and compression of the O-ring, equivalent to the terms $f_h A_{proj}$ and $f_c L_w$ from equation (C.3), respectively. The results from Figure C.10 shows that, for diameter sizes larger than 10 mm, the friction is almost completely governed by the O-ring compression. This means that changes in the O-ring dimensions and material properties will have the most influence in this order of magnitude. Towards smaller diameters, the pressure differential starts to have more influence and slightly increases the frictional losses again. However, because the O-ring compression remains the dominant term, it appears that the total losses will remain to decrease until the limit of 3 mm.

The fact that efficiency will increase for smaller cylinder diameters indicates that the scaling laws are in favor of miniaturization of fluidic components. Especially when output

forces between 5–20 N are desired, there is a very steep increase of efficiency towards the millimeter-range of diameters. In fact, to be able to achieve an output force of 5 N, a cylinder diameter of less than 6 mm is required in order to remain below the break-out force. For even smaller forces, the relative break-out force becomes too high and sealing methods without such stick-slip effects are required (e.g., liquid seals).

C.4.2. ADDING VALVES

Like the first hydraulic brake system (Loughead, 1917), pressure inside a hydraulic system can be distributed over multiple cylinders. Often, this is carried out in a master-slave system architecture, where a master actuator serves as an input and is connected to multiple slave actuators (e.g., Smit et al. (2015)). As an expansion to this concept, valves can be used to disconnect one or more slave actuators from the main circuit (e.g., Kargov et al. (2008)). This creates a separate circuit for the blocked slave actuators, while the other slave actuators are free to move with the master actuator. However, valves can add a substantial amount of mass and volume, as they rely on their own micro-actuator (e.g., solenoid, shape memory alloy) to actively block or pass fluid flow. To minimize this effect, valves often use a very small orifice to reduce the force necessary to block high pressure fluids. This results in a literal bottleneck and increases the flow resistance. The amount of slave actuators that can realistically be blocked with a single valve depends on the size of the valve orifice. For example, if a valve is linked to four slave actuators, it should also be able to accommodate the fluid flow to fully extend all four actuators. This gives rise to another trade-off given a fixed amount of slave actuators: less valves increase flow resistance per valve, whereas more valves increase mass and volume of the total system.

As an illustrative example, this was elaborated for a hydraulic dynamic hand orthosis design that uses water as working fluid and a total of 8 slave cylinders with a bore diameter of 4 mm and a 20 mm stroke (see Chapter 6). Fluid flow was then analyzed if all slave cylinders needed to be fully extended in 0.5 s. Two situations were assessed, one where each valve was linked with groups of four slave actuators (i.e., two finger elements) and one with two slave actuators per valve (i.e., one finger element). Additionally, by varying the diameter of the valve orifice, an estimate can be obtained of how a valve's design can influence flow characteristics. These orifices were varied between 0.40–1.00 mm, which require a valve's micro-actuator to exert a force of 0.25–1.6 N to block a 2 MPa flow, over a stroke of at least 0.10–0.25 mm to accommodate the fluid flow in an opened position.

Figure C.11 shows the overall schematic of these situations, along with the associated Reynolds numbers and presssure drops (estimated with extended Bernoulli equations) for each section of the circuit. These results show that, when two valves are used, turbulent flow is inevitable for the given flow rate. When four valves are used, orifices smaller than 0.60 mm should be avoided to prevent the formation of turbulent flow. Moreover, we find that pressure drops can rise up to an order of magnitude of 0.3 MPa (3 bar) if very small orifices (<0.40 mm) are used. Overall, it can be concluded that increasing valve orifice diameter has the most influence on the pressure drop. A doubling of the amount of valves can have a similar effect as increasing the valve orifice by only 0.10 mm. The amount of valves (i.e., the flow rate through the valve orifice) has the most influence on the Reynolds number and, at the same time, can increase overall functionality of the system.

To the author's knowledge, valves from the Lee Company (IEP Series, The Lee Company, Westbrook, CT, USA) and Gyger (Micro valve, Fritz Gyger AG, Gwatt,

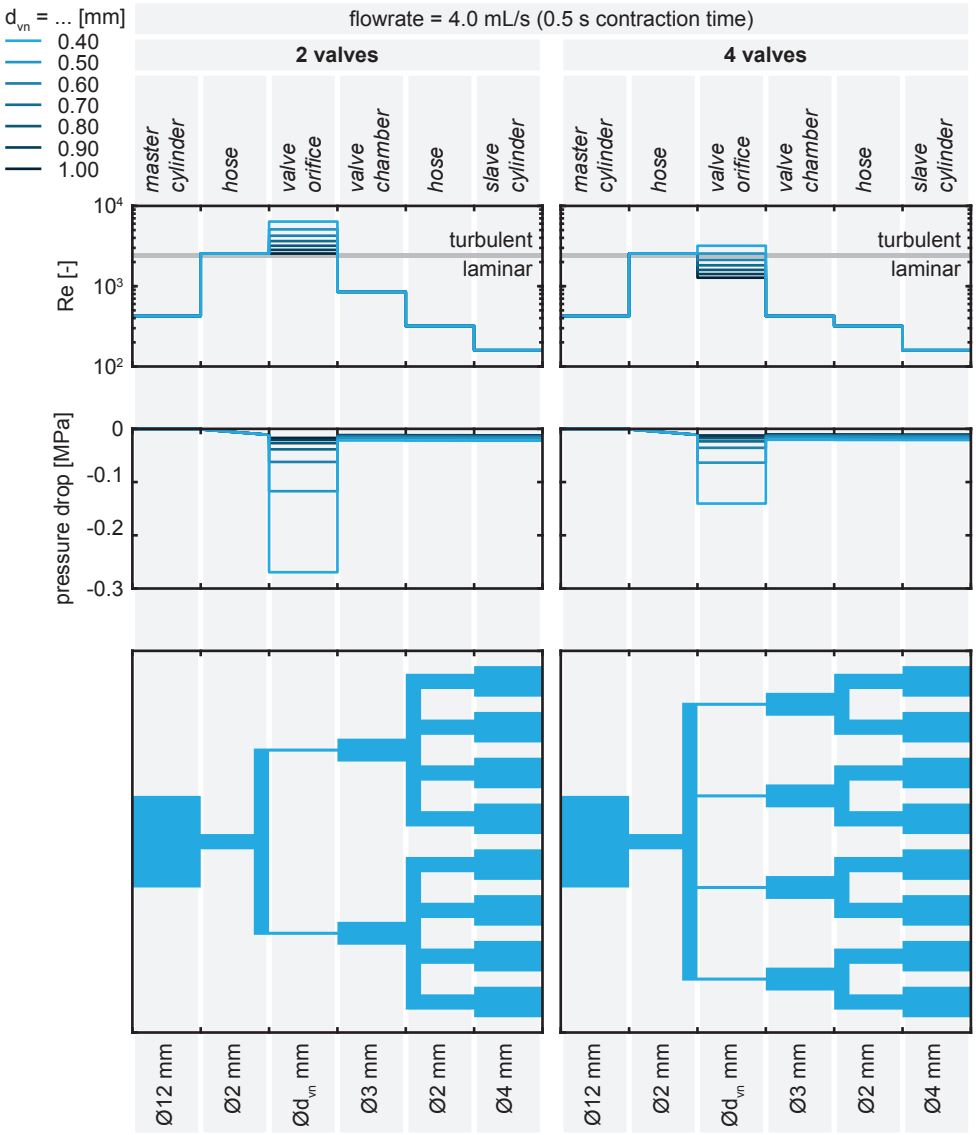

Figure C.11: Reynolds numbers and pressure drops for fluid flow (water) through a hydraulic circuit that uses a total of 8 slave cylinders to actuate a hypothetical dynamic hand orthosis. The lower figures illustrate the hydraulic circuit, along with the varying channel diameters, and serve as a label for the horizontal axes. The left figures depict a situation where only 2 valves are used, each operating 4 slave cylinders, whereas the right figures depict a situation with 4 valves, each operating 2 slave cylinders.

Switzerland) are currently the only commercially available valves that can block pressures higher than 2 MPa (up to 5 MPa) within a 10 mm diameter encasing. However, their valve orifices range between 0.40–0.60 mm, which still result in high pressure drops and potentially turbulent flow. Aside from the flow resistance, this increases the risk of cavitation, which occurs when the pressure locally drops below vapor pressure. Therefore, lower speeds need to be used or new valves need to be developed. In the case where a new valve is desired, selection of the micro-actuator in combination with a method to seal the fluid from the electronics is key. Because of the very low strokes that are required for the micro-actuator (i.e., 0.10–0.25 mm), sealing methods with stick-slip behavior are unsuitable because of the accompanied relative inefficiencies and inaccuracies.

C.4.3. COMPONENT INTEGRATION

Aside from taking advantage of fluidic phenomena, there are also design implications that limit the possibilities. Firstly, one that is quickly encountered when gathering and assembling components, is the size of the connectors and stiffness of the hoses. Especially in a prototyping phase, a system that facilitates quick (dis-)connecting of the hoses is favorable but results in bulky connectors. Additionally, the hoses available for miniature hydraulics (i.e., outer diameters of <3 mm) are scarce and their accompanying bending stiffness does not make it easy to route the hoses in a practical way.

Secondly, a closed hydraulic circuit cannot always be used to pull on the fluid. This causes the system pressure to decrease and the fluid to expand when below vapor pressure. Because a perfect vacuum is impossible to achieve, the maximum pressure differential with the atmosphere is only approximately 0.1 MPa (1 bar) and limits the attainable forces for a fluidic actuator. A bidirectional actuator (e.g., a double-acting piston-type actuator) is therefore often used to avoid this effect, but quickly increases volume occupation due to introduction of additional valves or hydraulic lines. Alternatively, a passive element (e.g., spring, flexible structure) at the slave actuator can be used to provide the return force, with the downside that the attainable forces and speeds are different between the directions of actuation. As suggested by Burkhard et al. (2017), a constant bias pressure can also be introduced (e.g., using pneumatic pressure), which increases the pressure differential with the atmosphere and therefore also the available pulling force.

Lastly, as with any hydraulic system with a closed circuit, air bubbles can develop from multiple sources: air that was dissolved in the fluid and exposed to low pressures; air that entered the system due to leakages; or, air that was trapped in the system to begin with. These bubbles decrease the bulk stiffness of the hydraulic system, which introduces mechanical delays and unwanted compliancy. Hence, in order to guarantee the characteristics of a hydraulic transmission over time, measures need to be taken in account to reduce the formation of bubbles inside the circuit. A combination of degassing the fluid, filling under vacuum pressure and the addition of a bias pressure to the circuit decreases the amount of dissolved air and risk of dropping below the fluid's vapor pressure. Alternative fluids like a biodegradable solution with ethylene glycol can also decrease the fluid's vapor pressure. However, this is accompanied by an increase in viscosity and therefore higher energetic losses due to fluid flow through small orifices. Over longer periods of time, any fluid needs to be de-aired. This requires the addition of bleeding valves to facilitate access to the working fluid and need to be taken in account

during the design of such a system. In tight spaces, this can be difficult to implement and affects the practical convenience of a design.

C.5. CONCLUSIONS & RECOMMENDATIONS

Due to a lack of available products in the millimeter-scale, miniature hydraulic systems were analyzed using scientific literature and general theories on fluid flow. In particular, its application in a closed hydraulic circuit was assessed. In this scenario, a hydraulic system provides efficient actuation, transparent transmission of mechanical work, and compact distribution and amplification of forces.

On a more specific component-level, it can be concluded that piston-type actuators with O-ring seals are the most feasible type of fluidic actuator to be used in the miniature scale. Scaling laws even suggest that, given a desired output force, smaller diameter cylinders with O-ring seals will result in higher force efficiencies. Additional testing is recommended to validate this deduction because it is based on empirical formula. As an alternative, although the attainable pressures limit their current feasibility, liquid seals have the potential to outperform O-ring seals due to a lack of stick-slip behavior.

The introduction of smaller cylinders also results in the requirement for higher pressures to accommodate the desired output force. Consequently, the development of smaller hydraulic components (e.g., hoses, connectors, valves) can be considered as equally important as actuator development. For example, if one were to successfully design a 2 mm bore hydraulic cylinder able to exert 20 N, it is uncertain whether this miniaturization remains useful if it requires a 5 mm diameter connector and a hose with a minimum bending radius of 30 mm. Additionally, the proposed range of actuator sizes and stroke speeds imply that currently available miniature hydraulic valves are inadequate. Research towards compact connectors, flexible high-pressure hoses and miniature hydraulic valve design is therefore warranted. In addition, solutions like integration of hydraulic functionalities (e.g., fluid transport, actuation) in structural or articulating components can further aid in the miniaturizability of hydraulic technology.

BIBLIOGRAPHY

Ab Patar, M. N. A. B., T. Komeda, C. Y. Low, and J. Mahmud (2015a). "Model-based systems engineering of a hand rehabilitation device". In: *Jurnal Teknologi*, 76 (4): 185–190. DOI: 10.11113/jt.v76.5496.

Ab Patar, M. N. A. B., T. Komeda, and J. Mahmud (2014). "Force assisted hand and finger device for rehabilitation". In: *2014 International Symposium on Technology Management and Emerging Technologies*. Bandung, pp. 133–138. DOI: 10.1109/ISTMET.2014.6936493.

Ab Patar, M. N. A. B., T. Komeda, J. Mahmud, and C. Y. Low (2015b). "Model Based Design of Finger Exoskeleton for Post Stroke Rehabilitation Using a Slotted Link Cam with Lead Screw Mechanism". In: *Industrial Engineering, Management Science and Applications 2015*. Ed. by M. Gen, K. J. Kim, X. Huang, and Y. Hiroshi. Vol. 349. Lecture Notes in Electrical Engineering. Berlin, Heidelberg, pp. 95–103. DOI: 10.1007/978-3-662-47200-2_11.

Ab Rahim, A. H., M. N. A. B. Ab Patar, A. T. M. Amin, and J. Mahmud (2013). "The Development of Finger Rehabilitation Device for Stroke Patients". In: *Applied Mechanics and Materials*, 393: 604–610. DOI: 10.4028/www.scientific.net/AMM.393.604.

Abbink, D. A., M. Mulder, and E. R. Boer (2012). "Haptic shared control: smoothly shifting control authority?" In: *Cognition, Technology & Work*, 14 (1): 19–28. DOI: 10.1007/s10111-011-0192-5.

Agarwal, P. and A. D. Deshpande (2015). "Impedance and force-field control of the index finger module of a hand exoskeleton for rehabilitation". In: *2015 IEEE International Conference on Rehabilitation Robotics (ICORR)*. Section II. Singapore, pp. 85–90. DOI: 10.1109/ICORR.2015.7281180.

Agarwal, P., J. Fox, Y. Yun, M. K. O'Malley, and A. D. Deshpande (2015). "An index finger exoskeleton with series elastic actuation for rehabilitation: Design, control and performance characterization". In: *The International Journal of Robotics Research*, 34 (14): 1747–1772. DOI: 10.1177/0278364915598388.

Agrawal, V., W. J. Peine, and B. Yao (2010). "Modeling of transmission characteristics across a cable-conduit system". In: *IEEE Transactions on Robotics*, 26 (5): 914–924. DOI: 10.1109/TRO.2010.2064014.

Agrawal, V., B. Yao, and W. J. Peine (2013). "Modeling of viscoelastic cable-conduit actuation for MRI compatible systems". In: *Journal of Dynamic Systems, Measurement, and Control*, 135 (5): 051004. DOI: 10.1115/1.4024079.

El-Aloul, B., K. N. Speechley, Y. Wei, P. Wilk, and C. Campbell (2019). "Fatigue in young people with Duchenne muscular dystrophy". In: *Developmental Medicine & Child Neurology*. DOI: 10.1111/dmcn.14248.

Alutei, A., A. Vaida, D. Mandru, and M. O. Tatar (2009). "Development of an Active Upper-Limb Orthosis". In: *International Conference on Advancements of Medicine and*

Health Care through Technology, pp. 405–408. DOI: 10.1007/978-3-642-04292-8_89.

AMES Technology, Inc. (n.d.). http://www.amesdevices.com/. Accessed 23 Oct 2015.

Amirabdollahian, F., S. Ates, A. Basteris, A. Cesario, J. H. Buurke, H. J. Hermens, D. Hofs, E. Johansson, G. Mountain, N. Nasr, S. M. Nijenhuis, G. B. Prange, N. Rahman, P. Sale, F. Schätzlein, B. van Schooten, and A. H. A. Stienen (2014). "Design, development and deployment of a hand/wrist exoskeleton for home-based rehabilitation after stroke - SCRIPT project". In: *Robotica*, 32 (08): 1331–1346. DOI: 10.1017/S0263574714002288.

Andersson, S., A. Söderberg, and S. Björklund (2007). "Friction models for sliding dry, boundary and mixed lubricated contacts". In: *Tribology International*, 40 (4): 580–587. DOI: 10.1016/j.triboint.2005.11.014.

Andry, N. (1743). *L'Orthopédie, ou l'art de prevenir et corriger dans les enfans, les difformités du corps*. George Fricx. URL: https://books.google.nl/books?id=GNFEAAAAcAAJ.

Arata, J., K. Ohmoto, R. Gassert, O. Lambercy, H. Fujimoto, and I. Wada (2013). "A new hand exoskeleton device for rehabilitation using a three-layered sliding spring mechanism". In: *2013 IEEE International Conference on Robotics and Automation (ICRA)*. Karlsruhe, pp. 3902–3907. DOI: 10.1109/ICRA.2013.6631126.

"Artificial muscle" (March 14, 1960). In: *LIFE*: 87–88.

Ates, S., C. J. W. Haarman, and A. H. A. Stienen (2016). "SCRIPT passive orthosis: design of interactive hand and wrist exoskeleton for rehabilitation at home after stroke". In: *Autonomous Robots*: 1–13. DOI: 10.1007/s10514-016-9589-6.

Ates, S., B. Leon, A. Basteris, S. M. Nijenhuis, N. Nasr, P. Sale, A. Cesario, F. Amirabdollahian, and A. H. A. Stienen (2014a). "Technical evaluation of and clinical experiences with the SCRIPT passive wrist and hand orthosis". In: *2014 7th International Conference on Human System Interactions (HSI)*. Costa da Caparica, pp. 188–193. DOI: 10.1109/HSI.2014.6860472.

Ates, S., J. Lobo-Prat, P. Lammertse, H. van der Kooij, and A. H. A. Stienen (2013). "SCRIPT passive orthosis: design and technical evaluation of the wrist and hand orthosis for rehabilitation training at home". In: *2013 IEEE International Conference on Rehabilitation Robotics (ICORR)*. Seattle, WA, pp. 1–6. DOI: 10.1109/ICORR.2013.6650401.

Ates, S., I. Mora-Moreno, M. Wessels, and A. H. A. Stienen (2015). "Combined active wrist and hand orthosis for home use: Lessons learned". In: *2015 IEEE International Conference on Rehabilitation Robotics (ICORR)*. Singapore, pp. 398–403. DOI: 10.1109/ICORR.2015.7281232.

Ates, S., I. M. Moreno, M. Wessels, P. Lammertse, and A. H. A. Stienen (2014b). "Three Stages of Development of the Robust SCRIPT Active Orthosis Session". In: *Design of Medical Devices Conference Europe Edition*. Delft, pp. 56–57.

Aubin, P., K. Petersen, H. Sallum, C. J. Walsh, A. Correia, and L. Stirling (2014). "A pediatric robotic thumb exoskeleton for at-home rehabilitation: the isolated orthosis for thumb actuation (IOTA)". In: *International Journal of Intelligent Computing and Cybernetics*, 7 (3). Ed. by D. Guilherme N. DeSouza: 233–252. DOI: 10.1108/IJICC-10-2013-0043.

Aw, K. C. and A. J. McDaid (2014). "Bio-applications of ionic polymer metal composite transducers". In: *Smart Materials and Structures*, 23 (7): 074005. DOI: 10.1088/0964-1726/23/7/074005.

Backus, D., P. Cordo, A. Gillott, C. Kandilakis, M. Mori, and A. M. Raslan (2014). "Assisted movement with proprioceptive stimulation reduces impairment and restores function in incomplete spinal cord injury". In: *Archives of Physical Medicine and Rehabilitation*, 95 (8): 1447–1453. DOI: 10.1016/j.apmr.2014.03.011.

Bae, J.-H., Y.-M. Kim, and I. Moon (2012). "Wearable hand rehabilitation robot capable of hand function assistance in stroke survivors". In: *2012 4th IEEE RAS & EMBS International Conference on Biomedical Robotics and Biomechatronics (BioRob)*. Rome, pp. 1482–1487. DOI: 10.1109/BioRob.2012.6290736.

Bain, G. I., N. Polites, B. G. Higgs, R. J. Heptinstall, and A. M. McGrath (2015). "The functional range of motion of the finger joints". In: *Journal of Hand Surgery (European Volume)*, 40 (4): 406–411. DOI: 10.1177/1753193414533754.

Baker, M. D., M. K. McDonough, E. M. McMullin, M. Swift, and B. F. BuSha (2011). "Orthotic hand-assistive exoskeleton". In: *2011 IEEE 37th Annual Northeast Bioengineering Conference (NEBEC)*. Troy, NY, pp. 1–2. DOI: 10.1109/NEBC.2011.5778523.

Balasubramanian, S., J. Klein, and E. Burdet (2010). "Robot-assisted rehabilitation of hand function". In: *Current Opinion in Neurology*, 23 (6): 661–670. DOI: 10.1097/WCO.0b013e32833e99a4.

Baqapuri, H. I., H. A. Nizami, S. Siddiqui, J. Iqbal, and U. Shahbaz (2012). "Prefabrication design of an actuated exoskeleton for traumatized and paralytic hands". In: *2012 International Conference of Robotics and Artificial Intelligence*. Rawalpindi, pp. 108–111. DOI: 10.1109/ICRAI.2012.6413404.

Bartels, B., R. F. Pangalila, M. P. Bergen, N. A. M. Cobben, H. J. Stam, and M. E. Roebroeck (2011). "Upper limb function in adults with Duchenne muscular dystrophy". In: *Journal of Rehabilitation Medicine*, 43 (9): 770–775. DOI: 10.2340/16501977-0841.

Basteris, A., S. M. Nijenhuis, A. H. A. Stienen, J. H. Buurke, G. B. Prange, and F. Amirabdollahian (2014). "Training modalities in robot-mediated upper limb rehabilitation in stroke: a framework for classification based on a systematic review". In: *Journal of NeuroEngineering and Rehabilitation*, 11 (1): 111. DOI: 10.1186/1743-0003-11-111.

Van Beek, A. (2009). *Advanced engineering design: Lifetime performance and reliability*. ISBN: 90-810406-1-8. Delft: TU Delft.

Bellofram Corporation (1998). *Bellofram rolling diaphragm design manual)*. Newell, WV. URL: http://bellofram diaphragm.com/wp-content/uploads/2017/03/brd-design-manual.pdf.

Ben-Tzvi, P. and Z. Ma (2015). "Sensing and Force-Feedback Exoskeleton (SAFE) Robotic Glove". In: *IEEE Transactions on Neural Systems and Rehabilitation Engineering*, 23 (6): 992–1002. DOI: 10.1109/TNSRE.2014.2378171.

Benjuya, N. and S. B. Kenney (1990). "Myoelectric hand orthosis". In: *Journal of Prosthetics & Orthotics*, 2 (2): 149–154.

Bennett, L. (1972). "Transferring load to flesh. Part III. Analysis of shear stress". In: *Bulletin of Prosthetics Research*, 10-17: 38–51.

Bergamasco, M., A. Frisoli, M. Fontana, C. Loconsole, D. Leonardis, M. Troncossi, M. M. Foumashi, and V. Parenti-Castelli (2011). "Preliminary results of BRAVO project: brain computer interfaces for Robotic enhanced Action in Visuo-motOr tasks." In: *2011 IEEE International Conference on Rehabilitation Robotics (ICORR)*. Zurich, p. 5975377. DOI: 10.1109/ICORR.2011.5975377.

Bergsma, A., J. Lobo-Prat, E. Vroom, P. Furlong, and J. L. Herder (2016). "1st Workshop on Upper-Extremity Assistive Technology for People with Duchenne: State of the art, emerging avenues, and challenges: April 27th 2015, London, United Kingdom". In: *Neuromuscular Disorders*, 26 (6): 386–393. DOI: 10.1016/j.nmd.2016.04.005.

Bi, Q. and C.-J. Yang (2011). "Design of a Hand Exoskeleton Rehabilitation Device". In: *Advanced Materials Research*, 328-330: 1778–1783. DOI: 10.4028/www.scientific.net/AMR.328-330.1778.

Bi, Q. and C.-J. Yang (2014). "Human-machine interaction force control: using a model-referenced adaptive impedance device to control an index finger exoskeleton". In: *Journal of Zhejiang University SCIENCE C*, 15 (4): 275–283. DOI: 10.1631/jzus.C1300259.

Bi, Q., C.-J. Yang, X.-L. Deng, and J.-C. Fan (2013). "Contacting Mechanical Impedance of Human Finger based on Uncertain System". In: *2013 IEEE/ASME International Conference on Advanced Intelligent Mechatronics (AIM)*. Wollongong, pp. 1619–1624.

Biddiss, E. and T. Chau (2008). "Dielectric elastomers as actuators for upper limb prosthetics: Challenges and opportunities". In: *Medical Engineering & Physics*, 30 (4): 403–418. DOI: 10.1016/j.medengphy.2007.05.011.

Bioness, Inc. (2013). *Ness H200 Brochure*. http://www.bioness.com/Documents/H200Consumer/H200_Wireless_Brochure_Update.pdf. Accessed 23 Oct 2015.

Birch, B., E. Haslam, I. Heerah, N. Dechev, and E. J. Park (2008). "Design of a continuous passive and active motion device for hand rehabilitation". In: *30th Annual International Conference of the IEEE Engineering in Medicine and Biology Society (EMBC)*. Vancouver, BC, pp. 4306–4309. DOI: 10.1109/IEMBS.2008.4650162.

Blake, D. J., A. Weir, S. E. Newey, and K. E. Davies (2002). "Function and genetics of dystrophin and dystrophin-related proteins in muscle". In: *Physiological Reviews*, 82 (2): 291–329. DOI: 10.1152/physrev.00028.2001.

Bos, R. A., C. J. W. Haarman, T. Stortelder, K. Nizamis, J. L. Herder, A. H. A. Stienen, and D. H. Plettenburg (2016a). "A structured overview of trends and technologies used in dynamic hand orthoses". In: *Journal of NeuroEngineering and Rehabilitation*, 13: 62. DOI: 10.1186/s12984-016-0168-z.

Bos, R. A., M. N. Mahmood, P. N. Kooren, S. Verros, M. I. Paalman, H. F. J. M. Koopman, and D. H. Plettenburg (2016b). "Measuring dynamic friction properties of Bowden cable systems". In: *The Anthology of the ISPO European Congress on Prosthetics and Orthotics*. Rotterdam, p. 45.

Bos, R. A., K. Nizamis, H. F. J. M. Koopman, J. L. Herder, M. Sartori, and D. H. Plettenburg (2018a). *SymbiHand DMD case study*. URL: https://www.youtube.com/watch?v=jpHjlFM0t3Y.

Bos, R. A., K. Nizamis, M. Sartori, H. F. J. M. Koopman, J. L. Herder, and D. H. Plettenburg (n.d.). *A case study with SymbiHand: an sEMG-controlled electrohydraulic hand orthosis for people with Duchenne muscular dystrophy*. Submitted.

Bos, R. A., D. H. Plettenburg, and J. L. Herder (July 2019). *Simplifying models and estimating grasp performance for comparing dynamic hand orthosis concepts*. DOI: 10.1371/journal.pone.0220147.

Bos, R. A., K. Nizamis, D. H. Plettenburg, and J. L. Herder (2018b). "Design of an electrohydraulic hand orthosis for people with Duchenne muscular dystrophy using commercially available components". In: *2018 International Conference on Biomedical*

Robotics and Biomechatronics (BioRob). Enschede, pp. 305–311. DOI: 10.1109/BIOROB.2018.8487196.

Bos, R. A. and D. H. Plettenburg (2019). "Miniaturization of hydraulic components". In: *7th Dutch Bio-Medical Engineering Conference*. Egmond aan Zee.

Bos, R. A., D. H. Plettenburg, and J. L. Herder (2017). "Exploratory design of a compliant mechanism for a dynamic hand orthosis: Lessons learned". In: *2017 International Conference on Rehabilitation Robotics (ICORR)*. London, pp. 603–608. DOI: 10.1109/ICORR.2017.8009314.

Bouzit, M., G. Burdea, G. Popescu, and R. Boian (2002). "The Rutgers Master II - New design force-feedback glove". In: *IEEE/ASME Transactions on Mechatronics*, 7 (2): 256–263. DOI: 10.1109/TMECH.2002.1011262.

Bowden, E. M. (1896). *New and improved mechanism for transmission of power*. Patent no. GB 25,325.

Bowden, E. M. (1897). *Improvements in and relating to brakes for velocipedes and other road vehicles*. Patent no. GB 14,402.

Bramah, J. (1897). *Obtaining and applying motive power*. Patent no. GB 2045.

Broadened Horizons, Inc. (n.d.). *PowerGrip Assisted Grasp Orthosis*. http://www.broadenedhorizons.com/powergrip. Accessed 25 Oct 2015.

Brokaw, E. B., I. Black, R. J. Holley, and P. S. Lum (2011). "Hand Spring Operated Movement Enhancer (HandSOME): a portable, passive hand exoskeleton for stroke rehabilitation". In: *IEEE Transactions on Neural Systems and Rehabilitation Engineering*, 19 (4): 391–399. DOI: 10.1109/TNSRE.2011.2157705.

Brown, P., D. Jones, S. K. Singh, and J. M. Rosen (1993). "The exoskeleton glove for control of paralyzed hands". In: *1993 IEEE International Conference on Robotics and Automation (ICRA)*. Atlanta, GA, pp. 642–647. DOI: 10.1109/ROBOT.1993.292051.

Bullock, I. M., J. Z. Zheng, S. De La Rosa, C. Guertler, and A. M. Dollar (2013). "Grasp frequency and usage in daily household and machine shop tasks". In: *IEEE Transactions on Haptics*, 6 (3): 296–308. DOI: 10.1109/TOH.2013.6.

Burkhard, N., S. Frishman, A. Gruebele, J. P. Whitney, R. Goldman, B. Daniel, and M. Cutkosky (2017). "A rolling-diaphragm hydrostatic transmission for remote MR-guided needle insertion". In: *2017 IEEE International Conference on Robotics and Automation (ICRA)*, pp. 1148–1153. DOI: 10.1109/ICRA.2017.7989137.

Burton, T. M. W., R. Vaidyanathan, S. C. Burgess, A. J. Turton, and C. Melhuish (2011). "Development of a parametric kinematic model of the human hand and a novel robotic exoskeleton". In: *2011 IEEE International Conference on Rehabilitation Robotics (ICORR)*. Zurich, pp. 1–7. DOI: 10.1109/ICORR.2011.5975344.

Burton, T. M. W., R. Vaidyanathan, S. C. Burgess, A. J. Turton, and C. Melhuish (2012). "Sensitivity Analysis of a Parametric Hand Exoskeleton Designed to Match Natural Human Grasping Motion". In: *Lecture Notes in Computer Science*. Ed. by G. Herrmann, M. Studley, M. Pearson, A. Conn, C. Melhuish, M. Witkowski, J.-H. Kim, and P. Vadakkepat. Vol. 7429. Bristol, pp. 390–401. DOI: 10.1007/978-3-642-32527-4_35.

Bushby, K., R. Finkel, D. J. Birnkrant, L. E. Case, P. R. Clemens, L. Cripe, A. Kaul, K. Kinnett, C. McDonald, S. Pandya, J. Poysky, F. Shapiro, J. Tomezsko, and C. Constantin (2010a). "Diagnosis and management of Duchenne muscular dystrophy, part 1: diagnosis, and

pharmacological and psychosocial management". In: *The Lancet Neurology*, 9 (1): 77–93. DOI: 10.1016/S1474-4422(09)70271-6.

Bushby, K., R. Finkel, D. J. Birnkrant, L. E. Case, P. R. Clemens, L. Cripe, A. Kaul, K. Kinnett, C. McDonald, S. Pandya, J. Poysky, F. Shapiro, J. Tomezsko, and C. Constantin (2010b). "Diagnosis and management of Duchenne muscular dystrophy, part 2: implementation of multidisciplinary care". In: *The Lancet Neurology*, 9 (2): 177–189. DOI: 10.1016/S1474-4422(09)70272-8.

Cappello, L., J. T. Meyer, K. C. Galloway, J. D. Peisner, R. Granberry, D. A. Wagner, S. Engelhardt, S. Paganoni, and C. J. Walsh (2018). "Assisting hand function after spinal cord injury with a fabric-based soft robotic glove". In: *Journal of NeuroEngineering and Rehabilitation*, 15 (1): 59. DOI: 10.1186/s12984-018-0391-x.

Carlson, J. D. and C. A. Trombly (1983). "The Effect of Wrist Immobilization on Performance of the Jebsen Hand Function Test". In: *American Journal of Occupational Therapy*, 37 (3): 167–175. DOI: 10.5014/ajot.37.3.167.

Carlson, L. B., B. Radocy, and P. D. Marschall (1991). "Spectron 12 Cable for Upper-Limb Prostheses". In: *Journal of Prosthetics & Orthotics*, 3 (3): 130. DOI: 10.1097/00008526-199106000-00010.

Carlson, L. B., B. D. Veatch, and D. D. Frey (1995). "Efficiency of Prosthetic Cable and Housing". In: *Journal of Prosthetics & Orthotics*, 7 (3): 96.

Carpi, F., A. Mannini, and D. De Rossi (2008). "Elastomeric contractile actuators for hand rehabilitation splints". In: *Electroactive Polymer Actuators and Devices (EAPAD)*. Ed. by Y. Bar-Cohen. Vol. 6927, p. 692705. DOI: 10.1117/12.774644.

Catalano, M. G., G. Grioli, E. Farnioli, A. Serio, C. Piazza, and A. Bicchi (2014). "Adaptive synergies for the design and control of the Pisa/IIT SoftHand". In: *The International Journal of Robotics Research*, 33 (5): 768–782. DOI: 10.1177/0278364913518998.

Cempini, M., M. Cortese, and N. Vitiello (2014a). "A powered finger–thumb wearable hand exoskeleton with self-aligning joint axes". In: *IEEE/ASME Transactions on Mechatronics*, 20 (2): 705–716. DOI: 10.1109/TMECH.2014.2315528.

Cempini, M., M. Cortese, and N. Vitiello (2015). "A Powered Finger-Thumb Wearable Hand Exoskeleton With Self-Aligning Joint Axes". In: *IEEE/ASME Transactions on Mechatronics*, 20 (2): 705–716. DOI: 10.1109/TMECH.2014.2315528.

Cempini, M., S. M. M. De Rossi, T. Lenzi, M. Cortese, F. Giovacchini, N. Vitiello, and M. C. Carrozza (2013). "Kinematics and design of a portable and wearable exoskeleton for hand rehabilitation". In: *2013 IEEE International Conference on Rehabilitation Robotics (ICORR)*. Seattle, WA. DOI: 10.1109/ICORR.2013.6650414.

Cempini, M., N. Vitiello, F. Giovacchini, S. M. M. De Rossi, T. Lenzi, A. Chiri, and M. C. Carrozza (2014b). *Wearable exoskeleton device for hand rehabilitation*. Patent no. WO 2014/033613 A2.

Chakravarthy, S., K. Aditya, and A. Ghosal (2014). "Experimental Characterization and Control of Miniaturized Pneumatic Artificial Muscle". In: *Journal of Medical Devices*, 8 (4): 041011. DOI: 10.1115/1.4028420.

Chan, C. L., S. Gobee, and D. Vickneswari (2014). "Finger Grip Rehabilitation Using Exoskeleton with Grip Force Feedback". In: *15th International Conference on Biomedical Engineering (IFBME)*. Ed. by J. Goh. Vol. 43. IFMBE Proceedings. Cham, pp. 520–523. DOI: 10.1007/978-3-319-02913-9.

Charoenseang, S. and S. Panjan (2011). “5-Finger Exoskeleton for Assembly Training in Augmented Reality”. In: *Virtual and Mixed Reality - New Trends*. Vol. 6773. Orlando, FL, pp. 30–39. DOI: 10.1007/978-3-642-22021-0_4.

Chen, D., Y. Yun, and A. D. Deshpande (2014a). “Experimental characterization of Bowden cable friction”. In: *2014 IEEE International Conference on Robotics and Automation (ICRA)*, pp. 5927–5933. DOI: 10.1109/ICRA.2014.6907732.

Chen, M., S. K. Ho, H. F. Zhou, P. M. K. Pang, X. L. Hu, D. T. W. Ng, and K. Y. Tong (2009). “Interactive rehabilitation robot for hand function training”. In: *2009 IEEE International Conference on Rehabilitation Robotics (ICORR)*. Kyoto, pp. 777–780. DOI: 10.1109/ICORR.2009.5209564.

Chen, Z., S. Fan, and D. Zhang (2014b). “An Exoskeleton System for Hand Rehabilitation Based on Master-Slave Control”. In: *Intelligent Robotics and Applications*, pp. 242–253. DOI: 10.1007/978-3-319-13966-1_25.

Chiri, A., M. Cempini, S. M. M. De Rossi, T. Lenzi, F. Giovacchini, N. Vitiello, and M. C. Carrozza (2012a). “On the design of ergonomic wearable robotic devices for motion assistance and rehabilitation”. In: *2012 Annual International Conference of the IEEE Engineering in Medicine and Biology Society*. San Diego, CA, pp. 6124–6127. DOI: 10.1109/EMBC.2012.6347391.

Chiri, A., F. Giovacchini, N. Vitiello, E. Cattin, S. Roccella, F. Vecchi, and M. C. Carrozza (2009). “HANDEXOS: Towards an exoskeleton device for the rehabilitation of the hand”. In: *2009 IEEE/RSJ International Conference on Intelligent Robots and Systems (IROS)*. St. Louis, MO, pp. 1106–1111. DOI: 10.1109/IROS.2009.5354376.

Chiri, A., N. Vitiello, F. Giovacchini, S. Roccella, F. Vecchi, and M. C. Carrozza (2012b). “Mechatronic design and characterization of the index finger module of a hand exoskeleton for post-stroke rehabilitation”. In: *IEEE/ASME Transactions on Mechatronics*, 17 (5): 884–894. DOI: 10.1109/TMECH.2011.2144614.

Chishiro, T., T. Ono, and S. Konishi (2013). “Pantograph mechanism for conversion from swelling into contraction motion of pneumatic balloon actuator”. In: *2013 IEEE 26th International Conference on Micro Electro Mechanical Systems (MEMS)*. Taipei, pp. 532–535. DOI: 10.1109/MEMSYS.2013.6474296.

Choi, B. H. and H. R. Choi (1999). “A semi-direct drive hand exoskeleton using ultrasonic motor”. In: *8th IEEE International Workshop on Robot and Human Interaction (RO-MAN)*. Pisa, pp. 285–290. DOI: 10.1109/ROMAN.1999.900354.

Choi, B. H. and H. R. Choi (2000). “SKK Hand Master-hand exoskeleton driven by ultrasonic motors”. In: *2000 IEEE/RSJ International Conference on Intelligent Robots and Systems (IROS)*. Vol. 2. Takamatsu, pp. 1131–1136. DOI: 10.1109/IROS.2000.893171.

Cincotti, C. C., S. O’Donnell, G. E. Zapata, C. M. Rabolli, and B. F. BuSha (2015). “Strength amplifying hand exoskeleton”. In: *2015 41st Annual Northeast Biomedical Engineering Conference (NEBEC)*. Troy, NY, pp. 1–2. DOI: 10.1109/NEBEC.2015.7117082.

Coffey, A. L., D. J. Leamy, and T. E. Ward (2014). “A novel BCI-controlled pneumatic glove system for home-based neurorehabilitation”. In: *36th Annual International Conference of the IEEE Engineering in Medicine and Biology Society*. Chicago, IL, pp. 3622–3625. DOI: 10.1109/EMBC.2014.6944407.

Colon, M., Y. Hamid, J. Lopez, L. Scully, S. Kim, and B. F. BuSha (2014). “3-D printed hand assisstive exoskeleton for actuated pinch and grasp”. In: *2014 40th Annual Northeast*

Bioengineering Conference (NEBEC). Boston, MA, pp. 1–2. DOI: 10.1109/NEBEC.2014.6972761.

Connelly, L., Y. Jia, M. L. Toro, M. E. Stoykov, R. V. Kenyon, and D. G. Kamper (2010). "A pneumatic glove and immersive virtual reality environment for hand rehabilitative training after stroke". In: *IEEE Transactions on Neural Systems and Rehabilitation Engineering*, 18 (5): 551–9. DOI: 10.1109/TNSRE.2010.2047588.

Connelly, L., M. E. Stoykov, Y. Jia, M. L. Toro, R. V. Kenyon, and D. G. Kamper (2009). "Use of a pneumatic glove for hand rehabilitation following stroke". In: *31st Annual International Conference of the IEEE Engineering in Medicine and Biology Society (EMBC)*. Minneapolis, MN, pp. 2434–2437. DOI: 10.1109/IEMBS.2009.5335400.

Conti, R., B. Allotta, E. Meli, and A. Ridolfi (2015). "Development, design and validation of an assistive device for hand disabilities based on an innovative mechanism". In: *Robotica*, FirstView: 1–15. DOI: 10.1017/S0263574715000879.

Corbett, E. A., E. J. Perreault, and T. A. Kuiken (2011). "Comparison of electromyography and force as interfaces for prosthetic control". In: *The Journal of Rehabilitation Research and Development*, 48 (6): 629–642. DOI: 10.1682/JRRD.2010.03.0028.

Cordo, P., H. Lutsep, L. Cordo, W. G. Wright, T. Cacciatore, and R. Skoss (2009). "Assisted movement with enhanced sensation (AMES): coupling motor and sensory to remediate motor deficits in chronic stroke patients". In: *Neurorehabilitation and Neural Repair*, 23 (1): 67–77. DOI: 10.1177/1545968308317437.

Cordo, P., S. Wolf, J.-S. Lou, R. Bogey, M. Stevenson, J. Hayes, and E. Roth (2013). "Treatment of severe hand impairment following stroke by combining assisted movement, muscle vibration, and biofeedback". In: *Journal of Neurologic Physical Therapy*, 37 (4): 194–203. DOI: 10.1097/NPT.0000000000000023.

Cornell University (n.d.). *Reuleaux Collection of Kinematic Mechanisms*. http://kmoddl.library.cornell.edu/model.php?m=reuleaux. Accessed 19 Nov 2015.

Cortese, M., M. Cempini, P. R. de Almeida Ribeiro, S. R. Soekadar, M. C. Carrozza, and N. Vitiello (2015). "A Mechatronic System for Robot-Mediated Hand Telerehabilitation". In: *IEEE/ASME Transactions on Mechatronics*, 20 (4): 1753–1764. DOI: 10.1109/TMECH.2014.2353298.

Croshaw, P. F. (1969). *Hardiman arm test*. Tech. rep. S-70-1019. General Electric Company.

Cruz-Jentoft, A. J., J. P. Baeyens, J. M. Bauer, Y. Boirie, T. Cederholm, F. Landi, F. C. Martin, J.-P. Michel, Y. Rolland, S. M. Schneider, E. Topinkova, M. Vandewoude, and M. Zamboni (2010). "Sarcopenia: European consensus on definition and diagnosis: Report of the European Working Group on Sarcopenia in Older People". In: *Age and Ageing*, 39 (4): 412–423. DOI: 10.1093/ageing/afq034.

Cruz, E. G. and D. G. Kamper (2010). "Use of a novel robotic interface to study finger motor control". In: *Annals of Biomedical Engineering*, 38 (2): 259–268. DOI: 10.1007/s10439-009-9845-4.

Cui, L., A. Phan, and G. Allison (2015). "Design and fabrication of a three dimensional printable non-assembly articulated hand exoskeleton for rehabilitation". In: *2015 37th Annual International Conference of the IEEE Engineering in Medicine and Biology Society (EMBC)*. Milan, pp. 4627–4630. DOI: 10.1109/EMBC.2015.7319425.

Cutkosky, M. (1989). "On grasp choice, grasp models, and the design of hands for manufacturing tasks". In: *IEEE Transactions on Robotics and Automation*, 5 (3): 269–279. DOI: 10.1109/70.34763.

CyberGrasp Systems LLC (2009). *CyberGrasp Brochure*. http://static1.squarespace.com/static/559c381ee4b0ff7423b6b6a4/t/5602fc01e4b07ebf58d480fb/1443036161782/CyberGrasp_Brochure.pdf. Accessed 30 Oct 2015.

Darras, B. T., D. T. Miller, and D. K. Urion (2010). "Dystrophinopathies". In: *GeneReviews®*. Updated 2014. URL: http://www.ncbi.nlm.nih.gov/pubmed/20301298.

de Carvalho, R. M. F., N. Mazzer, and C. H. Barbieri (2012). "Analysis of the reliability and reproducibility of goniometry compared to hand photogrammetry". In: *Acta Ortopédica Brasileira*, 20 (3): 139–149. DOI: 10.1590/S1413-78522012000300003.

Delph II, M. A., S. A. Fischer, P. W. Gauthier, C. H. M. Luna, E. A. Clancy, and G. S. Fischer (2013). "A soft robotic exomusculature glove with integrated sEMG sensing for hand rehabilitation". In: *2013 IEEE International Conference on Rehabilitation Robotics (ICORR)*. Seattle, WA, pp. 1–7. DOI: 10.1109/ICORR.2013.6650426.

Derler, S. and L.-C. Gerhardt (2012). "Tribology of Skin: Review and Analysis of Experimental Results for the Friction Coefficient of Human Skin". In: *Tribology Letters*, 45 (1): 1–27. DOI: 10.1007/s11249-011-9854-y.

Deshpande, A. D., N. Gialias, and Y. Matsuoka (2012). "Contributions of intrinsic visco-elastic torques during planar index finger and wrist movements". In: *IEEE Transactions on Biomedical Engineering*, 59 (2): 586–594. DOI: 10.1109/TBME.2011.2178240.

Dexta Robotics (n.d.[a]). http://www.dextarobotics.com/. Accessed 30 Oct 2015.

Dexta Robotics (n.d.[b]). *Dexmo: an exoskeleton for you to touch the digital world*. https://www.kickstarter.com/projects/1277630932/dexmo-an-exoskeleton-for-you-to-touch-the-digital. Accessed 30 Oct 2015.

DiCicco, M., L. Lucas, and Y. Matsuoka (2004). "Comparison of control strategies for an EMG controlled orthotic exoskeleton for the hand". In: *2004 IEEE International Conference on Robotics and Automation (ICRA)*. Vol. 2. April, pp. 1622–1627. DOI: 10.1109/ROBOT.2004.1308056.

DINED anthropometric database (n.d.). *Dutch adults, dined2004, 20–60 years*. http://dined.io.tudelft.nl/en/database.

Dollar, A. M. and H. Herr (2008). "Lower Extremity Exoskeletons and Active Orthoses:Challenges and State-of-the-Art". In: *IEEE Transactions on Robotics*, 24 (1): 144–158. DOI: 10.1109/TRO.2008.915453.

Dollar, A. M. and R. D. Howe (2011). "Joint coupling design of underactuated hands for unstructured environments". In: *International Journal of Robotics Research*, 30 (9): 1157–1169. DOI: 10.1177/0278364911401441.

Dollfus, P. and M. Oberlé (1984). "Technical note: preliminary communication a tridigital dynamic orthosis for tetraplegic patients". In: *Paraplegia*, 22 (2): 115–118. DOI: 10.1038/sc.1984.20.

Domalain, M., L. Vigouroux, F. Danion, V. Sevrez, and E. Berton (2008). "Effect of object width on precision grip force and finger posture". In: *Ergonomics*, 51 (9): 1441–1453. DOI: 10.1080/00140130802130225.

Dovat, L., O. Lambercy, R. Gassert, T. Maeder, T. Milner, T. C. Leong, and E. Burdet (2008). "HandCARE: A cable-actuated rehabilitation system to train hand function after stroke". In: *IEEE Transactions on Neural Systems and Rehabilitation Engineering*, 16 (6): 582–591. DOI: 10.1109/TNSRE.2008.2010347.

Eagle, M., S. V. Baudouin, C. Chandler, D. R. Giddings, R. Bullock, and K. Bushby (2002). "Survival in Duchenne muscular dystrophy: improvements in life expectancy since 1967 and the impact of home nocturnal ventilation". In: *Neuromuscular Disorders*, 12 (10): 926–929. DOI: 10.1016/S0960-8966(02)00140-2.

ERIKS bv (n.d.). *ERIKS O-ring Technical Handbook*. Alkmaar.

Ertas, I. H., E. Hocaoglu, D. E. Barkana, and V. Patoglu (2009). "Finger exoskeleton for treatment of tendon injuries". In: *2009 IEEE International Conference on Rehabilitation Robotics (ICORR)*. Kyoto, pp. 194–201. DOI: 10.1109/ICORR.2009.5209487.

Ertas, I. H., E. Hocaoglu, and V. Patoglu (2014). "AssistOn-Finger: an under-actuated finger exoskeleton for robot-assisted tendon therapy". In: *Robotica*, 32 (08): 1363–1382. DOI: 10.1017/S0263574714001957.

Ewbank, T. (1847). *Descriptive and historical account of hydraulic and other machinery for raising water*. Greeley & McElrath.

Fang, H., Z. Xie, and H. Liu (2009a). "An exoskeleton master hand for controlling DLR/HIT hand". In: *2009 IEEE/RSJ International Conference on Intelligent Robots and Systems (IROS)*. St. Louis, MO, pp. 3703–3708. DOI: 10.1109/IROS.2009.5354624.

Fang, H., Z. Xie, H. Liu, T. Lan, and J. Xia (2009b). "An exoskeleton force feedback master finger distinguishing contact and non-contact mode". In: *2009 IEEE/ASME International Conference on Advanced Intelligent Mechatronics*. Singapore, pp. 1059–1064. DOI: 10.1109/AIM.2009.5229726.

Farina, D. and M. Sartori (2016). "Surface electromyography for MAN-machine interfacing in rehabilitation technologies". In: *Surface Electromyography: Physiology, Engineering and Applications*, pp. 540–560. DOI: 10.1002/9781119082934.ch20.

Festo AG & Co. KG (2012). *ExoHand Brochure*. http://www.festo.com/net/SupportPortal/Files/156734/Brosch_FC_ExoHand_EN_lo.pdf. Accessed 19 Oct 2015.

Feyrer, K. (2015). *Wire ropes: tension, endurance, reliability*. 2nd ed. Springer-Verlag.

Fiorilla, A. E., F. Nori, L. Masia, and G. Sandini (2011). "Finger impedance evaluation by means of hand exoskeleton". In: *Annals of Biomedical Engineering*, 39 (12): 2945–2954. DOI: 10.1007/s10439-011-0381-7.

Fiorilla, A. E., N. G. Tsagarakis, F. Nori, and G. Sandini (2009). "Design of a 2-finger hand exoskeleton for finger stiffness measurements". In: *Applied Bionics and Biomechanics*, 6 (2): 217–228. DOI: 10.1080/11762320902920567.

Flores, P., J. Ambrósio, J. C. P. Claro, and H. M. Lankarani (2006). "Influence of the contact–impact force model on the dynamic response of multi-body systems". In: *Proceedings of the Institution of Mechanical Engineers, Part K: Journal of Multi-body Dynamics*, 220 (1): 21–34. DOI: 10.1243/146441906X77722.

Fontana, M., A. Dettori, F. Salsedo, and M. Bergamasco (2009). "Mechanical design of a novel Hand Exoskeleton for accurate force displaying". In: *2009 IEEE International Conference on Robotics and Automation (ICRA)*. Kobe, pp. 1704–1709. DOI: 10.1109/ROBOT.2009.5152591.

Fontana, M., F. Salsedo, S. Marcheschi, and M. Bergamasco (2013). "Haptic hand exoskeleton for precision grasp simulation". In: *Journal of Mechanisms and Robotics*, 5 (4): 041014. DOI: 10.1115/1.4024981.

Fu, Y., P. Wang, and S. Wang (2008). "Development of a multi-DOF exoskeleton based machine for injured fingers". In: *2008 IEEE/RSJ International Conference on Intelligent Robots and Systems (IROS)*. Nice, pp. 1946–1951. DOI: 10.1109/IROS.2008.4651208.

Fu, Y., P. Wang, S. Wang, H. Liu, and F. Zhang (2007). "Design and development of a portable exoskeleton based CPM machine for rehabilitation of hand injuries". In: *2007 IEEE International Conference on Robotics and Biomimetics (ROBIO)*. 60275033. Sanya, pp. 1476–1481. DOI: 10.1109/ROBIO.2007.4522382.

Fu, Y., Q. Zhang, F. Zhang, and Z. Gan (2011). "Design and development of a hand rehabilitation robot for patient-cooperative therapy following stroke". In: *2011 International Conference on Mechatronics and Automation (ICMA)*. Beijing, pp. 112–117. DOI: 10.1109/ICMA.2011.5985641.

Gael Langevin (n.d.). *Hand robot InMoov*. http://www.inmoov.fr/. Accessed 16 Jan 2016.

Gasser, B. W. and M. Goldfarb (2015). "Design and performance characterization of a hand orthosis prototype to aid activities of daily living in a post-stroke population". In: *2015 37th Annual International Conference of the IEEE Engineering in Medicine and Biology Society (EMBC)*. Milan, pp. 3877–3880. DOI: 10.1109/EMBC.2015.7319240.

Al-Ghathian, F. M. M. and M. S. Tarawneh (2005). "Friction Forces in O-ring Sealing". In: *American Journal of Applied Sciences*, 2 (3): 626–632. DOI: 10.3844/ajassp.2005.626.632.

Gilardi, G. and I. Sharf (2002). "Literature survey of contact dynamics modelling". In: *Mechanism and Machine Theory*, 37 (10): 1213–1239. DOI: 10.1016/S0094-114X(02)00045-9.

Goiriena, A., I. Retolaza, A. Cenitagoya, F. Martinez, S. Riafio, and J. Landaluze (2009). "Analysis of bowden cable transmission performance for orthosis applications". In: *2009 IEEE International Conference on Mechatronics (ICM)*. Málaga, Spain, pp. 1–6. DOI: 10.1109/ICMECH.2009.4957133.

Gopura, R. A. R. C., D. S. V. Bandara, K. Kiguchi, and G. K. I. Mann (2015). "Developments in hardware systems of active upper-limb exoskeleton robots: A review". In: *Robotics and Autonomous Systems*. DOI: 10.1016/j.robot.2015.10.001.

Guo, S., F. Zhang, W. Wei, F. Zhao, and Y. Wang (2014). "Kinematic analysis of a novel exoskeleton finger rehabilitation robot for stroke patients". In: *2014 IEEE International Conference on Mechatronics and Automation (ICMA)*. Tianjin, pp. 924–929. DOI: 10.1109/ICMA.2014.6885821.

Gupta, A., M. K. O'Malley, V. Patoglu, and C. Burgar (2008). "Design, Control and Performance of RiceWrist: A Force Feedback Wrist Exoskeleton for Rehabilitation and Training". In: *The International Journal of Robotics Research*, 27 (2): 233–251. DOI: 10.1177/0278364907084261.

Gustus, A., G. Stillfried, J. Visser, H. Jörntell, and P. van der Smagt (2012). "Human hand modelling: kinematics, dynamics, applications". In: *Biological Cybernetics*, 106 (11-12): 741–55. DOI: 10.1007/s00422-012-0532-4.

Gwynne, G. (1956). "Nylon vs. control cable friction". In: *Orthopedic & Prosthetic Appliance Journal*, 10 (3): 43–45.

Haghgoo, H. A., E. S. Pazuki, A. S. Hosseini, and M. Rassafiani (2013). "Depression, activities of daily living and quality of life in patients with stroke". In: *Journal of the Neurological Sciences*, 328 (1-2): 87–91. DOI: 10.1016/j.jns.2013.02.027.

Hahne, J. M., M. Markovic, and D. Farina (2017). "User adaptation in Myoelectric Man-Machine Interfaces". In: *Scientific Reports*, 7: Article no. 4437. DOI: 10.1038/s41598-017-04255-x.

Haley, S. M., W. I. Coster, Y. C. Kao, H. M. Dumas, M. A. Fragala-Pinkham, J. M. Kramer, L. H. Ludlow, and R. Moed (2010). "Lessons from use of the pediatric evaluation of disability inventory: where do we go from here?" In: *Pediatric Physical Therapy*, 22 (1): 69–75. DOI: 10.1097/PEP.0b013e3181cbfbf6.

Hamonet, C. and A. DeMontgolfier (1974). "A new myoelectric prehension orthosis". In: *Inter Clinic Information Bulletin*, 13 (5): 15–17.

Hart, R. L., K. L. Kilgore, and P. H. Peckham (1998). "A comparison between control methods for implanted FES hand-grasp systems". In: *IEEE Transactions on Rehabilitation Engineering*, 6 (2): 208–218. DOI: 10.1109/86.681187.

Hartopanu, S., M. Poboroniuc, F. Serea, D. Irimia, and G. Livint (2013). "Design of a hybrid FES-mechanical intelligent haptic robotic glove". In: *2013 17th International Conference on System Theory, Control and Computing (ICSTCC)*. Sinaia, pp. 687–692. DOI: 10.1109/ICSTCC.2013.6689040.

Hartopanu, S., M. Poboroniuc, F. Serea, and G. Livint (2014). "Towards human arm rehabilitation in stroke patients by means of a hybrid FES & robotic glove". In: *2014 International Conference and Exposition on Electrical and Power Engineering (EPE)*. Iasi, pp. 148–152. DOI: 10.1109/ICEPE.2014.6969886.

Hartwig, M. (2014). "Modern Hand- and Arm Rehabilitation: The Tyrosolution concept". In: *Neurology & Rehabilitation*, 2: 111–116.

Hasegawa, Y., T. Ariyama, and K. Kamibayashi (2012). "Pinching force accuracy affected by thumb sensation in human force augmentation". In: *2012 IEEE/RSJ International Conference on Intelligent Robots and Systems (IROS)*. Vilamoura, pp. 3943–3948. DOI: 10.1109/IROS.2012.6386081.

Hasegawa, Y., Y. Mikami, K. Watanabe, and Y. Sankai (2008). "Five-fingered assistive hand with mechanical compliance of human finger". In: *2008 IEEE International Conference on Robotics and Automation (ICRA)*. Pasadena, CA, pp. 718–724. DOI: 10.1109/ROBOT.2008.4543290.

Hasegawa, Y. and J. Muto (2013). "Superiority of pinching force accuracy augmented by exoskeletal support system". In: *2013 IEEE/RSJ International Conference on Intelligent Robots and Systems (IROS)*. Tokyo, pp. 3771–3776. DOI: 10.1109/IROS.2013.6696895.

Hasegawa, Y. and T. Suzuki (2015). "Thin and active fixture to hold finger for easy attachment and comfort of grasping support exoskeleton". In: *2015 IEEE International Conference on Robotics and Automation (ICRA)*. Seattle, WA, pp. 4973–4978. DOI: 10.1109/ICRA.2015.7139890.

Hasegawa, Y., J. Tokita, K. Kamibayashi, and Y. Sankai (2011). "Evaluation of fingertip force accuracy in different support conditions of exoskeleton". In: *2011 IEEE International Conference on Robotics and Automation (ICRA)*. Shanghai, pp. 680–685. DOI: 10.1109/ICRA.2011.5980512.

Hasegawa, Y., K. Watanabe, and Y. Sankai (2010). "Performance evaluations of hand and forearm support system". In: *2010 IEEE/RSJ International Conference on Intelligent Robots and Systems (IROS)*. Taipei, pp. 2645–2650. DOI: 10.1109/IROS.2010.5650355.

Hatem, S. M., G. Saussez, M. della Faille, V. Prist, X. Zhang, D. Dispa, and Y. Bleyenheuft (2016). "Rehabilitation of Motor Function after Stroke: A Multiple Systematic Review Focused on Techniques to Stimulate Upper Extremity Recovery". In: *Frontiers in Human Neuroscience*, 10 (September): 1–22. DOI: 10.3389/fnhum.2016.00442.

Heo, P., G. M. Gu, S. J. Lee, K. Rhee, and J. Kim (2012). "Current hand exoskeleton technologies for rehabilitation and assistive engineering". In: *International Journal of Precision Engineering and Manufacturing*, 13 (5): 807–824. DOI: 10.1007/s12541-012-0107-2.

Heo, P. and J. Kim (2014a). "Estimating grip forces with a tactilely transparent finger exoskeleton for pinch grip force assistance". In: *2014 IEEE Haptics Symposium*. Houston, TX, pp. 493–497. DOI: 10.1109/HAPTICS.2014.6775505.

Heo, P. and J. Kim (2014b). "Power-assistive finger exoskeleton with a palmar opening at the fingerpad". In: *IEEE Transactions on Biomedical Engineering*, 61 (11): 2688–2697. DOI: 10.1109/TBME.2014.2325948.

Heo, P., S. J. Kim, and J. Kim (2013). "Powered finger exoskeleton having partially open fingerpad for flexion force assistance". In: *2013 IEEE/ASME International Conference on Advanced Intelligent Mechatronics (AIM)*. Vol. 2. Wollongong, pp. 182–187. DOI: 10.1109/AIM.2013.6584089.

Herr, H. (2009). "Exoskeletons and orthoses: classification, design challenges and future directions". In: *Journal of NeuroEngineering and Rehabilitation*, 6 (1): 21. DOI: 10.1186/1743-0003-6-21.

Hesse, S., H. Kuhlmann, J. Wilk, C. Tomelleri, and S. G. B. Kirker (2008). "A new electromechanical trainer for sensorimotor rehabilitation of paralysed fingers: a case series in chronic and acute stroke patients". In: *Journal of NeuroEngineering and Rehabilitation*, 5 (21). DOI: 10.1186/1743-0003-5-21.

Hioki, M., H. Kawasaki, H. Sakaeda, Y. Nishimoto, and T. Mouri (2010). "Finger rehabilitation system using multi-fingered haptic interface robot controlled by surface electromyogram". In: *2010 3rd IEEE RAS and EMBS International Conference on Biomedical Robotics and Biomechatronics (BioRob)*. Tokyo, pp. 276–281. DOI: 10.1109/BIOROB.2010.5626938.

Ho, N. S. K., K. Y. Tong, X. L. Hu, K. L. Fung, X. J. Wei, W. Rong, and E. A. Susanto (2011). "An EMG-driven exoskeleton hand robotic training device on chronic stroke subjects: Task training system for stroke rehabilitation". In: *2011 IEEE International Conference on Rehabilitation Robotics (ICORR)*. Zurich, pp. 1–5. DOI: 10.1109/ICORR.2011.5975340.

Hocking, E. and N. Wereley (2013). "Fabrication and Characterization of Small-scale Pneumatic Artificial Muscles for a Bio-Inspired Robotic Hand". In: *51st AIAA Aerospace Sciences Meeting including the New Horizons Forum and Aerospace Exposition*. January. Reston, VA, pp. 1–11. DOI: 10.2514/6.2013-132.

Hoffman, H. B. and G. L. Blakey (2011). "New design of dynamic orthoses for neurological conditions". In: *NeuroRehabilitation*, 28 (1): 55–61. DOI: 10.3233/NRE-2011-0632.

Holmes, C. D., M. Wronkiewicz, T. Somers, J. Liu, E. Russell, D. Kim, C. Rhoades, J. Dunkley, D. Bundy, E. Galboa, and E. Leuthardt (2012). "IPSIHAND BRAVO: An improved EEG-based brain-computer interface for hand motor control rehabilitation". In: *2012 Annual International Conference of the IEEE Engineering in Medicine and Biology Society*. San Diego, CA, pp. 1749–1752. DOI: 10.1109/EMBC.2012.6346287.

Hong, M. B., S. J. Kim, and K. Kim (2012). "Development of a 10-DOF robotic system for upper-limb power assistance". In: *2012 9th International Conference on Ubiquitous Robots and Ambient Intelligence (URAI)*. Daejeon, pp. 61–62. DOI: 10.1109/URAI.2012.6462931.

Hong, M. B., S. J. Kim, T. Um, and K. Kim (2013a). "KULEX: An ADL power-assistance demonstration". In: *2013 10th International Conference on Ubiquitous Robots and Ambient Intelligence (URAI)*. Jeju, pp. 542–544. DOI: 10.1109/URAI.2013.6677333.

Hong, M., S. J. Kim, and K. Kim (2013b). "KULEX: ADL power assistant robotic system for the elderly and the disabled (Abstract for video)". In: *2013 10th International Conference on Ubiquitous Robots and Ambient Intelligence (URAI)*. Jeju, pp. 121–122. DOI: 10.1109/URAI.2013.6677487.

Howell, L. L. (2001). *Compliant mechanisms*. John Wiley & Sons.

Huber, J. E., N. A. Fleck, and M. F. Ashby (1997). "The selection of mechanical actuators based on performance indices". In: *Proceedings of the Royal Society A: Mathematical, Physical and Engineering Sciences*, 453 (1965): 2185–2205. DOI: 10.1098/rspa.1997.0117.

Iberall, T. (1997). "Human prehension and dexterous robot hands". In: *The International Journal of Robotics Research*, 16 (3): 285–299. DOI: 10.1177/027836499701600302.

Idrogenet, srl (2013). *Gloreha (Hand Rehabilitation Glove): summary of clinical results*. http://www.gloreha.com/images/pdf/GLOREHA%20Summary%20of%20Clinical%20Results.pdf. Accessed 23 Oct 2015.

Idrogenet, srl (n.d.). *Gloreha Lite*. http://gloreha.com/. Accessed 23 Oct 2015.

IJzerman, M. J., T. S. Stoffers, F. in 't Groen, M. A. P. Klatte, G. J. Snoek, J. H. C. Vorsteveld, R. H. Nathan, and H. J. Hermens (1996). "The NESS Handmaster orthosis: restoration of hand function in C5 and stroke patients by means of electrical stimulation". In: *Journal of Rehabilitation Sciences*, 9 (3): 86–89.

In, H. and K.-J. Cho (2012). "Evaluation of the antagonistic tendon driven system for SNU Exo-Glove". In: *2012 9th International Conference on Ubiquitous Robots and Ambient Intelligence (URAI)*. Daejeon, pp. 507–509.

In, H., K.-J. Cho, K. Kim, and B.-S. Lee (2011). "Jointless structure and under-actuation mechanism for compact hand exoskeleton". In: *2011 IEEE International Conference on Rehabilitation Robotics (ICORR)*. Zurich, pp. 1–6. DOI: 10.1109/ICORR.2011.5975394.

In, H., B. B. Kang, M. Sin, and K.-j. Cho (2015). "Exo-Glove: A Wearable Robot for the Hand with a Soft Tendon Routing System". In: *IEEE Robotics & Automation Magazine*, 22 (1): 97–105. DOI: 10.1109/MRA.2014.2362863.

Inmann, A. and M. Haugland (2001). "An instrumented object for evaluation of lateral hand grasp during functional tasks". In: *Journal of Medical Engineering & Technology*, 25 (5): 207–211. DOI: 10.1080/03091900110065951.

Interactive Motion Technologies (2013). *InMotion Robot-assisted Therapy: Evidence-Based Neurorehabilitation*. http://interactive-motion.com/wp-content/uploads/2013/10/EvidenceBasedNeurorehabilitation.pdf. Accessed 19 Oct 2015.

Interactive Motion Technologies (n.d.). *InMotion HAND™*. http://interactive-motion.com/healthcarereform/upper-extremity-rehabilitiation/inmotion-hand/. Accessed 19 Oct 2015.

Ionescu, M., I. C. Rosca, and B. C. Braun (2012). "Miniature Flexible Pneumatic Actuator". In: *Applied Mechanics and Materials*, 186: 291–296. DOI: 10.4028/www.scientific.net/AMM.186.291.

Iqbal, J., O. Ahmad, and A. Malik (2011a). "HEXOSYS II - towards realization of light mass robotics for the hand". In: *2011 IEEE 14th International Multitopic Conference*. Karachi, pp. 115–119. DOI: 10.1109/INMIC.2011.6151454.

Iqbal, J., D. G. Caldwell, and N. G. Tsagarakis (2015). "Four-fingered lightweight exoskeleton robotic device accommodating different hand sizes". In: *Electronics Letters*, 51 (12): 888–890. DOI: 10.1049/el.2015.0850.

Iqbal, J., H. Khan, N. G. Tsagarakis, and D. G. Caldwell (2014). "A novel exoskeleton robotic system for hand rehabilitation – conceptualization to prototyping". In: *Biocybernetics and Biomedical Engineering*, 34 (2): 79–89. DOI: 10.1016/j.bbe.2014.01.003.

Iqbal, J., N. G. Tsagarakis, and D. G. Caldwell (2010a). "A human hand compatible optimised exoskeleton system". In: *2010 IEEE International Conference on Robotics and Biomimetics*. Tianjin, pp. 685–690. DOI: 10.1109/ROBIO.2010.5723409.

Iqbal, J., N. G. Tsagarakis, and D. G. Caldwell (2011b). "A multi-DOF robotic exoskeleton interface for hand motion assistance". In: *2011 Annual International Conference of the IEEE Engineering in Medicine and Biology Society (EMBC)*. Boston, MA, pp. 1575–1578. DOI: 10.1109/IEMBS.2011.6090458.

Iqbal, J., N. G. Tsagarakis, and D. G. Caldwell (2011c). "Design of a wearable direct-driven optimized hand exoskeleton device". In: *ACHI 2011 - 4th International Conference on Advances in Computer-Human Interactions*. Gosier, pp. 142–146.

Iqbal, J., N. G. Tsagarakis, A. E. Fiorilla, and D. G. Caldwell (2010b). "A portable rehabilitation device for the hand". In: *2010 Annual International Conference of the IEEE Engineering in Medicine and Biology Society (EMBC)*. Buenos Aires, pp. 3694–3697. DOI: 10.1109/IEMBS.2010.5627448.

ISO/TC 168 (1989a). *Prosthetics and orthotics – Vocabulary – Part 1: General terms for external limb prostheses and external orthoses*. Tech. rep. 8549-1:1989. Geneva, Switzerland: International Organization for Standardization.

ISO/TC 168 (1989b). *Prosthetics and orthotics – Vocabulary – Part 3: Terms relating to external orthoses*. Tech. rep. 8549-3:1989. Geneva, Switzerland: International Organization for Standardization.

ISO/TC 168 (2007). *Prosthetics and orthotics – Categorization and description of external orthoses and orthotic components*. Tech. rep. ISO 13404:2007. Geneva, Switzerland: International Organization for Standardization.

Ison, M. and P. Artemiadis (2014). "The role of muscle synergies in myoelectric control: trends and challenges for simultaneous multifunction control". In: *Journal of Neural Engineering*, 11 (5): 051001. DOI: 10.1088/1741-2560/11/5/051001.

Ito, S., H. Kawasaki, Y. Ishigure, M. Natsume, T. Mouri, and Y. Nishimoto (2011). "A design of fine motion assist equipment for disabled hand in robotic rehabilitation system". In: *Journal of the Franklin Institute*, 348 (1): 79–89. DOI: 10.1016/j.jfranklin.2009.02.009.

JACE Systems (n.d.). http://www.jacesystems.com/. Accessed 20 Oct 2015.

Janssen, L. and M. Warmoeskerken (2006). *Transport phenomena data companion*. Delft: VSSD.

Janssen, M. M. H. P., J. C. M. Hendriks, A. C. H. Geurts, and I. J. M. de Groot (2016). "Variables associated with upper extremity function in patients with Duchenne muscular dystrophy". In: *Journal of Neurology*, 263 (9): 1810–1818. DOI: 10.1007/s00415-016-8193-1.

Janssen, M. M. H. P., A. Bergsma, A. C. H. Geurts, and I. J. M. de Groot (2014). "Patterns of decline in upper limb function of boys and men with DMD: an international survey". In: *Journal of Neurology*, 261 (7): 1269–1288. DOI: 10.1007/s00415-014-7316-9.

Jeong, U., H.-K. In, and K.-J. Cho (2013). "Implementation of various control algorithms for hand rehabilitation exercise using wearable robotic hand". In: *Intelligent Service Robotics*, 6 (4): 181–189. DOI: 10.1007/s11370-013-0135-5.

Jeong, U., H. In, H. Lee, B. B. Kang, and K.-j. Cho (2015). "Investigation on the control strategy of soft wearable robotic hand with slack enabling tendon actuator". In: *2015 IEEE International Conference on Robotics and Automation (ICRA)*. Seattle, WA, pp. 5004–5009. DOI: 10.1109/ICRA.2015.7139895.

Jo, I. and J. Bae (2013). "Kinematic analysis of a hand exoskeleton structure". In: *2013 10th International Conference on Ubiquitous Robots and Ambient Intelligence (URAI)*. Jeju, pp. 457–458. DOI: 10.1109/URAI.2013.6677310.

Jo, I. and J. Bae (2015). "Design and control of a wearable hand exoskeleton with force-controllable and compact actuator modules". In: *2015 IEEE International Conference on Robotics and Automation (ICRA)*. Seattle, WA, pp. 5596–5601. DOI: 10.1109/ICRA.2015.7139982.

Johansson, L., G. M. Hägg, and T. Fischer (2002). "Skin blood flow in the human hand in relation to applied pressure". In: *European Journal of Applied Physiology*, 86 (5): 394–400. DOI: 10.1007/s00421-001-0562-4.

Jones, C. L., F. Wang, R. Morrison, N. Sarkar, and D. G. Kamper (2014). "Design and development of the cable actuated finger exoskeleton for hand rehabilitation following stroke". In: *IEEE/ASME Transactions on Mechatronics*, 19 (1): 131–140. DOI: 10.1109/TMECH.2012.2224359.

Jones, C. L., F. Wang, C. Osswald, Xuan Kang, N. Sarkar, and D. G. Kamper (2010). "Control and kinematic performance analysis of an Actuated Finger Exoskeleton for hand rehabilitation following stroke". In: *2010 3rd IEEE RAS and EMBS International Conference on Biomedical Robotics and Biomechatronics (BioRob)*. Tokyo, pp. 282–287. DOI: 10.1109/BIOROB.2010.5626057.

Jones, L. A. and E. Piateski (2006). "Contribution of tactile feedback from the hand to the perception of force". In: *Experimental Brain Research*, 168: 298–302. DOI: 10.1007/s00221-005-0259-8.

Jung, I. Y., J. H. Chae, S. K. Park, J. H. Kim, J. Y. Kim, S. J. Kim, and M. S. Bang (2012). "The correlation analysis of functional factors and age with Duchenne muscular dystrophy". In: *Annals of Rehabilitation Medicine*, 36 (1): 22–32. DOI: 10.5535/arm.2012.36.1.22.

Kadowaki, Y., T. Noritsugu, M. Takaiwa, D. Sasaki, and M. Kato (2011). "Development of soft power-assist glove and control based on human intent". In: *Journal of Robotics and Mechatronics*, 23 (2): 281–291.

Kamper, D. G., E. G. Cruz, and M. P. Siegel (2003). *Stereotypical fingertip trajectories during grasp*. Tech. rep. 6, pp. 3702–3710. DOI: 10.1152/jn.00546.2003.

Kamper, D. G., T. George Hornby, and W. Z. Rymer (2002). "Extrinsic flexor muscles generate concurrent flexion of all three finger joints". In: *Journal of Biomechanics*, 35 (12): 1581–1589. DOI: 10.1016/S0021-9290(02)00229-4.

Kamper, D. G. and W. Z. Rymer (2000). "Quantitative features of the stretch response of extrinsic finger muscles in hemiparetic stroke". In: *Muscle & Nerve*, 23 (6): 954–961. DOI: 10.1002/(SICI)1097-4598(200006)23:6<954::AID-MUS17>3.0.CO;2-0.

Kaneko, M., M. Wada, H. Maekawa, and K. Tanie (1991). "A new consideration on tendon-tension control system of robot hands". In: *1991 IEEE International Conference on Robotics and Automation (ICRA)*. April, pp. 1028–1033. DOI: 10.1109/ROBOT.1991.131727.

Kang, Y.-S., Y.-G. Park, B.-S. Lee, and H. S. Park (2013). "Biomechanical evaluation of wrist-driven flexor hinge orthosis in persons with spinal cord injury". In: *Journal of Rehabilitation Research and Development*, 50 (8): 1129–1138. DOI: 10.1682/JRRD.2012.10.0189.

Karaszkiewicz, A. (1987). "Hydrodynamics of rubber seals for reciprocating motion, lubricating film thickness, and outleakage of O-seals". In: *Industrial & Engineering Chemistry Research*, 26 (11): 2180–2185. ISSN: 0888-5885. DOI: 10.1021/ie00071a002.

Kargov, A., T. Werner, C. Pylatiuk, and S. Schulz (2008). "Development of a miniaturised hydraulic actuation system for artificial hands". In: *Sensors and Actuators A: Physical*, 141 (2): 548–557. DOI: 10.1016/j.sna.2007.10.025.

Kargov, A., C. Pylatiuk, J. Martin, S. Schulz, and L. Döderlein (2004). "A comparison of the grip force distribution in natural hands and in prosthetic hands". In: *Disability and Rehabilitation*, 26 (12): 705–711. DOI: 10.1080/09638280410001704278.

Kawasaki, H., S. Ito, Y. Ishigure, Y. Nishimoto, T. Aoki, T. Mouri, H. Sakaeda, and M. Abe (2007). "Development of a Hand Motion Assist Robot for Rehabilitation Therapy by Patient Self-Motion Control". In: *2007 IEEE 10th International Conference on Rehabilitation Robotics (ICORR)*. Vol. 00. c. Noordwijk, pp. 234–240. DOI: 10.1109/ICORR.2007.4428432.

Kawasaki, H., S. Ito, Y. Nishimoto, H. Kimura, and H. Hayashi (2004). "Hand rehabilitation support system based on self-motion-control". In: *First IEEE Technical Exhibition Based Conference on Robotics and Automation*. Tokyo, pp. 55–56. DOI: 10.1109/TEXCRA.2004.1424994.

Kawasaki, H., S. Ito, Y. Nishimoto, S. Ueki, Y. Ishigure, and T. Mouri (2014). "Hand motion assist robot for rehabilitation therapy". In: *Journal of Robotics and Mechatronics*, 26 (1): 103–104.

Kazemi, H., R. E. Kearney, and T. E. Milner (2012). "A robotic interface to train grip strength, grip coordination and finger extension following stroke". In: *2012 Annual International Conference of the IEEE Engineering in Medicine and Biology Society*. Vol. 2012. San Diego, CA, pp. 3903–3906. DOI: 10.1109/EMBC.2012.6346820.

Kell, R. T., G. Bell, and A. Quinney (2001). "Musculoskeletal Fitness, Health Outcomes and Quality of Life". In: *Sports Medicine*, 31 (12): 863–873. DOI: 10.2165/00007256-200131120-00003.

Kelley, L. C. (1919). *Pedomotor*. Patent no. US1308675A.

Khanicheh, A., D. Mintzopoulos, B. Weinberg, A. A. Tzika, and C. Mavroidis (2008). "MR_CHIROD v.2: magnetic resonance compatible smart hand rehabilitation device

for brain imaging". In: *IEEE Transactions on Neural Systems and Rehabilitation Engineering*, 16 (1): 91–98. DOI: 10.1109/TNSRE.2007.910286.

Khanicheh, A., A. Muto, C. Triantafyllou, B. Weinberg, L. Astrakas, A. Tzika, and C. Mavroidis (2005). "MR Compatible ERF Driven Hand Rehabilitation Device". In: *2005 IEEE 9th International Conference on Rehabilitation Robotics (ICORR)*. Chicago, IL, pp. 7–12. DOI: 10.1109/ICORR.2005.1501039.

Khanicheh, A., A. Muto, C. Triantafyllou, B. Weinberg, L. Astrakas, A. Tzika, and C. Mavroidis (2006). "fMRI-compatible rehabilitation hand device". In: *Journal of NeuroEngineering and Rehabilitation*, 3 (1): 24. DOI: 10.1186/1743-0003-3-24.

Kim, D.-h., S. W. Lee, and H. S. Park (2014). "Feedback control of biomimetic exotendon device for hand rehabilitation in stroke". In: *36th Annual International Conference of the IEEE Engineering in Medicine and Biology Society (EMBC)*, pp. 3618–3621. DOI: 10.1109/EMBC.2014.6944406.

Kim, H.-M. and G.-S. Kim (2013). "Development of a finger-rehabilitation robot for fingers' flexibility rehabilitation exercise". In: *International Journal of Precision Engineering and Manufacturing*, 14 (4): 535–541. DOI: 10.1007/s12541-013-0073-3.

Kim, S. J. and J. Kim (2015). "MR-compatible hand exoskeleton for monitoring brain activity during active assistance". In: *2015 37th Annual International Conference of the IEEE Engineering in Medicine and Biology Society (EMBC)*. Milan, pp. 5752–5755. DOI: 10.1109/EMBC.2015.7319699.

Kim, Y.-m., S.-y. Jung, and I. Moon (2009). "Design of a wearable upper-limb rehabilitation robot using parallel mechanism". In: *ICROS-SICE International Joint Conference*. Fukuoka, pp. 785–789.

Kinetec SAS (2014). *Kinetec CPMs*. http://theratechequip.com/wp-content/uploads/2014/04/Kinetec-knee-hand-elbow1.pdf. Accessed 23 Oct 2015.

Kinetec SAS (n.d.). *Kinetec Maestra Portable CPM*. http://www.kinetec.fr/en. Accessed 23 Oct 2015.

King, C. E., K. R. Dave, P. T. Wang, M. Mizuta, D. J. Reinkensmeyer, A. H. Do, S. Moromugi, and Z. Nenadic (2014). *Performance Assessment of a Brain-Computer Interface Driven Hand Orthosis*. DOI: 10.1007/s10439-014-1066-9.

King, C. E., P. T. Wang, M. Mizuta, D. J. Reinkensmeyer, A. H. Do, S. Moromugi, and Z. Nenadic (2011). "Noninvasive brain-computer interface driven hand orthosis". In: *2011 Annual International Conference of the IEEE Engineering in Medicine and Biology Society (EMBC)*. Boston, MA, pp. 5786–5789. DOI: 10.1109/IEMBS.2011.6091432.

Kline, T., D. G. Kamper, and B. Schmit (2005). "Control system for pneumatically controlled glove to assist in grasp activities". In: *2005 IEEE 9th International Conference on Rehabilitation Robotics (ICORR)*. Vol. 2005. Chicago, IL, pp. 78–81. DOI: 10.1109/ICORR.2005.1501056.

Koyama, T., I. Yamano, K. Takemura, and T. Maeno (2002). "Multi-fingered exoskeleton haptic device using passive force feedback for dextrous telemanipulation". In: *2002 IEEE/RSJ International Conference on Intelligent Robots and Systems*. Lausanne, pp. 2905–2910.

Kragten, G. A., F. C. van der Helm, and J. L. Herder (2011). "A planar geometric design approach for a large grasp range in underactuated hands". In: *Mechanism and Machine Theory*, 46 (8): 1121–1136. DOI: 10.1016/j.mechmachtheory.2011.03.004.

Kragten, G. A. and J. L. Herder (2010). “The ability of underactuated hands to grasp and hold objects”. In: *Mechanism and Machine Theory*, 45 (3): 408–425. DOI: 10.1016/j.mechmachtheory.2009.10.002.

Kudo, S., K. Oshima, M. Arizono, Y. Hayashi, and S. Moromugi (2014). “Electric-powered glove for CCI patients to extend their upper-extremity function”. In: *2014 IEEE/SICE International Symposium on System Integration*. Tokyo, pp. 638–643. DOI: 10.1109/SII.2014.7028113.

Kuppens, P. R. and W. J. Wolfslag (2018). “A String-Based Representation and Crossover Operator for Evolutionary Design of Dynamical Mechanisms”. In: *IEEE Robotics and Automation Letters*, 3 (3): 1600–1607. DOI: 10.1109/LRA.2018.2800102.

Kurillo, G. and B. Bajd (2005). “Grip Force Control in Healthy Children and Children with Down Syndrome”. In: *EUROCON 2005 - The International Conference on "Computer as a Tool"*. Vol. 1, pp. 390–393. DOI: 10.1109/EURCON.2005.1629944.

Kwakkel, G., B. J. Kollen, and H. I. Krebs (2008). “Effects of robot-assisted therapy on upper limb recovery after stroke: a systematic review”. In: *Neurorehabilitation and Neural Repair*, 22 (2): 111–121. DOI: 10.1177/1545968307305457.

Lambercy, O., L. Dovat, R. Gassert, E. Burdet, C. L. Teo, and T. Milner (2007a). “A haptic knob for rehabilitation of hand function”. In: *IEEE Transactions on Neural Systems and Rehabilitation Engineering*, 15 (3): 356–366. DOI: 10.1109/TNSRE.2007.903913.

Lambercy, O., L. Dovat, V. Johnson, B. Salman, S. Wong, R. Gassert, T. Milner, T. C. Leong, and E. Burdet (2007b). “Development of a Robot-Assisted Rehabilitation Therapy to train Hand Function for Activities of Daily Living”. In: *2007 IEEE 10th International Conference on Rehabilitation Robotics (ICORR)*. Noordwijk, pp. 678–682. DOI: 10.1109/ICORR.2007.4428498.

Lambercy, O., D. Schröder, S. Zwicker, and R. Gassert (2013). “Design of a thumb exoskeleton for hand rehabilitation”. In: *Proceedings of the 7th International Convention on Rehabilitation Engineering and Assistive Technology*. ii. Singapore, Article No. 41.

Lampaert, S., B. Fellinger, J. Spronck, and R. van Ostayen (2018). “In-plane friction behaviour of a ferrofluid bearing”. In: *Precision Engineering*. in press. DOI: 10.1016/j.precisioneng.2018.05.013.

Landauer, K. S. (1958). “Methods and sources of stimulating interdisciplinary research”. In: *Annals of the New York Academy of Sciences*, 74 (1): 145–160. DOI: 10.1111/j.1749-6632.1958.tb39540.x.

Lawrence, E. S., C. Coshall, R. Dundas, J. Stewart, A. G. Rudd, R. Howard, and C. D. A. Wolfe (2001). “Estimates of the Prevalence of Acute Stroke Impairments and Disability in a Multiethnic Population”. In: *Stroke*, 32 (6): 1279–1284. DOI: 10.1161/01.STR.32.6.1279.

LeBlanc, M. A. (1985). “Evaluation of cable vs. hydraulic transmission of forces for body-powered arm prostheses”. In: *Proceedings of the 8th Annual RESNA Conference*. Memphis, TN, USA, pp. 71–73.

LeBlanc, M. A. (1990). “Current evaluation of hydraulics to replace the cable force transmission system for body-powered upper-limb prostheses”. In: 2 (3): 101–107. DOI: 10.1080/10400435.1990.10132159.

Lee, D. W., S. J. Lee, B. R. Yoon, J. Y. Jho, and K. Rhee (2014a). "Preliminary study on analysis of pinching motion actuated by electro-active polymers". In: *International Journal of Mechanical, Aerospace, Industrial and Mechatronics Engineering*, 8 (5): 922–924.

Lee, J. and J. Bae (2015). "Design of a hand exoskeleton for biomechanical analysis of the stroke hand". In: *2015 IEEE International Conference on Rehabilitation Robotics (ICORR)*. Singapore, pp. 484–489. DOI: 10.1109/ICORR.2015.7281246.

Lee, S. W., K. A. Landers, and H. S. Park (2014b). "Development of a biomimetic hand exotendon device (BiomHED) for restoration of functional hand movement post-stroke". In: *IEEE Transactions on Neural Systems and Rehabilitation Engineering*, 22 (4): 886–898. DOI: 10.1109/TNSRE.2014.2298362.

Lee, S. W., K. M. Wilson, B. A. Lock, and D. G. Kamper (2011). "Subject-Specific Myoelectric Pattern Classification of Functional Hand Movements for Stroke Survivors". In: *IEEE Transactions on Neural Systems and Rehabilitation Engineering*, 19 (5): 558–566. DOI: 10.1109/TNSRE.2010.2079334.

Lee, S. J., Y. J. Kim, G. H. Jeong, B. R. Yoon, J. Y. Jho, D. M. Kim, and K. Rhee (2012). "Computational analyses of pinching dynamics of a finger exoskeleton composed of IPMC actuators". In: *International Journal of Precision Engineering and Manufacturing*, 13 (12): 2135–2141. DOI: 10.1007/s12541-012-0283-0.

Lelieveld, M. J. and T. Maeno (2006). "Design and development of a 4 DOF portable haptic interface with multi-point passive force feedback for the index finger". In: *2006 IEEE International Conference on Robotics and Automation (ICRA)*. Orlando, FL, pp. 3134–3139. DOI: 10.1109/ROBOT.2006.1642178.

Lelieveld, M. J., T. Maeno, and T. Tomiyama (2006). "Design and development of two concepts for a 4 DOF portable haptic interface with active and passive multi-point force feedback for the index finger". In: *2006 ASME International Design Engineering Technical Conference (DETC)*. Philadelphia, PA, pp. 547–556. DOI: 10.1115/DETC2006-99111.

Lenzi, T., S. M. M. De Rossi, N. Vitiello, and M. C. Carrozza (2012). "Intention-based EMG control for powered exoskeletons." In: *IEEE Transactions on Biomedical Engineering*, 59 (8): 2180–2190. DOI: 10.1109/TBME.2012.2198821.

Leonardis, D., M. Barsotti, C. Loconsole, M. Solazzi, M. Troncossi, C. Mazzotti, V. P. Castelli, C. Procopio, G. Lamola, C. Chisari, M. Bergamasco, and A. Frisoli (2015). "An EMG-Controlled Robotic Hand Exoskeleton for Bilateral Rehabilitation". In: *IEEE Transactions on Haptics*, 8 (2): 140–151. DOI: 10.1109/TOH.2015.2417570.

Li, J., S. Wang, J. Wang, R. Zheng, Y. Zhang, and Z. Chen (2012). "Development of a hand exoskeleton system for index finger rehabilitation". In: *Chinese Journal of Mechanical Engineering*, 25 (2): 223–233. DOI: 10.3901/CJME.2012.02.223.

Li, J., R. Zheng, Y. Zhang, and J. Yao (2011). "iHandRehab: An interactive hand exoskeleton for active and passive rehabilitation". In: *2011 IEEE International Conference on Rehabilitation Robotics (ICORR)*. Zurich, pp. 1–6. DOI: 10.1109/ICORR.2011.5975387.

Li, Z. M. and J. Tang (2007). "Coordination of thumb joints during opposition". In: *Journal of Biomechanics*, 40 (3): 502–510. DOI: 10.1016/j.jbiomech.2006.02.019.

Liu, L., S. Miyake, N. Maruyama, K. Akahane, and M. Sato (2014). "Development of two-handed multi-finger haptic interface SPIDAR-10". In: *Eurohaptics*. Lecture Notes

in Computer Science. Versailles, pp. 176–183. DOI: 10.1007/978-3-662-44196-1_22.

Lobo-Prat, J., A. Q. L. Keemink, A. H. A. Stienen, A. C. Schouten, P. H. Veltink, and B. F. J. M. Koopman (2014a). "Evaluation of EMG, force and joystick as control interfaces for active arm supports." In: *Journal of Neuroengineering and Rehabilitation*, 11 (1): 68. DOI: 10.1186/1743-0003-11-68.

Lobo-Prat, J., P. N. Kooren, M. M. Janssen, A. Q. Keemink, P. H. Veltink, A. H. Stienen, and B. F. Koopman (2016). "Implementation of EMG-and force-based control interfaces in active elbow supports for men with duchenne muscular dystrophy: a feasibility study". In: *IEEE Transactions on Neural Systems and Rehabilitation Engineering*, 24 (11): 1179–1190. DOI: 10.1109/TNSRE.2016.2530762.

Lobo-Prat, J., P. N. Kooren, A. H. A. Stienen, J. L. Herder, B. F. J. M. Koopman, and P. H. Veltink (2014b). "Non-invasive control interfaces for intention detection in active movement-assistive devices". In: *Journal of NeuroEngineering and Rehabilitation*, 11 (1): 168. DOI: 10.1186/1743-0003-11-168.

Lobo-Prat, J., K. Nizamis, M. M. Janssen, A. Q. Keemink, P. H. Veltink, B. F. Koopman, and A. H. Stienen (2017). "Comparison between sEMG and force as control interfaces to support planar arm movements in adults with Duchenne: A feasibility study". In: *Journal of NeuroEngineering and Rehabilitation*, 14 (1): 1–17. DOI: 10.1186/s12984-017-0282-6.

Loconsole, C., D. Leonardis, M. Barsotti, M. Solazzi, A. Frisoli, M. Bergamasco, M. Troncossi, M. M. Foumashi, C. Mazzotti, and V. P. Castelli (2013). "An emg-based robotic hand exoskeleton for bilateral training of grasp". In: *2013 World Haptics Conference (WHC)*. Daejeon, pp. 537–542. DOI: 10.1109/WHC.2013.6548465.

Loughead, M. (1917). *Braking apparatus*. Patent no. 1,249,143.

Loureiro, R. C. V. and W. S. Harwin (2007). "Reach and grasp therapy: design and control of a 9-DOF robotic neuro-rehabilitation system". In: *2007 IEEE 10th International Conference on Rehabilitation Robotics (ICORR)*. Noordwijk, pp. 757–763. DOI: 10.1109/ICORR.2007.4428510.

Love, L. J., R. F. Lind, and J. F. Jansen (2009). "Mesofluidic actuation for articulated finger and hand prosthetics". In: *2009 IEEE/RSJ International Conference on Intelligent Robots and Systems, IROS 2009*: 2586–2591. DOI: 10.1109/IROS.2009.5353919.

Low, J.-H., M. H. Ang, and C.-H. Yeow (2015). "Customizable soft pneumatic finger actuators for hand orthotic and prosthetic applications". In: *2015 IEEE International Conference on Rehabilitation Robotics (ICORR)*. Singapore, pp. 380–385. DOI: 10.1109/ICORR.2015.7281229.

Lue, Y.-J., S.-S. Chen, and Y.-M. Lu (2017). "Quality of life of patients with Duchenne muscular dystrophy: from adolescence to young men". In: *Disability and Rehabilitation*, 39 (14): 1408–1413. DOI: 10.1080/09638288.2016.1196398.

Luo, X., R. V. Kenyon, T. Kline, H. C. Waldinger, and D. G. Kamper (2005a). "An Augmented Reality Training Environment for Post-Stroke Finger Extension Rehabilitation". In: *2005 IEEE 9th International Conference on Rehabilitation Robotics (ICORR)*. Chicago, IL, pp. 329–332. DOI: 10.1109/ICORR.2005.1501112.

Luo, X., T. Kline, H. C. Fischer, K. Stubblefield, R. V. Kenyon, and D. G. Kamper (2005b). "Integration of Augmented Reality and Assistive Devices for Post-Stroke Hand Opening

Rehabilitation". In: *2005 IEEE Engineering in Medicine and Biology 27th Annual Conference*. Shanghai, pp. 6855–6858. DOI: 10.1109/IEMBS.2005.1616080.

Ma, Z. and P. Ben-Tzvi (2015). "RML Glove - An Exoskeleton Glove Mechanism With Haptics Feedback". In: *IEEE/ASME Transactions on Mechatronics*, 20 (2): 641–652. DOI: 10.1109/TMECH.2014.2305842.

Machado, M., P. Moreira, P. Flores, and H. M. Lankarani (2012). "Compliant contact force models in multibody dynamics: Evolution of the Hertz contact theory". In: *Mechanism and Machine Theory*, 53: 99–121. DOI: 10.1016/j.mechmachtheory.2012.02.010.

Maciejasz, P., J. Eschweiler, K. Gerlach-Hahn, A. Jansen-Troy, and S. Leonhardt (2014). "A survey on robotic devices for upper limb rehabilitation." In: *Journal of NeuroEngineering and Rehabilitation*, 11 (1): 3. DOI: 10.1186/1743-0003-11-3.

Makaran, J. B., D. K. Dittmer, R. O. Buchal, and D. B. MacArthur (1993). "The SMART(R) Wrist-Hand Orthosis (WHO) for quadriplegic patients". In: *Journal of Prosthetics & Orthotics*, 5 (3): 3–6.

Makinson, J. B. (1971). *Research and Development Prototype for Machine Augmentation of Human Strength and Endurance*. Tech. rep. 196. General Electric Company.

Mali, U. and M. Munih (2006). "HIFE-haptic interface for finger exercise". In: *IEEE/ASME Transactions on Mechatronics*, 11 (1): 93–102. DOI: 10.1109/TMECH.2005.863363.

Martinez, L. A., O. O. Olaloye, M. V. Talarico, S. M. Shah, R. J. Arends, and B. F. BuSha (2010). "A power-assisted exoskeleton optimized for pinching and grasping motions". In: *2010 IEEE 36th Annual Northeast Bioengineering Conference (NEBEC)*. New York, NY, pp. 1–2. DOI: 10.1109/NEBC.2010.5458232.

Martini Leonard, J. (1984). *Practical seal design*. New York, NY: Marcel Dekker.

Masia, L., H. I. Krebs, P. Cappa, and N. Hogan (2007). "Design and characterization of hand module for whole-arm rehabilitation following stroke". In: *IEEE/ASME Transactions on Mechatronics*, 12 (4): 399–407. DOI: 10.1109/TMECH.2007.901928.

Matheson, E. and G. Brooker (2011). "Assistive Rehabilitation Robotic Glove". In: *Proceedings of Australasian Conference on Robotics and Automation*.

Matheson, E. and G. Brooker (2012). "Augmented robotic device for EVA hand manoeuvres". In: *Acta Astronautica*, 81 (1): 51–61. DOI: 10.1016/j.actaastro.2012.06.006.

Mattar, F. L. and C. Sobreira (2008). "Hand weakness in Duchenne muscular dystrophy and its relation to physical disability". In: *Neuromuscular Disorders*, 18 (3): 193–198. DOI: 10.1016/j.nmd.2007.11.004.

Mayhew, A., E. S. Mazzone, M. Eagle, T. Duong, M. Ash, V. Decostre, M. Vandenhauwe, K. Klingels, J. Florence, M. Main, F. Bianco, E. Henrikson, L. Servais, G. Campion, E. Vroom, V. Ricotti, N. Goemans, C. Mcdonald, and E. Mercuri (2013). "Development of the Performance of the Upper Limb module for Duchenne muscular dystrophy". In: *Developmental Medicine and Child Neurology*, 55 (11): 1038–1045. DOI: 10.1111/dmcn.12213.

Mayr, A., A. Kollreider, D. Ram, and L. Saltuari (2010). "An electromechanical device for distal upper limb training: preliminary results". In:

McConnell, A., X. Kong, and P. A. Vargas (2014). "A novel robotic assistive device for stroke-rehabilitation". In: *The 23rd IEEE International Symposium on Robot and Human Interactive Communication*. Edinburgh, pp. 917–923. DOI: 10.1109/ROMAN.2014.6926370.

Mehrholz, J., T. Platz, J. Kugler, and M. Pohl (2008). "Electromechanical and robot-assisted arm training for improving arm function and activities of daily living after stroke". In: *Cochrane Database of Systematic Reviews*, (4): CD006876. DOI: 10.1002/14651858.CD006876.pub2.

Memberg, W. D. and P. Crago (1997). "Instrumented objects for quantitative evaluation of hand grasp". In: 34 (1): 82–90.

Meng, Q. Y., S. L. Tan, H. L. Yu, Q. L. Meng, and Y. F. Fang (2014a). "Trajectory Planning and Realizing of an Exoskeleton Device for Hand Rehabilitation Based on sEMG Control". In: *Applied Mechanics and Materials*, 536-537: 1015–1020. DOI: 10.4028/www.scientific.net/AMM.536-537.1015.

Meng, Q. Y., S. L. Tan, H. L. Yu, Q. L. Meng, and J. H. Yi (2014b). "Research on Size Synthesis Optimization Design of a Bionic Exoskeleton for Index Finger Rehabilitation". In: *Advanced Materials Research*, 945-949: 1447–1450. DOI: 10.4028/www.scientific.net/AMR.945-949.1447.

Metzger, J.-C., O. Lambercy, A. Califfi, F. M. Conti, and R. Gassert (2014). "Neurocognitive Robot-Assisted Therapy of Hand Function". In: *IEEE Transactions on Haptics*, 7 (2): 140–149. DOI: 10.1109/TOH.2013.72.

Metzger, J.-C., O. Lambercy, D. Chapuis, and R. Gassert (2011). "Design and characterization of the ReHapticKnob, a robot for assessment and therapy of hand function". In: *2011 IEEE/RSJ International Conference on Intelligent Robots and Systems (IROS)*. San Francisco, CA, pp. 3074–3080. DOI: 10.1109/IROS.2011.6094882.

Metzger, J.-C., O. Lambercy, and R. Gassert (2012). "High-fidelity rendering of virtual objects with the ReHapticKnob - novel avenues in robot-assisted rehabilitation of hand function". In: *2012 IEEE Haptics Symposium (HAPTICS)*. Vancouver, BC, pp. 51–56. DOI: 10.1109/HAPTIC.2012.6183769.

Meyer, C. M., R. D. Shrosbree, and D. L. Abrahams (1979). "A method of rehabilitating the C6 tetraplegic hand". In: *Paraplegia*, 17: 170–175. DOI: 10.1038/sc.1979.35.

Mihelj, M., J. Podobnik, and M. Munih (2008). "HEnRiE - Haptic environment for reaching and grasping exercise". In: *2008 2nd IEEE RAS & EMBS International Conference on Biomedical Robotics and Biomechatronics*. Scottsdale, AZ, pp. 907–912. DOI: 10.1109/BIOROB.2008.4762810.

Mohamaddan, S. and T. Komeda (2010). "Wire-driven mechanism for finger rehabilitation device". In: *2010 IEEE International Conference on Mechatronics and Automation (ICMA)*. Xi'an, pp. 1015–1018. DOI: 10.1109/ICMA.2010.5588077.

Moromugi, S., T. Ishimatsu, H. Matsui, T. Ikeda, M. Mizuta, T. Koga, T. Tateishi, T. Saoyama, and M. Takashima (2010). "An electrical prehension orthosis operated through activity of mastication muscle". In: *SICE Annual Conference 2010*. Taipei, pp. 2030–2033.

Moromugi, S., K. Kawakami, K. Nakamura, T. Sakamoto, and T. Ishimatsu (2009). "A tendon-driven glove to restore finger function for disabled". In: *ICROS-SICE International Joint Conference*. Fukuoka, pp. 794–797.

Moromugi, S., T. Tanaka, T. Higashi, M. Q. Feng, and T. Ishimatsu (2013). "Pneumatically Driven Prehension Orthosis with Force Control Function". In: *Journal of Robotics and Mechatronics*, 25 (6): 973–982.

Mosher, R. S. (1967). "From Handyman to Hardiman". In: *SAE Technical Paper*: No. 670088. DOI: 10.4271/670088.

Mulas, M., M. Folgheraiter, and G. Gini (2005). "An EMG-controlled exoskeleton for hand rehabilitation". In: *2005 IEEE 9th International Conference on Rehabilitation Robotics (ICORR)*. Vol. 2005. Chicago, IL, pp. 371–374. DOI: 10.1109/ICORR.2005.1501122.

Naidu, D., R. Stopforth, G. Bright, and S. Davrajh (2011). "A 7 DOF exoskeleton arm: Shoulder, elbow, wrist and hand mechanism for assistance to upper limb disabled individuals". In: *IEEE Africon '11*. September. Livingstone, pp. 1–6. DOI: 10.1109/AFRCON.2011.6072065.

Naidu, D., R. Stopforth, G. Bright, and S. Davrajh (2012). "A Portable Passive Physiotherapeutic Exoskeleton". In: *International Journal of Advanced Robotic Systems*, 9: 1. DOI: 10.5772/52065.

Nakagawara, S., H. Kajimoto, N. Kawakami, S. Tachi, and I. Kawabuchi (2005). "An encounter-type multi-fingered master hand using circuitous joints". In: *2005 IEEE International Conference on Robotics and Automation (ICRA)*. Vol. 2005. Barcelona, pp. 2667–2672. DOI: 10.1109/ROBOT.2005.1570516.

Napier, J. R. (1956). "The prehensile movements of the human hand". In: *The Journal of Bone & Joint Surgery (British Volume)*, 38-B (4): 902–913.

NASA Johnson Space Center, G. (n.d.). *Robo-Glove: wearable technology that reduces the force needed to operate tools*. https://technology.nasa.gov//t2media/tops/pdf/MSC-TOPS-37.pdf. Accessed 25 Oct 2018.

Nathan, D. E. and M. J. Johnson (2007). "Design of a Grasp Assistive Glove for ADL-focused, Robotic Assisted Therapy after Stroke". In: *2007 IEEE 10th International Conference on Rehabilitation Robotics (ICORR)*. Noordwijk, pp. 943–950. DOI: 10.1109/ICORR.2007.4428537.

Nathan, D. E., M. J. Johnson, and J. R. McGuire (2009). "Design and validation of low-cost assistive glove for hand assessment and therapy during activity of daily living-focused robotic stroke therapy". In: *Journal of Rehabilitation Research and Development*, 46 (5): 587–602. DOI: 10.1682/JRRD.2008.04.0052.

Ngeo, J., T. Tamei, T. Shibata, M. F. Orlando, L. Behera, A. Saxena, and A. Dutta (2013). "Control of an optimal finger exoskeleton based on continuous joint angle estimation from EMG signals". In: *35th Annual International Conference of the IEEE Engineering in Medicine and Biology Society (EMBC)*. Osaka, pp. 338–341. DOI: 10.1109/EMBC.2013.6609506.

Nikas, G. K. (2010). "Eighty years of research on hydraulic reciprocating seals: review of tribological studies and related topics since the 1930s". In: *Proceedings of the Institution of Mechanical Engineers, Part J: Journal of Engineering Tribology*, 224 (1): 1–23. DOI: 10.1243/13506501JET607.

Nikas, G. K. and R. S. Sayles (2006). "Study of leakage and friction of flexible seals for steady motion via a numerical approximation method". In: *Tribology International*, 39 (9): 921–936. DOI: 10.1016/j.triboint.2005.09.003.

Nilsson, M., J. Ingvast, J. Wikander, and H. Von Holst (2012). "The Soft Extra Muscle system for improving the grasping capability in neurological rehabilitation". In: *2012 IEEE EMBS Conference on Biomedical Engineering and Sciences (IECBES)*. Langkawi, pp. 412–417. DOI: 10.1109/IECBES.2012.6498090.

Nishad, S. S., A. Dutta, and A. Saxena (2014). "Design and control of a three finger hand exoskeleton for translation of a slender object". In: *2014 11th International*

Conference on Ubiquitous Robots and Ambient Intelligence (URAI). Urai. Kuala Lumpur, pp. 179–184. DOI: 10.1109/URAI.2014.7057526.

Nizamis, K., W. Schutte, J. Goseling, and B. F. Koopman (2017). "Quantification of information transfer rate of the human hand during a mouse clicking task with healthy adults and one adult with Duchenne muscular dystrophy". In: *2017 International Conference on Rehabilitation Robotics (ICORR)*, pp. 1227–1232. DOI: 10.1109/ICORR.2017.8009417.

Nizamis, K., A. H. A. Stienen, D. G. Kamper, T. Keller, D. H. Plettenburg, E. J. Rouse, D. Farina, B. F. J. M. Koopman, and M. Sartori (2019). "Transferrable Expertise From Bionic Arms to Robotic Exoskeletons: Perspectives for Stroke and Duchenne Muscular Dystrophy". In: *IEEE Transactions on Medical Robotics and Bionics*, 1 (2): 88–96. DOI: 10.1109/TMRB.2019.2912453.

North Coast Medical, Inc. (n.d.). https://www.ncmedical.com/. Accessed 23 Oct 2015.

Nycz, C. J., T. Butzer, O. Lambercy, J. Arata, G. S. Fischer, and R. Gassert (2016). "Design and Characterization of a Lightweight and Fully Portable Remote Actuation System for Use With a Hand Exoskeleton". In: *IEEE Robotics and Automation Letters*, 1 (2): 976–983. DOI: 10.1109/LRA.2016.2528296.

Nycz, C. J., M. A. Delph, and G. S. Fischer (2015). "Modeling and design of a tendon actuated soft robotic exoskeleton for hemiparetic upper limb rehabilitation". In: *2015 37th Annual International Conference of the IEEE Engineering in Medicine and Biology Society (EMBC)*. Milan, pp. 3889–3892. DOI: 10.1109/EMBC.2015.7319243.

Obara, T. and S. Konishi (2012). "Multiarticular actuator composed of serially connected micropistons for wearable actuator". In: *2012 IEEE 25th International Conference on Micro Electro Mechanical Systems (MEMS)*. February. Paris, pp. 76–79. DOI: 10.1109/MEMSYS.2012.6170097.

Oboe, R., O. a. Daud, S. Masiero, F. Oscari, and G. Rosati (2010). "Development of a haptic teleoperation system for remote motor and functional evaluation of hand in patients with neurological impairments". In: *2010 11th IEEE International Workshop on Advanced Motion Control (AMC)*. Nagaoka, pp. 518–523. DOI: 10.1109/AMC.2010.5464078.

Ochoa, J. M., Y. Jia, N. Dev, and D. G. Kamper (2009). "Development of a portable actuated orthotic glove to facilitate gross extension of the digits for therapeutic training after stroke". In: *2009 31st Annual International Conference of the IEEE Engineering in Medicine and Biology Society (EMBC)*. Minneapolis, MN, pp. 6918–6921. DOI: 10.1109/IEMBS.2009.5333630.

Ochoa, J. M., D. G. Kamper, M. Listenberger, and S. W. Lee (2011). "Use of an electromyographically driven hand orthosis for training after stroke". In: *2011 IEEE International Conference on Rehabilitation Robotics (ICORR)*. Zurich, pp. 1–5. DOI: 10.1109/ICORR.2011.5975382.

Ochonski, W. (2005). "The attraction of Ferrofluid Bearings". In: *Machine Design*, 77 (21): 96–102.

Ockenfeld, C., R. K. Y. Tong, E. A. Susanto, S. K. Ho, and X.-L. Hu (2013). "Fine finger motor skill training with exoskeleton robotic hand in chronic stroke: Stroke rehabilitation". In: *2013 IEEE International Conference on Rehabilitation Robotics (ICORR)*. Seattle, WA, pp. 1–4. DOI: 10.1109/ICORR.2013.6650392.

Oomens, C. W. J., S. Loerakker, and D. L. Bader (2010). "The importance of internal strain as opposed to interface pressure in the prevention of pressure related deep tissue injury". In: *Journal of Tissue Viability*, 19 (2): 35–42. DOI: 10.1016/j.jtv.2009.11.002.

Orlando, M. F., H. Akolkar, A. Dutta, A. Saxena, and L. Behera (2010). "Optimal design and control of a hand exoskeleton". In: *2010 IEEE Conference on Robotics, Automation and Mechatronics (RAM)*. Singapore, pp. 72–77. DOI: 10.1109/RAMECH.2010.5513211.

Otsuka, T. and Y. Sankai (2010). "Development of exo-finger for grasp-assistance". In: *SCIS & ISIS*. Okayama, pp. 410–415.

Palli, G., G. Borghesan, and C. Melchiorri (2009). "Tendon-based transmission systems for robotic devices: models and control algorithms". In: *2009 IEEE International Conference on Robotics and Automation (ICRA)*. Kobe, pp. 4063–4068. DOI: 10.1109/ROBOT.2009.5152491.

Palli, G., G. Borghesan, and C. Melchiorri (2012). "Modeling, Identification, and Control of Tendon-Based Actuation Systems". In: *IEEE Transactions on Robotics*, 28 (2): 277–290. DOI: 10.1109/TRO.2011.2171610.

Palli, G., C. Natale, C. May, C. Melchiorri, and T. Würtz (2013). "Modeling and control of the twisted string actuation system". In: *IEEE/ASME Transactions on Mechatronics*, 18 (2): 664–673. DOI: 10.1109/TMECH.2011.2181855.

Pangalila, R. F., G. A. M. Van Den Bos, B. Bartels, M. P. Bergen, M. J. Kampelmacher, H. J. Stam, and M. E. Roebroeck (2015). "Quality of life of adult men with Duchenne muscular dystrophy in the Netherlands: Implications for care". In: *Journal of Rehabilitation Medicine*, 47 (2): 161–166. DOI: 10.2340/16501977-1898.

Park, H. S., Y. Ren, and L. Q. Zhang (2008). "IntelliArm: An exoskeleton for diagnosis and treatment of patients with neurological impairments". In: *2008 2nd Biennial IEEE RAS-EMBS International Conference on Biomedical Robotics and Biomechatronics (BioRob)*. Scottsdale, AZ, pp. 109–114. DOI: 10.1109/BIOROB.2008.4762876.

Park, J.-H., K.-s. Lee, K.-h. Jeon, D.-h. Kim, and H.-s. Park (2014). "Low cost and light-weight multi-DOF exoskeleton for comprehensive upper limb rehabilitation". In: *2014 11th International Conference on Ubiquitous Robots and Ambient Intelligence (URAI)*. Urai. Kuala Lumpur, pp. 138–139. DOI: 10.1109/URAI.2014.7057415.

Parker Hannifin Corporation O-ring Division (2007). *Parker O-Ring handbook (ORD 5700)*. Cleveland, OH: Parker Hannifin Corporation.

Pedrocchi, A., S. Ferrante, E. Ambrosini, M. Gandolla, C. Casellato, T. Schauer, C. Klauer, J. Pascual, C. Vidaurre, M. Gföhler, W. Reichenfelser, J. Karner, S. Micera, A. Crema, F. Molteni, M. Rossini, G. Palumbo, E. Guanziroli, A. Jedlitschka, M. Hack, M. Bulgheroni, E. D'Amico, P. Schenk, S. Zwicker, A. Duschau-Wicke, J. Miseikis, L. Graber, and G. Ferrigno (2013). "MUNDUS project: MUltimodal Neuroprosthesis for daily Upper limb Support." In: *Journal of NeuroEngineering and Rehabilitation*, 10: 66. DOI: 10.1186/1743-0003-10-66.

Peerdeman, B., G. Smit, S. Stramigioli, D. H. Plettenburg, and S. Misra (2012). "Evaluation of pneumatic cylinder actuators for hand prostheses". In: *2012 IEEE RAS & EMBS International Conference on Biomedical Robotics and Biomechatronics (BioRob)*. Rome, pp. 1104–1109. DOI: 10.1109/BioRob.2012.6290807.

Pehlivan, A. U., F. Sergi, and M. K. O'Malley (2015). "A Subject-Adaptive Controller for Wrist Robotic Rehabilitation". In: *IEEE/ASME Transactions on Mechatronics*, 20 (3): 1338–1350. DOI: 10.1109/TMECH.2014.2340697.

Peirs, J., D. Reynaerts, and H. Van Brussel (2001). "A miniature manipulator for integration in a self-propelling endoscope". In: *Sensors and Actuators A: Physical*, 92 (1-3): 343–349. DOI: 10.1016/S0924-4247(01)00570-2.

Pillsbury, T. E., C. S. Kothera, and N. M. Wereley (2015). "Effect of bladder wall thickness on miniature pneumatic artificial muscle performance". In: *Bioinspiration & Biomimetics*, 10 (5): 055006. DOI: 10.1088/1748-3190/10/5/055006.

Plettenburg, D. H. (2002). "A sizzling hand prosthesis. On the design and development of a pneumatically powered hand prosthesis for children". PhD thesis. Delft University of Technology.

Plettenburg, D. H. (2005). "Pneumatic actuators: A comparison of energy-to-mass ratio's". In: *2005 IEEE 9th International Conference on Rehabilitation Robotics (ICORR)*. Chicago, IL, pp. 545–549. DOI: 10.1109/ICORR.2005.1502022.

Plettenburg, D. H. (2006). *Upper extremity prosthetics: Current status & evaluation*. 1st ed. ISBN: 978-90-71301-75-9. Delft: VSSD.

Podobnik, J., M. Mihelj, and M. Munih (2009). "Upper limb and grasp rehabilitation and evaluation of stroke patients using HenRiE device". In: *2009 Virtual Rehabilitation International Conference*. Haifa, pp. 173–178. DOI: 10.1109/ICVR.2009.5174227.

Podobnik, J. and M. Munih (2010). "Robotic system for training of grasping and reaching". In: *XII Mediterranean Conference on Medical and Biological Engineering and Computing 2010*. Chalkidiki, pp. 703–706. DOI: 10.1007/978-3-642-13039-7_177.

Polotto, A., F. Modulo, F. Flumian, Z. G. Xiao, P. Boscariol, and C. Menon (2012). "Index finger rehabilitation/assistive device". In: *2012 4th IEEE RAS & EMBS International Conference on Biomedical Robotics and Biomechatronics (BioRob)*. Rome, pp. 1518–1523. DOI: 10.1109/BioRob.2012.6290676.

Polygerinos, P., K. C. Galloway, S. Sanan, M. Herman, and C. J. Walsh (2015a). "EMG controlled soft robotic glove for assistance during activities of daily living". In: *2015 IEEE International Conference on Rehabilitation Robotics (ICORR)*, pp. 55–60. DOI: 10.1109/ICORR.2015.7281175.

Polygerinos, P., K. C. Galloway, E. Savage, M. Herman, K. O. Donnell, and C. J. Walsh (2015b). "Soft robotic glove for hand rehabilitation and task specific training". In: *2015 IEEE International Conference on Robotics and Automation (ICRA)*. Seattle, WA, pp. 2913–2919. DOI: 10.1109/ICRA.2015.7139597.

Polygerinos, P., S. Lyne, Z. Wang, L. F. Nicolini, B. Mosadegh, G. M. Whitesides, and C. J. Walsh (2013). "Towards a soft pneumatic glove for hand rehabilitation". In: *2013 IEEE/RSJ International Conference on Intelligent Robots and Systems (IROS)*. Tokyo, pp. 1512–1517. DOI: 10.1109/IROS.2013.6696549.

Polygerinos, P., Z. Wang, K. C. Galloway, R. J. Wood, and C. J. Walsh (2015c). "Soft robotic glove for combined assistance and at-home rehabilitation". In: *Robotics and Autonomous Systems*, 73: 135–143. DOI: 10.1016/j.robot.2014.08.014.

Poole, A. D. and J. D. Booker (2011). "Design methodology and case studies in actuator selection". In: *Mechanism and Machine Theory*, 46 (5): 647–661. DOI: 10.1016/j.mechmachtheory.2010.12.009.

Popescu, D., M. Ivanescu, S. Manoiu-Olaru, M.-i. Burtea, and N. Popescu (2014). "Robotic glove development with application in robotics rehabilitation". In: *2014 International Conference and Exposition on Electrical and Power Engineering (EPE)*. Iasi, pp. 168–173. DOI: 10.1109/ICEPE.2014.6969890.

Popescu, D., M. Ivanescu, S. Manoiu-Olaru, L.-C. Popescu, and N. Popescu (2015). "Development of Robotic Gloves for Hand Rehabilitation Post-Stroke". In: *2015 20th International Conference on Control Systems and Computer Science*. Bucharest, pp. 838–844. DOI: 10.1109/CSCS.2015.95.

Popescu, N., D. Popescu, M. Ivanescu, D. Popescu, C. Vladu, C. Berceanu, and M. Poboroniuc (2013a). "Exoskeleton Design of an Intelligent Haptic Robotic Glove". In: *2013 19th International Conference on Control Systems and Computer Science*. Bucharest, pp. 196–202. DOI: 10.1109/CSCS.2013.21.

Popescu, N., D. Popescu, M. Poboroniuc, and C. D. Popescu (2013b). "Intelligent Haptic Robotic Glove for patients diagnosed with cerebrovascular accidents". In: *2013 17th International Conference on System Theory, Control and Computing (ICSTCC)*. Sinaia, pp. 717–721. DOI: 10.1109/ICSTCC.2013.6689045.

Pourghodrat, A. and C. a. Nelson (2014). "Miniature Fluidic Actuators for Surgical Robotics". In: *Journal of Medical Devices*, 8 (3): 030920. DOI: 10.1115/1.4027041.

Prange, G. B., M. J. A. Jannink, C. G. M. Groothuis-Oudshoorn, H. J. Hermens, and M. J. Ijzerman (2006). "Systematic review of the effect of robot-aided therapy on recovery of the hemiparetic arm after stroke." In: *Journal of Rehabilitation Research and Development*, 43 (2): 171–184. DOI: 10.1682/JRRD.2005.04.0076.

Pu, S.-W., H.-T. Chang, and J.-Y. Chang (2015). "Modeling and development of tension force measurement system for cable-driven hand exoskeleton robot". In: *2015 IEEE International Conference on Advanced Intelligent Mechatronics (AIM)*. Busan, pp. 635–640. DOI: 10.1109/AIM.2015.7222608.

Pu, S.-W., S.-Y. Tsai, and J.-Y. Chang (2014). "Design and development of the wearable hand exoskeleton system for rehabilitation of hand impaired patients". In: *2014 IEEE International Conference on Automation Science and Engineering (CASE)*. Taipei, pp. 996–1001. DOI: 10.1109/CoASE.2014.6899448.

Pursley, R. J. (1955). "Harness patterns for upper-extremity prostheses". In: *Artificial limbs*, 2 (3): 26–60.

Puzo, Z. C., T. A. Clark, and B. L. Ulrey (2014). "Development of an assistive device controlled by surface electromyogram signals". In: *2014 40th Annual Northeast Bioengineering Conference (NEBEC)*. Boston, MA, pp. 1–2. DOI: 10.1109/NEBEC.2014.6972912.

QAL Medical, LLC (2012). *WaveFlex Specifications Sheet*. http://qalmedical.com/qalmed/wp-content/uploads/sites/28/2013/11/QAL-Medical-6000X-WaveFlex-HandCPM-CPM.pdf. Accessed 6 Nov 2015.

QAL Medical, LLC (n.d.). http://qalmedical.com/. Accessed 6 Nov 2015.

Radder, B., A. Kottink, N. van der Vaart, D. Oosting, J. Buurke, S. Nijenhuis, G. Prange, and J. Rietman (2015). "User-centred input for a wearable soft-robotic glove supporting hand function in daily life". In: *2015 IEEE International Conference on Rehabilitation Robotics (ICORR)*. Singapore, pp. 502–507. DOI: 10.1109/ICORR.2015.7281249.

Raghavan, P. (2016). "Upper Limb Motor Impairment Post Stroke". In: *Physical Medicine and Rehabilitation Clinics of North America*, 26 (4): 599–610. DOI: 10.1016/j.pmr.2015.06.008.Upper.

Rahbek, J., B. Werge, A. Madsen, J. Marquardt, B. F. Steffensen, and J. Jeppesen (2005). "Adult life with Duchenne muscular dystrophy: observations among an emerging and

unforeseen patient population". In: *Pediatric Rehabilitation*, 8 (1): 17–28. DOI: 10.1080/13638490400010191.

Rahman, A. and A. Al-Jumaily (2012). "Design and Development of a Hand Exoskeleton for Rehabilitation Following Stroke". In: *Procedia Engineering*, 41: 1028–1034. DOI: 10.1016/j.proeng.2012.07.279.

Rahman, A. and A. Al-Jumaily (2013). "Design and development of a bilateral therapeutic hand device for stroke rehabilitation". In: *International Journal of Advanced Robotic Systems*, 10: Art. nr. A405. DOI: 10.5772/56809.

Ramirez, J., M. Alfaro, and I. Chairez (2015). "Electromyographic Driven Assisted Therapy for Hand Rehabilitation by Robotic Orthosis and Artificial Neural Networks". In: *VI Latin American Congress on Biomedical Engineering CLAIB 2014*. Ed. by A. Braidot and A. Hadad. Vol. 49. IFMBE Proceedings October 2014. Cham, pp. 75–78. DOI: 10.1007/978-3-319-13117-7_20.

Ramos-Murguialday, A., M. Schürholz, V. Caggiano, M. Wildgruber, A. Caria, E. M. Hammer, S. Halder, and N. Birbaumer (2012). "Proprioceptive Feedback and Brain Computer Interface (BCI) Based Neuroprostheses". In: *PLoS ONE*, 7 (10). Ed. by M. Hendricks: e47048. DOI: 10.1371/journal.pone.0047048.

Ramos, A., S. Halder, and N. Birbaumer (2009). "Proprioceptive feedback in BCI". In: *2009 4th International IEEE/EMBS Conference on Neural Engineering*. Antalya, Turkey, pp. 279–282. DOI: 10.1109/NER.2009.5109287.

RAUMEDIC AG (2018). *High-Pressure Tubing*. https://www.raumedic.com/fileadmin/user_upload/PDF/RAUMEDIC_company_EN.pdf. Accessed 29 Nov 2018.

Ravaud, R., G. Lemarquand, and V. Lemarquand (2009). "Magnetic pressure and shape of ferrofluid seals in cylindrical structures". In: *Journal of Applied Physics*, 106 (3): 034911. DOI: 10.1063/1.3187560.

Reha-Stim Medtec GmbH & Co. KG (2012). *Reha-Digit Flyer*. http://www.reha-stim.de/cms/assets/files/Flyer/Reha-Digit%20Flyer%20Englisch%202012.pdf. Accessed 16 Oct 2015.

Reha-Stim Medtec GmbH & Co. KG (n.d.). http://www.reha-stim.de/. Accessed 16 Oct 2015.

Rehab-Robotics Company Ltd. (n.d.). *Hand of Hope*. http://www.rehab-robotics.com/intro.html. Accessed 23 Oct 2015.

Reinkensmeyer, D. J. and M. L. Boninger (2012). "Technologies and combination therapies for enhancing movement training for people with a disability". In: *Journal of NeuroEngineering and Rehabilitation*, 9 (1): 17. DOI: 10.1186/1743-0003-9-17.

Ren, Y., H. S. Park, and L. Q. Zhang (2009). "Developing a whole-arm exoskeleton robot with hand opening and closing mechanism for upper limb stroke rehabilitation". In: *2009 IEEE International Conference on Rehabilitation Robotics (ICORR)*. Kyoto, pp. 761–765. DOI: 10.1109/ICORR.2009.5209482.

Richards, D. S., I. Georgilas, G. Dagnino, and S. Dogramadzi (2015). "Powered exoskeleton with palm degrees of freedom for hand rehabilitation". In: *2015 37th Annual International Conference of the IEEE Engineering in Medicine and Biology Society (EMBC)*. Milan, pp. 4635–4638. DOI: 10.1109/EMBC.2015.7319427.

Rijpkema, H. and M. Girard (1991). "Computer animation of knowledge-based human grasping". In: *ACM SIGGRAPH Computer Graphics*, 25 (4): 339–348. DOI: 10.1145/127719.122754.

Rosati, G., S. Cenci, G. Boschetti, D. Zanotto, and S. Masiero (2009). "Design of a single-dof active hand orthosis for neurorehabilitation". In: *2009 IEEE International Conference on Rehabilitation Robotics (ICORR)*. Kyoto, pp. 161–166. DOI: 10.1109/ICORR.2009.5209552.

Rosati, G., A. Rodà, F. Avanzini, and S. Masiero (2013). "On the Role of Auditory Feedback in Robot-Assisted Movement Training after Stroke: Review of the Literature". In: *Computational Intelligence and Neuroscience*, 2013: 1–15. DOI: 10.1155/2013/586138.

Rose, C. G., F. Sergi, Y. Yun, K. Madden, A. D. Deshpande, and M. K. O'Malley (2015). "Characterization of a hand-wrist exoskeleton, READAPT, via kinematic analysis of redundant pointing tasks". In: *2015 IEEE International Conference on Rehabilitation Robotics (ICORR)*. Singapore, pp. 205–210. DOI: 10.1109/ICORR.2015.7281200.

Rossi, J., E. Berton, L. Grélot, C. Barla, and L. Vigouroux (2012). "Characterisation of forces exerted by the entire hand during the power grip: effect of the handle diameter". In: *Ergonomics*, 55 (6): 682–692. DOI: 10.1080/00140139.2011.652195.

Rotella, M. F., K. E. Reuther, C. L. Hofmann, E. B. Hage, and B. F. BuSha (2009). "An orthotic hand-assistive exoskeleton for actuated pinch and grasp". In: *2009 IEEE 35th Annual Northeast Conference Bioengineering Conference*. Boston, MA, pp. 1–2. DOI: 10.1109/NEBC.2009.4967693.

Royal Vendors, Inc. (n.d.). *Package Vending Specs*. Last accessed February 14, 2018. URL: http://www.royalvendors.com/customer-service/technical-info/package-vending-specs/.

Ryder, S., R. M. Leadley, N. Armstrong, M. Westwood, S. de Kock, T. Butt, M. Jain, and J. Kleijnen (2017). "The burden, epidemiology, costs and treatment for Duchenne muscular dystrophy: an evidence review". In: *Orphanet Journal of Rare Diseases*, 12 (1): 79. DOI: 10.1186/s13023-017-0631-3.

Ryu, D., K. W. Moon, H. Nam, Y. Lee, C. Chun, S. Kang, and J. B. Song (2008). "Micro hydraulic system using slim artificial muscles for a wearable haptic glove". In: *2008 IEEE/RSJ International Conference on Intelligent Robots and Systems (IROS)*. Nice, pp. 3028–3033. DOI: 10.1109/IROS.2008.4651159.

Ryu, J., W. P. Cooney, L. J. Askew, K.-N. An, and E. Y. Chao (1991). "Functional ranges of motion of the wrist joint". In: *The Journal of Hand Surgery*, 16 (3): 409–419. DOI: 10.1016/0363-5023(91)90006-W.

Saebo, Inc. (n.d.[a]). Accessed 20 Oct 2015. URL: http://www.saebo.com/.

Saebo, Inc. (n.d.[b]). *SaeboGlove Brochure*. Accessed 16 Jan 2017. URL: https://www.saebo.com/wp-content/uploads/2016/01/SaeboGlove-Brochure.pdf.

Santello, M., M. Flanders, and J. F. Soechting (1998). "Postural hand synergies for tool use". In: *The Journal of Neuroscience*, 18 (23): 10105–10115.

Santello, M., M. Bianchi, M. Gabiccini, E. Ricciardi, G. Salvietti, D. Prattichizzo, M. Ernst, A. Moscatelli, H. Jörntell, A. M. Kappers, K. Kyriakopoulos, A. Albu-Schäffer, C. Castellini, and A. Bicchi (2016). "Hand synergies: Integration of robotics and neuroscience for understanding the control of biological and artificial hands". In: *Physics of Life Reviews*, 17: 1–23. DOI: 10.1016/j.plrev.2016.02.001.

Sarakoglou, I., N. G. Tsagarakis, and D. G. Caldwell (2004). "Occupational and physical therapy using a hand exoskeleton based exerciser". In: *2004 IEEE/RSJ International*

Conference on Intelligent Robots and Systems (IROS). Vol. 3. Sendai, pp. 2973–2978. DOI: 10.1109/IROS.2004.1389861.

Sartori, M., G. Durandau, S. Došen, and D. Farina (2018). "Robust simultaneous myoelectric control of multiple degrees of freedom in wrist-hand prostheses by real-time neuromusculoskeletal modeling". In: *Journal of Neural Engineering*, 15 (6): 066026. DOI: 10.1088/1741-2552/aae26b.

Sartori, M., J. van de Riet, and D. Farina (2019). "Estimation of phantom arm mechanics about four degrees of freedom after targeted muscle reinnervation". In: *IEEE Transactions on Medical Robotics and Bionics*, 1 (1): 58–64. DOI: 10.1109/TMRB.2019.2895791.

Sasaki, D., T. Noritsugu, M. Takaiwa, and H. Konishi (2014). "Control method based on EMG for power assist glove using self-organizing maps". In: *International Journal of Automation Technology*, 8 (2): 177–185.

Sasaki, D., T. Noritsugu, H. Yamamoto, and M. Takaiwa (2004). "Wearable power assist device for hand grasping using pneumatic artificial rubber muscle". In: *2004 SICE Annual Conference*. Sapporo, pp. 655–660. DOI: 10.1109/ROMAN.2004.1374840.

Sato, K., K. Minamizawa, N. Kawakami, and S. Tachi (2007). "Haptic telexistence". In: *ACM SIGGRAPH 2007*, p. 10. DOI: 10.1145/1278280.1278291.

Saudabayev, A., Z. Rysbek, R. Khassenova, and H. Atakan Varol (2018). "Data Descriptor: Human grasping database for activities of daily living with depth, color and kinematic data streams". In: *Scientific Data*, 5: Article no. 180101. DOI: 10.1038/sdata.2018.101.

Sauerbruch, F. (1916). *Die willkürlich bewegbare künstliche hand: eine anleitung für chirurgen und techniker*. ISBN: 978-3642649196. Berlin: Julius Springer.

Saxena, A. and G. K. Ananthasuresh (1998). "Topological synthesis of compliant mechanisms using the optimality criteria method". In: *7th AIAA/USAF/NASA/ISSMO Symposium on Multidisciplinary Analysis and Optimization*. Reston, Virigina, pp. 1900–1910. DOI: 10.2514/6.1998-4953.

Schabowsky, C. N., S. B. Godfrey, R. J. Holley, and P. S. Lum (2010). "Development and pilot testing of HEXORR: hand EXOskeleton rehabilitation robot". In: *Journal of NeuroEngineering and Rehabilitation*, 7 (1): 36. DOI: 10.1186/1743-0003-7-36.

Schiele, A. (2008). "Performance difference of Bowden Cable relocated and non-relocated master actuators in virtual environment applications". In: *2008 IEEE/RSJ International Conference on Intelligent Robots and Systems (IROS)*. Nice, pp. 3507–3512. DOI: 10.1109/IROS.2008.4650891.

Schiele, A. and F. C. T. van der Helm (2006). "Kinematic Design to Improve Ergonomics in Human Machine Interaction". In: *IEEE Transactions on Neural Systems and Rehabilitation Engineering*, 14 (4): 456–469. DOI: 10.1109/TNSRE.2006.881565.

Schiele, A., P. Letier, R. Q. van der Linde, and F. C. T. van der Helm (2006). "Bowden cable actuator for force-feedback exoskeletons". In: *2006 IEEE/RSJ International Conference on Intelligent Robots and Systems (IROS)*. Beijing, pp. 3599–3604. DOI: 10.1109/IROS.2006.281712.

Schuurmans, J., R. Q. van der Linde, D. H. Plettenburg, and F. C. T. van der Helm (2007). "Grasp force optimization in the design of an underactuated robotic hand". In: *2007 IEEE 10th International Conference on Rehabilitation Robotics (ICORR)*. Noordwijk, pp. 776–782. DOI: 10.1109/ICORR.2007.4428513.

Shafi, U. A., A. Pervez, F. A. Kamal, R. Ejaz, U. S. Khan, and J. Iqbal (2013). "Design and fabrication of an actuated hand exoskeleton for stroke and post traumatic rehabilitation". In: *International Conference on Innovations in Engineering and Technology (ICIET)*. Bangkok, pp. 176–180. DOI: 10.15242/IIE.E1213515.

Shashaty, A. J. (1981). "The Reduction of Capstan Effectiveness by Cable Bending Resistance". In: *Journal of Engineering for Industry*, 103 (3): 319. DOI: 10.1115/1.3184491.

Shields, B. L., J. A. Main, S. W. Peterson, and A. M. Strauss (1997). "An anthropomorphic hand exoskeleton to prevent astronaut hand fatigue during extravehicular activities". In: *IEEE Transactions on Systems, Man, and Cybernetics - Part A: Systems and Humans*, 27 (5): 668–673. DOI: 10.1109/3468.618265.

Sigmund, O. (2001). "A 99 line topology optimization code written in Matlab". In: *Structural and Multidisciplinary Optimization*, 21 (2): 120–127. DOI: 10.1007/s001580050176.

Sigmund, O. (1997). "On the Design of Compliant Mechanisms Using Topology Optimization". In: *Mechanics of Structures and Machines*, 25 (4): 493–524. DOI: 10.1080/08905459708945415.

Sigrist, R., G. Rauter, R. Riener, and P. Wolf (2013). "Augmented visual, auditory, haptic, and multimodal feedback in motor learning: A review". In: *Psychonomic Bulletin & Review*, 20 (1): 21–53. DOI: 10.3758/s13423-012-0333-8.

Sindrey, R. and G. M. Bone (2009). "Position Tracking Control of a Miniature Water Hydraulic Rotary Actuator". In: *Journal of Dynamic Systems, Measurement, and Control*, 131 (6): 061003. DOI: 10.1115/1.3223563.

Skalsky, A. J. and C. M. McDonald (2012). "Prevention and Management of Limb Contractures in Neuromuscular Diseases". In: *Physical Medicine and Rehabilitation Clinics of North America*, 23 (3): 675–687. DOI: 10.1016/j.pmr.2012.06.009.

Slack, M. and D. Berbrayer (1992). "A myoelectrically controlled wrist-hand orthosis for brachial plexus injury: a case study". In: *Journal of Prosthetics & Orthotics*, 4 (3): 171–174.

Smit, G., D. H. Plettenburg, and F. C. T. van der Helm (2013). "Design and evaluation of two different finger concepts for body-powered prosthetic hand". In: *Journal of Rehabilitation Research and Development*, 50 (9): 1253–1266. DOI: 10.1682/JRRD.2012.12.0223.

Smit, G., D. H. Plettenburg, and F. C. T. van der Helm (2015). "The lightweight Delft Cylinder Hand, the first multi-articulating hand that meets the basic user requirements". In: *IEEE Transactions on Neural Systems and Rehabilitation Engineering*, 23 (3). DOI: 10.1109/TNSRE.2014.2342158.

Smith, G. E. (1908). "The most ancient splints". In: *British Medical Journal*, 1 (2465): 732–736. DOI: 10.1136/bmj.1.2465.732.

Solano, B. and C. Rotinat-Libersa (2011). "Compact and Lightweight Hydraulic Actuation System for High Performance Millimeter Scale Robotic Applications: Modeling and Experiments". In: *Journal of Intelligent Material Systems and Structures*, 22 (13): 1479–1487. DOI: 10.1177/1045389X11418860.

Song, K.-t. and Y.-y. Chai (2013). "Compliance control of wearable robotic fingers for rehabilitation applications". In: *2013 CACS International Automatic Control Conference (CACS)*. Sun Moon Lake, pp. 306–311. DOI: 10.1109/CACS.2013.6734151.

Sooraj, R., N. Akshay, T. G. Jeevan, and R. R. Bhavani (2013). “Design and Analysis of a Parallel Haptic Orthosis for Upper Limb Rehabilitation.” In: *International Journal of Engineering and Technology*, 5 (1): 444–451.

Stanic, I. (2018). “Orthotic arm”. In: *The birth of humanoid robotics - 50th anniversary of the Robotics Centre at the Institute "Mihailo Pupin"*. Belgrade: Museum of Science and Technology.

Stergiopoulos, P., P. Fuchs, and C. Laurgeau (2003). “Design of a 2-finger hand exoskeleton for VR grasping simulation”. In: *Eurohaptics*. Dublin, pp. 80–93.

Steutel, P. (2010). “Design of a fully compliant under-actuated finger with a monolithic structure and distributed compliance”. M.Sc. Thesis. Delft University of Technology.

Stienen, A. H. A., E. E. G. Hekman, H. T. Braak, A. M. M. Aalsma, F. C. T. Van Der Helm, and H. Van Der Kooij (2010). “Design of a rotational hydroelastic actuator for a powered exoskeleton for upper limb rehabilitation”. In: *IEEE Transactions on Biomedical Engineering*, 57 (3): 728–735. DOI: 10.1109/TBME.2009.2018628.

Suarez-Escobar, M., J. A. Gallego-Sanchez, and E. Rendon-Velez (2016). “Mechanisms for linkage-driven underactuated hand exoskeletons: conceptual design including anatomical and mechanical specifications”. In: *International Journal on Interactive Design and Manufacturing (IJIDeM)*. DOI: 10.1007/s12008-015-0297-9.

Sun, Z., G. Bao, Q. Yang, and Z. Wang (2006). “Design of a Novel Force Feedback Dataglove Based on Pneumatic Artificial Muscles”. In: *2006 International Conference on Mechatronics and Automation*. 50375034. Luoyang, pp. 968–972. DOI: 10.1109/ICMA.2006.257756.

Sun, Z., X. Miao, and X. Li (2009). “Design of a bidirectional force feedback dataglove based on pneumatic artificial muscles”. In: *2009 International Conference on Mechatronics and Automation*. Changchun, pp. 1767–1771. DOI: 10.1109/ICMA.2009.5246223.

Surendra, W. A., A. P. Tjahyono, and K. C. Aw (2012). “Portable and Wearable Five-Fingered Hand Assistive Device”. In: *2012 19th International Conference on Mechatronics and Machine Vision in Practice (M2VIP)*. Auckland, pp. 431–435.

Tadano, K., M. Akai, K. Kadota, and K. Kawashima (2010). “Development of grip amplified glove using bi-articular mechanism with pneumatic artificial rubber muscle”. In: *2010 IEEE International Conference on Robotics and Automation (ICRA)*. Anchorage, AK, pp. 2363–2368. DOI: 10.1109/ROBOT.2010.5509393.

Taheri, H., J. B. Rowe, D. Gardner, V. Chan, K. Gray, C. Bower, D. J. Reinkensmeyer, and E. T. Wolbrecht (2014). “Design and preliminary evaluation of the FINGER rehabilitation robot: controlling challenge and quantifying finger individuation during musical computer game play”. In: *Journal of NeuroEngineering and Rehabilitation*, 11 (1): 10. DOI: 10.1186/1743-0003-11-10.

Taheri, H., J. B. Rowe, D. Gardner, V. Chan, D. J. Reinkensmeyer, and E. T. Wolbrecht (2012). “Robot-assisted Guitar Hero for finger rehabilitation after stroke”. In: *2012 Annual International Conference of the IEEE Engineering in Medicine and Biology Society*. San Diego, CA, pp. 3911–3917. DOI: 10.1109/EMBC.2012.6346822.

Takagi, M., K. Iwata, Y. Takahashi, S. I. Yamamoto, H. Koyama, and T. Komeda (2009). “Development of a grip aid system using air cylinders”. In: *2009 IEEE International Conference on Robotics and Automation (ICRA)*. Kobe, pp. 2312–2317. DOI: 10.1109/ROBOT.2009.5152246.

Takahashi, C. D., L. Der-Yeghiaian, V. H. Le, and S. C. Cramer (2005). "A robotic device for hand motor therapy after stroke". In: *2005 IEEE 9th International Conference on Rehabilitation Robotics (ICORR)*. Vol. 2005. Chicago, IL, pp. 17–20. DOI: 10.1109/ICORR.2005.1501041.

Tan, H. Z., B. Eberman, M. A. Srinivasan, and B. Cheng (1994). "Human factors for the design of force-reflecting haptic interfaces". In: *American Society of Mechanical Engineers, Dynamic Systems and Control Division*, 55-1: 353–359.

Tang, T., D. Zhang, T. Xie, and X. Zhu (2013a). "An exoskeleton system for hand rehabilitation driven by shape memory alloy". In: *2013 IEEE International Conference on Robotics and Biomimetics (ROBIO)*. Shenzhen, pp. 756–761. DOI: 10.1109/ROBIO.2013.6739553.

Tang, Z., S. Sugano, and H. Iwata (2011). "A novel, MRI compatible hand exoskeleton for finger rehabilitation". In: *2011 IEEE/SICE International Symposium on System Integration (SII)*. Kyoto, pp. 118–123. DOI: 10.1109/SII.2011.6147430.

Tang, Z., S. Sugano, and H. Iwata (2012). "Design of an MRI compatible robot for finger rehabilitation". In: *2012 IEEE International Conference on Mechatronics and Automation (ICMA)*. Chengdu, pp. 611–616. DOI: 10.1109/ICMA.2012.6283177.

Tang, Z., S. Sugano, and H. Iwata (2013b). "Design and evaluation of an one DOF finger rehabilitation device". In: *2013 IEEE/ASME International Conference on Advanced Intelligent Mechatronics (AIM)*. Wollongong, pp. 822–827. DOI: 10.1109/AIM.2013.6584195.

Tang, Z., S. Sugano, and H. Iwata (2013c). "A finger exoskeleton for rehabilitation and brain image study". In: *2013 IEEE International Conference on Rehabilitation Robotics (ICORR)*. Seattle, WA, pp. 1–6. DOI: 10.1109/ICORR.2013.6650446.

Taylor, C. L. and R. J. Schwarz (1955). "The Anatomy and Mechanics of the Human Hand". In: *Artificial Limbs*, 2 (2): 22–35. DOI: 10.1016/B0-08-043749-4/09065-0.

Thurston, A. J. (2007). "Pareé and prosthetics: the early history of artificial limbs". In: *ANZ Journal of Surgery*, 77 (12): 1114–1119. DOI: 10.1111/j.1445-2197.2007.04330.x.

Timmermans, A. A. A., H. A. M. Seelen, R. D. Willmann, and H. Kingma (2009). "Technology-assisted training of arm-hand skills in stroke: concepts on reacquisition of motor control and therapist guidelines for rehabilitation technology design". In: *Journal of Neuroengineering and Rehabilitation*, 6 (1): 1. DOI: 10.1186/1743-0003-6-1.

Tjahyono, A. P., K. C. Aw, H. Devaraj, W. A. Surendra, E. Haemmerle, and J. Travas-Sejdic (2013). "A five-fingered hand exoskeleton driven by pneumatic artificial muscles with novel polypyrrole sensors". In: *Industrial Robot: An International Journal*, 40 (3): 251–260. DOI: 10.1108/01439911311309951.

Tong, K. Y., S. K. Ho, P. M. K. Pang, X. L. Hu, W. K. Tam, K. L. Fung, X. J. Wei, P. N. Chen, and M. Chen (2010). "An intention driven hand functions task training robotic system". In: *2010 Annual International Conference of the IEEE Engineering in Medicine and Biology Society (EMBC)*. Buenos Aires, pp. 3406–3409. DOI: 10.1109/IEMBS.2010.5627930.

Tong, K. Y., P. M. K. Pang, M. Chen, S. K. Ho, H. Zhou, and D. T. W. Chan (2013). *Wearable power assistive device for helping a user to move their hand*.

Torgerson, C. (1997). *Continuous passive motion device for the hand and a method of using the same*. Patent no. US 5,697,892.

Toya, K., T. Miyagawa, and Y. Kubota (2011). "Power-Assist Glove Operated by Predicting the Grasping Mode". In: *Journal of System Design and Dynamics*, 5 (1): 94–108. DOI: 10.1299/jsdd.5.94.

Truelsen, T., B. Piechowski-Jóźwiak, R. Bonita, C. Mathers, J. Bogousslavsky, and G. Boysen (2006). "Stroke incidence and prevalence in Europe: A review of available data". In: *European Journal of Neurology*, 13 (6): 581–598. DOI: 10.1111/j.1468-1331.2006.01138.x.

Tu, X., L. Yu, and J. He (2012). "Design of a Wearable Quantitative Muscle Rehabilitation Evaluation Robotic Hand Device". In: *Lecture Notes in Electrical Engineering*. Ed. by X. Wang, F. Wang, and S. Zhong. Vol. 138. Lecture Notes in Electrical Engineering. London, pp. 1753–1761. DOI: 10.1007/978-1-4471-2467-2_208.

Tyromotion GmbH (n.d.). http://tyromotion.com/. Accessed 23 Oct 2015.

Tzafestas, C. (2003). "Whole-hand kinesthetic feedback and haptic perception in dextrous virtual manipulation". In: *IEEE Transactions on Systems, Man, and Cybernetics - Part A: Systems and Humans*, 33 (1): 100–113. DOI: 10.1109/TSMCA.2003.812600.

Tzemanaki, A., D. Raabe, and S. Dogramadzi (2011). "Development of a novel robotic system for hand rehabilitation". In: *2011 24th International Symposium on Computer-Based Medical Systems (CBMS)*. Bristol, pp. 1–6. DOI: 10.1109/CBMS.2011.5999150.

Udupa, G., P. Sreedharan, P. Sai Dinesh, and D. Kim (2014). "Asymmetric Bellow Flexible Pneumatic Actuator for Miniature Robotic Soft Gripper". In: *Journal of Robotics*, 2014 (Article ID 902625): 1–11. DOI: 10.1155/2014/902625.

Ueki, S., H. Kawasaki, S. Ito, Y. Nishimoto, M. Abe, T. Aoki, Y. Ishigure, T. Ojika, and T. Mouri (2012). "Development of a hand-assist robot with multi-degrees-of-freedom for rehabilitation therapy". In: *IEEE/ASME Transactions on Mechatronics*, 17 (1): 136–146. DOI: 10.1109/TMECH.2010.2090353.

Unluhisarcikli, O., B. Weinberg, M. Sivak, A. Mirelman, P. Bonato, and C. Mavroidis (2010). "A robotic hand rehabilitation system with interactive gaming using novel Electro-Rheological Fluid based actuators". In: *2010 IEEE International Conference on Robotics and Automation (ICRA)*. Anchorage, AK, pp. 1846–1851. DOI: 10.1109/ROBOT.2010.5509806.

Ushiba, J., A. Morishita, and T. Maeda (2014). "A task-oriented brain-computer interface rehabilitation system for patients with stroke hemiplegia". In: *2014 4th International Conference on Wireless Communications, Vehicular Technology, Information Theory and Aerospace & Electronic Systems (VITAE)*. Aalborg, pp. 1–3. DOI: 10.1109/VITAE.2014.6934416.

Veijgen, N. K., M. A. Masen, and E. van der Heide (2013). "Variables influencing the frictional behaviour of in vivo human skin". In: *Journal of the Mechanical Behavior of Biomedical Materials*, 28: 448–461. DOI: 10.1016/j.jmbbm.2013.02.009.

Verros, S., N. Mahmood, L. Peeters, J. Lobo-Prat, A. Bergsma, E. Hekman, G. J. Verkerke, and B. Koopman (2018). "Evaluation of Control Interfaces for Active Trunk Support". In: *IEEE Transactions on Neural Systems and Rehabilitation Engineering*, 26 (10): 1965–1974. DOI: 10.1109/TNSRE.2018.2866956.

De Volder, M. and D. Reynaerts (2009). "Development of a hybrid ferrofluid seal technology for miniature pneumatic and hydraulic actuators". In: *Sensors and Actuators A: Physical*, 152 (2): 234–240. DOI: 10.1016/j.sna.2009.04.010.

De Volder, M. and D. Reynaerts (2010). "Pneumatic and hydraulic microactuators: a review". In: *Journal of Micromechanics and Microengineering*, 20 (4): 043001. DOI: 10.1088/0960-1317/20/4/043001.

Vos, T. et al. (2016). "Global, regional, and national incidence, prevalence, and years lived with disability for 310 diseases and injuries, 1990–2015: a systematic analysis for the Global Burden of Disease Study 2015". In: *The Lancet*, 388 (10053): 1545–1602. DOI: 10.1016/S0140-6736(16)31678-6.

Vukobratovic, M., D. Hristic, and Z. Stojiljkovic (1974). "Development of active anthropomorphic exoskeletons". In: *Medical & Biological Engineering*, 12 (1): 66–80. DOI: 10.1007/BF02629836.

Vukobratovic, M. K. (2007). "When were active exoskeletons actually born?" In: *International Journal of Humanoid Robotics*, 04 (3): 459–486. DOI: 10.1142/S0219843607001163.

Vukobratovic, M. K. and B. Borovac (2004). "Zero-moment point — thirty five years of its life". In: *International Journal of Humanoid Robotics*, 1 (01): 157–173. DOI: 10.1142/S0219843604000083.

Wagner, K. R., N. Lechtzin, and D. P. Judge (2007). "Current treatment of adult Duchenne muscular dystrophy". In: *Biochimica et Biophysica Acta*, 1772 (2): 229–237. DOI: 10.1016/j.bbadis.2006.06.009.

Wagner, M. B., P. J. J. Vignos, C. Carlozzi, and A. L. Hull (1993). "Assessment of hand function in Duchenne muscular dystrophy". In: *Archives of physical medicine and rehabilitation*, 74 (8): 801–804.

Wagner, M. B., P. J. Vignos, and C. Carlozzi (1989). "Duchenne muscular dystrophy: A study of wrist and hand function". In: *Muscle & Nerve*, 12 (3): 236–244. DOI: 10.1002/mus.880120313.

Wakimoto, S., K. Suzumori, and K. Ogura (2011). "Miniature Pneumatic Curling Rubber Actuator Generating Bidirectional Motion with One Air-Supply Tube". In: *Advanced Robotics*, 25: 1311–1330. DOI: 10.1163/016918611X574731.

Wang, F., M. Shastri, C. L. Jones, V. Gupta, C. Osswald, X. Kang, D. G. Kamper, and N. Sarkar (2011a). "Design and control of an actuated thumb exoskeleton for hand rehabilitation following stroke". In: *2011 IEEE International Conference on Robotics and Automation (ICRA)*. Shanghai, pp. 3688–3693. DOI: 10.1109/ICRA.2011.5980099.

Wang, J., J. Li, Y. Zhang, and S. Wang (2009a). "Design of an exoskeleton for index finger rehabilitation". In: *31st Annual International Conference of the IEEE Engineering in Medicine and Biology Society (EMBC)*. Minneapolis, MN, pp. 5957–5960. DOI: 10.1109/IEMBS.2009.5334779.

Wang, S., J. Li, Y. Zhang, and J. Wang (2009b). "Active and Passive Control of an Exoskeleton with Cable Transmission for Hand Rehabilitation". In: *2009 2nd International Conference on Biomedical Engineering and Informatics*. Tianjin, pp. 1–5. DOI: 10.1109/BMEI.2009.5305113.

Wang, S., J. Li, and R. Zheng (2010a). "A Resistance Compensation Control Algorithm for a Cable-Driven Hand Exoskeleton for Motor Function Rehabilitation". In: *Intelligent Robotics and Applications*, pp. 398–404. DOI: 10.1007/978-3-642-16587-0_37.

Wang, S., J. Li, and R. Zheng (2010b). "Active and passive control algorithm for an exoskeleton with bowden cable transmission for hand rehabilitation". In: *2010 IEEE*

International Conference on Robotics and Biomimetics. Tianjin, pp. 75–79. DOI: 10.1109/ROBIO.2010.5723306.

Wang, S., J. Li, R. Zheng, Z. Chen, and Y. Zhang (2011b). "Multiple rehabilitation motion control for hand with an exoskeleton". In: *2011 IEEE International Conference on Robotics and Automation (ICRA)*. Shanghai, pp. 3676–3681. DOI: 10.1109/ICRA.2011.5979696.

Watanabe, H., K. Ogata, T. Okabe, and T. Amano (1978). "Hand orthosis for various finger impairments–the K U finger splint". In: *Prosthetics and Orthotics International*, 2 (2): 95–100. DOI: 10.1080/03093647809177776.

Watanabe, K., H. Morishita, T. Mori, and T. Sato (2005). "Grasping objects with the prototype of index-finger PIP joint motion amplifier for assisting rheumatoid arthritis patients". In: *2005 IEEE/ASME International Conference on Advanced Intelligent Mechatronics*. Monterey, CA, pp. 875–880. DOI: 10.1109/AIM.2005.1511119.

Watanabe, K., H. Morishita, T. Mori, and T. Sato (2007). "A Prototype of Index-Finger PIP Joint Motion Amplifier for Assisting Patients with Impaired Hand Mobility". In: *2007 IEEE International Conference on Robotics and Automation (ICRA)*. April. Rome, pp. 4146–4151. DOI: 10.1109/ROBOT.2007.364116.

Wee, T. B. and S. Y. Ling (2011). "Development of a Puppetry Robotic Glove System for the Rehabilitation of Upper Limb Functions". In: *5th International Conference on Rehabilitation Engineering & Assistive Technology*. Singapore, Article no. 18.

Wege, A. and G. Hommel (2005). "Development and control of a hand exoskeleton for rehabilitation of hand injuries". In: *2005 IEEE/RSJ International Conference on Intelligent Robots and Systems (IROS)*. Edmonton, AB, pp. 3046–3051. DOI: 10.1109/IROS.2005.1545506.

Wege, A. and G. Hommel (2006). *Embedded System Design for a Hand Exoskeleton*. ISBN: 978-1-4020-4932-3. Dordrecht: Springer Netherlands, pp. 169–176. DOI: 10.1007/1-4020-4933-1.

Wege, A., K. Kondak, and G. Hommel (2006). "Force Control Strategy for a Hand Exoskeleton Based on Sliding Mode Position Control". In: *2006 IEEE/RSJ International Conference on Intelligent Robots and Systems (IROS)*. Beijing, pp. 4615–4620. DOI: 10.1109/IROS.2006.282169.

Wege, A., K. Kondak, and G. Hommel (2005). "Mechanical design and motion control of a hand exoskeleton for rehabilitation". In: *2005 IEEE International Conference Mechatronics and Automation*. Vol. 1. July. Niagara Falls, pp. 155–159. DOI: 10.1109/ICMA.2005.1626539.

Wege, A. and A. Zimmermann (2007). "Electromyography sensor based control for a hand exoskeleton". In: *2007 IEEE International Conference on Robotics and Biomimetics (ROBIO)*. Sanya, pp. 1470–1475. DOI: 10.1109/ROBIO.2007.4522381.

Wei, W., S. Guo, F. Zhang, J. Guo, Y. Ji, and Y. Wang (2013). "A novel upper limb rehabilitation system with hand exoskeleton mechanism". In: *2013 IEEE International Conference on Mechatronics and Automation (ICMA)*. Takamatsu, pp. 285–290. DOI: 10.1109/ICMA.2013.6617932.

Wei, W., W. Zhang, S. Guo, X. Zhao, and Y. Wang (2014). "Development of an upper limb rehabilitation robot system for bilateral training". In: *2014 IEEE International Conference on Mechatronics and Automation (ICMA)*. Tianjin, pp. 930–935. DOI: 10.1109/ICMA.2014.6885822.

Weichbrodt, J., B.-M. Eriksson, and A.-K. Kroksmark (2018). "Evaluation of hand orthoses in Duchenne muscular dystrophy". In: *Disability and Rehabilitation*, 40 (23): 2824–2832. DOI: 10.1080/09638288.2017.1347721.

Weir, R. F., C. W. Heckathorne, and D. S. Childress (2001). "Cineplasty as a control input for externally powered prosthetic components." In: *Journal of Rehabilitation Research and Development*, 38 (4): 357–363.

Weiss, P., L. Heyer, T. F. Munte, M. Heldmann, A. Schweikard, and E. Maehle (2013). "Towards a parameterizable exoskeleton for training of hand function after stroke". In: *2013 IEEE International Conference on Rehabilitation Robotics (ICORR)*. Seattle, WA, pp. 1–6. DOI: 10.1109/ICORR.2013.6650505.

White, F. M. (1991). *Viscous Fluid Flow*. 2nd ed. ISBN: 0-07-069712-4. New York: McGraw-Hill.

White, F. M. (2011). *Fluid Mechanics*. 7th ed. ISBN: 978-0-07-352934-9. New York: McGraw-Hill.

Whitney, J. P., M. F. Glisson, E. L. Brockmeyer, and J. K. Hodgins (2014). "A low-friction passive fluid transmission and fluid-tendon soft actuator". In: *2014 IEEE/RSJ International Conference on Intelligent Robots and Systems (IROS)*. Chicago, IL, USA, pp. 2801–2808. DOI: 10.1109/IROS.2014.6942946.

Williams, A. N. and J. Williams (2004). "'Proper to the duty of a chirurgeon': Ambroise Paré and sixteenth century paediatric surgery". In: *Journal of the Royal Society of Medicine*, 97 (9): 446–449. DOI: 10.1258/jrsm.97.9.446.

Winter, S. H. and M. Bouzit (2007). "Use of magnetorheological fluid in a force feedback glove". In: *IEEE Transactions on Neural Systems and Rehabilitation Engineering*, 15 (1): 2–8. DOI: 10.1109/TNSRE.2007.891401.

Wiste, T. E., S. A. Dalley, H. Atakan Varol, and M. Goldfarb (2011). "Design of a Multigrasp Transradial Prosthesis". In: *Journal of Medical Devices*, 5 (3): 031009. DOI: 10.1115/1.4004653.

Wolbrecht, E. T., D. J. Reinkensmeyer, and A. Perez-Gracia (2011). "Single degree-of-freedom exoskeleton mechanism design for finger rehabilitation". In: *2011 IEEE International Conference on Rehabilitation Robotics (ICORR)*. Zurich, pp. 1–6. DOI: 10.1109/ICORR.2011.5975427.

World Health Organization (2002). *Towards a Common Language for Functioning, Disability and Health: ICF*. URL: http://www.who.int/classifications/icf/icfbeginnersguide.pdf.

World Health Organization (2011). *World report on disability 2015*. URL: http://whqlibdoc.who.int/publications/2011/9789240685215_eng.pdf.

World Health Organization (2015). *World health statistics 2015*. URL: http://apps.who.int/iris/bitstream/handle/10665/170250/9789240694439_eng.pdf.

World Health Organization (2017). *The need to scale up rehabilitation*. URL: http://www.who.int/disabilities/care/NeedToScaleUpRehab.pdf.

Worsnopp, T. T., M. A. Peshkin, J. E. Colgate, and D. G. Kamper (2007). "An actuated finger exoskeleton for hand rehabilitation following stroke". In: *2007 IEEE 10th International Conference on Rehabilitation Robotics (ICORR)*. Noordwijk, pp. 896–901. DOI: 10.1109/ICORR.2007.4428530.

Wu, J., J. Huang, Y. Wang, and K. Xing (2010). "A Wearable Rehabilitation Robotic Hand Driven by PM-TS Actuators". In: *Lecture Notes in Computer Science*. Vol. 6425. PART 2. Shanghai, pp. 440–450. DOI: 10.1007/978-3-642-16587-0_41.

Wu, J., J. Huang, Y. Wang, and K. Xing (2012). "RLSESN-based PID adaptive control for a novel wearable rehabilitation robotic hand driven by PM-TS actuators". In: *International Journal of Intelligent Computing and Cybernetics*, 5 (1): 91–110. DOI: 10.1108/17563781211208242.

Wu, J., J. Huang, Y. Wang, K. Xing, and Q. Xu (2009). "Fuzzy PID control of a wearable rehabilitation robotic hand driven by pneumatic muscles". In: *2009 International Symposium on Micro-NanoMechatronics and Human Science*. Nagoya, pp. 408–413. DOI: 10.1109/MHS.2009.5352012.

Wurth, S. M. and L. J. Hargrove (2014). "A real-time comparison between direct control, sequential pattern recognition control and simultaneous pattern recognition control using a Fitts' law style assessment procedure". In: *Journal of NeuroEngineering and Rehabilitation*, 11 (1): 91. DOI: 10.1186/1743-0003-11-91.

Würtz, T., C. May, B. Holz, C. Natale, G. Palli, and C. Melchiorri (2010). "The twisted string actuation system: modeling and control". In: *2010 IEEE/ASME International Conference on Advanced Intelligent Mechatronics*. Montreal, ON, Canada, pp. 1215–1220. DOI: 10.1109/AIM.2010.5695720.

Xia, J. and W. K. Durfee (2011). "Modeling of Tiny Hydraulic Cylinders". In: *IFPE Conference Proceedings*, (25): 657–662.

Xia, J. and W. K. Durfee (2014). "Experimentally Validated Models of O-Ring Seals for Tiny Hydraulic Cylinders". In: *ASME/BATH 2014 Symposium on Fluid Power and Motion Control*. 1. Bath, V001T01A019. DOI: 10.1115/FPMC2014-7825.

Xia, J. and W. K. Durfee (2013). "Analysis of Small-Scale Hydraulic Actuation Systems". In: *Journal of Mechanical Design*, 135 (9): 091001. DOI: 10.1115/1.4024730.

Xing, K., J. Huang, Q. Xu, and Y. Wang (2009). "Design of a wearable rehabilitation robotic hand actuated by pneumatic artificial muscles". In: *2009 7th Asian Control Conference*. Hong Kong, pp. 740–744.

Xing, K., Q. Xu, J. He, Y. Wang, Z. Liu, and X. Huang (2008). "A wearable device for repetitive hand therapy". In: *2nd Biennial IEEE RAS & EMBS International Conference on Biomedical Robotics and Biomechatronics (BioRob)*. Scottsdale, AZ, pp. 919–923. DOI: 10.1109/BIOROB.2008.4762789.

Yagn, N. (1890). *Apparatus for facilitating walking, running, and jumping*. Patent no. US420179A.

Yamada, Y., T. Morizono, K. Sato, H. Shibuya, T. Shimohira, Y. Umetani, T. Yoshida, and S. Aoki (2004). "Proposal of a SkilMate Hand and its component technologies for extravehicular activity gloves". In: *Advanced Robotics*, 18 (3): 269–284. DOI: 10.1163/156855304322972440.

Yamada, Y., T. Morizono, S. Sato, T. Shimohira, Y. Umetani, T. Yoshida, and S. Aoki (2001). "Proposal of a SkilMate finger for EVA gloves". In: *2001 IEEE International Conference on Robotics and Automation (ICRA)*. Vol. 2. Seoul, pp. 1406–1412. DOI: 10.1109/ROBOT.2001.932807.

Yamaura, H., K. Matsushita, R. Kato, and H. Yokoi (2009). "Development of hand rehabilitation system for paralysis patient - universal design using wire-driven mechanism". In: *31st Annual International Conference of the IEEE Engineering in*

Medicine and Biology Society (EMBC). Minneapolis, MN, pp. 7122–7125. DOI: 10.1109/IEMBS.2009.5332885.

Yap, H. K., J. C. H. Goh, and R. C. H. Yeow (2015a). "Design and Characterization of Soft Actuator for Hand Rehabilitation Application". In: *IFMBE Proceedings*. Vol. 45, pp. 367–370. DOI: 10.1007/978-3-319-11128-5_92.

Yap, H. K., J. H. Lim, F. Nasrallah, J. C. H. Goh, and R. C. H. Yeow (2015b). "A soft exoskeleton for hand assistive and rehabilitation application using pneumatic actuators with variable stiffness". In: *2015 IEEE International Conference on Robotics and Automation (ICRA)*. Seattle, WA, pp. 4967–4972. DOI: 10.1109/ICRA.2015.7139889.

Yap, H. K., J. H. Lim, F. Nasrallah, F.-Z. Low, J. C. H. Goh, and R. C. H. Yeow (2015c). "MRC-glove: A fMRI compatible soft robotic glove for hand rehabilitation application". In: *2015 IEEE International Conference on Rehabilitation Robotics (ICORR)*. 65. Singapore, pp. 735–740. DOI: 10.1109/ICORR.2015.7281289.

Yap, H. K., J. H. Lim, F. Nasrallah, and C. H. Yeow (2017). "Design and preliminary feasibility study of a soft robotic glove for hand function assistance in stroke survivors". In: *Frontiers in Neuroscience*, 11: 547. DOI: 10.3389/fnins.2017.00547.

Yeong, C. F., K. Baker, A. Melendez-Calderon, E. Burdet, and E. D. Playford (2010). "ReachMAN to help sub-acute patients training reaching and manipulation". In: *2010 IEEE Conference on Robotics, Automation and Mechatronics (RAM)*. Singapore, pp. 90–95. DOI: 10.1109/RAMECH.2010.5513206.

Yeong, C. F., A. Melendez-Calderon, R. Gassert, and E. Burdet (2009). "ReachMAN: A personal robot to train reaching and manipulation". In: *2009 IEEE/RSJ International Conference on Intelligent Robots and Systems (IROS)*. St. Louis, MO, pp. 4080–4085. DOI: 10.1109/IROS.2009.5354837.

Zhang, F., Y. Fu, T. Wang, Q. Zhang, S. Wang, and B. Guo (2013). "Research on sensing and measuring system for a hand rehabilitation robot". In: *2013 IEEE International Conference on Robotics and Biomimetics (ROBIO)*. December. Shenzhen, pp. 50–55. DOI: 10.1109/ROBIO.2013.6739434.

Zhang, F., L. Hua, Y. Fu, H. Chen, and S. Wang (2014). "Design and development of a hand exoskeleton for rehabilitation of hand injuries". In: *Mechanism and Machine Theory*, 73: 103–116. DOI: 10.1016/j.mechmachtheory.2013.10.015.

Zhang, M., A. R. Turner-Smith, and V. C. Roberts (1994). "The reaction of skin and soft tissue to shear forces applied externally to the skin surface". In: *Proceedings of the Institution of Mechanical Engineers*, 208 (4): 217–222. DOI: 10.1243/PIME_PROC_1994_208_291_02.

Zheng, D. Y., M. Luo, and S. S. Yang (2013). "Design of a mechanical exoskeleton system for improving hand-gripping force". In: *Advanced Materials Research*, 663: 708–712. DOI: 10.4028/www.scientific.net/AMR.663.708.

Zheng, R. and J. Li (2010). "Kinematics and workspace analysis of an exoskeleton for thumb and index finger rehabilitation". In: *2010 IEEE International Conference on Robotics and Biomimetics*. Tianjin, pp. 80–84. DOI: 10.1109/ROBIO.2010.5723307.

Zhu, T. L., J. Klein, S. A. Dual, T. C. Leong, and E. Burdet (2014). "reachMAN2: A compact rehabilitation robot to train reaching and manipulation". In: *2014 IEEE/RSJ International Conference on Intelligent Robots and Systems (IROS)*. Iros. Chicago, IL, pp. 2107–2113. DOI: 10.1109/IROS.2014.6942845.

Zupan, M., M. Ashby, and N. Fleck (2002). “Actuator Classification and Selection — The Development of a Database”. In: *Advanced Engineering Materials*, 4 (12): 933–940. DOI: 10.1002/adem.200290009.

CURRICULUM VITÆ

November 3, 1989
Born in Houten, The Netherlands.

2002-2008
VWO at College de Heemlanden in Houten, The Netherlands.

2008-2011
BSc Mechanical Engineering at Delft University of Technology in Delft, The Netherlands.

- Minor in Biomedical Engineering.
- BSc thesis entitled *"Exploring a solar updraft tower at small scale"*.

2011-2013
MSc Biomedical Engineering at Delft University of Technology in Delft, The Netherlands.

- Specialization in Biomechatronics.
- MSc thesis entitled *"Cosmetic glove stiffness compensation for body-powered hand prostheses: Design of a novel negative stiffness element"*.
- Graduated with distinction.

2014-2018
PhD Candidate at Delft University of Technology in Delft, The Netherlands.

- Research on novel tools and technologies to be used in dynamic hand orthoses (e.g. hand exoskeletons), with applications for stroke patients and boys that suffer from Duchenne Muscular Dystrophy.
- PhD thesis entitled *"Mechanical design of dynamic hand orthoses: Expanding technology with comprehensive overviews and alternative pathways"*.

2015–*present*
Joined the board as treasurer of the Hand Fund, a foundation with a primary mission to financially support applied scientific research and development of hand and arm prostheses and orthoses.

2019–*present*
Innovation Engineer at Wilgenhaege in Hoofddorp, The Netherlands

- Research & mechanical design on innovative technologies.
- Clean energy storage of durable energy.

ACKNOWLEDGMENTS

The acknowledgments; to many it is the first thing they will read in a PhD thesis, for me it is the last thing that I am writing. Yes, a PhD can feel pretty lonely sometimes, but writing sections like this makes me realize how much support I had around me. During this period there were so many people who I have met, who have helped me and who have provided me with the distraction that I needed. I like to think that my PhD research has given me more personal growth than professional knowledge, and I hope I was able to express my gratitude to the people around me *during* this process and not after—so this section does not become like a reversed obituary. Nonetheless, here come the thank-you-notes.

The first one to thank is you: the reader. I assume that if you made it here, you are either interested in the person behind this thesis or are wondering whether your name is listed. So thank you [insert your name], your attention is the most valuable gift to give!

All this work was never possible without my daily supervisor: **Dick**. All the way from project courses during my BSc minor program, my MSc graduation project and now my PhD research, I have gotten to know you as a supervisor that devotes attention and interest to your students, and more importantly encourages to explore. You gave me a work mentality that I will take with me, which is to maintain a broad but critical view, to aim for simple solutions and to have fun while you are at it. This mentality was strengthened by my promotor: **Just**, who was Dick's perfect partner-in-crime in supervision. Your ability to get to the core of any problem in minutes continues to amaze me and has helped me to develop the scientific value in my thesis. Whenever I was feeling stuck or down, a meeting with the three of us always helped me to regain confidence and stride forward, thank you for inspiring me.

Within the Delft Institute of Prosthetics and Orthotics, I want to thank **Mona**, **Gerwin** and **Jan** for the many discussions on the ins and outs of upper limb prosthetics and orthotics. The occasional walk-ins and monthly 'bring-your-own-lunch meetings' organized by Dick made me feel I was part of a team. I thoroughly enjoyed the meetings with Jan, which was filled with crucial advice, many learning moments and getting carried away with off-topic matters. Another thank you goes to everyone who had to put up with me and/or my technical drawings in the workshop. Believe it or not, in my last few months, I wore safety glasses, a dust coat and hardened shoes every time!

My office room was the space where I could share my initial frustrations on Matlab, listen to weekend stories and have meaningful personal conversations. It was also a space with a dynamic occupation, so I was fortunate enough to have met with and learned from many people, some of who I still call my friends. Thank you for giving me a listening ear and a fun environment to work in **Xavier**, **Hoda**, **Paulos**, **Joost**, **Bram**, **Lixin**, **Frederico**, **Pier**, **Ingrid**, **Karen**, **Mojtaba**, **Jinne**, **Maryam**, **Mana** and **Sara**.

Outside of Delft I was part of a larger consortium called Symbionics, an amazing group of people that spanned between Amsterdam–Enschede and Maastricht–Groningen. A big thanks to everyone who made this possible and who saw it through, specifically also **Arno**,

Herman, **Bart** and **Micha** for your crucial inputs and occasional guidance. Thank you to **Kostas**, **Stergios**, **Niek**, **Bob**, **Claudia**, **Teun**, **Koen**, **Hans**, **Roy**, **Nauzef**, **Laura**, **Anouk** and **Arjen** for all the advisory talks and fun times at conferences and meetings, and definitely for the (tree-)climbing, e-stepping, campfiring, log-throwing and card-gaming during our amazing self-organized weekend outings. Kostas, through our collaboration in our final year, your limitless energy and enthusiasm has pushed me further than I could on my own. That, and our compatible sense of humor might have played a role as well... Thank you for time, energy, and letting me sleep on your couch a few times.

A big part of my third year was my research visit to Festo's headquarters in Esslingen am Neckar, Germany. During the three months that I spent there, I seemed the weird one out trying to do hydraulics in a big pneumatic institute. Regardless, the knowledge on fluidics was boundless and by working within the R&D department I have learned to quickly turn hunches into demonstrators, ideas into prototypes, and a Weihnachtsmarkt into a bad headache. Thank you **Metin** for your hospitality, your expertise and for saving my PhD files when I burned my motherboard. Thank you to **Simon**, **Daniel**, **Daniel**, **Daniel** (yes there were three), **Tobias**, **Markus**, **Stefan**, **Mathias**, **Michael**, **Lars** and **Gebhard** for making me feel welcome, for the enjoyable coffee conversations and for exposing me to German culture. This visit would not have been possible without **Jan** from the Dutch branch of Festo, thank you for your interest in this project and for creating this opportunity.

This thesis would not be this way without the time and effort of numerous graduating BSc and MSC students I had the privilege of supervising. **Davey**, **Arthur**, **Wietske**, **Kenneth**, **Daan**, **Edwin**, **Els**, **Guido**, **Jeroen**, **Panayiotis**, **Rik** and **Kevin**: I thoroughly enjoyed getting to know you all and go through your graduation project together. All your work has found its way in this thesis in one way or another.

I always felt that a big part of one's job is what you do afterwards. One of the biggest contributors to emptying my mind is the weekly volleyball practice, a team which I got to know simultaneously with my PhD, thank you **Sandra**, **Gitty**, **Francien**, **Sanny**, **Leanne**, **Ingeborg**, **José**, **Hildy**, **Marit**, **Nynke**, **Joost**, **Bernd**, **Mike**, **Dennis**, **Roeland**, **Coen** and **Erik**! In the comfort of our own homes yet still together, I had a blast during the weekly games and shenanigans together with **Andi**, **Bart**, **Casper**, **Dave**, **Diana**, **Reea** & **Roy**, thank you! To **Rosanne**, **Maarten**, **Chantal** and **Daniel**, thank you for the silly trips, card games and house visits. **Rens**, I will always remember our good times as roommates during our studies and will strive to beat you at least once with one of your party games (help me **Renske**!). **Frans Willem**, thank you for the numerous nights with western/mafia movies and specialty beers. **René**, you are the best big brother I can imagine, with your time and attention you have helped me get through various engineering problems, rants and mental blocks for countless times. **Esther**, thank you for your unfiltered competitiveness while playing 30 Seconds and shared laugh attacks while gambling for Sinterklaas gifts. I can only imagine the great example you two are setting for Jesper and the little girl that is almost bursting out during my defense ceremony. **Johan** and **Fabiënne**, thank you for your never-ending interest, spontaneous life lessons and for always making me feel proud of my own work. To my parents, **Jozef** and **Thérèse**, thank you for providing me with words that are always supporting, with ears that are always listening and with a place that always feels like home.

The most important to thank is my best friend, my girlfriend and my wife. **Esmé**, thank you for helping me get through this one particular storm and for the unconditional support you have given me during the rainy and sunny days. You taught me how to take steps back, reminded me to celebrate the small victories and extensively discussed with me how to make sense of... well everything. You inspire me to be a better person every day.